University of Southampton

Faculty of Medicine

Human Development and Health

Risk stratification in sudden cardiac death:
Engineering novel solutions in heart failure

by

James A Rosengarten

Thesis for the degree of Doctor of Medicine

July 2014

Final Version December 2014

UNIVERSITY OF SOUTHAMPTON

ABSTRACT

FACULTY OF MEDICINE

Human Development and Health

Doctor of Medicine

RISK STRATIFICATION IN SUDDEN CARDIAC DEATH: ENGINEERING NOVEL SOLUTIONS IN HEART FAILURE

By James Alexander Rosengarten

Sudden cardiac death (SCD) risk is reduced by implantable cardioverter defibrillator (ICD) use in appropriately selected patients. Established markers such as impairment of left ventricular function and QRS duration are non specific for arrhythmic death and therefore many patients receive ICD therapy from which they gain no benefit, either due to survival without arrhythmia or death from pump failure. Both myocardial scar and serum protein biomarkers have potential as SCD risk stratifiers, but novel solutions are needed to deliver non invasive tests that are suitable for point of care testing. The aims of this thesis were to explore novel assessment methods for the risk stratification of SCD, with particular focus on heart failure.

Several approaches were chosen to explore these concepts: (i) meta-analysis to assess the utility of fragmented QRS, (ii) retrospective evaluation of ECG and CMR to assess ECG markers of repolarisation and (iii) QRS scoring, (iv) prospective evaluation of an automated QRS scoring algorithm to predict myocardial scar, (v) artificial intelligence machine learning techniques to develop and validate an algorithm capable to classifying ECG scar, and (vi) a novel high resolution proteomic technique to propose biomarkers of SCD risk, validated using ELISA (vii). The hypothesis is that novel clinical tools, encompassing technologies and techniques which could stretch across the clinical landscape from primary to specialised care services, can be identified as indicators of ICD benefit in patients at risk of SCD.

My results indicate that simpler ECG markers such as T-peak-end, fQRS and QRS scoring have a significant association with myocardial scar, although the strength of association varies according to scar characteristics, and is not specific. The specificity of these markers for mode of death is also weak. Computerised algorithms can serve to speed up manual ECG scoring, whilst maintaining overall accuracy, but greatest potential is seen in using a novel marker, custom developed using artificial intelligence techniques. I also found that candidate serum biomarkers, predictive of death or ventricular arrhythmia, could be identified through high resolution proteomic techniques. Clinical and technical validation with ELISA is possible.

Novel non invasive markers, such as serum proteins and computer ECG analysis may be valuable tools to improve risk prediction. The incremental benefit of these tools to determine prognosis, and select those who will most benefit from ICD therapy, can now be addressed by future prospective studies.

Table of contents

List of figures

List of tables

Declaration of authorship

I, James Alexander Rosengarten, declare that this thesis:

Risk stratification in sudden cardiac death: engineering novel solutions in heart failure.

and the work presented in it are my own and has been generated by me as the result of my own original research.

I confirm that:

1. This work was done wholly or mainly while in candidature for a research degree at this University;

2. Where any part of this thesis has previously been submitted for a degree or any other qualification at this University or any other institution, this has been clearly stated;

3. Where I have consulted the published work of others, this is always clearly attributed;

4. Where I have quoted from the work of others, the source is always given. With the exception of such quotations, this thesis is entirely my own work;

5. I have acknowledged all main sources of help;

6. Where the thesis is based on work done by myself jointly with others, I have made clear exactly what was done by others and what I have contributed myself;

7. Parts of this work have been published as:

Original papers:

Rosengarten JA, Scott PA, Morgan, JM. Fragmented QRS for the prediction of sudden cardiac death: a meta-analysis. Europace. In press.

Scott PA, **Rosengarten JA**, Shahed A, Yue AM, Murday DC, Roberts PR, Peebles CR, Harden SP, Curzen NP, Morgan JM. The relationship between left ventricular scar and ventricular repolarization in patients with coronary artery disease: insights from late gadolinium enhancement magnetic resonance imaging. Europace. 2013 Jun;15(6):899-906.

Rosengarten JA, Scott PA, Chiu OKH, Shambrook JS, Curzen NP, Morgan JM. Can QRS scoring predict left ventricular scar and clinical outcomes? Europace. 2013 Jul;15(7):1034–41.

Bono V, Mazomenos EB, Chen T, **Rosengarten JA**, Acharyya A, Maharatna K, Morgan JM, Curzen, N. Development of an automated updated Selvester QRS scoring system using SWT-based QRS fractionation detection and classification. IEEE J Biomed Health Inform. 2014 Jan;18(1):193–204.

Dima S-M, Panagiotou C, Mazomenos EB, **Rosengarten J**, Maharatna K, Gialelis JV, Curzen, N, Morgan J. On the Detection of Myocadial Scar Based on ECG/VCG Analysis. IEEE Trans Biomed Eng. 2013 Dec;60(12):3399–409.

Abstracts:

J.A. Rosengarten, S.M. Dima, C. Panagiotou, P.A. Scott, K.H.O. Chui, E.B. Mazomenos, K. Maharatna, N.P. Curzen, J. Morgan. Novel non invasive detection of arrhythmia substrate using supervised learning support vector machine. Europace (2013) 15 (suppl 2): ii11.

J.A. Rosengarten, P.A. Scott, S.E. Larkin, S. Garbis, N.P. Curzen, P.A. Townsend, J.M. Morgan. High resolution multidimensional proteomics detects candidate arrhythmia biomarkers. Europace (2013) 15 (suppl 2): ii118.

J.A. Rosengarten, P.A. Scott, S.E. Larkin, S. Garbis, N.P. Curzen, P.A. Townsend, J.M. Morgan. High Resolution Multidimensional Proteomics Detects Candidate Arrhythmia Biomarkers. Heart 2013 99: A45-46

J.A. Rosengarten, S.M. Dima, C. Panagiotou, P.A. Scott, K.H.O. Chui, E.B. Mazomenos, K. Maharatna, N.P. Curzen, J. Morgan. Novel Non Invasive Detection of Arrhythmia Substrate Using Support Vector Machine Learning. Heart 2013 99: A46

Signed:

……

Date:

……

Acknowledgements

I would especially like to thank Professor John Morgan for his constant guidance, support and encouragement. My thanks also go to Professor Mark Hanson who gave invaluable advice and supervision, and to Professor Nick Curzen who provided insightful commentary and helpful direction.

I am extremely grateful to Dr. Paul Scott. Much of my work built upon the foundations laid by his research. He collected the initial CMR scar quantification for a separate study that naturally lead on to the exploration of ECG parameters and the relationship with scar in Chapter 4. Some of this initial analysis was also used in Chapter 5. He also established the biobank of serum samples used in Chapter 8 and 9. He was also kind enough to verify my extracted data used in the meta-analysis (Chapter 3).

I acknowledge and thank Dr. Koushik Maharatna and his team at the School of Electronics and Computer Science for the close collaboration in coding the software used in automated QRS scoring (Chapter 6) and the machine learning algorithm used for ECG scar classification (Chapter 7).

I thank Professor Paul Townsend and Dr. Sam Larkin for their help, advice and guidance on biomarker discovery and validation, and thank Dr. Spiros Garbis for his involvement in the final steps of the biomarker discovery process by performing the proteomic analysis.

I would like to thank Dr. James Shambrook for his guidance and tutoring me in the CMR scar quantification used in Chapters 6 and 7.

I thank the medical students who took an interest in my work. Anwar Shahed helped perform the QT and Tpeak-end measurements used for assessing reproducibility in Chapter 4, and Oscar Chiu was involved in the QRS scoring and CMR scar quantification used in Chapters 5 and 6.

I would like to thank Medtronic for providing the financial support that made this work possible, and the research team at Southampton, with whom I learnt to appreciate the value of strong coffee and good cake.

Lastly, I owe a tremendous amount to my wife Nicci, and daughter Ava. They provided me with an escape during the research and gave me the space to complete this thesis.

Abbreviations

ACE-I	angiotensin-converting enzyme inhibitor
ACS	acute coronary syndrome
ADC	analogue to digital converter
AF	atrial fibrillation
AMI	acute myocardial infarction
ANOVA	analysis of variance
ANP	atrial natriuretic peptide
ARB	angiotensin II receptor blocker
ARVC	arrhythmogenic right ventricular cardiomyopathy
ATP	anti-tachycardia pacing
AUC	area under the curve
AVID	Antiarrhythmics versus Implantable Defibrillators trial
BBB	bundle branch block
BNP	B-type natriuretic peptide
CABG	coronary artery bypass grafting
CAD	coronary artery disease
CASH	Cardiac Arrest Study Hamburg
CI	confidence iterval
CIDS	Canadian Implantable Defibrillator Study
CIED	cardiac implantable electronic device
CMR	cardiac magnetic resonance imaging
CRP	C-reactive protein
CRT	cardiac resynchronization therapy
DCM	dilated cardiomyopathy
DEFINITE	Defibrillators in Non-Ischaemic Cardiomyopathy Treatment Evaluation
DSP	digital signal processing
ECG	Electrocardiogram
ELISA	enzyme-linked immunosorbent assay
FWHM	full width at half maximum
Gd	Gadolinium
GDF	growth differentiation factor
HF	heart failure
HPLC	high performance liquid chromatography
HR	hazard ratio
HRP	horseradish peroxidase

HRV	heart rate variability
hsCRP	highly sensitive C-reactive protein
ICC	intraclass correlation coefficient
ICD	implantable cardioverter defibrillator
iTRAQ	Isobaric Tag for Relative and Absolute Quantification
LAFB	left anterior fascicular block
LBBB	left bundle branch block
LGE-CMR	late gadolinium enhancement-cardiac magnetic resonance imaging
LPCAT	Lysophosphatidylcholine acyltransferase 2
LR	likelihood ratio
LV	left ventricular
LVEDV	left ventricular end diastolic volume
LVEF	left ventricular ejection fraction
LVH	left ventricular hypertrophy
MADIT	Multicenter Automatic Defibrillator Implantation Trial
MALDI	Matrix-Assisted Laser Desorption/Ionization
MI	myocardial infarction
MIBG	metaiodobenzylguanidine
MRI	magnetic resonance imaging
MRM-MS	multiple reaction monitoring mass spectrometry
MS	mass spectrometry
MS/MS	tandem mass spectrometry
MTWA	microvolt T-wave alternans
MUSTT	Multicenter Unsustained Tachycardia Trial
NICE	National Institute for Health and Care Excellence
NICM	non-ischaemic cardiomyopathy
NPV	negative predictive value
NS	non-significant
NSVT	non-sustained ventricular tachycardia
NYHA	New York Heart Association
PAF	platelet activating factor
PCI	percutaneous coronary intervention
PES	programmed electrical stimulation
PPV	positive predictive value
PRIME	Prospective Epidemiological Study of Myocardial Infarction
PTM	post translational protein modification
PVC	premature ventricular contraction

QTc	corrected QT interval
QTD	QT dispersion
QUIPS	Quality in Prognosis Studies
QUORUM	Quality of Reporting of Meta-analyses
RBBB	right bundle branch block
ROC	receiver operating characteristic
RWMA	regional wall motion abnormalities
SAECG	signal-averaged ECG
SCD	sudden cardiac death
SD	standard deviation
SELDI	surface-enhanced laser desorption/ionization
SOPIWG	Standard Operating Procedure Integration Working Group
SVM	support vector machine
TOF	time of flight
TpTe	T peak to T end interval
VA	ventricular arrhythmia
VDAC1	voltage-dependent anion-selective channel protein 1
VF	ventricular fibrillation
VT	ventricular tachycardia

1 Introduction

1.1 Heart Failure

1.1.1 Definition, aetiology and epidemiology

Heart failure (HF) is the final common syndrome of many differing heart diseases. The aetiology is varied, but a cardiac output insufficient to meet metabolic demands activates maladaptive neurohormonal and circulatory responses. The result is a complex syndrome in which patients have the following features: [1]

Symptoms typical of HF such as shortness of breath at rest or during exertion, fatigue, tiredness, ankle swelling.

and

Signs typical of HF such as tachycardia, tachypnoea, pulmonary crackles, pleural effusion, raised jugular venous pressure, peripheral oedema, hepatomegaly

and

Objective evidence of a structural or functional abnormality of the heart at rest (cardiomegaly, third heart sound, cardiac murmurs, echocardiographic abnormality, raised natriuretic peptide concentration)

Despite the decline in other cardiovascular conditions, the prevalence of HF continues to rise, partly due to the increased life expectancy of an ageing population, but also due to better survival from cardiovascular disease in earlier life.[2,3] The prevalence of HF is 2-3% and rises sharply in the elderly, where between 10 and 20% of those aged 70-80 years old are affected. Men are more frequently affected in the younger age groups, where coronary disease is the biggest cause. In the elderly, prevalence is equal between the sexes.[1]

HF is the cause of 5% of acute hospital admissions and is seen in 10% of inpatients. These figures fail to take account of patient episodes in which HF is a co-morbid diagnosis, or the aetiology, rather than where HF itself is coded as the final diagnosis. The direct and indirect cost of HF in the United States is estimated at close to $40 billion.[4] Hospital admissions account for the largest proportion of HF spending, with the total cost running at 4% of NHS expenditure.[5]

HF can develop due to any structural or functional deterioration of the heart. This can occur through diseases of the myocardium, pericardium, valves or great vessels, or

development of rhythm disturbance. Coronary artery disease leading to myocardial ischaemia and loss of viable heart muscle is implicated in ~70% if cases. Valve disease accounts for 10% and cardiomyopathies a further 10%. The remaining cases are due to drugs, toxins, metabolic, infective and infiltrative causes. HF secondary to high circulatory output conditions, such as anaemia, thyrotoxicosis and Paget's disease are reversible with treatment of the primary cause.[1] Even in the absence of symptoms, disorders of cardiac function are considered to be precursors of symptomatic HF, known to have an adverse prognosis and should be regarded with the same importance.[6]

The majority of cases are caused by left ventricular (LV) impairment. An arbitrary distinction can be made between systolic HF and HF with preserved ejection fraction. Although the inclusion criteria for most HF trials have included dilated hearts with reduced left ventricular ejection fraction (LVEF), most patients with HF have evidence of systolic and diastolic HF, and although systolic ejection fraction may be normal, LV compliance and systolic shortening velocities, myocardial strain and strain rate are reduced. [67]

1.1.2 Prognosis

Despite advances in therapy and management, HF remains lethal. HF can be implicated in 1 in 8 deaths, and 20% have HF as the primary cause of death.[4] Since definitions vary, mortality risk is difficult to define, but does steadily increase after a new diagnosis, and is as "malignant" as common cancers.[8] 1-year mortality is 10-20% and at 5 years it reaches 40-60%.[39] 5 year mortality can be as high as 75% after first hospitalisation for HF.[10]

A review of Medicare patients in the USA reported a fall in 30-day mortality from 12.8% in 1993 to 10.7% in 2006.[11] A study of patients hospitalised in Scotland between 1986 and 2003 reported a decline in 30-day mortality after first hospitalization with HF, from 24.4% to 16.2% in men and 20% to 16.9% in women, with differences persisting at 1-year and 5-year follow-up.[12] Although there have been improvements in both short and long-term outcomes for those diagnosed with HF, the prognosis remains poor.

1.1.3 Mode of Death

Describing and understanding the mechanism of death in HF may enable identification of high-risk individuals and provide insight into the clinical course of the syndrome, and the appropriate targeting of therapeutic interventions, such as drugs or electrical devices, including the implantable cardioverter defibrillator (ICD). The importance of reporting such data in epidemiological studies has long been recognised; of the 461

subjects who developed HF in the Framingham study, 55% of men and 24% of women had died within 4 years of diagnosis (a mortality rate more than six times the general population). Around 50% of these deaths were sudden.[13] More recent epidemiological evidence seems discrepant. Mehta *et al*. reported mode of death from 396 patients newly diagnosed with HF. 51 cardiovascular deaths were recorded, of which 52% were due to progressive HF and 22% due to sudden cardiac causes.[14]

It is difficult to be certain if differences in the reported rates of death in these and other epidemiological studies may just be due to changes in contemporary practice. A study by Cubbon *et al*. compared 2 prospective cohort studies of outpatients with chronic HF.[15] The studies predominantly differed in their rates of β-adrenoceptor antagonist prescribing; 8.5% in the historical cohort (1993-95) and 80% in the contemporary cohort (2006-2009). There was a significant 32% reduction in all cause mortality, driven by a reduction in sudden cardiac death (SCD) (34% v 13%) whilst progressive HF death remained broadly similar (41% v 37%). Whilst these rates are low overall, perhaps since these cohorts did not include hospitalized patients, the study serves to support that assertion that the mechanism of death in HF can be modulated with therapeutic interventions.

Evidence is also available from randomised controlled trials (RCTs) of HF interventions. Patients enrolled in MERIT-HF, investigating the effect of metoprolol in HF, died of a sudden cardiac cause in 60% of all death cases.[16] However, most the patients enrolled in the study had New York Heart Association class (NYHA) II-III symptoms, perhaps limiting applicability to a more general HF population. Data published at the same time investigated the effect of spironolactone on patients with severe HF (NYHA III-IV). This reported sudden death occurring in 35%, and pump failure in up to 60%. [17] More recently, the ATLAS study enrolled 3164 patients (83% NYHA class III-IV) to investigate the effects of lisinopril.[18] Analysis of the 1224 cardiovascular deaths in this trial reported 48% as sudden and 36% due to pump failure. Each of these studies enrolled patients with established disease, and this in itself may account for the differences reported. Such trials are subject to survival bias, since only patients surviving the highest risk period are available for recruitment.

In addition to changes in enrolment and contemporary practice, differences in reporting may also reflect the use of differing definitions of HF, a lack of uniformity in classification the mode of death, and the methods used to adjudicate the mode of death.[19] However, a standardised definition was used in a contemporary study of 10538 patients with HF (51% NYHA II-III) enrolled across 6 randomised trials and registries. SCD was described as unexpected death in a clinically stable patient,

typically within 1 hour of symptom onset, from documented or presumed cardiac arrhythmia and without a clear non-cardiac cause. Pump failure death was defined as progressively reduced cardiac output and failure of organ perfusion. Of 2014 deaths, 50% were SCD, and 34% died of pump failure.[20]

These data serve to highlight that although HF deaths are due to SCD or pump failure, there is uncertainty about the true balance between these mechanisms. The limitations in the data may be due to changes in contemporary practice, selection or survival bias or standardisation in definition.

1.2 Sudden Cardiac Death

1.2.1 Definition

Sudden cardiac death is natural death from cardiac causes, heralded by abrupt loss of consciousness within one hour of the onset of acute symptoms; pre-existing heart disease may have been present, but the time and mode of death are unexpected. [21] It is a matter of debate when an unexpected death should be labelled “sudden” and “how” the cardiac origin of death should be ascertained.[22] As sophistication of clinical trials improves, and new therapies target specific mechanisms, the need to objectively and precisely classify cause of cardiac death has become increasingly important. The practical consequence of classifying a death as sudden cardiac is the presumption that such deaths are due to ventricular tachyarrhythmias. Although in most cases this is the case, other mechanisms may also lead to instantaneous death, such as cardiac rupture or massive pulmonary embolism.[23] Efforts have been made in defining SCD to make arrhythmic death more likely and the duration of the terminal event has been shortened to an hour, rather than 24 hours as was previously the case. Of course, death may still be arrhythmic, even if it does not occur suddenly.

1.2.2 Incidence

SCD incidence is estimated to vary from between 200,000 and 450,000 according to inclusion criteria and geography, with similar rates in Europe and the USA, but with variation according to local rates of coronary disease. The most widely used estimates are in the region 300,000 to 350,000 annually. [422] Globally, the yearly burden of SCD has been estimated to reach between 4 and 5 million.[24] When the temporal definition is 1 hour from onset of symptoms, 13% of all natural deaths are due to SCD, whereas when using a 24hour definition, this rises to 18.5%.[2526]

1.2.3 Populations at risk

Most SCD occurs in individuals with previously undiagnosed cardiovascular disease. For this reason, attributing SCD to one pathology or another remains a challenge. Although the absolute numbers may vary, it is widely accepted that ischaemic heart disease, whether active coronary lesions, acute myocardial infarction (MI) or myocardial scar, accounts for around 80% of SCD events.[27] Around 10-15% of cases are seen in those with reduced LVEF but no evidence of coronary artery disease (CAD), categorised as non-ischaemic cardiomyopathy (NICM). [28] Only a small proportion of cases (5-10%) occur in those with a structurally normal heart, and many of these cases will be due to a genetic abnormality affecting the function of cellular membrane proteins. These so called "channelopathies" are conditions, frequently inherited, that modify the electrical properties of the heart, making primary arrhythmic events, and therefore SCD, more likely.

Patients with reduced LVEF, a history of HF, and survivors of cardiac arrest are most at risk of experiencing SCD, and have the highest case fatality rates.[29] However, when analysing the absolute numbers of SCD, it is clear that these highest risk clinical subgroups do not generate the greatest number of events and that most cases of SCD events occur in lower risk populations who are less well defined and poorly studied. Identifying these unique populations is important to improve risk stratification and tailor personalised therapy.[30] However, it is the highest risk subgroups that are most clearly identified and therefore have been studied most closely through observation and interventional trials.

1.2.4 Mechanisms of SCD

The exact mechanism of a SCD is difficult to establish. Very few patients are under direct observation or electrocardiogram (ECG) monitoring at the time of demise, and therefore the arrhythmic cause for SCD is frequently determined retrospectively. Despite many individuals expressing the myocardial substrate necessary for developing a life threatening arrhythmia, only a small number of those go on to die suddenly. It is the interplay of the anatomical or electrical substrate and a transient triggering event, whether ischaemic, neurohormonal, pharmacological or metabolic that results in an arrhythmic mechanism of death.[31]

VT degenerating into ventricular fibrillation (VF) is the most common electrical sequence of events in SCD. In those without underlying CAD or NICM, polymorphic VT or torsade de pointes (TdP), caused by genetic or acquired cardiac abnormalities such as channelopathies, may be the initiating fatal arrhythmia. [32]

The largest series of deaths occurring during continuous ECG recording was reported in 1989, and included data from 9 case series of ambulant patients (i.e. not suffering an acute MI or in the end stages of disease).[33] In these 157 patients experiencing SCD, 62% of patients had VT/VF, 8% had primary VF, 13% had polymorphic VT or TdP and 17% had bradycardia.

Patients in the end stages of HF have a different distribution of arrhythmias.[34] One series reporting on 216 patients, stabilized in hospital for advanced HF, demonstrated that of 20 sudden deaths, 62% of patients had severe bradycardia or pulseless electrical activity, and that 38% had VT/VF.[35]

Even in the normal heart myocardial cells exhibit different action potential characteristics, refractoriness, and conduction velocities that lead to electrical heterogeneity. This heterogeneity can become extreme under circumstances such as acute ischaemia, regional sympathetic dysfunction or unequal stretch, leading to conditions in which VF can develop.[31] Electrical re-entry forms the basis of the majority of VT and VF, resulting from dispersion of repolarisation and heterogeneity. The anatomical substrate for these events is myocardial scar, and it is the border zone between healthy and scarred tissue with islands of viable myocardium that creates this (further discussion in 1.10). In the majority of cases scar is associated with healed MI, but similar mechanisms arise in surgery, hypertrophy, myocarditis or fibrosis. Monomorphic VT is a result of a single re-entrant circuit with a single exit site whereas polymorphic VT has more complex circuits and is dependent on long-short conduction sequences, long QT intervals and early after-depolarisations. Transition from organized VT to VF, or development of primary VF, is usually from simultaneous ventricular activation by multiple localized areas of micro-re-entry circuits. [36]

1.3 Implantable Cardioverter Defibrillator Therapy

In its simplest form, an ICD is system consisting of a power source and programmable computer circuitry, inside an implantable canister, connected to electrodes, generally sited within the venous system and cardiac chambers, capable of sensing life threatening ventricular arrhythmias. Following successful detection, ICD therapy involves delivering energy between the electrodes and active canister. When required, a capacitor in the device accumulates charge from the battery and which in turn enables the rapid discharge of energy required for successful defibrillation. In the face of electrical heterogeneity and re-entry circuits, this shock depolarizes the critical mass of the heart muscle with the aim restoring a normal heart rhythm.

Modern devices also function as a pacemaker generator and can deliver low energy pacing for bradycardia, and rapid pacing (anti-tachycardia pacing, ATP) to achieve cardioversion without delivering a shock.

The clinical utility of the ICD in humans was first demonstrated in 1980[37], at a time when the epidemiology of SCD, discussed in the previous sections, was just becoming understood. Throughout the decade, the technology was refined from a non-programmable, committed defibrillator, to a programmable ICD capable of sensing slower VT in addition to VF.[38] At the same time, lead technology evolved from an apical cup, to epicardial patch, until finally bipolar defibrillation between two intracardiac coils was possible. This enabled the implant procedure to move from an open chest thoracotomy of several hours to transvenous procedure performed under conscious sedation. The very first patients were SCD survivors experiencing recurrent VF, remote from MI. The developments in technology enabled the treatment to be considered in those too sick to undergo major surgery or indeed patients who were considered at risk of SCD but had not suffered a life-threatening episode. However, in this early era, the cost efficacy of ICD therapy was difficult to prove. Device interrogation was very limited, and even where information about shock delivery was available, it was not possible to adjudicate whether it had been life saving. In addition, mechanical or electrical failure, infection, and surgical complications varied considerably.[3839] Nonetheless, ICD use became accepted treatment for survivors of SCD (known as secondary prevention) with strong advocates for its use as first line treatment in these patients. It was only in the early 1990s that clinical trial evidence was emerging to support this.

1.4 Randomised trials of ICD therapy

1.4.1 Secondary prevention

The Antiarrhythmics versus Implantable Defibrillators (AVID) trial was the first and largest randomized trial of ICDs for secondary prevention.[40] 1016 patients with resuscitated VF or symptomatic VT and LVEF<40% were assigned to ICD (93% transvenous) or antiarrhythmic drug treatment (96% amiodarone). At 3 years follow-up, mortality was reduced by 29% in patients with defibrillators implanted. Further analysis suggested that the improved survival in the ICD group was limited to those with LVEF<35%.[41]

The Canadian Implantable Defibrillator Study (CIDS) compared ICD with amiodarone in 659 survivors of SCD or haemodynamically unstable VT. ICD implantation resulted in a

non-significant reduction in all cause mortality (p=0.14) and arrhythmic mortality (p=0.09) over 5 years.[42] Significant ICD benefit was seen in the highest risk quartile composed of older patients with LVEF<35% or class III HF.[43]

The Cardiac Arrest Study Hamburg (CASH) included 288 cardiac arrest survivors, but unlike CIDS and AVID did not include haemodynamically significant VT. There was a 23% fall in all-cause mortality with ICD treatment compared with a group taking amiodarone or metoprolol.[44] This failed to reach significance (p=0.08) but could be explained by observing that the mean LVEF was higher than AVID, and around 10% of participants did not have structural heart disease. Notably, over half the CASH ICD group received epicardial lead systems requiring a thoracotomy, leading to a higher post-operative mortality than contemporary practice.

These apparent differences in efficacy were addressed in a meta-analysis of the three trials.[45] It showed a significant reduction in death from any cause with the ICD with a hazard ratio (HR) of 0.72 (95% confidence interval (CI) 0.60-0.87, P=0006) and reduction in arrhythmic death (HR 0.50, 95% CI 0.37-0.67, P<0.0001). Patients with LVEF≤35% derived more benefit from ICD therapy than those with better LV function (P=0.011). It is important to note that overall survival was only extended by a mean of 4.4 months at 3 years. Beyond this the curves for all-cause mortality did not diverge, whereas a reduction in arrhythmic death continued to steadily diverge, suggesting that competing death from non-arrhythmic causes may reduce the benefit of the ICD. This introduces a key question of this thesis: how can ICD therapy be targeted more effectively?

1.4.2 Primary prevention of SCD

Several studies have assessed the efficacy of ICD therapy for the prevention of SCD in high-risk populations (primary prevention). Broadly, these trials were conducted in populations classified according to underlying anatomical substrate.

1.4.2.1 Primary prevention of SCD in ischaemic heart disease

The **CABG-Patch** trial recruited 900 patients scheduled for elective coronary bypass surgery with LVEF≤35% and abnormal signal-averaged ECG (see 1.8.4 for further details), and randomized them to ICD (all epicardial systems) or no treatment.[46] Over a mean 32 month follow-up there was no difference in overall or cardiac mortality. Secondary analysis showed that the ICD did reduce arrhythmic death, offset by an increase in non-arrhythmic death.

The Multicenter Automatic Defibrillator Implantation Trial (**MADIT**) included patients with LVEF<35% and recent MI, screened with programmed electrical stimulation (PES)

(see also 1.7).[47] Patients with inducible VT or VF were enrolled in the study if inducibility could not be suppressed by procainamide. 196 patients were randomized to ICD or "conventional" therapy, decided at the discretion of the investigator (80% amiodarone). The trial was terminated prematurely when about 75% of planned enrolment had occurred, because of marked benefit derived from ICD treatment in all cause mortality (HR 0.46, 95% CI 0.26-0.82, P=0.009).

The Multicenter Unsustained Tachycardia Trial (**MUSTT**) was a randomized trial of electrophysiologically guided antiarrhythmic therapy in patients with CAD, LVEF≤40% and asymptomatic, non-sustained ventricular tachycardia (NSVT).[48] The complex study design involved all 2202 patients undergoing PES. The 35% with inducible VT were then randomized to conservative management or EP guided treatment. Those in whom a first line antiarrhythmic failed to prevent VT induction were further randomized to ICD therapy or another agent, until all patients received an effective drug, or ICD. At 5 years cardiac arrest or death from arrhythmia was less frequent amongst patients who received ICDs (9%) compared to inducible patients receiving antiarrhythmics (34%) or those conservative management (32%) (P<0.001).

The **MADIT II** included patients with LVEF ≤30% but without evidence of sustained VT/VF.[49] Patients were excluded if experiencing MI within 1 month or CABG or coronary angioplasty with 2 months. 1232 patients were randomized to ICD (742) or conventional therapy (490). Over a mean follow up of 20 months the mortality rates were 19.8% in the conventional therapy group and 14.2% in the defibrillator group (HR 0.69, 95% CI 0.51-0.93).

The Defibrillator in Acute Myocardial Infarction Trial was a randomized study of ICD versus standard care in patients recruited 6-40 days following acute MI.[50] Inclusion criteria were LVEF <35% and depressed heart rate variability (a marker of autonomic function). There was no difference in the primary outcome of overall mortality between the two groups: an increase in non-arrhythmic death offset any reduction in arrhythmic death.

1.4.2.2 Primary prevention of SCD in NICM

In the Cardiomyopathy Trial, patients with recent onset dilated cardiomyopathy (DCM) and LVEF≤30% were randomised to ICD or standard therapy. The trial was terminated early due to the low all-cause mortality in the control group at one year. Cumulative survival was not significantly different between the two groups out to 4 years. This highlights the different disease process of this population where prognosis is varied and spontaneous recovery of LVEF possible.

The Amiodarone Versus Implantable Cardioverter Defibrillator Randomized Trial (**AMIOVIRT**) randomized 103 patients with NICM, LVEF<35% and asymptomatic VT to receive either amiodarone or ICD.[51] This study was also stopped early when it was clear that survival in both groups was not statistically different.

In the Defibrillators in Non-Ischaemic Cardiomyopathy Treatment Evaluation (**DEFINITE**) study, 458 patients with NICM, LVEF ≤35% and NSVT or ventricular ectopy, were randomized to receive ICD plus medical therapy, or medical therapy alone. During a mean follow up of 29±14.4 months, there was no significant difference in overall mortality, but there was a reduction sudden arrhythmic deaths in the ICD group (HR 0.20, 95% CI 0.06-0.71, P=0.006).

1.4.2.3 Primary prevention of SCD in heart failure of any cause

The Sudden Cardiac Death in Heart Failure Trial (SCD-HeFT) included patients with NYHA class II or III HF and a LVEF ≤35%. The aetiology of the HF was CAD in 52% and NICM in 48% (making it the largest randomized trial of NICM). In total 2521 patients were randomly assigned to conventional therapy plus placebo, conventional therapy plus amiodarone, or conventional therapy plus ICD. The primary end point was death from any cause. During a median follow up of 45.5 months the risk of death on amiodarone was similar to placebo (P=0.53), whilst ICD therapy was associated with a decreased risk of death (HR 0.77, 97.5% CI 0.62-0.96, P=0.007). There was an absolute decrease in mortality at 5 years of 7.2%, regardless of aetiology. The reduction in mortality with ICD therapy was greatest amongst NYHA class II but was not seen in NYHA class III.

1.4.2.4 Meta-analysis of primary prevention ICD trials

The benefits of primary prevention ICD therapy have been the subject of several meta-analyses, although those including contemporary practice have included results from patients receiving "cardiac resynchronization therapy" which in itself can influence mortality and morbidity.[52532854] Theuns *et al.* performed a pooled analysis of eight trials[55] including 5343 patients (including all discussed above except MUSTT due to the non randomized methodology of selecting ICD recipients) and concluded that ICDs significantly reduced the arrhythmic mortality (relative risk 0.40, 95% CI 0.27-0.67) and all cause mortality (RR 0.73, 95% CI .64-0.82) (Figure 1.1 and Figure 1.2). The benefit of ICD therapy was similar for CAD and NICM and based on inclusion criteria of the trials, seen in those with LVEF ≤35%, more than 40 days post MI and ≥3 months post coronary revascularization.

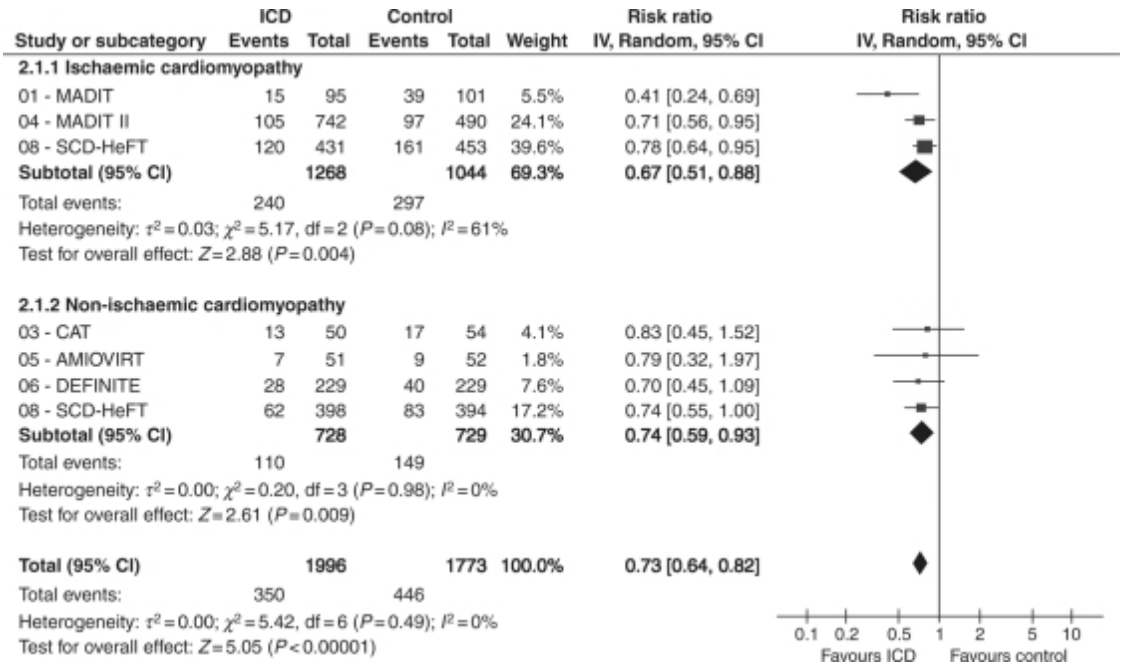

Figure 1.1 All-cause mortality among patients with ischaemic or non-ischaemic heart disease randomized to implantable cardioverter-defibrillator (ICD) vs. conventional therapy in primary prevention. For each randomized trial, the number of deaths (Events) and the number assigned (Total) are shown. The point estimates of the relative risk (RR) for individual studies are represented by squares with 95% confidence intervals (CIs) shown as bars. The midpoint of the diamond represents the overall pooled estimate of the RR, and the 95% CI is represented by the horizontal tips of the diamond. AMIOVIRT, Amiodarone vs. Implantable Defibrillator Randomized Trial; CAT, Cardiomyopathy Trial; DEFINITE, Defibrillators in Non-Ischemic Cardiomyopathy Treatment Evaluation; MADIT, Multicenter Automatic Defibrillator Implantation Trial; SCD-HeFT, Sudden Cardiac Death in Heart Failure Trial. Reproduced from Theuns et al. [55]

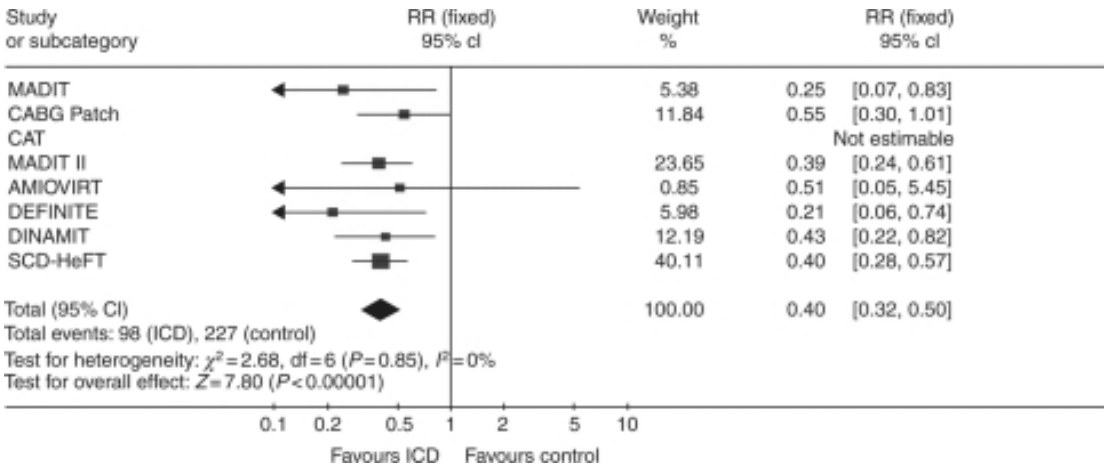

Figure 1.2 Arrhythmic mortality among primary prevention trials. For each randomized trial, the number of deaths (n) *and the number assigned* (N) *are shown. The point estimates of the relative risk (RR) for individual studies are represented by squares with 95% confidence intervals (CIs) shown as bars. The midpoint of the diamond represents the overall pooled estimate of the RR, and the 95% CI is represented by the horizontal tips of the diamond. Reproduced from Theuns et al.* [55]

1.5 Selection of patients for ICD: SCD Risk Stratification

The discussion thus far has established that SCD is a major healthcare problem. Approximately half of deaths related to heart disease are sudden, and the majority of these are due to VT/VF. Around 50% of SCD events are the first manifestation of cardiac disease. Without intervention, survival following cardiac arrest is poor. ICD therapy is effective in reducing the incidence of SCD death due to cardiac arrhythmia. Its use in survivors of cardiac arrest, and in the primary prevention of SCD in those at highest risk is established.

ICD therapy is not without limitations. The technology itself is expensive, with high upfront costs,[56] although cost efficacy has been proven in both North American and European settings.[5758] Inappropriate therapies, device malfunction and system infection are all associated with significant morbidity and mortality.[59] Importantly, ICD use does not eliminate death. Analysis of trial data suggests that SCD may still occur in ICD recipients.[60] Of course, some recipients will go on to die from pump failure, even having received life saving therapy for ventricular arrhythmia (VA), and others still will go on to die from non cardiac causes.

Evaluating these statements must lead to the conclusion that ICD therapy is more effective in some populations than others. “High-risk” individuals must be identified in order to reduce the number presenting with SCD. In addition, there are individuals fulfilling criteria for ICD implantation that never go on to receive life saving therapy. Lastly, there are those in whom ICD therapy is indicated, but risk of non-SCD prevails. Many current recipients of ICD therapy have no potential to benefit from that therapy as they are at low SCD risk but our current approaches to risk stratification do not allow their identification.

1.5.1 Guidelines for the selection of patients for ICD therapy

Current national and international guidance exists for the selection of patients for ICD therapy. [616263] Whilst it is recognized that secondary prevention of SCD is indicated for survivors of cardiac arrest and symptomatic VA regardless of LVEF, recommendations for primary prevention of SCD are based primarily on reduced LVEF, reflecting the primary selection criterion in the trials of ICD therapy. European and North American guidelines recommend ICD implantation in those with prior MI (≥40 days), or NICM, and LVEF ≤35%. Those with HF not meeting these criteria may need further risk stratification based upon symptoms and EP study.[6263]

In England and Wales, the National Institute for Health and Care Excellence (NICE) technology appraisal has recently offered updated guidance. Amongst those with HF,

ICD therapy is recommended for SCD primary prevention based solely upon LVEF ≤35% without symptoms worse than NYHA III.[61] This is in contrast to previous guidance that required further qualification with risk stratifiers such as electrophysiology (EP) testing or ambulatory ECG monitoring.[64]

1.6 Left ventricular systolic ejection fraction

The negative relationship between LVEF and increasing mortality was recognized in early observational studies[65] and this association persists despite contemporary therapies for CAD and HF, and regardless of aetiology.[66] Solomon *et al*. studied 7599 patients enrolled in a trial of the angiotensin II receptor blocker (ARB), Candesartan.[67] Participants had symptomatic HF of varying aetiology. Each 10% reduction in LVEF (below 45%) was independently associated with a significant increase in death due to any cause, including SCD (48% increase in RR).

LVEF is easy to measure, non invasive and reasonably reproducible. Depressed LV systolic function was therefore used for selection in the trials assessing the impact of ICD therapy on SCD, with LVEF ≤40% identifying a high risk group who benefitted from intervention.[46–49,68,69] These primary prevention trials were designed to evaluate the utility of ICD therapy in high-risk groups, defined mainly by LVEF, and not to evaluate different variables, including LVEF, as risk stratifiers. Thus, they show that a reduced LVEF is associated with an increased SCD risk and that ICD therapy improves survival, but do not establish LVEF as the optimal risk stratification variable.

Although LVEF has been shown to identify high-risk patients of both ischaemic and non-ischaemic aetiology in whom ICD therapy confers survival benefit, there remain limitations in its performance as a SCD risk stratification tool.

First, although the ICD reduces risk of death in cardiomyopathy patients, most such patients never experience therapy from their ICD in the form of shock or ATP, and thus the specificity of LVEF to predict SCD is poor. Data from 7 large RCTs was examined in a systematic review of appropriate ICD therapy and SCD.[70] In the 5 trials with inclusion criteria of LVEF≤35%, less than one third experienced appropriate therapy. These findings are consistent with registry data, where around 50% do not receive appropriate ICD therapy.[5871] In an observational study of 2296 French ICD recipients, implanted according to contemporary guidelines, rates of appropriate therapy were around 11 shocks per 100 patient years.[72]

Second, the sensitivity of reduced LVEF to predict SCD is relatively low. In a review of 8 studies using LVEF to predict SCD after MI, mean sensitivity ranged from 22-59%.[73] This

is also seen when LVEF is considered as a SCD risk stratifier in the general population. The Oregon Sudden Unexpected Death Study was an observation of all cases of SCD occurring in Multnomah County, Oregon. Of those 121 cases who had undergone LV evaluation before death, LVEF was ≤35% in only 30%. The majority, therefore, of new SCD cases will not be identified as high risk based on LVEF stratification.

Lastly, the specificity of LVEF for mode of death is poor. Although patients with low LVEF, compared to preserved LVEF, have an increased risk of SCD, risk of non-SCD is also increased.[7475] Therefore, a considerable number will not benefit from ICD therapy due to the competing risk of non-preventable, non-arrhythmic death.

1.7 Electrophysiology studies

Invasive EP assessment through PES can be used to induce arrhythmia. In those with a history of MI and reduced LVEF, [4748] CAD and syncope,[76] cardiac arrest survivors,[404244] or asymptomatic NSVT[77], induction of monomorphic VT is associated with a high risk of future events. However, non inducibility may not confer a benign prognosis: patients in MUSTT and MADIT who were not inducible remained at high risk of SCD.[48,49] In addition, amongst those with NICM, the predictive value of PES is limited.[78,79] Polymorphic VT or VF is often induced, without significant predictive value.

1.8 Electrocardiography

1.8.1 Ambulatory ECG

Complex ventricular ectopy, defined as >10 ventricular premature beats/hour in a 24-hour Holter recording and/or NSVT, was associated with increased mortality in survivors of MI.[6580] However, the positive predictive value (PPV) of an abnormal Holter recording in this patient population is low. In the modern era of CAD treatments there is a declining incidence of post MI arrhythmia, and contemporary evidence suggests that NSVT may only be predictive of SCD in those with preserved LVEF.[75]

The predictive value of NSVT in patients with NICM is also uncertain. In the initial Marburg Cardiomyopathy Study, NSVT was not a significant predictor of arrhythmia risk,[81] although subsequent analysis of patients in the database showed that ≥10beats of NSVT were associated with a higher risk of sustained VT/VF or SCD.

1.8.2 Microvolt T-wave alternans

Microvolt T-wave alternans (MTWA) is defined as a change in T-wave amplitude, width or shape that occurs in alternate beats, detected by digital signal processing (see 1.11). The changes are thought to represent temporal and spatial heterogeneity of dispersion of ventricular repolarisation. Several studies have demonstrated an

association of MTWA and arrhythmic events, but have been limited by small sample sizes and disparate patient populations. A meta-analysis of 19 studies comprising 2608 patients with CAD, NICM and healthy participants, found a PPV of 19.3% and a negative predictive value (NPV) of 97.2%.[82] This study left doubt as to incremental benefit of MTWA compared to other risk stratifiers. A more recent meta-analysis sought to address this, and found that although the technique had a reasonable NPV for predicting VT, MTWA testing does not provide additional SCD risk discrimination in populations already indicated for ICD insertion.[83] The value of MTWA in risk stratification may actually be in deciding which patients are least likely to benefit from ICD insertion. The prospective Alternans Before Cardioverter Defibrillator trial was the first to use MTWA to guide prophylactic ICD insertion in those with LVEF ≤40% and NSVT. MTWA achieved a PPV and NPV similar to PES.[84]

All of these studies report a high level of indeterminate results (up to 50%) due to technical factors such as signal noise, or atrial fibrillation (AF), ventricular ectopy or failure to achieve target heart rate. This is a significant limitation of the technique that may restrict its usefulness. [85]

1.8.3 Measures of cardiac autonomic modulation

The amount of short- and long-term variability in heart rate reflects the vagal and sympathetic function of the autonomic nervous system. Heart rate variability (HRV) can be assessed using various methods by measuring ECG recordings over short (0.5-5 minutes) or longer (24 hour) periods. Time domain methods include the standard deviation (SD) of beat-to-beat R-R interval differences within the recording period. Spectral analysis involves measures of the frequency domain, providing not just variability but also the number of heart rate fluctuations per second.[86]

Reduced HRV has been associated with an increased mortality risk among survivors of acute MI and those with chronic HF.[8788] In a contemporary multicentre study, 1284 patients with a recent MI had HRV measured. During 21 months of follow up, low HRV significantly predicted a high risk of (all cause) cardiac mortality, independent of LVEF.[89] However, in a study where all patients were treated with early percutaneous coronary intervention (PCI), the incidence of significantly depressed HRV, was very low, and consequently the PPV was poor.[90] Nonetheless, in the current era, attenuated HRV measured >6 weeks after acute MI is associated with risk of death or VA, and provides more powerful prognostic information when compared to early measurements.[91] Equally, amongst those with chronic NICM, assessed in DEFINITE, significant differences were seen in mortality rates between those with normal and depressed HRV.

It is likely that HRV is a predictor of both SCD and non-SCD, and therefore its use in determining need for ICD therapy may be limited. The largest observational study found that reduced HRV is a stronger predictor of non-SCD than SCD.[75] However, patients with normal HRV measures, even post MI, are at very low risk of mortality.[92]

Other measures of cardiac autonomic function including *baroreflex sensitivity*, *deceleration capacity of heart rate* and *heart rate turbulence* have all been shown to have association with all-cause or cardiac mortality, although none has been shown to predict SCD.[66]

1.8.4 Signal-averaged ECG

The signal-averaged ECG (SAECG) is a test to identify the presence of ventricular late potentials (VLPs), which represent slowed conduction through a diseased myocardium due to the presence of fibrosis or scar correlating with the substrate for ventricular arrhythmias. VLPs are high frequency, low amplitude signals that have microvolt amplitudes and therefore require high resolution ECG recording for identification. Many studies have looked at the prognostic value of SAECG in post MI patients. Studies completed before the era of early reperfusion consistently reported that an abnormal SAECG in the post-infarction period confers up to an 8-fold increase in risk of an arrhythmic event.[93,94] In the MUSTT study population an abnormal SAECG was a strong predictor of arrhythmic and total cardiac mortality.[95] However, with increasing use of primary PCI, the prognostic value of SAECG has become less clear.[9697] Bauer *et al* performed SAECGs in 968 patients following acute MI, 91% of whom underwent PCI, and found that the presence of VLPs was not significantly associated with cardiac death or a serious arrhythmic event during a median follow-up of 34 months.[97] These results are supported by the outcome of the CABG-Patch trial where patients with abnormal SAECG were randomised to ICD or usual care. ICD implantation conferred no survival benefit, despite a reduction in arrhythmic deaths, suggesting SAECG was not specific for SCD.[46]

The value of SAECG in risk stratifying patients with NICM is less well studied, and the available data are conflicting.[98] Newer methods of SAECG analysis may be of use in overcoming technical limitations, although in the NICM population such methods have predicted total cardiac mortality and non SCD rather than arrhythmia.[99]

1.8.5 QRS duration

QRS duration is a simple measure that reflects intraventricular conduction time. Ventricular scar or fibrosis, the substrate of ventricular arrhythmia, creates increased

dispersion of depolarisation and repolarisation, resulting in prolonged QRS duration. There is an association with cardiac mortality, although QRS duration often increases and LV function decreases, and independent prediction of mortality risk is not clear.[100,101] In addition, it does not seem to be a strong predictor of SCD. In MUSTT, delayed QRS conduction was associated with increased mortality but there was no link with inducible VT.[102] The PainFree RX II trial investigated efficacy of ATP versus shock therapy for VT/VF in 431 CAD patients receiving ICDs. QRS duration did not predict the delivery of appropriate therapy for VT or VF.[103]

Amongst those with NICM the data is sparse, although more consistent. In both the observational studies and the few available published reports from RCTs, QRS duration was not shown to have significant predictive value for selecting patients at increased risk of SCD or total cardiac mortality.[8168104]

1.8.6 QT interval

The QT interval is a measure of slowed or inhomogeneous ventricular repolarisation. The association between prolonged QT interval and increased mortality was first noted amongst patients with acute MI.[105] The link is strongest in patients with the inherited channelopathy, long QT syndrome, itself the subject of considerable research and debate over risk stratification for SCD, and beyond the scope of this thesis.[106]

Large population studies among patients with and without known CAD reported a 2- to 3- fold increase in cardiac mortality risk when QT corrected for heart rate (QTc) was >420 to 440ms.[107-109] However, prospective evaluations of high-risk patients with LV systolic dyfunction did not corroborate these findings, although in some studies a modest PPV was found.[110111] In addition, specificity for SCD after adjustment for other cardiovascular risk factors is poor.[112] These differences might be due to several reasons, including wide overlap in QT interval measurements between subjects with and without events, and difficulties in measuring the QT interval accurately in some leads due to T-U wave abnormalities. QT dispersion (QTD) index is the maximal interlead QT interval variability in a 12 lead ECG and has been proposed as a better estimate of repolarisation inhomogeneity. In the general population abnormal QTD confers increased risk of cardiac and total mortality,[113] although appears not to be an independent predictor in high risk populations with prior MI and HF.[114]

1.8.7 Tpeak to Tend

The interval from the peak of the T wave to the end of the T wave on the 12-lead ECG (Tpeak to Tend interval, TpTe) is another measure of ventricular repolarisation. Ventricular wedge preparation experiments suggested TpTe represents increased

transmural dispersion,[115-117118119] although animal studies using intact hearts,[116,120] and simulation studies[121] have challenged this and suggest that it is a measure of global dispersion of repolarisation. However, it is hypothesised that prolongation of this interval represents a period of potential vulnerability to re-entrant arrhythmias.

The measure has been investigated in 101 patients undergoing primary PCI for acute MI. Haarmark *et al*. found a prolonged TpTe >100ms to be associated with increased all cause mortality over a mean 22 months of follow up,[122] with similar findings found in a larger study of 488 patients by Tatlisu *et al*..[123] In this group, TpTe was also associated with in-hospital VT/VF although long-term arrhythmia or SCD was not explored. However, in 76 patients with prior MI receiving ICD therapy, TpTe was significantly longer in those receiving appropriate ICD therapy for VT/VF than those not. TpTe was an independent predictor of ventricular arrhythmias even after adjustment for age, LVEF and QRS duration (HR 1.16, 95% CI 1.04-1.30, P=0.01).

TpTe in the general population has also been studied. The Oregon Sudden Unexpected Death Study compared 353 SCD cases (where resting ECG was available) to 342 age and gender matched CAD controls and examined the association of TpTe.[124] TpTe was significantly prolonged in SCD cases compared to controls, independent of age, gender, QTc, QRS duration and LVEF.

TpTe was also examined in the Finnish population-based Health 2000 Study.[125] In this work automated ECG analysis was performed to measure TpTe, in addition to other T-wave morphology parameters reflecting repolarisation dispersion. Over 7.7 years, 17% of 307 deaths were sudden. Although these other measures were associated with SCD, TpTe was shorter, rather than prolonged, in those dying of any cause, and not independent of baseline factors, nor associated with SCD.

1.8.8 Early repolarisation

The presence of early repolarisation of the QRS complex is now recognized to have prognostic significance in some individuals and may have a potential role to play in SCD risk prediction.[126] Elevation of the QRS-ST junction (J point) by 0.1mV in at least 2 leads (other than V1 to V3) has been demonstrated to occur in patients with a structurally normal heart resuscitated from VF. Haissaguerre *et al*. found ER more frequently in 206 cases compared to 412 matched controls.[127] Several studies have examined ER in the general population and reported an association with increased risk of cardiac death and SCD, although the prevalence and relative risk was varied.[128129130] It is also likely that the risk varies according to location and pattern of ER; inferolateral ST segment notching confers greater risk than an upsloping QRS-ST segment and it is

possible that baseline changes represent an evolving disease process with risk of death increasing many years after first observation.[131]

However, the significance of these changes in those with structural heart disease and HF is less established. Patel *et al*. analysed the ECGs of CAD patients with an ICD implanted for conventional indications. After adjustment for LVEF, early repolarisation was more common in 60 cases experiencing appropriate ICD therapy for VT/VF than age and sex matched controls (32% versus 8%, P=0.005). They also reported that notching of the J point was the most frequently seen ER change, and that slurring or elevation of the J point was not associated with arrhythmia.

There has also been interesting speculation that the existence of ER changes confers an increase risk of VA in the event of an acute ischaemic event. To answer this question, 432 SCD cases occurring in the context of an acute coronary event were matched to 532 acute coronary event controls who did not experience life threatening arrhythmia.[132] 14.4% of those who died displayed ER changes, compared to 7.9% of survivors (P=0.001), and although the overall prevalence was low, it adds plausibility to this mechanistic link.

1.9 Imaging Studies

The utility of imaging in risk stratification is established primarily as a means of estimating LVEF. Echocardiography, contrast and radionuclide ventriculography, and magnetic resonance imaging (MRI) have all been used in this regard. However, modalities capable of defining new aspects of cardiac function and anatomy are finding a place in routine clinical use.

1.9.1 Radionuclide studies

Single positron emission computed tomography and positron emission tomography are radionuclide techniques able to visualize myocardial scar as fixed perfusion defects. These techniques have been used to demonstrate an association between myocardial scar and cardiovascular mortality during long-term follow-up,[133][134] and prediction of arrhythmic death and VT recurrence.[135]

In addition, autonomic function can be assessed using markers such as metaiodobenzylguanidine (MIBG) that acts as a noradrenaline analogue. This has been used in both CAD and NICM patients as an independent predictor of death in several studies.[136,137] A prospective study in CAD and NICM patients demonstrated MIBG as a predictor of a composite cardiovascular end point, including cardiac death and

arrhythmias.[138] Furthermore, extent of MIBG defect has been correlated with occurrence of appropriate ICD therapies.[139]

1.9.2 Cardiac magnetic resonance imaging

Cardiac magnetic resonance imaging (CMR) with contrast enhancement has the highest spatial resolution for assessment of scar tissue and has further increased the understanding of the pathophysiology of SCD in patients with ischaemic heart disease.[140] Gadolinium (Gd) based contrast agents rapidly diffuse outside the capillaries, but are unable to cross intact cellular membranes. In acutely infarcted tissue, cell membrane breakdown allows the entry of Gd, with a consequent increase in concentration and signal intensity, or "hyperenchancement" on T1-weighted MR images.[141] When imaging chronically infarcted collagenous scar, the increased extracellular matrix traps the contrast, and T1-weighted MRI sequences acquired 10 minutes after intravenous Gd permit detection of scar areas as small as 0.16g.[142] This technique is known as late gadolinium enhancement-cardiac magnetic resonance imaging (LGE-CMR). The extent and characteristics of scar tissue detected by LGE-CMR have been related to increased risk of cardiac death and VA.[140,143,144,145] Furthermore, defining different signal intensity thresholds on LGE-CMR permits differentiation and quantification of the core infarct zone and the peri-infarct or border zone. These areas represent bundles of viable myocardium intermingling with fibrous tissue,[146] the extent of which has been suggested as a powerful predictor of cardiac death and ventricular arrhythmias.[143,144147] However, these studies have been limited by small sample size, and the contribution of core and peri-infarct zone in the prediction of SCD is unclear.

The Defibrillators to Reduce Risk by MRI Evaluation trial was designed to evaluate the efficacy of the ICD in patients with previous MI and an infarct mass >10% of LV mass (by MRI) who were not candidates for an ICD by the current LVEF criteria.[148] The trial was stopped because of poor enrolment but represents a change from established risk strategies for ICD selection.

1.10 The ECG as a marker of scar

The ECG is a biomedical signal reflecting the electrical activation of the heart. In the resting state, myocardial cells are polarized with a positive surface charge, and when activated they become depolarized with a negative surface charge. If a stimulus activating a cell will create a potential electrical difference between adjacent cells, and a current will flow. This current will have a positive "head" and a negative "tail". A unipolar electrode, or positive bipolar electrode, will record a positive or upward deflection when orientated toward the oncoming activation front. Likewise, when the activation front is directed away from the electrode, a negative or downward deflection

is recorded. Since the electromagnetic activation has both magnitude and direction, it can be described as a vector. Electrical activity occurs synchronously in more than one region of the heart, so the ECG recording electrodes reflect the net or resultant force at that point, which may be several synchronous electrical vectors travelling in different directions. The six unipolar precordial electrodes record activity in the horizontal plane, and the limb electrodes record activity in the frontal plane as bipolar limb leads. The resulting 12 leads of a standard ECG reflect the three dimensional activation.

Ventricular depolarisation is reflected on the ECG as the QRS complex. Left ventricular endocardium is activated near the terminations of the left bundle branch slightly before the right ventricular endocardium. Activation of the septum is mainly left to right but does proceed in both directions. The entire endocardium is activated rapidly via the Purkinje network. The middle inferior septum and anterior wall in the area of the insertion of the anterior papillary muscle are the earliest activated. The more thinly walled right ventricle has an earlier epicardial breakthrough than the thicker LV wall. The base and posterior of the heart are the latest areas to be excited.[149] Although the normal QRS will vary, an understanding of typical activation enables detection of atypical features, which may reflect myocardial scar.

Coronary artery occlusion without timely reperfusion leads to myocardial necrosis and ultimately replacement with collagen scar. Necrotic tissue is electrically inert and cannot be activated or depolarized. Full thickness, or *transmural,* scar results in an electrical window in the muscle, and an electrode orientated towards this scar will reflect the electrical activity of the distant healthy tissue beyond.[150] Where this activity is directed away from the electrode, a negative complex will be recorded, and by convention this first negative deflection is named a Q wave. Early experimental work using needle electrodes falsely concluded that only transmural infarction could deform the forces of depolarisation and produce a Q wave.[151] Although these findings were later retracted, the concept of the Q wave as a marker of full thickness infarction persisted for many years. [152][153] It was only later that independent review of pathological data concluded that there was no real association between Q waves and transmural infarction.[154][155][156] Necrotic tissue alters depolarisation by a number of mechanisms including dispersion, slow conduction and localized block.[157] For this reason, an electrode directed toward infarcted tissue can record not just a Q wave but also a reduced amplitude R wave. Many scars are not truly transmural because they have significant viable subepicardial myocardium surviving over their central region. These subendocardial infarcts have an outer border zone of interdigitating collagenous scar and viable electrically active myocardium that determines the local electrical field

generated from an infarcted region. The activation fronts must thread their way through the complex border zone and as these waves approach each other toward the epicardial centre, they tend to cancel out much of the current fields coming from the scar. This local disruption of the activation front accounts for the high frequency splintering and notching of the QRS complex, and low amplitude high frequency late potentials seen beyond the end of the QRS, both discussed later.[158]

In the contemporary era, advanced imaging techniques have become the gold standard in diagnosing myocardial scar. Although echocardiography, nuclear scintigraphy and positron emission tomography have limited accuracy in subendocardial infarcts, LGE-CMR has high spatial resolution that can detect acute and chronic myocardial infarction in humans.[159][160] These techniques have looked again at the association between ECG changes and MI. A study performed in Chicago looked at the ability of Gd contrast to detect healed MI in a group of 82 participants with known recent myocardial infarct, NICM or healthy myocardium.[142] Delayed hyperenhancement accurately detected chronic infarction. Less than half those with Q waves had full thickness, transmural scar. Moon *et al* looked again at this question through the use of LGE-CMR.[161] Amongst 100 patients with previous MI, Q waves were predictive of larger infarction, rather than transmural extent. Almost all patients with transmural infarction had at least one non-transmural segment, regardless of presence of Q waves.

1.10.1 Fragmented QRS

These observations have prompted comparison of Q wave with other ECG changes thought to be due to infarction. Conduction delay due to local disruption of activation can be seen as fragmentation of QRS complexes on the 12 lead ECG.[162] Das *et al*. found by chance observation that conduction delay leading to an RSR' pattern was associated with regional wall motion abnormalities (RWMA) assessed by left ventriculography.[163] This ECG finding was formally assessed in patients referred for cardiac stress testing by nuclear perfusion analysis.[164] Fragmented QRS (fQRS) was defined by the presence of an additional R wave (R') or notching in the nadir of the S wave, or the presence of >1 R' in 2 contiguous leads, corresponding to a major coronary artery territory (Figure 1.3). Typical bundle branch block (BBB) with a QRS≥120ms was excluded. 479 patients were included in the final analysis. In the prediction of myocardial scar, presence of fQRS was more sensitive than a Q wave (85.6% v 36.3%), although Q wave presence was a more specific sign than fQRS (99.2% v 89%). NPV was 87.6% compared to 70.0% for Q wave presence.

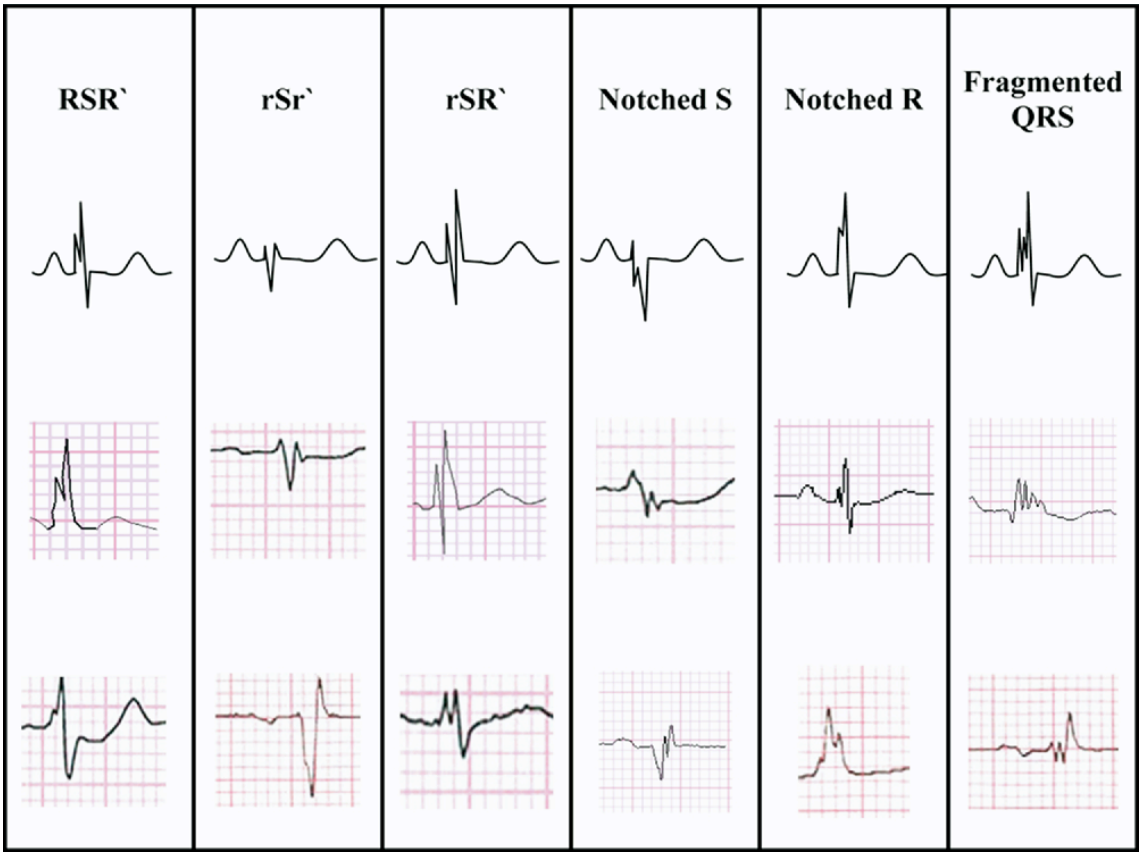

Figure 1.3 Different morphologies of fractionated QRS (fQRS) on a 12-lead ECG according to Das et al.[164]

The group then went on to look at 998 patients referred for nuclear investigation of CAD.[165] This larger study did not specifically report scar, but did find that those with fQRS were more likely to have reversible or non reversible perfusion defects. With a mean follow up of 57±23 months all cause mortality was higher in the 273 patients with fQRS compared to those without, although Kaplan-Meier analysis revealed no significant difference between the fQRS group and Q waves for cardiac events or mortality, nor was fQRS an independent predictor of mortality.

Das *et al*. again looked at the utility of fQRS, but included patients with broad QRS.[166] In the presence of QRS duration ≥120ms, fragmentation was defined as >2 notches of the R wave or S wave. Similar criteria were used whether the wide QRS was due to typical BBB, premature ventricular contraction (PVC) or ventricular pacing. In this study, scar was not just defined as fixed perfusion defect on nuclear perfusion imaging, but also RWMA associated with coronary occlusion. The final analysis included 879 patients with approximately a third each having BBB, PVC or ventricular pacing. Q wave analysis was not performed. Sensitivity was 86.8% and specificity was 92.5% with a NPV of 87.5%. Results were similar across the different groups. In this study, an analysis of survival over 29±18 months revealed a significantly higher mortality in the wide fQRS

group compared to those without fQRS, independent of other variables including age and LVEF.

In patients with CAD, fQRS is thought to be present due to myocardial scar. The studies discussed above take a varied approach in defining myocardial scar and it is not known whether an increase in cardiac events and mortality is due to an association with scar, or whether fQRS itself is an independent predictor of risk. Within this framework, it is important to identify SCD risk, which may be preventable with ICD therapy, as opposed to non-modifiable mortality or morbidity risk. The reported association between fQRS and cardiovascular events is in part driven by infarction and revascularization, and it is possible that fQRS is not associated with SCD risk itself. However, the authors speculate that the non significant mortality difference might be because of higher rates of revascularization and ICD use in the fQRS group.[165] This was further investigated in a study of 125 patients with ischaemic cardiomyopathy and primary prevention ICD implant. fQRS was a stronger predictor of appropriate ICD therapy over the 14±6 months follow up than Q wave, QRS duration, BBB or LVEF, and was associated with a significantly decreased arrhythmia free survival compared to non fQRS patients (p=0.001).[167] The same investigators also looked at the association of SCD and fQRS in 105 patients with non ischaemic cardiomyopathy receiving primary or secondary prevention ICD implant.[168] fQRS was present in 54 patients and was associated with a decreased event free survival and an increased risk of appropriate ICD therapy. A separate group retrospectively evaluated primary prevention ICD recipients. Of 394 patients, event free survival was similar between those with and without fQRS.[169]

The use of fQRS to predict appropriate ICD therapy in the MADIT II population has been retrospectively investigated.[170] MADIT II enrolled 1232 patients ≥21 years of age, with prior history of MI one month or more before, and an LVEF of ≤30%.[49] Patients were randomized to ICD plus conventional therapy or conventional therapy alone. 1040 patients had ECGs suitable for fQRS analysis and were followed up over a mean 20 months looking for the occurrence of SCD or appropriate ICD therapy. Overall 32.6% of all patients had fQRS, with most seen in the inferior leads. As a group overall, fQRS patients had lower LVEF and more diabetes. Presence of fQRS was associated with a 38% increase in SCD or appropriate ICD therapy (p=0.041), but no significant increase in SCD alone, or all cause mortality. The results were driven by a strong association between SCD and inferior fQRS in patients with left bundle branch block (LBBB), with less significant hazard associated with fQRS in other ECG territories.

This study leaves a number of unanswered questions. Although the whole population studied had previous MI, the presence of fQRS was only around one third. Surgical or percutaneous revascularization was performed in half these study patients, and this will have reduced scar formation. No CMR or other scar imaging was available from this study, but the investigators found no association between location of fQRS and Q waves. Notwithstanding the previous discussions about Q wave sensitivity, it would appear that presence of fQRS is not due to previous infarction. It is also unclear why risk of SCD or appropriate ICD therapy was so much worse in those with LBBB and inferior fQRS. The authors postulate that LBBB may mask anterior and lateral fQRS changes.

These observations are interesting in highlighting that this ECG marker of risk may be shared between disease groups that may not share a similar mechanism or distribution of scar. Indeed, there is also evidence that amongst individuals with Brugada syndrome, survivors of VF have a higher incidence of fQRS compared to syncope or asymptomatic groups.[171]

The value of fQRS as a prognostic tool for arrhythmic death is therefore unclear. Whether or the not any risk is conveyed due to an association with myocardial scar, the results of these studies leave doubt as to whether fQRS might be an effective risk stratification tool for SCD.

1.10.2 Selvester QRS scoring

The Selvester QRS score was first described in 1970s, borne from early computer simulations of ventricular excitation.[172] A 53-criteria/32 point scoring system was developed, tested and reported using a learning set of 100 biplane ventriculograms from patients with angiographically proven CAD. A refined and slightly simplified version of the score was evaluated in post mortem studies [173–175] and subsequently validated in clinical practice.[176]

The original scoring system was found to be poorly calibrated in younger males, due to increased voltages common in this age group, and older females due to lower voltages commonly seen. The original validation studies had shown the score to perform best in those aged 40-50 in whom the criteria were originally established.[177] The score was also limited to those ECGs free of conduction defects, such as BBB.

It was only more recently that QRS scoring received renewed interest. Several studies exploited improvements in LGE-CMR, comparing in vivo scar quantification with QRS scoring. Engblom *et al*. examined the ECGs of 25 patients with chronic LV scar due to

anterior MI, and found significant, but only moderate correlation between QRS score and LGE-CMR (r=0.40).[178] The group also studied 29 patients with first time reperfused MI. LGE-CMR scar and QRS score (performed a week after infarction) were well correlated (r=0.79).[179] Bang *et al*. looked at how performance of QRS scoring changed moving from the acute to chronic phase after MI.[180] In 31 patients, correlation between ECG and CMR scar was significant only at baseline and at 6 months, but not at 1 month. The strength of correlation was weak (r=0.39) at baseline but improved at 6 months (r=0.43). Geerse similarly looked at how QRS scoring changed between <1 week and >2 months following acute MI.[181] In this study of 13 patients, correlation between LGE-CMR and QRS score infarct size was moderate at baseline (r=0.59) and remained so at follow up (r=0.54). Weir also looked at a similar cohort, concentrating just on 34 patients with anterior infarction.[182] Correlation between QRS score and LGE-CMR scar was moderate at baseline (r=0.56) and improved at 24 weeks (r=0.78).

It is important to recognise that these studies all excluded patients with ECG confounders. More recently, a new QRS score was published, now including adjustments for dealing with age and gender, in addition to criteria for awarding points in the presence of ECG confounders (Figure 1.4).[183] This was evaluated in 162 patients with LVEF ≤35% due to ischaemic and non ischaemic causes.[184] Overall correlation between QRS score and LGE-CMR was strong (r=0.74). Of perhaps greater significance, the study also found an association between increasing QRS score and arrhythmogenesis, in the form of VT induction. Whilst there are clear limitations with VT induction as a surrogate for SCD (see 1.7), an ECG marker of myocardial scar as a risk stratifier is attractive. The same group investigated the association between QRS score and VT/VF in the SCD-HeFT trial.[185] Whilst the 797 patients included in this study had no “gold-standard” LGE-CMR scar imaging, the absence of QRS scar points identified a low risk group experiencing fewer events (HR 0.52, 95% CI 0.31-0.88).

The Selvester QRS score as a marker of myocardial scar clearly has some value. However, the accuracy of scar quantification through this tool is not clear. The data are discrepant. These findings might be due to chronicity, location or other physical characteristics of the scar. Even with this in mind, the ability of the QRS score to predict clinical outcomes, or utility as a risk stratifier remains unclear. Furthermore, whether conveyance of risk is due to reflection of myocardial scar, or some other factor, is not clear and warrants further investigation.

1.11 Signal Processing

Physiological processes in the human body are subject to biological, electrical and mechanical control. Such systems may manifest as detectable biomedical signals, and

with understanding of the processes involved, it is possible to observe the signal and interpret information about the performance and disease status of the system. The electrical manifestation of cardiac contractility can be recorded in clinical practice as an ECG.

Paired electrodes form the positive and negative poles of an ECG lead. The standard 12 lead ECG is acquired using 4 limb electrodes and 6 chest electrodes. The frontal plane bipolar leads I, II and III form Einthoven's triangle, and the unipolar augmented limb leads aVR, aVL, aVF, which take a zero potential negative pole. The precordial electrodes record the horizontal plane leads of V1-V6. [150] The standard ECG plots the time varying voltage amplitude acquired in each lead. Typical diagnostic features of the ECG are present in the morphology of the waveform, and changes in the rhythm of the heartbeat, or *periodicity* of the waveform. Both of these are features of the *time domain*. Pattern recognition, and knowledge of the amplitude and duration measurements seen in normal and diseased states, enables the clinician to use the ECG as a diagnostic tool. However, there is further electrophysiological information contained within the recorded signal, and if these features can be manipulated and presented in an accessible manner, further markers of risk may be identified.

QRS Scoring

Patient ID _____ QRS duration _____ Amplitude adjust _____
(↑1%/yr age 20-54; ↓1%/yr >55 yrs; ↓10% for females

Age & gender _____ QRS axis _____ Duration adjust _____ RAO(**, ***)Yes/No
(↓ 10% for females)

Lead	RBBB Criteria	Pts	LAFB Criteria	Pts	LAFB + RBBB Criteria	Pts	LVH Criteria	Pts	No Confounders Criteria	Pts
I	Q ≥ 30 ms	1	Q ≥ 30 ms	1	Q ≥ 30 ms	1	Q ≥ 30 ms	1	Q ≥ 30 ms	1
	R/Q ≤ 1	1	R/Q ≤ 1	1	R/Q ≤ 1	1	R/Q ≤ 1	1	R/Q ≤ 1	1
	R ≤ 0.2 mV		R ≤ 0.2 mV		R ≤ 0.2 mV		R ≤ 0.2 mV		R ≤ 0.2 mV	
II	Q ≥ 40 ms	2	Q ≥ 40 ms	2	Q ≥ 40 ms	2	Q ≥ 40 ms	2	Q ≥ 40 ms	2
	Q ≥ 30 ms	1	Q ≥ 30 ms	1	Q ≥ 30 ms	1	Q ≥ 30 ms	1	Q ≥ 30 ms	1
aVL	Q ≥ 30 ms	1	Q ≥ 40 ms	1	Q ≥ 40 ms	1	Q ≥ 40 ms	1	Q ≥ 30 ms	1
	R/Q ≤ 1	1	R/Q ≤ 1	1	R/Q ≤ 1	1	R/Q ≤ 1	1	R/Q ≤ 1	1
aVF	Q ≥ 50 ms	3	Q ≥ 50 ms	3	Q ≥ 50 ms	3	Q ≥ 60 ms	3	Q ≥ 50 ms	3
	Q ≥ 40 ms	2	Q ≥ 40 ms	2	Q ≥ 40 ms	2	Q ≥ 50 ms	2	Q ≥ 40 ms	2
	Q ≥ 30 ms	1	Q ≥ 30 ms	1	Q ≥ 30 ms	1	Q ≥ 40 ms	1	Q ≥ 30 ms	1
	R/Q ≤ 1	2	R/Q ≤ 1	2	R/Q ≤ 1	2	R/Q ≤ 1	2	R/Q ≤ 1	2
	R/Q ≤ 2	1	R/Q ≤ 2	1	R/Q ≤ 2	1	R/Q ≤ 2	1	R/Q ≤ 2	1
V1 Ant.	Q ≥ 50 ms	2			Q ≥ 50 ms	2	any QR			
	any Q	1	any QR	1	any Q	1	(or any Q if *)	1	any Q	1
	Init R ≤ 20 ms						NtchInit40			
V1 Post.**			R/S ≥ 1	1		1	R/S ≥ 1	1	R/S ≥ 1	1
	Init R ≥ 60 ms	2	R ≥ 50 ms	2	Init R ≥ 60 ms	2	R ≥ 50 ms	2	R ≥ 50 ms	2
	Init R ≥ 1.5 mV		R ≥ 1mV		Init R ≥ 1.5 mV		R ≥ 1mV		R ≥ 1mV	
	Init R ≥ 50 ms	1	R ≥ 40 ms	1	Init R ≥ 50 ms	1	R ≥ 40 ms	1	R ≥ 40 ms	1
	Init R ≥ 1.0 mV		R ≥ 0.7 mV		Init R ≥ 1.0 mV		R ≥ 0.7 mV		R ≥ 0.7 mV	
			Q≤0.2&S≤0.2mV	1			Q≤0.2&S≤0.2 mV	1	Q≤0.2&S≤0.2mV	1
V2 Ant.	Q ≥ 50 ms	2			Q ≥ 50 ms	2				
	any Q	1	any QR	1	any Q	1	any QR	1	any Q	1
	R ≤ 10 ms		R ≤ 10 ms		R ≤ 10 ms		(or any Q if *)		R ≤ 10 ms	
	R ≤ 0.1mV		R ≤ 0.1mV		R ≤ 0.1mV		NtchInit40		R ≤ 0.1mV	
V2 Post.**			R/S ≥ 1.5	1			R/S ≥ 1.5	1	R/S ≥ 1.5	1
	Init R ≥ 70 ms	2	R ≥ 60 ms	2	Init R ≥ 70 ms	2	R ≥ 60 ms	2	R ≥ 60 ms	2
	Init R ≥ 2.5 mV		R ≥ 2 mV		Init R ≥ 2.5 mV		R ≥ 2 mV		R ≥ 2 mV	
	Init R ≥ 50 ms	1	R ≥ 50 ms	1	Init R ≥ 50 ms	1	R ≥ 50 ms	1	R ≥ 50 ms	1
	Init R ≥ 2.0 mV		R ≥ 1.5 mV		Init R ≥ 2.0 mV		R ≥ 1.5 mV		R ≥ 1.5 mV	
			Q≤0.3&S≤0.3mV	1			Q≤0.3&S≤0.3mV	1	Q≤0.3&S≤0.3mV	1
V3	Q ≥ 30 ms	2	Q ≥ 30 ms	2	Q ≥ 30 ms	2	QR& (Q ≥ 30 ms)	2	Q ≥ 30 ms	2
	R ≤ 10 ms		R ≤ 10 ms		R ≤ 10 ms		NtchInit40	1	R ≤ 10 ms	
	Q ≥ 20 ms	1	Q ≥ 20 ms	1	Q ≥ 20 ms	1	any QR		Q ≥ 20 ms	1
	R ≤ 20 ms		R ≤ 20 ms		R ≤ 20 ms		(or any Q if *)		R ≤ 20 ms	
V4	Q ≥ 20 ms	1	Q ≥ 20 ms	1	Q ≥ 20 ms	1	Q ≥ 20 ms	1	Q ≥ 20 ms	1
	R/Q ≤ 0.5	2	R/Q ≤ 0.5	2	R/Q ≤ 0.5	2	R/Q ≤ 0.5	2	R/Q ≤ 0.5	2
	R/S ≤ 0.5		R/S ≤ 0.5		R/S ≤ 0.5		R/S ≤ 0.5		R/S ≤ 0.5	
	R/Q ≤ 1	1	R/Q ≤ 1	1	R/Q ≤ 1	1	R/Q ≤ 1	1	R/Q ≤ 1	1
	R/S ≤ 1		R/S ≤ 1		R/S ≤ 1		R/S ≤ 1		R/S ≤ 1	
	R ≤ 0.5 mV		R ≤ 0.5 mV		R ≤ 0.5 mV		R ≤ 0.5 mV		R ≤ 0.5 mV	
	NtchInit40		NtchInit40		NtchInit40		NtchInit40		NtchInit40	
V5	Q ≥ 30 ms	1	Q ≥ 30 ms	1	Q ≥ 30 ms	1	Q ≥ 30 ms	1	Q ≥ 30 ms	1
	R/Q ≤ 1	2	R/Q ≤ 1	2	R/Q ≤ 1	2	R/Q ≤ 1	2	R/Q ≤ 1	2
	R/S ≤ 1		R/S ≤ 1		R/S ≤ 1		R/S ≤ 1		R/S ≤ 1	
	R/Q ≤ 2	1	R/Q ≤ 2	1	R/Q ≤ 2	1	R/Q ≤ 2	1	R/Q ≤ 2	1
	R/S ≤ 2		R/S ≤ 1.5		R/S ≤ 1.5		R/S ≤ 2		R/S ≤ 2	
	R ≤ 0.6 mV		R ≤ 0.6 mV		R ≤ 0.6 mV		R ≤ 0.6 mV		R ≤ 0.6 mV	
	NtchInit40		NtchInit40		NtchInit40		NtchInit40		NtchInit40	
V6	Q ≥ 30 ms	1	Q ≥ 30 ms	1	Q ≥ 30 ms	1	Q ≥ 30 ms	1	Q ≥ 30 ms	1
	R/Q ≤ 1	2	R/Q ≤ 1	2	R/Q ≤ 1	2	R/Q ≤ 1	2	R/Q ≤ 1	2
	R/S ≤ 1		R/S ≤ 1		R/S ≤ 1		R/S ≤ 1		R/S ≤ 1	
	R/Q ≤ 3	1	R/Q ≤ 3	1	R/Q ≤ 3	1	R/Q ≤ 3	1	R/Q ≤ 3	1
	R/S ≤ 3		R/S ≤ 2		R/S ≤ 2		R/S ≤ 3		R/S ≤ 3	
	R ≤ 0.6 mV		R ≤ 0.6 mV		R ≤ 0.6 mV		R ≤ 0.6 mV		R ≤ 0.6 mV	
	NtchInit40		NtchInit40		NtchInit40		NtchInit40		NtchInit40	
Total	Points		Points		Points		Points		Points	
	%LV Infarct (3 x #pts)	____	% LV Infarct (3 x #pts)	____	%LV Infarct (3 x #pts)	____	% LV Infarct (3 x #pts)	____	% LV Infarct (3 x #pts)	____

Lead	LBBB Criteria	Pts
I	any Q	1
	R/Q ≤ 1	2
	R/S ≤ 1	
	R/Q ≤ 15	1
	R/S ≤ 15	
II	Q ≥ 40 ms	2
	Q ≥ 30 ms	1
	R/Q ≤ 0.5	1
	R/S ≤ 0.5	
aVL	Q ≥ 50 ms	2
	Q ≥ 40 ms	1
	R/S ≤ 0.5	2
	R/Q ≤ 0.5	
	R/S ≤ 1	1
	R/Q ≤ 1	
aVF	Q ≥ 50 ms	2
	Q ≥ 40 ms	1
	R/Q ≤ 0.5	1
	R/S ≤ 0.5	
V1 Ant.***	NchInit40	1
	R ≥ 0.3 mV	2
	R ≥ 30 ms	
	R ≥ 0.2 mV	1
	R ≥ 20 ms	
V1 Post	S/S' ≥ 2.0	3
	S/S' ≥ 1.5	2
	S/S' ≥ 1.25	1
V2 Ant.***	NchInit40	1
	R ≥ 0.4 mV	2
	R ≥ 30 ms	
	R ≥ 0.3 mV	1
	R ≥ 20 ms	
V2 Post	S/S' ≥ 2.5	3
	S/S' ≥ 2.0	2
	S/S' ≥ 1.5	1
V5	any Q	1
	R/R' ≥ 2	2
	R/R' ≥ 1	1
	R/S ≤ 2	
	R ≤ 0.5 mV	1
V6	Q ≥ 20 ms	1
	R/R' ≥ 2	2
	R/R' ≥ 1	1
	R/S ≤ 2	
	R ≤ 0.6 mV	1
Total	Points	

%LV Infarct (3 * #pts) ____

* (for LVH) If ≥4 other points in leads I, aVL, V4, V5 or V6 then count QS in V1-V3

** (RAO) If P positive amp in V1 ≥0.1 mV or aVF *P* ≥ .175 mV, then exclude V1-V2 Post criteria

*** (RAO) If P positive amp in V1 ≥0.1 mV or aVF *P* ≥ .175 mV, then exclude V1-V2 R-criteria points

Figure 1.4 QRS scoring. Points are awarded according to all ECG leads (except III and aVR) with respect to conduction type (columns). In left bundle branch block (LBBB) points are awarded in fewer leads. 1 point estimates 3% LV scar. Where criteria differ between confounder groups, this is highlighted.

1.11.1 The ECG Signal

In its simplest form, the ECG signal can be considered as a waveform formed of a number of sine waves with differing frequencies. When describing a sine wave, such as depicted in Figure 1.5, we consider a number of properties:

The *amplitude*, A, is the peak deviation from zero

The *frequency*, f, is number of oscillations (or cycles) per second

The *wavelength*, λ, the distance over which a wave's shape repeats

The *phase*, ϕ, specifies where in the cycle the oscillation is at t=0

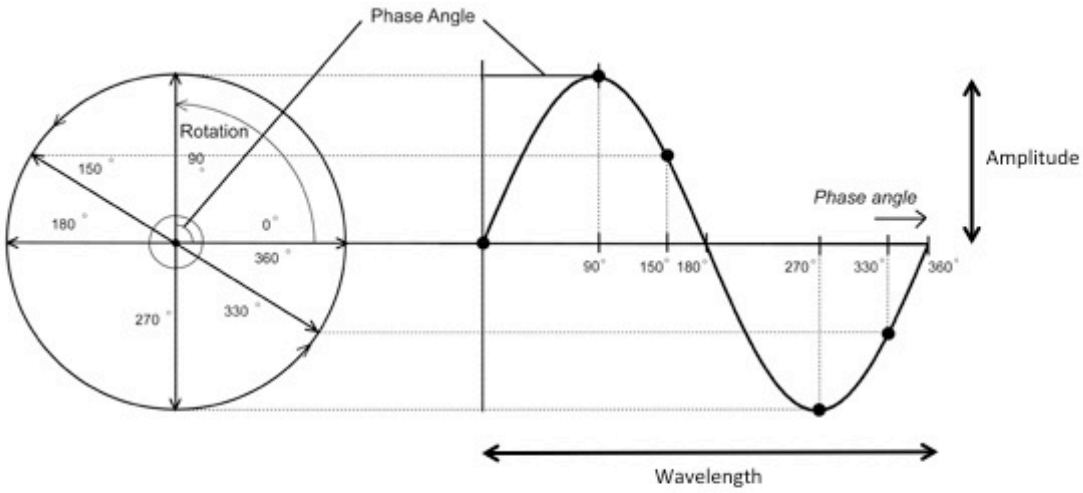

Figure 1.5 Sine wave, generated by plotting the constantly changing angle of rotation against time. One cycle, or wavelength, or the sine wave is depicted.

We can also identify the *fundamental* frequency of a signal as the lowest frequency wave contained within a signal. The *bandwidth* is the difference between the upper and lower frequencies comprising a signal.

The heart rate forms the fundamental frequency of the ECG. A heart rate of 30 beats per minute (bpm) gives us 0.5Hz, although heart rates below 40bpm (0.67Hz) are uncommon. Most diagnostic information in adults contained in the QRS complex is between ≈10Hz and 100Hz, although low amplitude, high frequency components as high as 500Hz have been reported.[186] The lowest frequency of T waves is approximately 1 to 2Hz.[187]

1.11.2 Signal Acquisition

The electrocardiograph is a sophisticated galvanometer, a sensitive electromagnet, which can detect and record changes in electromagnetic potential. Surface silver chloride (AgCl) electrodes act as a transducer, converting ionic conduction into electronic conduction. This is recorded as a continuous signal of varying voltage amplitude. In order that the output be displayed in a standard ECG format, the signal must undergo conditioning. The standard ECG is calibrated such that 1mV will result in a 10mm deflection. The changes in electromagnetic potential are in the range 10μV to 5mV and must be amplified. Pre-processing may also be necessary to remove artefact, or *noise*, that would also otherwise undergo amplification, avoiding unnecessary signal processing later in the analysis and improving the signal to noise ratio (S/N).[188]
Filtering of the analogue signal is achieved with a combination of capacitors, resistors, inductors and operational amplifiers to attenuate signals below (*high-pass* filters) or above (*low-pass* filters) the desired range. The result is a band-pass response allowing just the required *passband* signal to be processed further.[189]

Low-frequency noise is characterised by baseline wander, caused by drift in the range below 0.5Hz, due to movement and respiration. Historically this was addressed by a low frequency cut-off of 0.5Hz, although this resulted in marked distortion of repolarisation producing artifactual ST segment deviation.[190] Thus, recommendations changed to include the now standard 0.05Hz low frequency cut-off that preserves fidelity of repolarisation but does not eliminate baseline drift. These issues are somewhat overcome with newer software filters employed after digital conversion, capable of preserving the ST segment. Where these are used, recent recommendations support a relaxed lower frequency cut-off of up to 0.67Hz.[187]

High frequency noise is most frequently a result of electromagnetic *powerline* interference at 50/60Hz caused by mains electricity. The upper sampling frequency is determined by the need for accuracy in recording rapid upstroke velocities, peak amplitudes and waves of small duration.[191] A high frequency cut-off of at least 150Hz for adult ECGs is recommended.[186] Since powerline interference lies within the passband signal, a notched, narrowband 50 or 60Hz filter is employed.

An exception to these limits concerns pacemaker stimulus outputs that are in general shorter in duration than 0.5ms and would not be detected with the high frequency cut off. In practice, since low-pass filters have an imperfect transition that might result in aliasing (see below), systems tend to *oversample*, at rates of up to 15000 per second, before any signal conditioning is applied. As a consequence, a circuit can detect and

separate out pacing spikes, send information about pacemaker timing to the system microprocessor and insert artificial pacing spikes on the displayed ECG.[192]

1.11.3 Analogue to Digital Conversion

The ECG is analogue, a *continuous* signal whose voltage amplitude varies over time and is constantly fluctuating. This analogue signal must be digitally sampled to enable computer analysis, or *digital signal processing* (DSP) to be undertaken. DSP encompasses the mathematic techniques and algorithms used to manipulate, and analyse, these signals. [193] A digital signal is produced by an analogue to digital converter (ADC) and is formed of discrete values, determined by *sampling* and *quantization* (Figure 1.6). In the case of the ECG, where the independent variable is time, the sampling rate determines the number of values per second. The voltage amplitude is the dependent variable, whose continuous signal is converted to discrete values by quantization. The number of possible values is determined by the resolution of the ADC. The resolution is expressed in binary form as *bits*. A 12 bit ADC can convert a continuous signal into 2^{12}=4096 discrete values, or levels. The rounding error between the true value and the output digitized value results in *noise* known as quantization error, and the number of bits determines the precision of the data.

1.11.4 Sampling Theorem

An analogue signal, if properly sampled, can be reconstructed from the digital signal. The Nyquist-Shannon sampling theorem indicates that faithful reconstruction is only possible if the sampling rate is higher than twice the highest frequency of the signal.[194][195] Figure 1.7 demonstrates various analogue signals represented as continuous lines and digital samples represented as square markers. Figure 1.7b represents a sine wave with a frequency of 90Hz being sampled at 1000Hz. The wave has a frequency 0.09 of the sampling rate. There are 11.1 samples taken over each complete cycle and the analogue wave can be exactly reconstructed from these series of digital points. Likewise, Figure 1.7c is a wave with a frequency 310Hz which is 0.31 of the sampling rate (1000Hz), and the analogue wave is uniquely represented by the digital samples. However, Figure 1.7d represents a wave with a frequency of 950Hz, sampled at 1000Hz, that gives rise to only 1.05 samples per cycle. In this case however, the analogue signal cannot be reconstructed from the points since the digital signal is misrepresented as a sine wave of 50Hz. This is an example of improper sampling since it was not twice the highest frequency of the signal, the so-called *Nyquist* rate. Such a situation leads to *aliasing* whereby frequencies above the Nyquist rate are incorrectly detected as lower frequencies.

At a simple level, DSP techniques are based on the principle of *superposition*. [196] The signal being processed is broken down into simple components, and each component analysed individually. The resulting signal can then be reformed. The techniques used to separate out the signal components are known as transformations. One such example is the Fourier transform, based on decomposing the signal into sinusoids. The goal of such decomposition is to present the complex signal in a simple form. The resulting waves can then be subject to mathematical analysis not possible with the raw signal.

As discussed, the ECG is a widely available tool in clinical practice. Although there is some published data to support the utility of an ECG score in detecting myocardial scar, the evidence for its widespread use is lacking. Furthermore, the ECG is scored on time domain features, and no studies to date have looked at ECG signal processing techniques to detect, quantify or categorise myocardial scar.[197]

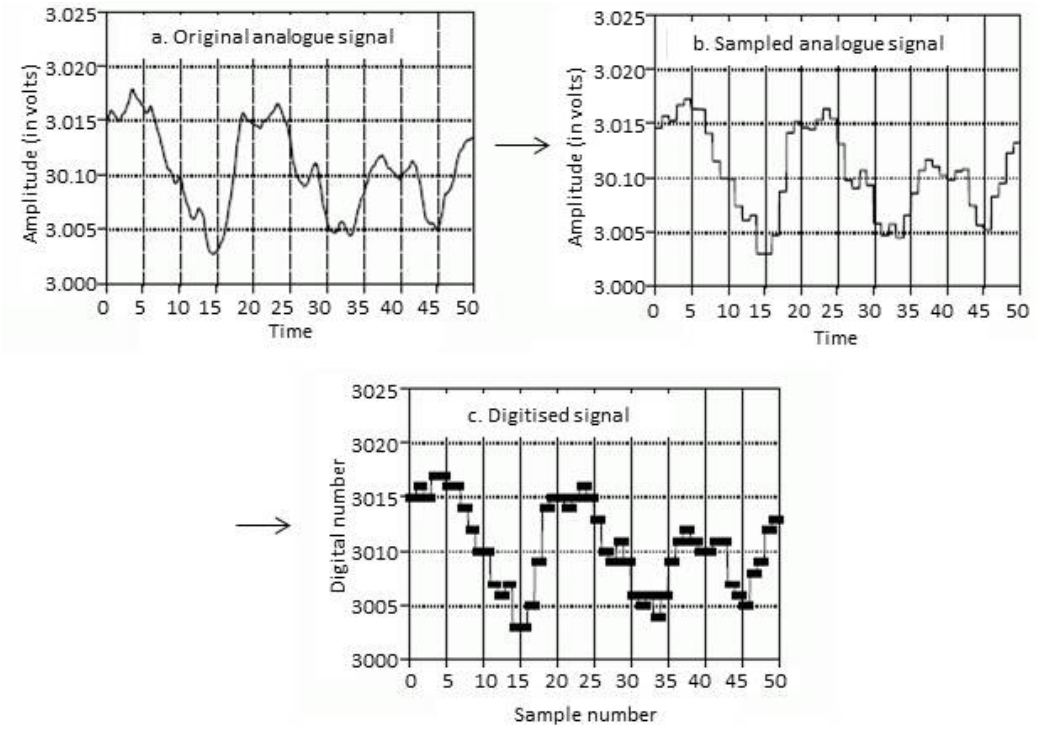

Figure 1.6 Digitisation of the analogue wave, sampled with a 12 bit analogue to digital converter. Adapted from Smith, SW.[196]

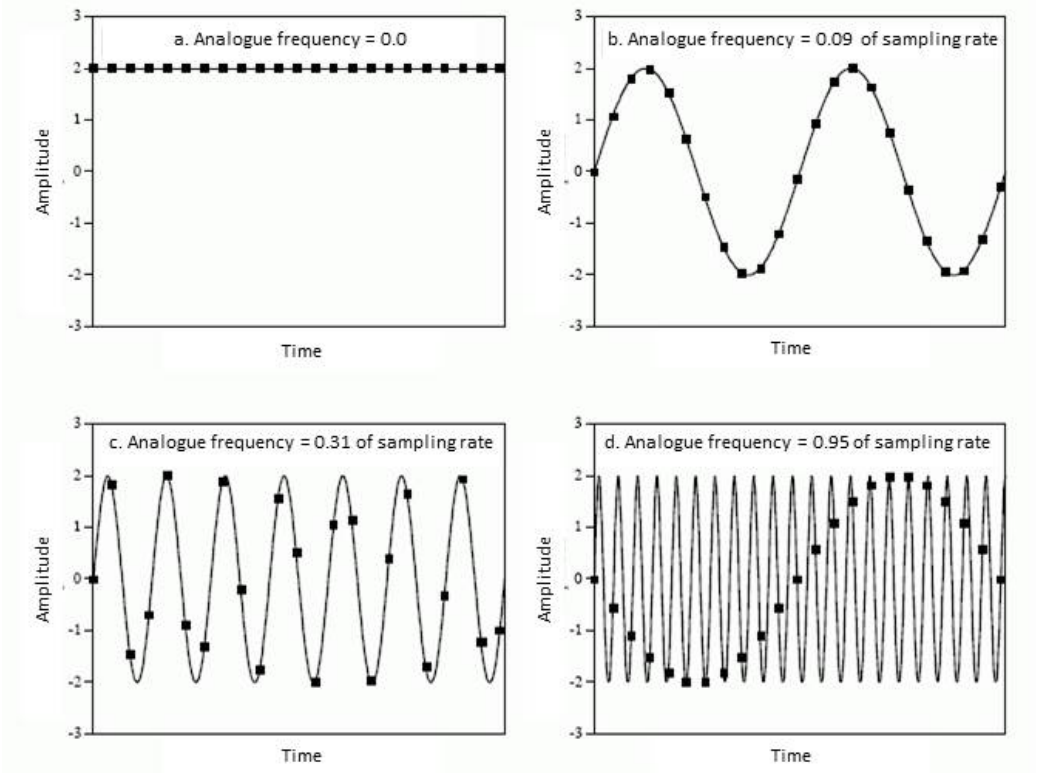

Figure 1.7 Illustration of proper and improper sampling. Figures (a), (b), and (c) illustrate proper sampling, since the sampling frequency is less than the Nyquist frequency. This results in a unique digital waveform that can be faithful reconstructed. Figure (d) demonstrates undersampling, resulting in aliasing, and consequently the continuous signal cannot be reconstructed. Adapted from Smith.[196]

1.12 Machine learning

1.12.1 Overview

Machine learning (ML) is a form of artificial intelligence using computer algorithms to make sense of large data sets. By identifying patterns in digital information, the "machine" can refine its model through processing new data. The resulting algorithm seeks to forecast a future outcome based upon what it has "learnt".[198] Classification of previously unseen data is used to predict the behaviour of one or more random variables.[199] ML methods are numerous, and can be broadly divided into *supervised* or *unsupervised* learning methods. Supervised learning relies on a set of training examples, where each input is paired with a desired output. The ML algorithm analyses the training data and produces a *function* that can be used for mapping new examples. Unsupervised learning is based on *data mining* methods such as *clustering* that seek to categorise objects based on similarity to other objects in a group.

Machine learning approaches are used in everyday life from finance to retail. "Big data" from loyalty cards, credit ratings, internet browsing and purchase history is used to refine targeted advertising. Facial recognition in photography is enabled by machine learning of the patterns that describe the faces of our human subjects, refined by past successes or failures.

Within medicine, computing has been used for many years to store, categorise and process data.[200][201] The use of digital systems for biomedical signals has seen an explosion in data in a format that is readily processed, but more importantly is beyond the capability of any clinician to process in real time, or indeed exploit to its full potential. Where traditional statistical modelling explores the relationship of independent predictor variable X and dependent variable Y, machine learning has no specific requirement for a specific hypothesis. Instead, the primary hypothesis is that there is a pattern in the predictor variables that will identify the outcome. This drives unbiased research about predictor variables that might otherwise be overlooked.[198]

Whilst not new, ML has benefited from advances in computational power and numerical algorithms.[199] Traditional techniques in the 1980s and 1990s were based on *frequentist* statistics, inferring conclusions due to the frequency or proportion of data, based upon high probabilities of known variables. In contrast, *Bayesian* inference allows probabilities to be associated with unknown parameters.

Despite the potential benefits of ML, mainstream acceptance of the techniques into point of care medicine is limited. There are several potential reasons for this. First, the expertise required to design, code and validate a machine learning approach is vastly different from that learnt by physicians at medical school and beyond. Computer scientists and biomedical engineers are experts in these fields, generating research using simulated data and archived biomedical signals, with mathematical proof used as validation for the work. If the software itself is not publically shared, the reproducibility of such approaches cannot be assessed.[202] The human condition is not binary, and appraisal of the research should reflect this and use tools familiar to clinical research.

Second, outside of specialist academic and commercial institutions, there is little in the way of collaboration between engineers and practicing clinicians.[203] This lack of dialogue may limit the potential that technology can deliver in medicine, in particular how ML can address the everyday needs of doctors. In addition, if the engineer fails to appreciate the subtleties of everyday diagnostics, engineered solutions may become too rigid in their outcomes.

Third, ML research is not frequently published in the medical literature. Hypothesis free research and lack of a specific aim may mean editors are less likely to find merit in such work.[198] In addition, the machine algorithm could be considered a *black box*, where the input and output is understood, but the complex internal workings are opaque, and appraisal by journal reviewers may not be possible. Commercially sensitive algorithms are not shared, being withheld from the public domain.

Since the 1980s, the number of ML articles indexed on MEDLINE per year has increased to nearly 5000. Over the same period, those published in core clinical journals has only risen to 200 per year (Figure 1.8).[204] Applications are varied and widespread, from bioinformatics to robotics. Indeed, much of the mass spectrometry output used in the experimental work in Chapter 8 is generated with commercial software utilizing ML methods such as hierarchical clustering. The novel work I describe in Chapter 7 features a custom support vector machine (SVM) used in the classification of ECGs. Therefore, for the remainder of this section I shall focus on the techniques relevant to this work.

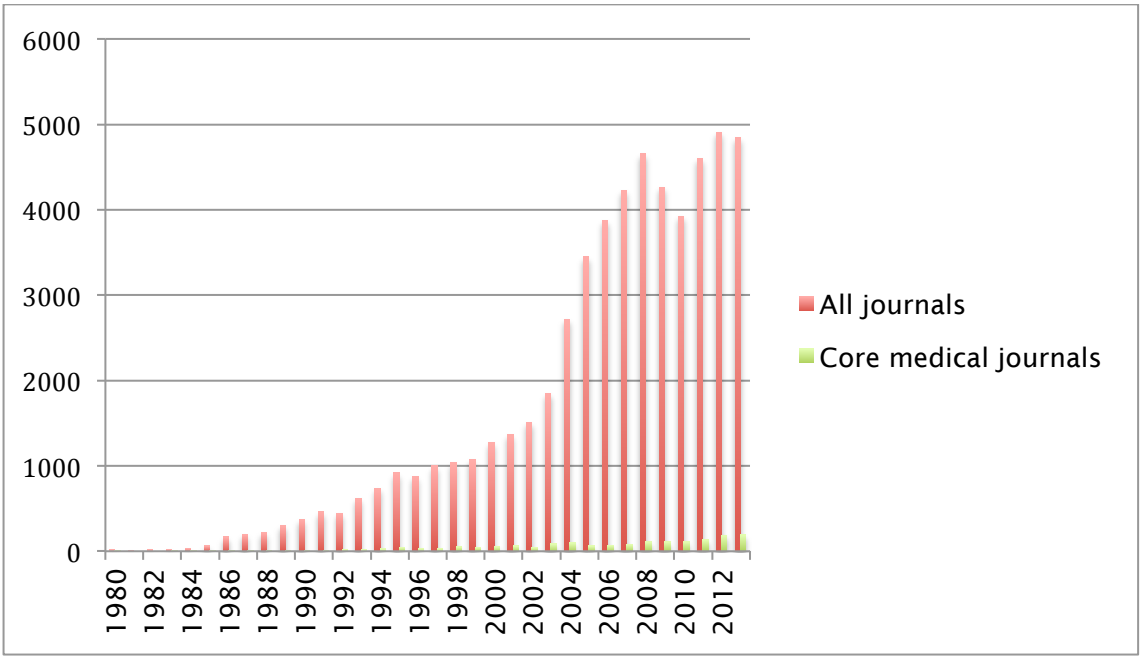

Figure 1.8 MEDLINE citations of "machine learning" articles between 1980 and 2013.

1.12.2 Support vector machines

An SVM is a supervised machine learning method. Given training examples belonging to one of two categories, an SVM training algorithm builds a classifier that assigns new examples into these two categories, or classes. The algorithm can be explained by four basic concepts[205] illustrated in Figure 1.9. Consider a situation in which novel tests, ROSE1 and JAME2 are used to detect HF. Based on the result a HF diagnosis is reached. In order to classify the disease status of the unknown dot in the figure, the SVM must learn to tell the difference between the two groups.

1.12.2.1 The separating hyperplane

Figure 1.9a demonstrates that the test results separate the diseased (red dots) from healthy (green dots) patients. It can be seen that if expression of JAME2 is twice that of ROSE1, HF can be classified. The clustering of the groups can be separated with a line between the two, depicted in Figure 1.9b. Subsequent prediction is determined according to which side of the line the unknown point falls.

Such separating lines can be drawn with no matter how many predicting tests are used. Figure 1.9c represents a single test, in one-dimensional space. The clustering can be separated with a single point. In three-dimensions, a plane is needed to separate the space (Figure 1.9d). This concept can be extrapolated into higher dimensions, where the separating line is a *hyperplane*.

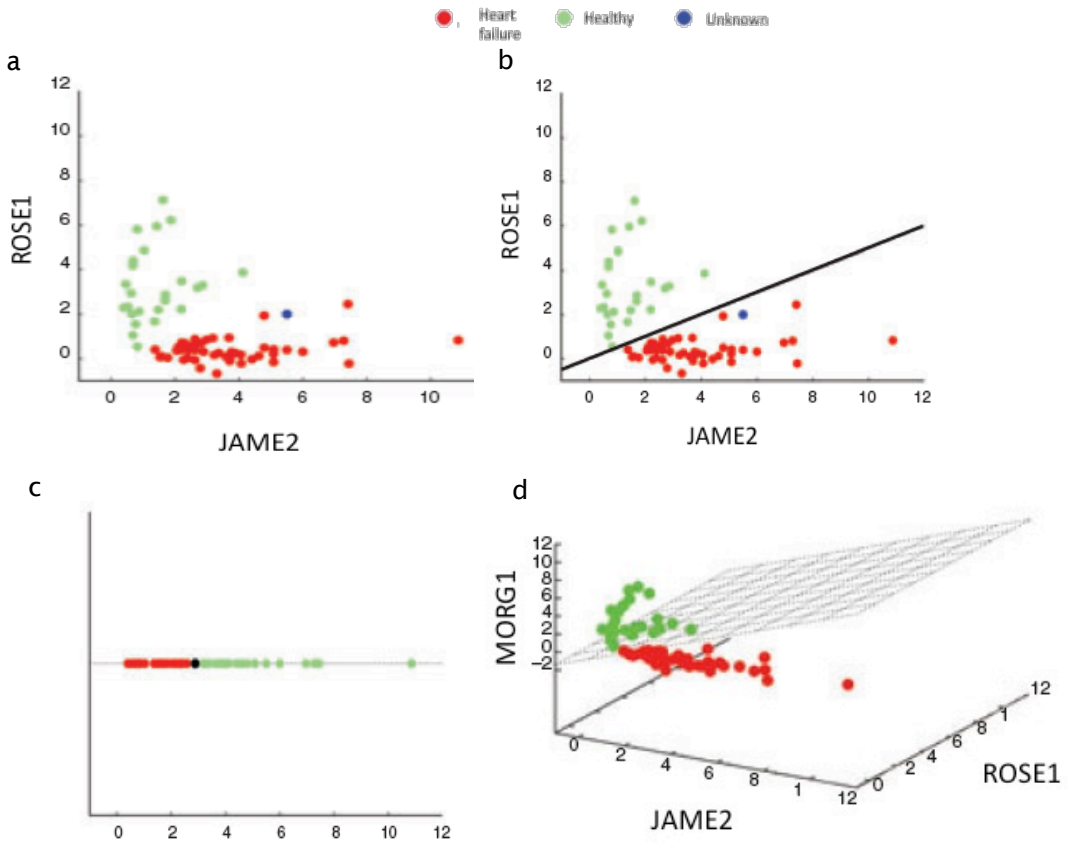

Figure 1.9 Lines of separation. a) Tests ROSE1 and JAME2 cluster the results. Lines of separation in b), c) and d). See text for explanation.

1.12.2.2The maximum-margin hyperplane

The goal of the SVM is to identify a line that separates the HF patients from healthy. In two-dimensional space, the line depicted in Figure 1.9b achieves this. There are however several such lines that would achieve the same (Figure 1.10a) The most effective plane for the SVM is that which adopts maximal distance from all points, whilst still separating the two classes (Figure 1.10b). This is the maximum-margin separating hyperplane, and serves to maximize the SVM's ability to predict the correct classification of previously unseen examples.[206] The training points closest to the hyperplane are known as *support vectors*.

1.12.2.3 The soft margin

Most real data sets cannot be separated with a straight line. Outliers exist, causing a point to fall "erroneously" on the wrong side of the hyperplane. The SVM can be trained to handle cases like this by adding a *soft margin*, allowing some points to fall in an unpredicted location without affecting the whole algorithm. This soft margin is

set to allow a certain number of outliers, without compromising the size of the maximum-margin hyperplane.

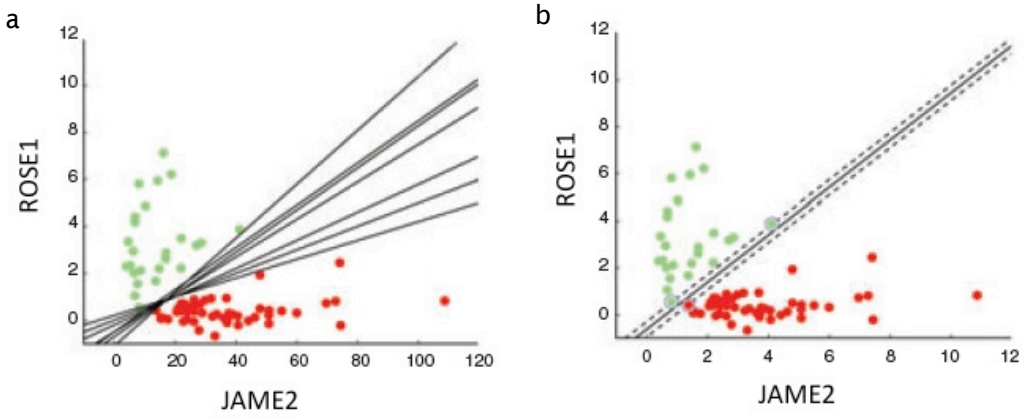

Figure 1.10 The maximum margin hyperplane. (a) Several lines would achieve separation of heart failure (green) and healthy (red). (b) The most effective line is that which adopts maximal distance from all points. See text for further explanation.

1.12.2.4 The kernel function

The kernel function provides a solution to data that cannot be separated by a single plane. Figure 1.11a demonstrates single dimension data where disease expression is clustered around zero and healthy expression has large absolute values. No single point can separate the two classes. By introducing a kernel function the data can be transformed to a new dimension where a single plane can then separate the data. The values in Figure 1.11b were squared, allowing for a single line of separation. In general, a kernel function projects data from a low dimension space to a space of higher dimension where the data is separable. Figure 1.11c is an example of second dimension data that is transformed into four-dimensional space where it is separated with a single plane. This space cannot be pictured, but the resulting separation can be projected back down to the original two dimensions.

For any given data set there exists a kernel function that allows the data to be linearly separated. However, projecting into very high-dimensional spaces can be problematic due to the *curse of dimensionality*: as the number of variables increases, the number of possible solutions increases exponentially. Consequently it becomes harder for any algorithm to select a correct solution. Figure 1.11d displays the same data as Figure 1.11c, but the projected hyperplane comes from a very high-dimensional kernel function. The resulting SVM is very specific to the training data, suffering with *overfitting*, and is unable to categorise correctly when presented with new data.

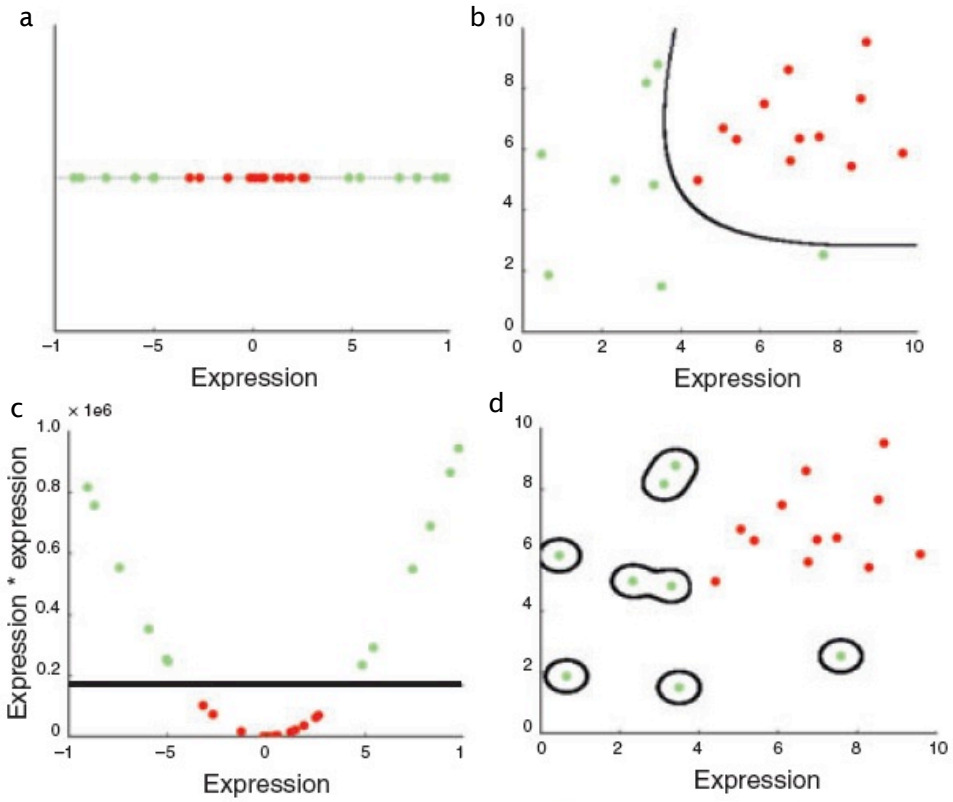

Figure 1.11 The kernel function provides the solution required to separate the data. No signal point can separate the data in (a). By transforming the same data to a new dimension (b) a single line of separation is possible. (c) and (d) represent more complex transformations. See text for further explanation.

1.12.3 Support vector machine learning, cardiovascular prognosis and the electrocardiogram

The use of SVM to support decision-making in cardiovascular disease has increased in line with other machine learning methods. Some approaches have used this technique to improve upon binary classification of biomedical signals, in particular the ECG. Whilst computerized analysis of the ECG is not necessarily novel, real time identification of ECG waveforms can be resource intensive, especially in a mobile platform where processing power may be constrained. Therefore methods to improve the reliability of heartbeat identification are desirable. Osowski *et al.* used a SVM to classify ECG beats into 13 categories including sinus rhythm, BBB, premature beats, ventricular flutter and fused paced beats.[207] They reported around a 2% error rate in classifying 12785 beats using this method, comparing favourably to other classifiers, even where these were limited to fewer categories. Mohebbi *et al.* presented an AF detection algorithm, using a SVM to categorise signals based upon time and frequency domain features, in addition to non-linear measures of fluctuance.[208] They reported

99% sensitivity and 100% specificity in categorizing 388 ECGs after training on 764 known recordings. Like many such experiments in the engineering literature, the ECG data in these studies was obtained from the Massachusetts Institute of Technology PhysioBank signal database.[209] Whilst this resource enables engineers to access human biomedical signals, these data must be interpreted with caution due to variable quality of signal, selection bias of archived data and the limited medical information available about individual subjects. Nonetheless, these studies represent a move toward efficient and accurate classification of arrhythmia. Such tools are not designed to improve upon human interpretation, but do serve to automate tasks that are impossible to perform in a continuous or parallel fashion. In addition, computer classification is reproducible and not subject to inter- or intra-observer error.

Some studies have utilized SVM learning beyond just automating human interpretation. Such applications are essential when dealing with multiple predictors, non linear associations and hidden interactions, where black box algorithms outperform human assessment. Namavar *et al*. used data from 35 Canadian patients who had undergone ambulatory ECG recording in the course of their clinical care.[210] An SVM algorithm, trained according to time and frequency *wavelet* features, was 92% sensitive and 75% specific for future VF or VT. Parveneh *et al*. trained an SVM algorithm to predict spontaneous termination of AF according to measures of HRV in 1minute recordings taken from 30 training records in the PhysioBank database.[211] Testing on 50 separate recordings from the same data source, the algorithm achieved >80% accuracy, performing better than other non SVM classifiers. Shandilya *et al*. trained an SVM to predict the success of external defibrillation, based upon pre-shock defibrillator recordings of 34 successful and 56 unsuccessful defibrillations, achieving 90% sensitivity and 79% specificity.[212] Lastly, Ramirez-Villegas used a SVM for pattern recognition when utilizing several non linear measures of HRV.[213] The authors hypothesized that non-linear HRV analysis would outperform classical HRV measures in predicting individuals with increased cardiovascular risk (but not outcomes). Such non-linear data could only be combined into a predictive algorithm by use of a machine learning technique. The SVM was trained using 60 records from a healthcare provider database and tested on 30 records from the same database, and outperformed classical HRV measures ($P<0.001$).

SVM techniques have also been used to improve localization of postinfarction VT.[214] Yokokawa *et al*. took 34 patients with prior MI and undertook EP studies to generate voltage and pace maps. The SVM was trained with digitized 12 lead ECG data recorded during pace mapping, and then validated in 58 VTs in 33 patients. No other information such as infarct location, BBB morphology or axis was used. The algorithm

was able to determine the site of VT origin with 88% accuracy, compared to between 7%-54% for previously published "manual" methods.

These algorithms all use SVM learning to classify data in a manner not possible through human processing. Where several complex time or frequency domain features are considered in combination, only a machine learning approach can create the predictor algorithm. Such studies are however limited by the lack of clinical rigor in experimental protocol, relatively small sample sizes and testing through cross validation rather than separate test populations. In contrast, whilst the Yokokawa experiment was a well designed study utilizing new clinical data, the authors chose not to describe the computer science is any detail. This highlights the divide between work published in clinical and engineering journals. More importantly, omitting these details limits validation of the algorithm by other groups.

1.13 Biomarkers

1.13.1 Inflammatory Markers

In view of the association of SCD and CAD, and the mechanistic role of plaque rupture, markers of inflammation may have a role in risk stratification.

C-reactive protein (CRP), an acute phase reactant, has been studied in detail, with recent developments in analysis of highly sensitive CRP (hsCRP) enabling evaluation that remains subclinical. HsCRP has a predictive value for development of coronary disease,[215] and is elevated on post mortem analysis of those with severe coronary disease dying suddenly compared to non cardiac deaths.[216] In CAD patients with ICD implants, hsCRP was significantly higher in those receiving appropriate therapy.[217] When considering SCD in the general population, analyses from the Physicians' Health Study showed that elevated CRP levels were an independent risk factor for SCD in males (RR 2.78, 95% CI 1.35-5.72, P=0.06),[218] although there was no risk association found in a similar nested case-control study of healthy women,[219] nor in the Prospective Epidemiological Study of Myocardial Infarction (PRIME) cohort (see below).[220]

Interleukin (IL) 6 is another inflammatory marker associated with CAD. PRIME investigated IL-6 as a risk marker amongst 9771 asymptomatic males enrolled in a multicentre cohort study.[220] Over 10 years IL-6 was associated with an increased risk of SCD (HR 2.06, 95% CI 1.20-7.81). In contrast, the same study did not find an association between hsCRP and SCD.

1.13.2 Myocyte injury

Myocyte injury may occur in response to ischaemia, oxidative stress, neurohormonal activation or inflammation, and in these circumstances, proteins associated with myocyte contraction are released into blood. Cardiac troponin T (cTn) is associated with total mortality in both acute and chronic HF, regardless of aetiology.[221222] More recently, amongst 4431 ambulatory participants of the community-based cohort, Cardiovascular Health Study, cTnT, measured with a high sensitivity assay at baseline, was associated with SCD.[223] Over a median follow up of 13.1 years, higher levels of cTnT carried a HR of 2.04 (95% CI 1.78-2.34), although after adjustment for lower LVEF, HF and MI the association was attenuated (HR 1.26, 95% CI 1.05-1.62), reinforcing that cTn is not specific for SCD.

1.13.3 Myocyte stress

Natriuretic peptides are hormones associated during cardiac haemodynamic stress. In clinical practice they are semi-quantitative markers of cardiac stress and HF, related to the extent of atrial, ventricular and valvular dysfunction. In patients with acute dyspnoea they can guide diagnostic investigations and management, and have a role in guiding therapy in established HF.[22462] Several studies have evaluated the ability of B-type natriuretic peptide (BNP) to predict risk of SCD or appropriate ICD therapies in at risk groups. Scott *et al*. performed a meta-analysis of 14 studies and found BNP predicted SCD with a relative risk of 3.68 (95% CI 1.90-7.14) in patients without ICDs, and predicted VA with a relative risk of 2.54 (95% CI 1.87-3.44) in patients with ICDs.[225] Subsequent studies have indicated that this risk also exists in apparently healthy populations, including females,[219] and older, non-whites.[226]

Soluble ST2 is a serum protein upregulated in response to mechanical stress of cardiac myocytes, increased following MI.[227] It has been shown to predict all-cause mortality in the post-MI setting, as well as in patients with CAD and NICM.[228229] In a nested case-control study of 36 SCD cases and 63 controls, sST2 was predictive of SCD in ambulant HF patients of mixed aetiology.[230] The prognostic value of sST2 was independent of other clinical variables, and provided complementary information to NT-proBNP.

1.13.4 Multimarker strategies for predicting SCD

Whilst individual biomarkers may be associated with cardiovascular outcomes, including SCD, the additional benefit of these markers in HF patients who already fulfil ICD criteria is unclear. As outlined below, few studies have determined whether measuring a panel of multiple biomarkers can provide incremental benefit over and above each individual result.

Population-based epidemiological studies have evaluated the multimarker strategy. In general populations these approaches seem to offer little additional discrimination for cardiovascular events over and above traditional risk factors. A cohort study of 5067 participants without cardiovascular disease examined the use of a combination of CRP, natriuretic peptides, cystatin C and lipoprotein-associated phospholipase 2 in predicting cardiovascular risk. Gains over "traditional" risk factors such as smoking, blood pressure and diabetes were minimal.[231] In those already at high risk, however, the strategy may be beneficial. In ageing populations or those with renal disease, varying combinations of these same biomarkers did provide prognostic information.[231-234] These divergent findings are largely attributable to differences in the study populations. Conventional risk factors perform poorly in those with already high baseline risk, and thus additional markers will be additive.[235] For the purposes of identifying those with most potential to gain from ICD therapy, multiple biomarkers should be evaluated in those already considered at high risk, rather than in general populations where the event rate is low and incremental benefit over traditional cardiovascular risk factors will be small.

Scott *et al*. investigated whether five plasma biomarkers, chosen for biological plausibility after literature review, would predict survival in an ICD population.[236] BNP, growth differentiation factor-15 (GDF-15), sST2, CRP and IL-6 were measured in 156 patients attending for routine device follow up. In this population, the study found that sST2, BNP, IL-6 and GDF-15 were predictors of all cause mortality (death not preventable with ICD therapy). Patients surviving with ICD therapy had significantly higher BNP than those surviving without ICD therapy (P=0.01). Using a multivariable model, sST2 and BNP identified patients surviving without ICD therapy, patients at risk of ICD therapy but not death, and patients with a high risk of death. The event rate in the study was low over 15±3 months follow up, but the approach is interesting in modifying the risk profile of patients considered high risk and identifying those who die despite ICD therapy and those who survive without needing it.

1.13.5 Biomarker Discovery and Proteomics

Biomarker discovery research has traditionally focused on the study of individual molecular indicators of clinical condition. Hypothesis-driven approaches to validating protein makers are well established, based upon contemporary understanding of cellular pathways and pathophysiology. However, an overreliance on this strategy may limit the translation of fundamental research into new clinical applications, not least because assessment of candidate proteins necessitates a targeted approach. Analysis is necessarily limited, both due to assay requirements and the scope of interactive and multivariate processing.[237]

Systems approaches enable strategies in which multiple biomarkers are assayed together as a system. Resultant markers more accurately reflect the underlying biological interactions than a traditional approach focused on a single protein. Heart failure is a complex clinical phenotype and the biological interactions leading to arrhythmic SCD are such that a single gene biomarker could never explain. Furthermore, genetic variation between patients is likely to be wide, even if the final common process is similar.[237]

Techniques capable of analysis of DNA and RNA enable rapid and global profiling of gene expression. However, the presence of genetic material does not always correlate with the presence of the encoded protein because of processes such as alternative mRNA splicing, RNA editing, and post translational protein modification (PTM).[238] The human genome contains about 23000 transcription units, and is virtually constant in all cells under all conditions. On the other hand, the protein profile, or *proteome*, is far more complex, undergoing dynamic changes as it responds to autocrine, paracrine, and endocrine factors, bloodborne mediators, temperature, drug treatment, and developing disease over time. When taking into account the splice variants and precursor/cleaved forms of each gene/protein, the proteome actually contains about 500,000 proteins. When considering the numerous post-translationally modified states of each protein, the number reaches into millions.[239]

Expression of proteins differs greatly between different cells and organs, and depends among others on differentiation state, and environmental and internal conditions. The proteome is highly dynamic, with transient modifications occurring at the second-to-minute time scale. Hence, it is the proteome that best reflects the complement of proteins expressed in a certain cell/tissue under specified conditions. There is compelling justification for the direct and large-scale analysis of proteins, and since the concept was proposed over 30 years ago, techniques to investigate the proteome have evolved considerably.[240][238] In theory, every disease may be uncovered and characterised by its unique panel of up- and down-regulated proteins, perhaps to the point where this were more relevant than a single protein biomarker.[241]

1.14 Proteomics

Proteomics involves the identification, characterization and quantification of the proteome within whole cells, tissues and body fluids.[242] Clinical proteomics applies these techniques within medicine in an effort to accelerate the discovery of new drug targets and protein disease markers useful for in vitro diagnosis. [243]

1.14.1 Workflow

The general principle of biomarker discovery through proteomics involves differential expression of proteins between disease and control groups. The process involves several steps including sample preparation, protein extraction and separation, and identification. These steps differ by technology platform, but all rely on a combination of laboratory processing and computer, or *in silico,* processing to identify proteins, in particular through high-resolution mass spectrometry.

1.14.2 Mass spectrometry

Mass spectrometry (MS) is an analytical technique capable of accurately measuring the molecular weights of individual components in a given sample. A mass spectrometer comprises three major parts: ion source, analyser, and detector.[244] Sample molecules are ionized and converted into gas phase in the ion source, separated according to their mass to charge ratio (m/z) in the analyser, and finally detected by the charge induced. The *m/z* profile can be compared between samples, resulting in a list of differentially expressed protein peaks. The MS spectrum of each peak is compared with theoretical values based upon in silico translation of DNA sequences into proteins, from which peptide masses are computed.[244]

1.14.3 Biological samples

In general, sample sources for proteomic study can be of human or animal origin, and be solid tissue, body fluid or cell. Animal models of MI and HF have been extensively characterized and such tissue can minimize clinical heterogeneity and ensure sample standardization[238] and can overcome difficulties with obtaining suitable human cardiac tissue from biopsy or autopsy.[245] However, it is important to appreciate that even where human tissue is used, proteins differentially expressed in the heart may not be detected in blood. It is not well understood how protein expression in tissues reflects measurable levels in serum.[246] In contrast, blood provides the most clinical relevant source of circulating biomarkers, and is the largest and deepest version of the human proteome. Its collection is minimally invasive, low risk and cheap, and processing to plasma or serum is a routine task in clinical labs.[244] It is therefore the most appropriate source for conducting biomarker discovery.

The serum or plasma proteome is subject to changes not solely caused by pathological processes. Factors such as age, circadian rhythm, stress, medication and fasting may affect the protein profile, and thus the pre-analytical phase is a crucial part of the biomarker discovery workflow.[244] Even minor deviations in the pre-analytical phase, for example variation in the type of collection tube or delay in sample processing, may

lead to false conclusions.[247] Standard operating procedures for blood collection and processing are published and provide a framework for experimental design.[248]

1.14.4 Gel based separation

The majority of cardiac proteome research has been carried out using two-dimensional electrophoresis (2DE).[238] The complex proteome sample is added to a polyacrylamide gel across which a current is applied. Proteins are separated in the first dimension according to their charge properties (isoelectric point [pI]), followed by their separation in the second dimension according to the relative molecular mass (M_r) (Figure 1.12). The resulting protein spots are identified on MS, frequently by peptide mass fingerprinting.[244]

Although these steps are labour intensive, the technique is advantageous in that it can provide information regarding protein isoforms and PTMs in addition to expression levels, and has been successfully used in tissue analysis.[249] However, this approach is limited by the relatively narrow dynamic range (~10^4) and bias towards detection of highly abundant proteins. It is also less effective at detecting hydrophobic proteins and proteins with extreme pI and M. These limitations make it less suitable for plasma or serum analysis.[250]

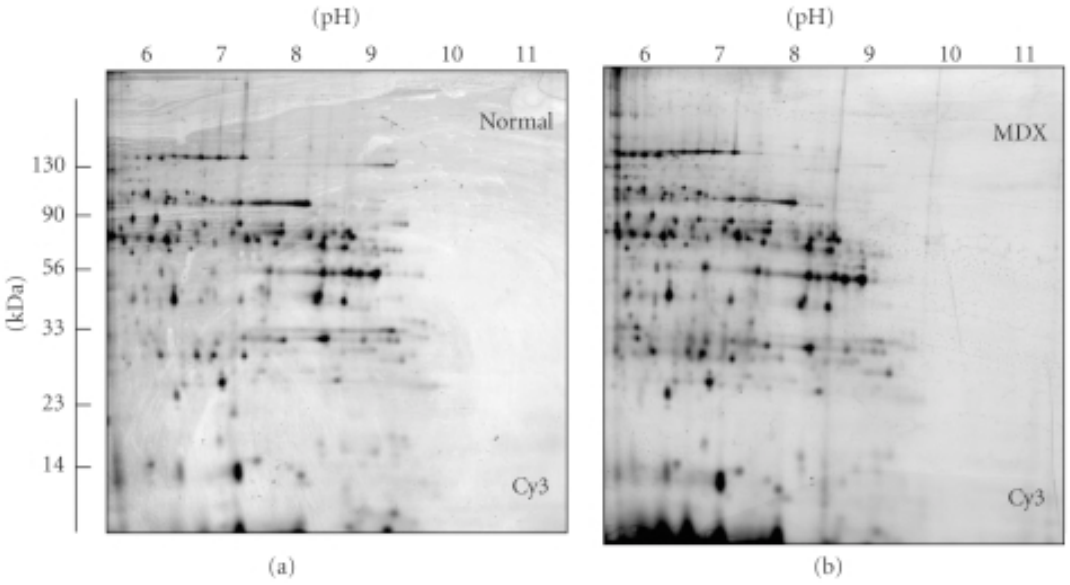

Figure 1.12 2D gel electrophoretic protein analysis of normal murine cardiac tissue (a) and muscular dystrophy mouse model (b). The first dimension scale (pH) and second dimension (kDa) are indicated. Adapted from Lewis et al.[251]

1.14.5 Proteomic profiling

Direct MS analysis of a sample can provide rapid insight into its protein profile. The most common technique utilizes Matrix-Assisted Laser Desorption/Ionization (MALDI)

to introduce ionized proteins into the MS. Specimens are dried and spotted on a target with a light absorbing matrix molecule, before being vaporized with nanosecond laser pulses.[252] This technique enables an acquisition of wide *m/z* range, but in analysis of complex samples, such as serum, low abundance samples remain undetected.[244] A variation of the MALDI technique partially solves this difficulty by reducing sample complexity. Surface-enhanced laser desorption/ionization (SELDI) is a chip based method that binds only a subset of the proteome, prior to MS on the same chip, resulting in a pattern of *m/z* peaks. The technique is particularly suitable for analysing the low-molecular weight proteome. However, quantification and identification of the proteins rather than just *m/z* peaks is not possible from the process.

1.14.6 Gel free separation

Gel-free systems are increasingly utilized for proteomic-based experiments.[250] These approaches take advantage of the automation, throughput and sensitivity of that can be provided by techniques based upon a combination of liquid chromatography and tandem mass spectrometry (MS/MS). A tandem mass spectrometer is an instrument capable of isolating a precursor ion, fragmenting it, and detecting resulting fragments.[253]

A typical experiment involves cleavage of complex protein mixture by a sequence specific protease (typically trypsin) into peptide fragments.[244] This generates a huge number of different tryptic peptides that precludes direct MS analysis and instead the resulting peptide mixture must be separated, typically through liquid chromatography.[238]

Multidimensional Protein Identification Technology (MudPIT) is an approach that first separates peptides using strong cation exchange chromatography, thereby separating on the basis of charge, and then by elution through a reverse-phase (RP) resin, resolving peptides on the basis of hydrophobicity.[254255] Eluted peptides then undergo electrospray ionization into the MS/MS where peptide ions are selectively fragmented via collision activated dissociation. The resulting spectra are recorded and referenced against a protein database, providing a snapshot of large-scale protein expression at a given point in time.[256]

1.14.7 Quantitative proteomics

Whilst the advances in MS and bioinformatics have enabled comprehensive protein identification, full exploitation of the proteomic technique for biomarker discovery requires quantitative and comparative analysis.

So-called “label-free” quantification simply compares the MS signal intensities between individual sample experiments. Whilst this approach can be applied to limitless samples and does not add to the complexity of the MS spectra, different peptides ionize differently during individual experiments. Their intensities may therefore vary from run to run and introduce both systematic and random errors in quantification.

Stable isotope labelling seeks to deal with these errors by analysing all samples simultaneously as a single experiment. To distinguish the samples during the analysis they are first labelled with reagents containing stable istopes. The labelled proteins or peptides still have identical ionization and chromatographic properties and will therefore behave “normally” during all steps of the experiment as if they were not labelled. However, the resulting *m/z,* shifted by a specific molecular mass, will identify the sample, whilst the relative intensity will quantify the proteins.[255] The Isobaric Tag for Relative and Absolute Quantification (iTRAQ) method uses labels composed of a reactive group, a reporter group, and a balancer group.[257] The sum molecular weight of these three parts is constant and therefore the peptide appears as a single MS peak, but during MS/MS tag becomes fragmented and it is the signal intensity of the reporter groups that gives relative peptide concentration. This technique is limited to a maximum of 8 samples simultaneously, usually representing pooled samples from clinical groups of interest.

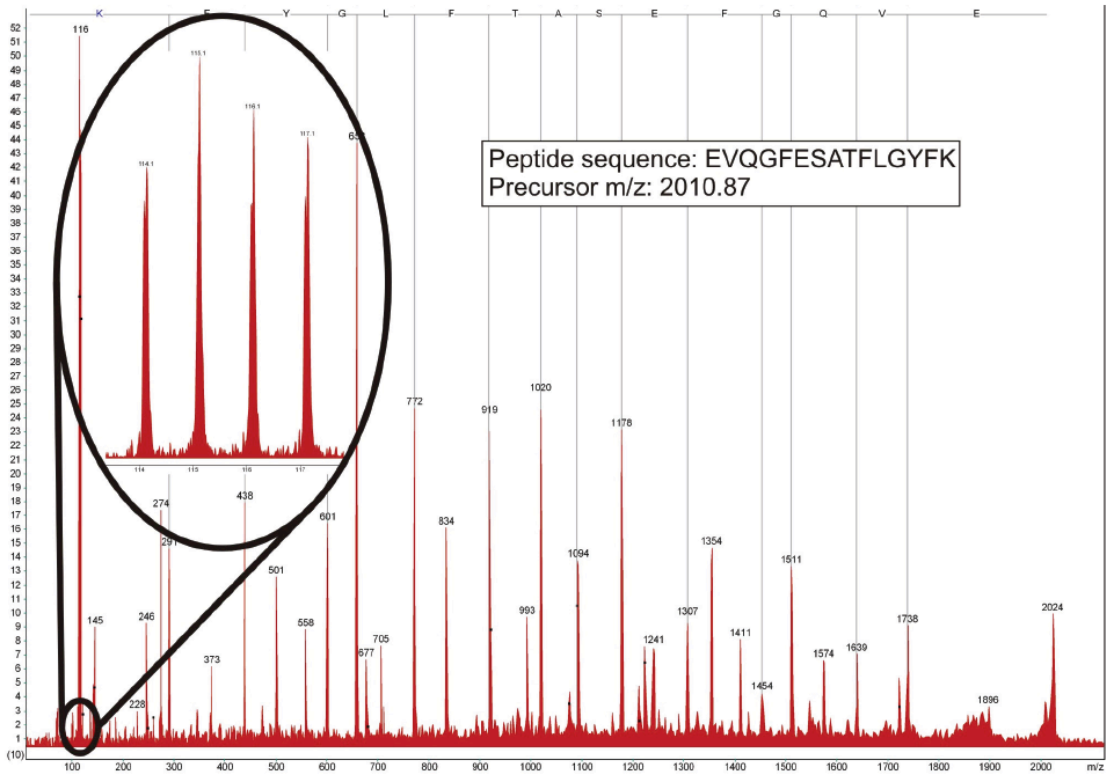

Figure 1.13 Representative iTRAQ MS spectrum. A peptide of m/z 2010.87 was selected for fragmentation analysis, generated from four samples. iTRAQ quantitation can be read in the low

m/z region (magnified view). The relative intensity of the peptide in each sample is reflected in the intensity of the four peaks.

1.14.8 Challenges of the blood proteome

The plasma or serum proteome reflects the sum of all secreted molecules, cell turnover proteins released at low level, and distinct clonal immunoglobulins. The $>10^6$ different molecules result in an enormous depth to the proteome with a huge dynamic range of 10^{12} over which proteins must be detected.[258] The task is further complicated when considering that approximately half the total protein mass is accounted for by just one protein, albumin, with ~99% of the proteome represented by just 20 very high-abundance proteins.[244] In-depth analysis of the less abundant proteins requires techniques to reduce the complexity of the sample.

One such method often implemented is the removal of proteins which are in high abundance and therefore offer no potential for risk identification. Immunoaffinity depletion is an approach employing immobilized polyclonal antibodies to bind to defined proteins and their isoforms, resulting in significant reduction of complexity and dynamic range of the proteome, leading in turn to a higher number of identified proteins, improved sequence coverage and more accurate protein quantification.[259] However, this approach is not without limitations, since some of the high abundance proteins, in particular albumin, act as carrier molecules for other less abundant proteins. Thus by removing the carrier proteins, these potentially interesting molecules may be lost as well.[260]

1.14.9 A high resolution approach to serum proteomics

Garbis *et al.* considered the difficulties of proteomic analysis in human serum, acknowledging the unmet need for high-resolution proteomic analysis across a wide range of molecular masses and concentrations. In a proof-of-principle study, clinical sera from patients with benign prostate hyperplasia underwent a modified MudPIT approach.[261] Rather than subjecting the sample to immunodepletion prior to the MudPIT standard of tryptic digestion followed by chromatography based upon charge and hydrophobicity, the novel method incorporates size-exclusion chromatography for the prefractionation of serum proteins followed by their dialysis exchange and solution phase trypsin proteolysis before hydrophilic interaction chromatography. In the experiment the samples were processed according to the novel method and two more standard approaches. All MS/MS and data processing steps were equivalent. The new method resulted in detection of 2000 proteins, across a wide analytical range incorporating 12 orders of magnitude, well beyond the standard approaches only detecting around one quarter of this.

Although this method has been applied to serum of those with prostate hyperplasia, it may represent a step change in the potential for disease state discovery by proteomics. To date, there have been no studies in HF utilizing this high resolution MudPIT method.

1.14.10 Validation

Although proteomics plays a major role in the discovery phase of potential biomarkers, validation is necessary by more traditional methods.[245] Whilst this is of greatest importance where the biomarker candidate is detected in tissue that would not be suitable for routine clinical sampling, even with serum/plasma proteins there is still a need for clinical validation. The enzyme-linked immunosorbent assay (ELISA) is a commonly used technique. Analytes from samples are captured by immobilized antibodies fixed to a plate surface. An enzyme linked detecting antibody is added which is then activated by the addition of a substance that changes colour or fluoresces when catalysed.[250] However, these traditional validation techniques are limited due to cross-reactivity of antibodies, restricted availability of reagents and the nanogram/millilitre concentration of candidates.[245] Targeted methods such as multiple reaction monitoring mass spectrometry (MRM-MS) can selectively detect specific peptide populations without the need for a specific antibody, and this may provide a more robust method for validation.[262250] Nonetheless, technology such as ELISA is clinically accepted, widely used in daily practice and is suitable as a first line in biomarker validation.

1.14.11 Proteomics for biomarker discovery in heart failure

Proteomic techniques have been used in cardiovascular medicine. Several studies have used animal models or human biopsy and transplant tissue to define the cardiac proteome and gain a better understanding of the pathophysiology of CAD and HF.[263264265266267]However, the use of serum or plasma clinical proteomics in developing diagnostic biomarker candidates has been less widespread, with few studies examining prognosis and arrhythmia prediction in HF.

Jones *et al*. used MALDI to evaluate the diagnostic value of proteins in 100 HF patients and 100 controls.[268] Of 67 differentially expressed protein peaks, 6 peaks were predictive of HF, independent of BNP. This experiment demonstrated the validity of a multimarker approach in HF diagnostics, but did not offer any insight into prognosis.

My research group carried out a pilot study to identify potential serum biomarkers associated with HF, and to prospectively explore the association of these biomarkers with mortality and the occurrence of ventricular arrhythmias.[269] Using the SELDI

platform to analyse serum from 141 ICD patients, 5 protein peaks were associated with all-cause mortality, but not occurrence of appropriate ICD therapy (Figure 1.14). Although novel, the experimental findings were limited by the SELDI technique. Only around 100 *m/z* peaks were identified, and the peptide identity of the differentially expressed proteins remained unknown.

Most recently, Hollander *et al.* used iTRAQ labelling and MALDI MS to propose biomarker signatures of those with recovered heart function following HF.[270] They retrospectively identified 39 patients with end stage HF and 20 healthy controls in whom serum had been stored. All 39 patients went on to have cardiac transplantation, but only 18 were considered clinically "recovered" after transplant. It was the differential expression of proteins between these patients and another group of 23 patients who had end stage HF that was examined. In all, from 138 proteins identified, 18 were differentially expressed. They hypothesized that the biomarkers of recovered transplant recipients would be of use in determining which stable heart HF patients receiving medical therapy would recover LV function. They went on to use targeted MS to validate the markers in 39 patients with HF receiving medical therapy. 30 patients had recovery of LVEF and HF symptoms, whilst 9 patients did not. 17 of the 18 markers were identified, and a multimarker panel of these was significantly predictive of HF recovery. However, this study highlights the complexity in experimental design that becomes necessary when attempting to identify prognostic biomarkers. The clinical value of a biomarker of recovery is in the symptomatic HF patient, but in this case the candidate markers are drawn from a clinically distinct group. Although the MALDI platform only identified 138 protein peaks, it is the first such study to identify the proteins themselves, with the majority involved in coagulation, inflammation, cell adhesion, proteolysis and development. Nonetheless, the choice of proteomic platform seems critical to create a truly unbiased approach to biomarker discovery.

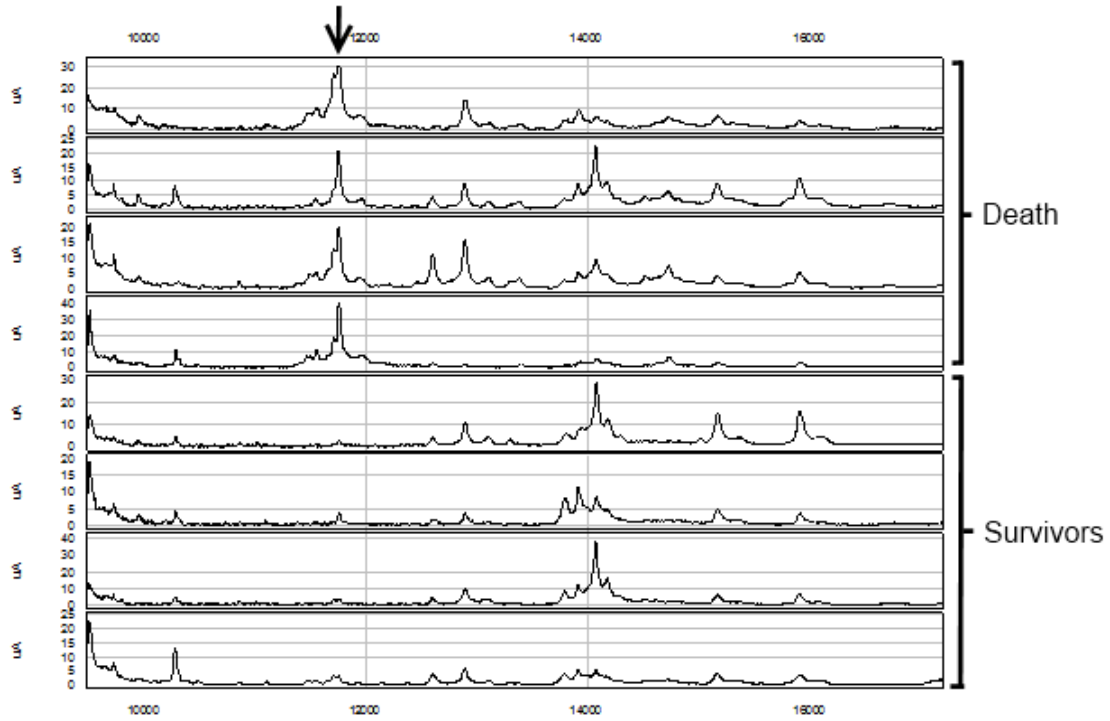

Figure 1.14 Mass spectra, 10 to 16 kDa, expanded and aligned for 4 patients that died during follow-up and 4 patients that survived. Peak intensity for biomarker peak m/z 11834 (arrow) is higher in patients that died versus those that survived. The x-axis is the ratio of mass-to-charge (m/z) and the y-axis represents peak intensity.

1.15 Aims

The overall aim of this thesis was to explore novel methods of non invasive risk stratification in sudden cardiac death. The specific aims of the research were:

i. To use meta-analysis to determine the accuracy of fQRS in predicting all cause mortality and SCD (Chapter 1).
ii. To evaluate the relationship between surface ECG markers of repolarisation and the extent and distribution of LV scar (Chapter 4).
iii. To determine whether the Selvester QRS score is a surrogate for LV scar burden, whether the score varies with scar characteristics and if QRS score can meaningfully predict SCD (Chapter 5).
iv. To determine whether automated analysis improves feasibility and accuracy of QRS scoring, and whether the tool could be used to screen an unselected population of LV scar (Chapter 6).
v. To use machine learning techniques to train an SVM algorithm capable of screening ECGs for presence of myocardial scar (Chapter 7).
vi. To determine if a novel high resolution proteomic technique could be used to identify candidate biomarkers reflective of SCD risk (Chapter 8).
vii. To use ELISA techniques to provide clinical and technical validation of candidate biomarkers (Chapter 9).

2 General Methods

2.1 Outline

This thesis contains 7 separate experiments corresponding to the background and aims outlined in the introduction, each detailed in individual chapters. Each study is presented in full, including the methodology, results and discussion pertinent to the specific work.

2.2 Setting

All original research was conducted at University Hospital Southampton NHS Foundation Trust. This hospital serves 1.3million people living in Southampton and South Hampshire, in addition to tertiary cardiac services to around 3 million people in central southern England and the Channel Islands.

2.3 Ethical considerations

All work was undertaken in accordance with the Declaration of Helsinki and according to the principles of Good Clinical Practice.

Ethical approval for prospective study was granted by the Research Ethics Committees of South Central – Oxford A [11/SC/0548] (Chapters 6 and 7) and South Hampshire and Southwest Hampshire (A) [08/H0502/54] (Chapters 8 and 9).

2.4 Data handling and record keeping

Data was collected and retained in accordance with the Data Protection Act 1998. Study documents (paper and electronic) were retained in a secure location during and after the relevant trial had finished. All essential documents and source data, including any medical records where entries related to the research have been made, will be retained for a minimum period of 5 years following the end of the study. A 'DO NOT DESTROY' label stating the time after which the documents can be destroyed was placed on the outer cover of relevant medical records.

2.5 Cardiac Magnetic Resonance

The CMR data acquisition in Chapters 4, 5, 6 and 7 was performed in an identical fashion. All patients were scanned on a cardiac dedicated 1.5-T Siemens Avanto MRI (Siemens, Germany). After initial localiser sequences, a stack of steady-state free precession cine images were acquired in the short axis plane from the level of the

mitral valve annulus to the LV apex. Following this, 0.15 mmol/kg gadobenate dimeglumine (Multihance, Bracco SpA, Milan, Italy) was administered intravenously. Short axis LGE images were acquired using a 3D segmented inversion recovery fast gradient echo sequence (3D IR turboFLASH) in two breath holds. An appropriate time to inversion was selected to null the normal myocardium.

Ejection fraction and volumes were analysed on commercially available post-processing software (Argus, Siemens, Germany). Short-axis cine images were used to measure end-diastolic volume, end-systolic volume and LVEF by standard methods. Papillary muscles were regarded as part of the blood pool.

In Chapters 4 and 5, scar analysis was performed using semiautomated software developed at my institution as a plugin to the open-source DICOM viewer OsiriX (OsiriX Project, Geneva, Switzerland).[271] In Chapters 6 and 7, scar analysis was performed using semiautomated software (cmr42 v3.4, Circle Cardiovascular Imaging Inc., Calgary, Canada). Endocardial and epicardial LV myocardial borders were manually delineated on the short axis LGE-CMR images. For each patient the maximum signal intensity (SI) within an infarct region in each image of the LV stack was automatically determined and scar was defined as myocardium with a signal intensity ≥50% of the maximum SI (full width at half maximum, FWHM). Scar was automatically segmented and any areas identified as scar by the software but not deemed to be scar by the user were excluded manually.

3 Fragmented QRS for the prediction of sudden cardiac death: a meta-analysis

3.1 Introduction

Sudden cardiac death (SCD) risk is reduced by Implantable Cardioverter Defibrillator (ICD) use in appropriately selected patients. Impairment of LV function and QRS duration are used as risk discriminants in current guidelines, but result in many patients receiving ICD therapy from which they gain no benefit, as a minority receive appropriate treatment for life threatening arrhythmias. Furthermore, ICD implantation carries procedural risk and long term morbidity related to device malfunction, need for device replacement and unnecessary or inappropriate shock delivery.[59272] Therefore approaches are needed that identify patients with greatest potential to benefit from ICD therapy.

Extent of LV scar, characterized CMR-LGE, is associated with the occurrence of spontaneous VA in patients receiving ICD therapy.[145] However, CMR-LGE has limitations as a risk stratification tool. It is not a bedside test or widely available due to the expense and clinical expertise required. By contrast, the 12-lead ECG is easily available and its use as a marker for scar could offer powerful benefit. Conduction delay due to local disruption of activation can be seen as fragmentation of QRS complexes on the 12-lead ECG. [162] Fragmented QRS (fQRS) has been proposed as a marker of myocardial scarring and may be associated with worse cardiovascular outcomes in both CAD and non-ischemic cardiomyopathy (NICM).[164273] Several studies have reported discrepant results in this regard and it remains unclear whether fQRS could be of use in SCD risk stratification. This meta-analysis was undertaken to determine the accuracy of fQRS in predicting all-cause mortality and SCD, and its potential in risk stratification.

3.2 Methods

3.2.1 Literature Search

All published data relating the presence of fQRS to cardiovascular arrhythmia end points were identified. The electronic databases MEDLINE and Embase, as well as the Cochrane Library were searched to find primary references and reviews, supplemented by manual searches through published bibliographies. The following search terms were used: (arrhythmias, cardiac OR ventricular fibrillation OR

tachycardia, ventricular OR death, sudden OR death, sudden, cardiac OR defibrillators, implantable OR implantable defibrillator OR defibrillator) AND (QRS or ECG) AND (fragmented or fragmentation) OR (fQRS).

The search was restricted to adults (older than 18 years of age) in English language peer-reviewed journals from 1966 to February 2014.

3.2.2 Study Selection

Studies were selected if the relationship between presence of fQRS, according to the method described by Das[164], and one or more arrhythmic end points (SCD, resuscitated cardiac arrest, occurrence of VA or appropriate ICD therapy) and/or mortality (cardiac or all-cause) was described. Studies recruiting patients with predominantly CAD or NICM, with follow up for ≥6 months were eligible for inclusion.

Studies only including patients with hypertrophic cardiomyopathy, congenital heart disease, Brugada syndrome and Chagas' disease, or those describing fQRS on vectorcardiography, magnetocardiography and signal averaged ECG, were excluded.

3.2.3 Bias Assessment

The internal validity of studies was assessed using the Quality in Prognosis Studies (QUIPS) tool.[274] Publication bias was evaluated by generating a funnel plot of the logarithm of effect size against the standard error for each trial.

3.2.4 Statistical Analysis

Studies were evaluated individually and data extracted according to mortality and/or arrhythmic end points before being pooled for analysis using Review Manager[275] and Meta-DiSc[276] software. Subgroup analyses were also performed, evaluating patients according to CAD or NICM aetiology, presence of ICD, and LVEF. The effect size is presented as the relative risk ratio (RR), and likelihood ratio (LR) indicating how many times more (or less) likely a patient experiencing an endpoint is to express fQRS.[277] Statistical heterogeneity was evaluated using the I^2 statistic and its 95% CI and in all cases a random effects model was used to account for significant statistical variation. [278279] Meta-regression analysis, using the linear weighted inverse variance method, was performed to evaluate the potential influence of baseline characteristics.

3.3 Results

3.3.1 Search results

The search strategy yielded 260 citations. Of these, 226 studies were excluded by title or abstract and 34 were retrieved for detailed evaluation (Figure 3.1). 19 studies were excluded as they did not present suitable mortality or arrhythmic end point data, or did not include a majority of patients with CAD or NICM. 3 studies used an alternative definition for fQRS[280281], or had only very short term follow up data[282] and were therefore excluded.

This left 12 studies for analysis, of which 8 reported results for both mortality and arrhythmia end points. A further 3 studies examined the association of fQRS and death only, and 1 study examined the association of fQRS and SCD or VA only.

3.3.2 Study quality

The methodological quality of the included studies was generally good, without high risk of bias (Table 3.1). 7 studies did not give clear data concerning loss to follow up and therefore the relationship between fQRS and outcome may be different for completing and non-completing participants. In addition, it was not clear how one study accounted for potential confounders, raising the small possibility of result distortion. The funnel plot did not suggest evidence of publication bias (not shown).

3.3.3 Study Characteristics

The 12 studies enrolled 5307 patients (Table 3.2) of whom 225 were excluded due to classification in the source study as "wide QRS" without reporting of fQRS[273,283], 36 excluded due to non CAD aetiology (see below)[284], and a further 37 classified as "transient fQRS", expressing QRS fragmentation following an ischemic event which disappeared before hospital discharge (mean stay 3.8days).[285] From the remaining 5009 patients, 4938 were included in the analysis of mortality, and 3758 in the analysis of arrhythmia end points.

Overall, most of the participants were male (78%) and had a history of CAD (60%). 39% of study participants had an ICD implanted. The mean/median LVEF was 35% and QRS duration was 111ms. Three distinct study populations were seen:

i. Four studies recruited recipients of ICDs or cardiac resynchronization therapy (CRT), with an entry requirement or mean/median LVEF of 45% or less. [169,273,284,286]
ii. Five studies included patients with HF, either with stable symptoms[283,287-289], or following a decompensated episode[290].

iii. Lastly, three studies recruited patients with CAD, either following the first episode of an acute coronary syndrome (ACS) with follow up in a chronic phase[285] or whilst undergoing investigation for stable CAD[166,291]. These studies had mean/median LVEF of 40% or greater.

Six studies had a population of both CAD or NICM[169,273,286–288,290]. The study by Apiyasawat *et al.* enrolled patients with ICDs implanted for a wide range of diseases. The results were presented in such a way that most non CAD or NICM patients could be excluded from this analysis, although a small number of patients with arrhythmogenic right ventricular cardiomyopathy (ARVC) were reported together with CAD/NICM endpoints and these could not excluded from the meta-analysis.[284] The study by Pei *et al.* presented data in such a way that end point data was analysed for the whole population but could also be extracted for subgroup analysis of patients with NICM and CAD. Two studies enrolled only patients with NICM[283,289], whereas three included only CAD.[166,285,291] In four studies, all patients had a cardiac implantable electronic device (CIED),[169,273,284,286] and since the study by Cheema *at al.* provided end point data for those with and without ICDs, these data were used in the subgroup analysis.

3.3.4 Data synthesis

3.3.4.1 fQRS and risk of mortality

During a mean/median follow up of 14-53 months, 1140 out of 4938 patients died. Death was more common in patients with fQRS (RR 1.71, 95% CI 1.02-2.85) (Figure 3.2). Significant heterogeneity existed across the studies (P <0.00001, I^2=94%). Pooled LRs were calculated. The summary positive LR was 1.475 (95% CI 0.980-2.220) and negative LR was 0.757 (95% CI 0.574-0.998). There was statistical heterogeneity for the positive LR (p=0.000 I^2=94.9) and negative LR (p=0.000 I^2=94.2). A sensitivity analysis failed to identify a single study to account for heterogeneity but did demonstrate the analysis was sensitive to the aetiology of the study population. In the subgroup of 3 studies that only included patients with CAD (n=1325) the RR was 1.80 (95% CI 1.14-2.84) without significant heterogeneity (I^2=44%, P=0.17) [166,285,291] and in the NICM subgroup (n=738), the RR was 3.97, (95% CI 3.25-4.85) without heterogeneity (I^2=0%, P=0.58).[283,288,289] Summary estimates in other subgroups are given in Table 3.3. Of particular note, fQRS in the subgroup of 3 studies with mean/median LVEF>35% was associated with greater risk of mortality without statistical heterogeneity, when compared to the 7 studies with mean/median

LVEF ≤35%. fQRS in the subgroup with QRS duration ≥120ms was also associated with greater risk of mortality than QRS <120ms. However, meta-regression analysis showed no statistically significant influence of LVEF on the diagnostic odds ratio of fQRS as a predictor of mortality (P=0.907) or QRS duration (P=0.931).

3.3.4.2 fQRS and risk of ventricular arrhythmia

During a mean/median follow up of 14-49 months, 406 out of 3758 patients experienced an arrhythmic end point. Events were more common in patients with fQRS (RR 2.20, 95% CI 1.05-4.62) (Figure 3.3). Significant heterogeneity existed across all studies (P<0.00001, I^2=90). The summary positive LR was 1.535 (95% CI 1.035-2.278, I^2 92.3 P=0.000) and negative LR was 0.641 (95% CI 0.423-0.972, I^2=92.2% P=0.000). A sensitivity analysis demonstrated that the heterogeneity was sensitive to the studies by Cheema *et al.*, Forleo *et al.* and Das *et al.*. Excluding them from the analysis had only a small effect on the overall pooled estimate of RR (2.87, 95% CI 1.94-4.34) but removed any significant heterogeneity (I^2=0%, P=0.58). Summary estimates are given in Table 3.3. Of note, fQRS was associated with VA risk in both CAD and NICM, although the risk appeared greater in the later subgroup. Three studies only recruited patients with an ICD (n=1118), choosing a VA end point based on appropriate ICD therapy or ATP.[169,273,284] The pooled RR from these studies was 2.17 (95% CI 0.78-6.07, I^2=82%, P=0.004). The study by Cheema *et al.* reported appropriate ICD shocks (but not ATP) in the subgroup with ICDs, and including these data in the pooled estimate resulted in a RR of 1.66 (95% CI, 0.70-3.95, I^2=86%, P<0.0001). Restricting the analysis to the 2 studies with no ICD recipients (and therefore a much less rigid endpoint of VA diagnosed on ambulatory ECG monitoring) did not change this risk estimate appreciably (RR 1.46, 95% CI 0.61-3.53, I^2=0%, P=0.89).[285,289]

Meta-regression analysis showed no significant effect of LVEF (P=0.77) or QRS duration (P=0.77) on the diagnostic odds ratio of fQRS as a predictor of arrhythmic events. Excluding the study by Apiyasawat *et al.* (in case of influence due to the inclusion of patients with ARVC) resulted in RR of 2.06 (95% CI 0.90-4.70).

3.4 Discussion

This meta-analysis, including data from >5000 patients with CAD or NICM, has demonstrated that fQRS is associated with an increased risk of mortality and VA events.

fQRS is proposed as a tool to identify patients expressing fatal cardiovascular risk, and within that framework, it is important to identify SCD risk, as opposed to risk of non-modifiable mortality resulting from pump failure death.

Recording sudden death endpoints can be a challenge, and defining when an arrhythmic event should be considered a surrogate of SCD is difficult.[19292] This analysis included VA detected by ambulatory monitoring and CIED, in addition to appropriate ICD therapy. An important observation is that there was no increase in mortality risk in the subgroup of patients with CIEDs (predominantly ICDs), whereas fQRS was associated with mortality in the population as a whole. Since ICDs prevent sudden arrhythmic deaths, all-cause mortality might be driven by sudden death, and that fQRS may be more suited as a marker of SCD risk.

Two of the most robust markers of arrhythmia risk, frequently used to guide ICD therapy, are LVEF and QRS duration. Novel risk markers, such as fQRS, need to add incremental value to established risk markers if their use is to be exploited.[30] When considering just those patients with LVEF≤35%, RR of death or VA was not significant. Reduced LVEF is a strong predictor of both SCD and pump failure death and it is likely that in this subgroup fQRS did not add any discriminatory value. However, in those with LVEF>35%, fQRS was associated with around a two-fold risk of mortality and up to five times the risk of VA. In addition, amongst those with QRS<120ms, fQRS was not associated with an increased risk of mortality, but did convey a risk of VA of up to seven times. This meta-analysis cannot assess whether fQRS does add incremental benefit to established methods of risk stratification, but these observations nonetheless deserve attention.

fQRS has long been thought of as a marker of myocardial scar, causing conduction local disruption of activation, seen as fragmentation of QRS complexes on the 12-lead ECG.[162] In patients being assessed by left ventriculography, QRS conduction delay leading to an RSR' pattern was observed more frequently amongst patients with LV aneurysm than without.[163] This finding lead to the more formal definition by Das *et al.,* and analysis of fQRS in patients referred for cardiac stress testing by nuclear perfusion analysis.[164] fQRS was more sensitive than Q wave in detecting myocardial scar (85.6% v 36.3%), although Q wave presence was a more specific sign (99.2% v 89%). Further work by the group also related fQRS to myocardial necrosis,

although it is important to appreciate that the definition varied widely, including reversible and non reversible nuclear perfusion defects and regional wall motion abnormality on echocardiography or left ventriculography.[165,166]

It is plausible that the risks of mortality and VA in the presence of fQRS are due to an association of myocardial scar, but since few studies relate fQRS to both scar burden and relevant clinical endpoints, this conclusion cannot be firmly drawn. It is equally possible that fQRS is a predictor of risk that is independent of scar. MADIT II enrolled patients with ischemic heart disease and LVEF≤ 30%.[49] A retrospective analysis of this study found fQRS present in only around one third of patients, despite a history of MI.[170] In addition, there was no association between location of fQRS and Q waves. The study (presenting data in such a way that it could not be included in this meta-analysis), found fQRS associated with a 38% increase in SCD or appropriate ICD therapy. This leaves further doubt that fQRS risk is conferred due to an association with scar.

The meta-analysis included patients with CAD or NICM. The pattern of scar in these conditions differs to an extent that one might not expect uniform changes in localized conduction delay.[293] Despite this, risks of mortality and VA are seen with fQRS in both CAD and NICM. It is also noteworthy that the risk was greater in NICM patients, although compared to studies recruiting only patients with CAD, these patients had worse LVEF, and these findings are likely to represent a sicker patient population rather than specifically worse outcomes in the presence of fQRS.

3.5 Limitations

Although this meta-analysis was performed with strict methodology and included high quality studies, inherent limitations exist with this technique. There was considerable variability in study designs, and although statistical heterogeneity was managed with appropriate use of random effects analysis, patient populations and endpoint definitions did vary.

Most studies recruited a mixed population of NICM and CAD patients, with differing entry requirements for LVEF, QRS width and CIED status. Although subgroup analysis was possible, not all studies reported results suitable for pooling in this way.
As mentioned in the discussion, definitions used for SCD endpoint varied from a clinical diagnosis, through to a surrogate based upon ambulatory monitoring of VA, or ICD therapy. Even amongst those with ICD based SCD definitions, there was variation whether ICD delivery of antitachycardia therapy was included as SCD

surrogate endpoint, and ICD programming within and between studies was not standardized.

In several instances not all patients in a population were included in the original study due to limitations in the 12-lead ECG interpretation. Although studies reported good inter-observer agreement, accurate detection of fQRS requires a high quality ECG recording. In addition, several studies excluded patients with wide QRS or paced ECGs, even though definitions for fQRS in these conditions exist. In this meta-analysis there was no significant difference when these studies were excluded (not shown) but it is unknown whether the patients excluded from the original study might have had an impact on event rates.

Lastly, none of the studies in this meta-analysis evaluation included the use of fQRS in a randomized fashion. No conclusions can be made as to whether fQRS can aid in the selection of patients for ICD therapy.

3.6 Conclusion

fQRS is associated with all-cause mortality and the occurrence of SCD. These risks are seen in patients with CAD or NICM, and may be greater in those with LVEF>35%, with SCD risk worse in those with QRS duration <120ms. In the presence of fQRS, the RR of SCD is greater than that of all-cause mortality. These findings suggest that fQRS has the potential to indicate risk of SCD but the incremental benefit of fQRS as a risk stratifier, compared to current tools, should be assessed in a randomized, prospective setting.

	1. Study Participation	2. Study Attrition	3. Prognostic Factor Measurement	4. Outcome Measurement	5. Study Confounding	6. Statistical Analysis and Reporting
Das 2008	Low	Medium	Low	Low	Low	Low
Cheema	Low	Medium	Low	Low	Low	Low
Das 2010	Low	Low	Low	Low	Low	Low
Forleo	Low	Low	Low	Low	Low	Low
Rickard	Low	Medium	Low	Low	Low	Low
Sha	Low	Medium	Low	Low	Low	Low
Pei	Low	Low	Low	Low	Medium	Low
Yan	Low	Medium	Low	Low	Low	Low
Ahn	Low	Medium	Low	Low	Low	Low
Lorgis	Low	Low	Low	Low	Low	Low
Ozcan	Low	Medium	Low	Low	Low	Low
Apiyasawat	Low	Low	Low	Low	Low	Low

Table 3.1 QUIPS analysis of internal validity. Risk assessment is listed for six areas of potential study bias.

Study Name	Year	n	Study Population	Aetiology	QRS (ms)	LVEF inclusion	CAD %	Mean age (years)	Male (%)	LVEF (%)	QRS width (ms)	ICD (%)	SCD definition	follow up (months)	Death	SCD
Das	2008	879	Stable CAD	CAD	>120	Any	100	67	97	44	≥120	14	n/a	29	233	n/a
Cheema	2010	842	Stable HF	Mixed	Any	<=35%	79	66	78	26	30%≥120	52	Appropriate ICD shocks/SCD	40	191	99
Das	2010	184	ICD recipients	Mixed	<120	<=40%	68	63	90	29	100	100	Appropriate ICD shocks or ATP	16.6	19	41
Forleo	2011	392	Consecutive ICD recipients	Mixed	any	<=35%	61	66	85	27	130	100	Appropriate ICD shocks or ATP	26.3	64	37
Rickard	2011	232	Consecutive CRT recipients	Mixed	Any	<=40%	53	64	74	24	162	94	n/a	52.8	89	n/a
Sha	2011	80	Stable HF	NICM	Any	<=40%	0	54	68	30	95	8	ICD shocks or ATP/external CV/VT ablation	14	6	7
Pei	2012	1570	Stable HF	Mixed	Any	*<=45/50%	64	62	78	u/k	102	2	Appropriate ICD shocks/SCD	36	408	102
Yan	2012	176	Stable CAD	CAD	<120	>=45%	100	68	82	57	93	0	n/a	36	9	n/a
Ahn	2013	86	Stable HF	NICM	Any	<45%	0	55	62	25	120	0	VF/VT>100bpm >3 beats	36.9	3	3
Lorgis	2013	270	Post ACS	CAD	<120	Any	100	66	69	52	80	0	VF/VT>100bpm >3 beats	27.8	39	16
Ozcan	2013	227	Post HF admission	Mixed	<120	<35%	63	65	69	31	120	5	SCD	48.5	49	25
Apiyasawat	2014	71	Consecutive ICD recipients	Mixed	Any	Any	42	53	82	42	103	100	Appropriate ICD shocks or ATP	21.3	n/a	17
Total/Mean		5009					61	62	78	36	111	39		32	101	39

*<=45% in NICM and <=50% in CAD

Table 3.2 Summary of Study Characteristics. CAD, coronary artery disease; NICM, non-ischemic cardiomyopathy; LVEF, left ventricular ejection fraction; ICD, implantable cardioverter defibrillator; CRT, cardiac resynchronization therapy; ATP, anti-tachycardia pacing; SCD, sudden cardiac death; CV, cardioversion.

	Mortality				Sudden cardiac death			
Summary estimates	Relative risk ratio (95% CI)	Patient no.	Events	No. of studies	Relative risk ratio (95% CI)	Patient no.	Events	No. of studies
All	1.71(1.02-2.85)	4938	1140	11	2.20(1.05-4.62)	3758	406	9
Subgroups:								
CAD patients only	1.80(1.14-2.84)	1325	281	3	3.38(0.78-14.66)	1268	118	2
NICM patients only	3.97(3.25-4.85)	738	195	3	5.02(3.13-8.04)	738	66	3
CIED patients	1.13(0.91-1.41)	1245	268	4	1.66(0.70-3.95)	1118	182	3
LVEF≤35%	1.45(0.94-2.24)	2045	421	7	1.64(0.77-3.48)	1813	212	6
LVEF>35%	1.80(1.14-2.84)	1325	281	3	2.38(1.00-5.61)	377	36	2
QRS≥120ms	1.75(1.18-2.59)	1818	438	5	1.36(0.55-3.38)	705	65	3
QRS<120ms	1.13(0.54-2.35)	1368	245	4	3.83(1.96-7.48)	2211	242	5

Table 3.3 Summary estimates of relative risk rations of fQRS to predict mortality and sudden cardiac death. CI, confidence interval; CAD, coronary artery disease; NICM, non-ischemic cardiomyopathy; CIED, cardiac implantable electronic device; LVEF, left ventricular ejection fraction.

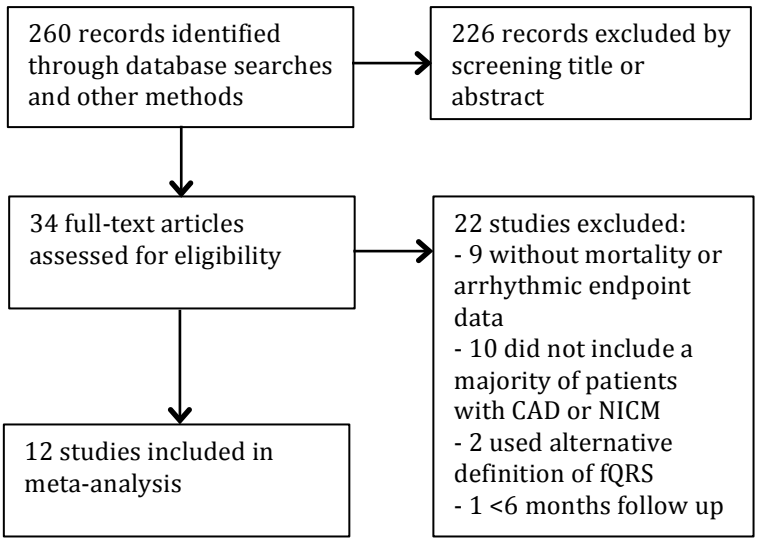

Figure 3.1 QUORUM flow diagram for the selection of articles included in the meta-analysis.

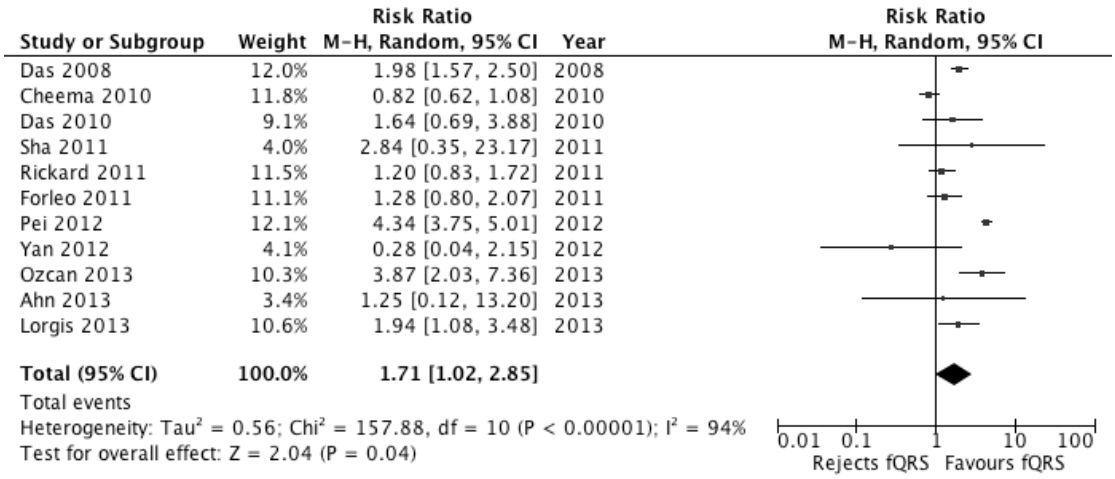

Figure 3.2 Summary of the relative risk of mortality in patients with fQRS. The size of the square for each study is proportional to the sample size. Weighting refers to the contribution of each individual study to the pooled result and was determined using the random effects model as detailed in the statistical section. For an explanation of the statistical tests used, please see the 'Statistics' section. CI, confidence interval.

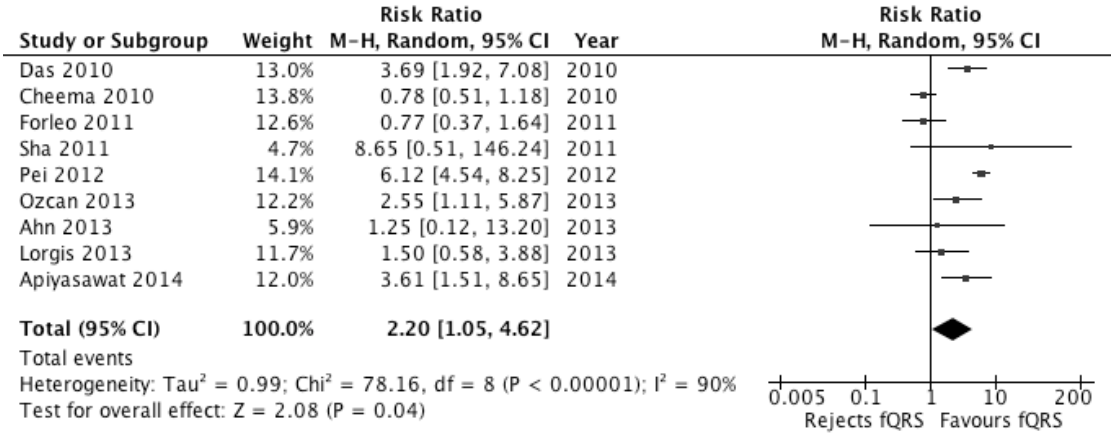

Figure 3.3 Summary of the relative risk of ventricular arrhythmia in patients with fQRS. The size of the square for each study is proportional to the sample size. Weighting refers to the contribution of each individual study to the pooled result and was determined using the random effects model as detailed in the statistical section. For an explanation of the statistical tests used, please see the 'Statistics' section. CI, confidence interval.

4 Ventricular repolarisation and myocardial scar

4.1 Introduction

The surface ECG markers of ventricular repolarisation, namely QTc, QTD and the TpTe, are associated with ventricular arrhythmogenesis in long QT syndrome where the mechanistic link is well established.[294] Such markers are also associated with the occurrence of SCD in the general population, as well as HF patients.[124,295,296] However in these populations the pathophysiological relationship with arrhythmogenesis is less clear.

LGE-CMR is known to accurately and reproducibly identify areas of myocardial scar, as well as discriminate between subendocardial and transmural scar more accurately than the surface ECG.[297] The extent of scar quantified by LGE-CMR has been shown to predict all-cause mortality in patients with CAD and delivery of appropriate anti-tachycardia therapy in patients fitted with ICDs.[298,299] In this context the role of scar in arrhythmogenesis is well established.[300] The relationship between the extent and distribution of LV scar, defined by LGE-CMR, and surface ECG markers of repolarisation, has however not been investigated. The aim of this study was to evaluate this relationship in a patient population with CAD known to be at high SCD risk.

4.2 Methods

4.2.1 Study Context

The study was conducted in a retrospective observational manner at the Wessex Cardiothoracic Unit, a regional cardiothoracic centre serving a population of approximately 3 million people.

4.2.2 Study Population

The study population consisted of consecutive CAD patients who underwent LGE-CMR prior to ICD implantation over a 4-year period (2006-2009). All patients had either been identified to be at high SCD risk using conventional risk stratification markers or experienced a prior life-threatening ventricular arrhythmia.

In these patients CAD had been defined as ≥70% stenosis in at least 1 epicardial coronary vessel on angiography and/or history of MI or coronary revascularization. All patients had undergone diagnostic coronary angiography with images reviewed by an expert physician.

4.2.3 CMR scar assessment

All patients were scanned according to the methods described in section 2.5 Cardiac Magnetic Resonance with scar assessment performed using OsiriX semiautomated analysis (Figure 4.1).

Two complementary aspects of scar were considered: (1) Total scar volume, quantified as a percentage of the total LV myocardial volume; (2) the transmural extent of scar.

The transmural scar assessment encompassed transmurality, which was split into quartiles (1-25%, 26-50%, 51-75% and 76-100%) and the number of segments of myocardium based on a standard American Heart Association 17-segment model, with each quartile of scar quantified.[301] CMR analysis was performed blinded to the clinical outcomes and ECG assessment.

To evaluate intra- and inter-observer agreement for the scar analysis methodology the per cent scar assessment was repeated in 15 patients by the same observer and 15 patients by a second observer, blinded to the results of the initial analysis.

4.2.4 Electrocardiographic Measurements

Repolarisation parameters were measured on standard resting 12-lead ECGs (25 mm/s, 10 mm/mV) acquired immediately prior to ICD implantation. The median time from the CMR being performed to the ECG being recorded was 15 days (6 to 159 days). ECGs were digitally scanned and measurements made with the use of digital callipers (Cardio Calipers version 3.3; Iconico Inc., New York, New York, USA) at approximately 400% magnification (Figure 4.1). All data was recorded prospectively but analysed retrospectively. Analysis was performed by a single investigator blinded to the patients' details. The repolarisation parameters measured (QTc, QTD and TpTe) were chosen based on previous studies[124,295,296].

The QT and QT peak intervals were measured in all 12 leads of each ECG. The QT interval was defined as the time interval between the initial deflection of the QRS complex and the point at which a tangent can be drawn to the steepest portion of the terminal part of T-wave, which crosses the isoelectric line.[302] The QT peak was measured from the beginning of the QRS until the peak of the T-wave. In the case of negative or biphasic T waves, the QT peak was measured to the nadir of the T wave. When U waves were present, the QT interval was measured to the nadir of the curve between the T and U waves, with the aid of a tangential method. T waves with amplitude <0.15 mV were not analysed. The measurement of each parameter was

obtained by averaging 2 consecutive beats. For each lead TpTe was obtained from the difference between the QT and QT peak intervals. The TpTe value quoted for each patient represented the average of the TpTe values in each lead. QTD was defined as the difference between the longest and shortest measured QT intervals on each ECG. The QTc value quoted represented the maximum value in all leads and was corrected for heart rate using Bazett's formula[303].

4.2.5 Patient Follow-up

As these study patients were ICD recipients they were followed up at 6 monthly intervals in office or remotely. Appropriate ICD therapy was defined as: (i) delivery of ATP for ventricular tachycardia (VT); (ii) delivery of shock therapy for VT or VF; and confirmed as such by analysis of stored electrograms by two electrophysiologists blinded to the CMR and ECG analyses.

4.2.6 Statistics

Categorical variables are expressed as numbers (percentages) and compared using Fisher's exact test. Normally distributed continuous variables are expressed as mean±SD and compared using Student's *t*-test. Variables not normally distributed are expressed as median (lower quartile to upper quartile).

The relationship between repolarisation variables (QTc, QTD and TpTe) and scar variables (percentage scar and number of segments with quartiles of scar transmurality) was explored in patients grouped based on the amount of scar. Patients were grouped into tertiles for percentage scar. The number of segments of scar for each quartile of transmurality was used to group transmural and non-transmural scar patients. The analysis of variance (ANOVA) test was used to compare the repolarisation variables across patient groups.

Univariable and multivariable regression analyses were performed to evaluate whether the association between subendocardial scar and repolarisation was independent of potential confounders. Diabetes, amiodarone use, LVEF and QRS width were chosen as covariables after initial analysis and in the light of previous studies that have demonstrated an association between these variables and ventricular repolarisation.[304] The multivariable analysis was performed using a general linear model.

The relationship between the repolarisation markers (QTc, QTD and TpTe) and delivery of appropriate ICD therapy was explored using univariable Cox proportional hazards analyses. For completeness clinical and CMR variables were also entered into the analysis though these results have been previously reported.[299]

Intra- and inter-observer agreement for scar quantification measurements were calculated using the intraclass correlation coefficient (ICC) for absolute agreement.

Statistical analyses were performed on SPSS Version 17 (SPSS Inc., Chicago, IL, USA). In all analyses a p value of <0.05 was considered significant.

4.3 Results

4.3.1 Patient Characteristics

During the study period there were 257 new ICD implants for CAD, of which 64 (25%) had an LGE-CMR prior to device implantation and were included in the study. The characteristics of patients who had an LGE-CMR (n=64) and were included in the study were broadly similar to those who did not have an LGE-CMR (n=193) (Table 4.1). However, patients that did not have LGE-CMR were significantly more likely to have had a previous MI than patients that did have a scan (92 vs. 77%, p=0.003).

Baseline demographics of the 64 patients included in the study are shown in Table 4.1. There was a balanced distribution of primary and secondary indication patients (48% vs. 52% respectively), signalling no selection bias based upon prior arrhythmia. Patients were on optimal medical therapy for HF (beta-blockade in 86% and angiotensin-converting enzyme inhibitor (ACE-I)/ARB in 88%).

In all patients LGE-CMR was performed to guide the need for potential revascularisation prior to ICD implantation. This included an assessment of myocardial viability in all patients, as well as an assessment of ischaemic burden in the majority of patients (73%, n=47).

4.3.2 CMR Variables

In the study population median LVEF was 30% (22 to 39%), mean end-systolic volume 192±96 mls and mean end-diastolic volume 269±97 mls. Fifty-eight patients (91%) had evidence of scar on the late enhancement images. The median amount of scar was 12.6% (5.9-21.2%). Only a minority of patients (n=9, 14%) had one or more segments of subendocardial scar (1-25% transmurality). In contrast most patients had evidence of semi-transmural (51-75% transmurality) (n=38, 59%) and transmural scar (76-100% transmurality) (n=48, 75%).

The ICC for per cent scar quantification was 0.91 for intra-observer agreement and 0.89 for inter-observer agreement (p<0.001 for both), demonstrating high reproducibility.

4.3.3 Repolarisation Variables and Relationship to Scar Indices

In the study population mean QTc was 472±56 ms, mean QTD 69±45ms and mean TpTe 85±18ms.

There was a significant association between the number of LV segments with subendocardial scar, defined as scar with 1-25% transmurality, and markers of repolarisation (Table 4.2) The greater the number of segments of subendocardial scar, the higher the value of QTc (p=0.009), QTD (p=0.026) and TpTe (0.029). However there was no association between the repolarisation variables and per cent LV scar or the number of LV segments with scar greater than 25% transmurality (Table 4.2 and Table 4.3)

Regression analysis evaluated whether the association of subendocardial scar with QTc, QTD and TpTe was independent of other variables that may influence ventricular repolarisation (

Table 4.4). When corrected for the presence of diabetes, amiodarone use, QRS width and LVEF the number of LV segments with subendocardial scar remained strongly associated with QTc (P=0.003), QTD (p=0.002) and TpTe (p=0.008).

4.3.4 Relationship of Repolarisation Parameters to the Occurrence of Appropriate ICD Therapy

During a mean follow-up of 19±10 months 19 (30%) patients received appropriate ICD therapy. Five (8%) patients died but predictors of death were not evaluated in view of the small number of patients. The ICD VT treatment zone lower setting was similar in patients who did, and did not, receive appropriate ICD therapy (147±26 beats per minute [bpm] vs. 149±23 bpm respectively; p=0.83). The distribution of appropriate ICD therapies was:

No episodes of appropriate ICD therapy – 45 patients
Appropriate ICD therapy for VT (rate <182bpm) only – 10 patients
Appropriate ICD therapy for fast VT (rate ≥182bpm) – 8 patients
Appropriate ICD therapy for VF – 1 patient

Univariable Cox proportional hazards analyses assessed the relationship between the markers of repolarisation (as well as other clinical and CMR variables) and the

occurrence of appropriate ICD therapy (Table 4.5). As previously described there was a strong association between appropriate ICD therapy and the scar parameters per cent scar (p=0.02) and number of transmural (76-100% transmurality) scar segments (p=0.001), but not the number of segments with subendocardial (1-25% transmurality) scar (p=0.48).[299] Furthermore, there was no significant association between the occurrence of appropriate ICD therapy and QTc (p=0.33), QTD (p=0.39) and TpTe (p=0.53). In view of the lack of association between the repolarisation markers and appropriate ICD therapy in univariable analyses multivariable analysis was not performed.

4.4 Discussion

In this small retrospective study of patients with CAD at high SCD risk there was a strong association between the extent of subendocardial LV scar, defined by LGE-CMR, and prolonged QTc, QT dispersion and TpTe. Furthermore, this association was independent of the presence of diabetes, amiodarone use, QRS width and LVEF, factors that may affect ventricular repolarisation. However, there was no association between any of the repolarisation markers or the extent of LGE-CMR defined subendocardial scar and the delivery of appropriate ICD therapy.

The finding that repolarisation markers did not predict the delivery of appropriate ICD therapy in this cohort is consistent with the results of previous studies performed in HF patients undergoing device implantation. Lellouche *et al*. evaluated a range of ECG markers of repolarisation and the occurrence of appropriate ICD therapy in 100 patients undergoing CRT defibrillator implantation.[305] Neither baseline QTD nor TpTe were independent predictors of appropriate ICD therapy. In addition Chalil *et al*. investigated the association of ECG repolarisation parameters and SCD or resuscitated cardiac arrest in 75 patients undergoing CRT implantation without defibrillator therapy.[306] In this study too, baseline QTc, QTD and TpTe were not predictive of events. Although these studies were relatively small, taken together the results suggest that baseline QTD and TpTe are not significant predictors of the occurrence of SCD or appropriate ICD therapy in patients with significant LVEF impairment undergoing device implantation.

ECG markers of ventricular repolarisation have consistently demonstrated an association with the occurrence of arrhythmic events in patients with long QT syndrome. QTc, TpTe and QTD have all shown an association with the occurrence of ventricular arrhythmias or death, and QTc is consistently one of the strongest predictors of cardiac events.[294] These ECG parameters have also been evaluated as markers of SCD in the general population. QTc and QTD were first proposed as

markers of increased mortality risk in the general population over a decade ago, however results have been inconsistent. While a number of large population-based studies have found a strong association between these markers and all-cause mortality or SCD others have not.[114,295,296] More recently Panikkath *et al*. evaluated the association of TpTe and SCD in a population-based case-control study of 353 cases of SCD and 342 matched controls.[124] Mean TpTe was significantly greater in cases than controls ($p<0.0001$), and remained a significant predictor of SCD when adjusted for age, sex, QTc, QRS duration and LVEF.

In patients with long QT syndrome enhanced dispersion of repolarisation provides a proarrhythmic substrate for the occurrence of torsades de pointes, which may degenerate into VF resulting in SCD.[294] As such, in long QT syndrome QTc, QTD and TpTe are direct markers of the arrhythmogenic substrate that underlies SCD risk. In the general population, or selected patients with depressed LVEF, the arrhythmias that are most likely to cause SCD are VT (that may subsequently degenerate into VF) and primary VF, rather than polymorphic VT.[33] In contrast to long QT syndrome the mechanism by which prolonged QTc, QTD and TpTe may be associated with SCD in the general population is less clear.

Most studies of SCD in the general population have suggested that around three quarters of patients that die suddenly have CAD.[307] Furthermore, these risks are not only confined to patients with current or previous ST-elevation MI (MI). Despite modern management the 5-year risk of death following non-ST-segment elevation (subendocardial) MI is up to 11%.[308] The results raise the possibility that in some patients prolonged QTc, QTD and TpTe may be associated with the occurrence of SCD as markers of previous subendocardial MI, rather than as indicators of increased dispersion of repolarisation.

The discrepancy between the results of the population-based studies and those performed in patients with CRT devices is unclear, however it may be partly related to the differences in study population. Two different mechanisms of ventricular arrhythmogenesis are thought to underlie the majority of SCD cases. In some patients arrhythmias occur in the context of acute myocardial ischaemia, which may arise in patients with or without previous myocardial scar.[309] In other cases, ventricular arrhythmias arise from an anatomical substrate, which is most commonly ventricular scar from a previous MI, without clear evidence of an ischemic trigger.[14] In patients with advanced HF undergoing CRT implantation, SCD is more likely to occur due to ventricular arrhythmias arising from chronic LV scar.[298] However in the general

population SCD most commonly occurs due to acute ischemia.[309] QTc, QTD and TpTe may be more strongly associated with one mechanism of SCD than another.

However the new finding is that prolonged QTc, TpTe and QT dispersion are associated with the presence of subendocardial, rather than transmural scar. This finding is consistent with both clinical and laboratory data. Chauhan *et al*. compared early post-MI changes in QTc and QTD in 40 patients with a non Q-wave MI and 69 patients with a Q wave MI.[310] Although QTc and QTD were prolonged in both sets of patients, those with non Q-wave infarcts had significantly greater increases than patients with Q-wave infarcts ($p<0.05$ for both ECG parameters). Yan *et al*. explored the effect of excision of the endocardium on myocardial repolarisation in an arterially perfused canine LV wedge preparation.[118] They found that excising the endocardium, as essentially occurs in a subendocardial infarction, prolonged ventricular repolarisation time of the M cells, the cells whose repolarisation determines the end of the T wave.[118] It is interesting to speculate that the use of LGE-CMR to identify subendocardial scar could help to refine the understanding of abnormal repolarisation and its importance in arrhythmogenesis, both as a pathophysiological mechanism and as a non-invasive marker. Likewise, the simplicity of an ECG marker of abnormal repolarisation might identify those who need imaging as part of SCD risk assessment. However these findings require confirmation in a larger study powered to look at population screening and mortality end-points.

Although it is widely acknowledged that a significant dispersion of repolarisation exists in the human heart, there is debate as to whether this dispersion is predominantly due to a repolarisation gradient from base to apex, or transmurally.[311] Interestingly in this study the main determinant of prolonged QTc, QTD and TpTe was the number of LV segments with subendocardial scar (1-25%), rather than the total amount of scar or the number of segments with more transmural scar (>25%). These findings are more supportive of a transmural repolarisation gradient being the predominant factor in determining dispersion of ventricular repolarisation, at least in patients with CAD and depressed LVEF. However, this study is too small to draw definitive conclusions regarding this issue.

4.4.1 Limitations

This is an observational study and has the limitations inherent in such a study design. The apparent association demonstrated between subendocardial scar and markers of repolarisation may be due to an unmeasured confounding factor. I included only a small number of patients and these findings need repeating in a larger cohort of patients.

Only patients with CAD who had undergone LGE-CMR prior to ICD implantation were included. The rationale for doing this was to evaluate the relationship between the ECG repolarisation markers and LV scar in a population of patients at high SCD risk. However, as a consequence of the specific inclusion criteria it may not be possible to generalise these findings to other patient populations. In addition the majority of patients (80%) were men and it again may not be possible to generalise the results to women. Furthermore, during the 4-year study period only 25% of new ICD implants for patients with CAD had an LGE-CMR prior to device implantation. Although the baseline demographics of ICD recipients who did and did not have an LGE-CMR were broadly similar, LGE-CMR is an expensive investigation and there may well be some selection bias related to local referral patterns not adequately captured by this baseline demographic data.

Different methods are available for the measurement of QTc, QTD and TpTe, as well as the correction of these variables for heart rate. The use of these alternative methods may have had some impact on the results.

Lastly, there are a number of different methods for the quantification of scar. Although scar quantification using this methodology is reproducible, it is unclear how well it correlates with infarct size in this dataset and using a different methodology may have yielded different results.

4.5 Conclusion

In this small retrospective study of patients with CAD at high SCD risk there was a strong independent association between the presence of subendocardial LV scar, quantified by LGE-CMR, and prolonged QTc, QTD and TpTe. However, there was no association between any of repolarisation markers and the delivery of appropriate ICD therapy. ECG analysis could be a tool to select on a population basis those that need imaging as part of SCD risk assessment.

	All new ICD Implants (n=257)		
	LGE-CMR (n=64)	No LGE-CMR (n=193)	P value
Age (years)	66±11	69±9	0.06
Male, n (%)	51 (80)	168 (87)	0.16
History of AF, n (%)	17 (27)	65 (34)	0.35
Diabetes, n (%)	17 (27)	53 (27)	1.0
Hypertension, n (%)	30 (47)	70 (36)	0.14
Previous MI, n (%)	49 (77)	177 (92)	0.003
Previous PCI, n (%)	13 (20)	35 (18)	0.71
Previous CABG, n (%)	21 (33)	85 (44)	0.14
Any previous pre-ICD revascularization, n (%)	28 (44)	109 (56)	0.08
Device Type, n (%)			
ICD single chamber	8 (12)	35 (18)	0.34
ICD dual chamber	32 (50)	91 (47)	0.77
CRT-D	24 (38)	67 (35)	0.76
ICD VT treatment zone lower setting (bpm)	148±24	149±19	0.65
Resting heart rate (bpm)	64±13	67±11	0.09
QRS width (ms)	122±31	125±29	0.44
ICD indication, n (%)			
Primary Prevention	31 (48)	82 (42)	0.47
Secondary prevention	33 (52)	111 (58)	-
Beta-blocker, n (%)	55 (86)	142 (74)	0.06
ACE-I/ARB, n (%)	56 (88)	165 (85)	0.84
Amiodarone, n (%)	15 (23)	52 (27)	0.63
Creatinine (µmol/l)	111±35	121±36	0.05
Haemoglobin (g/dl)	130±16	132±18	0.43

AF, atrial fibrillation; MI, myocardial infarction; PCI, percutaneous intervention; CABG, coronary artery bypass grafting; VT, ventricular tachycardia; ACE-I, angiotensin-converting enzyme inhibitor; ARBs, angiotensin II receptor blockers.

Table 4.1 Clinical characteristics of all new ICD implants during the study period, presented on the basis of whether they had an LGE-CMR prior to ICD implantation.

Scar transmurality	Number of scar segments for each quartile of scar transmurality			P value
	0 segments	1 segment	≥2 segments	
1-25% Transmurality				
Patient number (n=64)	55	6	3	
QTc (ms)	464±48	506±90	548±32	0.009
QTD (ms)	64±38	86±58	131±96	0.026
TpTe (ms)	82±17	95±22	106±23	0.029
26-50% Transmurality				
Patient number (n=64)	27	10	17	
QTc (ms)	467±62	480±54	470±48	0.75
QTD (ms)	76±43	65±41	64±53	0.65
TpTe (ms)	80±17	86±16	90±21	0.23
51-75% Transmurality				
Patient number (n=64)	26	21	17	
QTc (ms)	467±57	475±54	475±58	0.87
QTD (ms)	61±38	78±46	73±53	0.41
TpTe (ms)	81±16	85±19	90±20	0.30
76%-100% Transmurality				
Patient number (n=64)	16	15	33	
QTc (ms)	468±56	461±53	479±57	0.57
QTD (ms)	77±52	60±49	70±40	0.59
TpTe (ms)	81±21	84±14	87±18	0.63

Table 4.2 Relationship between the amount of transmural and non-transmural scar and ECG markers of repolarisation. Data are given for each quartile of scar transmurality. Group comparisons were made using the ANOVA test.

Repolarisation variables	Patients grouped by tertiles of increasing per cent scar			P value
	0-8.1% (n=21)	8.2-19.2% (n=22)	>19.2% (n=21)	
QTc (ms)	451±48	490±64	472±48	0.07
QTD (ms)	61±38	76±50	71±47	0.55
TpTe (ms)	78±14	89±19	87±19	0.09

Table 4.3 Relationship between per cent LV scar and surface ECG markers of repolarisation. Patients are grouped into tertiles of increasing scar. Group comparisons were made using the ANOVA test.

	P values					
	QTc		QTD		TpTe	
	Univariable	Multivariable	Univariable	Multivariable	Univariable	Multivariable
No. of segments of subendocardial scar	0.002	0.003	0.001	0.002	0.002	0.008
Diabetes	0.70	0.83	0.81	0.82	0.80	0.91
Amiodarone	0.058	0.036	0.007	0.008	0.003	0.004
QRS width	<0.001	<0.001	0.22	0.39	0.008	0.022
LVEF	<0.001	0.022	0.21	0.61	0.049	0.36

Table 4.4 Association of the number of segments of subendocardial (1-25%) scar and QTC, QTD and Tpeak-end in univariable and multivariable regression models.

	Univariable Analysis	
	P value	Hazard Ratio (95% CI)
Clinical variables		
Age (per year)	0.26	0.98 (0.94-1.02)
History of AF	0.20	0.45 (0.13-1.53)
Amiodarone use	0.04	0.12 (0.02-0.97)
Any previous pre-ICD revascularization	0.04	0.30 (0.09-0.95)
ECG variables		
QRS width (per 10 ms increase)	0.13	0.88 (0.75-1.04)
QTc (per 10ms increase)	0.33	0.96 (0.88-1.04)
QTD (per 10ms increase)	0.39	0.95 (0.84-1.07)
TpTe (per 10ms increase)	0.53	0.92 (0.71-1.19)
CMR variables		
LVEF (per 10% decrease)	0.86	1.03 (0.76-1.39)
Per cent scar (per 10% increase)	0.02	1.75 (1.09-2.81)
Number of affected segments by transmurality in a 17-segment model:		
1% to 25%	0.48	0.67 (0.22-2.04)
26% to 50%	0.77	0.95 (0.68-1.34)
51% to 75%	0.15	0.72 (0.45-1.13)
76% to 100%	0.001	1.40 (1.15-1.70)

Table 4.5 Relationship between clinical, ECG and CMR parameters and the occurrence of appropriate ICD therapy in univariable Cox proportional hazards models.

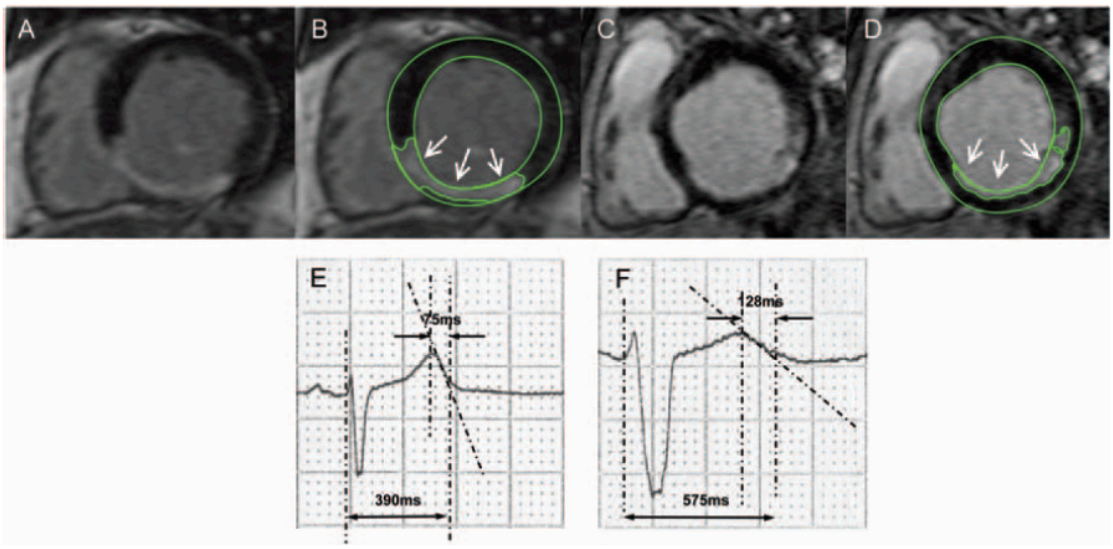

Figure 4.1 Short-axis LGE-CMR images from two patients with different patterns of LV scar. Images A and C are the plain LGE-CMR images. In B and D the images have been loaded on to customised software, the epi- and endocardium outlined manually and the infarct core automatically detected. In patient 1 (images A and B) there is a predominantly transmural inferoseptal scar (arrows). In contrast, in patient 2 (images C and D) there is an inferoposterior scar which is predominantly subendocardial (arrows).

5 Can QRS Scoring Predict Left Ventricular Scar and Clinical Outcomes?

5.1 Introduction

Sudden cardiac death (SCD) risk is reduced by Implantable Cardioverter Defibrillators (ICD) in appropriately selected patients. Impairment of LV function and QRS duration are used as risk discriminants in current guidelines, but result in many patients receiving an ICD from which they gain no benefit, as only the minority receive appropriate treatment for life threatening arrhythmias. Furthermore, ICD implantation carries procedural risk and long term morbidity related to device malfunction, need for device replacement and unnecessary or inappropriate shock delivery.[59272] Therefore approaches are needed that identify patients with greatest potential to benefit from ICD therapy.

Extent of LV scar, characterised by CMR-LGE, is associated with the occurrence of spontaneous ventricular arrhythmias in patients receiving ICD therapy.[299] However, CMR-LGE has limitations as a risk stratification tool. It is not a bedside test or widely available due to the expense and clinical expertise required. By contrast, the 12 lead ECG is easily available and its use as a marker for scar burden could offer powerful benefit.
The Selvester QRS score is derived from ECG analysis to quantify LV scar. “Points” are awarded for duration and amplitude criteria, adjusted according to conduction pattern (see methods).[183] Although it is reported that the score is significantly associated with LV scar, the strength of that correlation is unclear.[178,180–182,184] This may be due to the selected study populations, or scar characteristics such as transmural thickness and surface area. In addition, there is only circumstantial evidence that QRS scoring predicts clinical outcomes due to association with scar.[185]

Therefore, this study investigates Selvester scoring in an ICD population, in whom both myocardial scar and clinical outcome data is established, to determine if (a) the Selvester QRS score is a surrogate of scar burden (b) the performance of the score varies according to scar characteristics, and (c) QRS score can meaningfully predict SCD.

5.2 Methods

5.2.1 Study Population

This is a retrospective, observational study conducted at the Wessex Cardiothoracic Unit, a regional cardiothoracic centre serving a population of ≈3 million people. The study population has previously been described in detail, and consists of consecutive patients with CAD who had undergone LGE-CMR before ICD implantation over a 4-year period (2006 to 2009).[299]

5.2.2 QRS Scoring

ECG analysis was performed on standard resting 12 lead ECGs, recorded immediately prior to ICD implantation. Recordings were digitally scanned, displayed at 400% magnification and measured using on screen callipers (Cardio Calipers v3.3, Iconico, USA). An experienced cardiologist scored the ECG according to the published 50-criteria/31-point modified Selvester QRS method.[312] In summary, ECGs are first categorised according to conduction pattern: LBBB or RBBB, left anterior fascicular block (LAFB), left ventricular hypertrophy (LVH), right ventricular hypertrophy, RBBB+LAFB, or a normal pattern. Points are then awarded in leads I, II, aVL, aVF, and V1 through V6 according to presence of QRS notching, duration and amplitude criteria. The criterion thresholds are adjusted to account for younger men with increased voltage and older women with lower voltages. Each point represents 3% of myocardial scar (Figure 5.1 and Figure 5.2). With training, the score can be manually calculated in less than 10 minutes. Automated techniques have been developed but are not commercially available and were not used in this study. Scoring was repeated at a separate sitting on 15 patients by the same scorer to evaluate intraobserver error. In addition, a second scorer evaluated the ECG in 15 cases. Both scorers were independent and blinded to the CMR scar analysis.

5.2.3 CMR scar assessment

All patients were scanned according to the methods described in section 2.5 Cardiac Magnetic Resonance with scar assessment performed using OsiriX semiautomated analysis. Scar was measured in terms of (1) the amount of scar, quantified as a percentage of the total LV myocardial volume, (2) the total epicardial and endocardial scar surface area, and (3) the transmural extent of scar. For the transmural scar assessment, LV myocardium was divided according to the standard American Heart Association 17-segment model.[301] Scar thickness was split into quartiles (1% to 25%, 26%-50%, 51-75% and 76%-100%). A segment with no scar extending beyond 25% thickness was considered as subendocardial, and a segment with any scar extension between 76%-100% thickness was classified as transmural.

5.2.4 Study Follow-Up and End Points

All patients were followed at 3 to 6 month intervals via either a hospital visit or a remote management system. According to contemporary evidence, >2 episodes of ATP were programmed in the VT zone.[313] Patients under remote follow-up were also seen at the hospital every 6 months. At each visit, the patient was clinically assessed and the device interrogated. The occurrence of any ICD therapy was recorded. The two study end points were:

(i) appropriate ICD therapy and

(ii) all-cause mortality,

chosen to explore the ability of Selvester scoring to predict arrhythmic SCD versus non SCD. Appropriate ICD therapy was defined as ATP for VT or shock therapy for VT or VF. Correct arrhythmia detection or discrimination was confirmed by analysis of stored electrograms by 2 electrophysiologists blinded to the CMR analysis and QRS score.

5.3 Statistical Analysis

Categorical variables are expressed as numbers (percentages) and compared using Fisher's exact test. Normally distributed continuous variables are expressed as mean±SD and compared using Student's t-test. Variables not normally distributed are expressed as median (lower quartile to upper quartile).

The relationship between the QRS score and the LV scar variables was determined by Spearman's rank correlation and Bland-Altman plots used to analyse the agreement between the methods. Nonparametric receiver operating characteristic (ROC) curves were used to assess the ability of the QRS score to diagnose the presence of CMR-LGE scar.

The relationship between Selvester QRS score and study end points was also explored using univariate Cox proportional hazards models. Hazard ratios were calculated by constructing multivariable Cox models including QRS score and variables previously shown to be associated with increased risk (age, creatinine, AF, and QRS duration) and adjusting for LV end diastolic volume (LVEDV) and LVEF [314]. For the end-point of ventricular arrhythmia, multivariable analysis was not performed as there was no significant association with QRS score in univariable analyses.

Survival difference in the study population, stratified according to low or high QRS score was depicted using the Kaplan-Meier method. Differences in event rate between groups over time were compared using the Wilcoxon test of Breslow.

Unadjusted and adjusted HRs with their corresponding 95% CIs are reported.

Intra-observer and inter-observer agreement for ECG measurements were calculated using the ICC for absolute agreement. Statistical analyses were performed on SPSS Version 19 (IBM SPSS, Chicago, IL, USA). In all analyses a p value of <0.05 was considered significant.

5.4 Results

5.4.1 Study Patients

Sixty-four consecutive patients with CAD who had both LGE-CMR and new ICD implant and were included in the study. The average age was 66±11 years, 51 (80%) were male, and all patients were on optimised medical therapy for HF. There was a balanced distribution of primary and secondary indication patients (48% vs. 52% respectively). The ICD VT treatment zone lower setting was similar in patients who did, and did not, experience study end-points (147±26 beats per minute (bpm) vs. 149±23bpm respectively; p=0.83).

5.4.2 CMR Variables

Median time from CMR to ICD implantation was 15 days (6-159). In the study population median LVEF was 30% (22 to 39%). The mean end-systolic volume was 192±96 mls and mean end-diastolic volume 269±97mls. Fifty-eight patients (91%) had evidence of scar tissue on the late enhancement images. The median amount of scar was 12.6% (5.9-21.2%). Only a minority of patients (n=9, 14%) had one or more segments of subendocardial scar (1-25% transmurality). In contrast most patients had evidence of transmural scar (76-100% transmurality) (n=48, 75%).

5.4.3 QRS scoring

62 patients (97%) had at least 1 QRS point. Median QRS score was 6 (3-9) equal to estimated LV scar of 21% (9%-27%). Baseline characteristics were similar between those with low score (<6points) and high score (≥6) (Figure 5.1)

5.4.4 Reproducibility of QRS scoring

The ICC was 0.94 for intra-observer error and 0.94 for inter-observer error indicating an excellent reproducibility.

5.4.5 QRS Scores to Identify CMR Late-Gadolinium Enhancement

QRS scores correctly identified the presence of scar in 57/58 (98%) patients. However, only 1/6(17%) patients with no scar were correctly identified. Only 17/59 (29%) patients had anatomically matched QRS score and scar.

Analysis of QRS score as predictor of scar showed an area under the ROC curve of 0.66 (95% CI, 0.39 to 0.94). A cut-off of QRS score 1 resulted in a sensitivity of 98.3% (89.5-99.9), specificity of 16.7% (0.80% to 63.5%) and accuracy of 90.6%. A cut-off of 5 increased specificity to 50% (13.9% to 86.0%), with a sensitivity of 67.2% (53.5% to 78.6%), and accuracy of 65.6% (Figure 5.3).

5.4.6 QRS Score as an estimate of CMR-LGE Scar Characteristics

As a continuous variable, there was moderate correlation between QRS score and CMR scar (*r*=0.42 P=0.001) (Figure 5.4) and CMR scar surface area (*r*=0.41 P=0.001). Bland Altman analysis revealed a mean difference between ECG derived and CMR scar size of 6.0% (Figure 5.5).

Amongst those patients with evidence of subendocardial scar (n=9), there was no significant correlation with CMR scar. However, when considering those patients with some transmural scar (n=48), there was moderate correlation between QRS score and CMR scar (*r*=0.49 P<0.001). The strongest correlation was seen in those patients with transmural scar only (n=16, *r*=0.62 P=0.01).

5.4.7 Outcomes

During a mean follow-up of 42±13 months 28 (44%) patients received appropriate ICD therapy and 14 (22%) patients died.

5.4.8 Appropriate ICD therapy

Increasing QRS score was not a significant risk for VT/VF occurrence (any appropriate ICD therapy) (HR=0.99; CI=0.91-1.09; P=0.88), even when stratified according to transmural scar burden, ECG confounder or scar location. There was no correlation between QRS score and rate of VA defined as number of therapies per year.

5.4.9 All cause mortality

QRS score as a continuous variable was significantly related to mortality (HR=1.16; 95% CI=1.03 to 1.30; P=0.01). QRS remained the only significant risk in a multivariable model, adjusted for clinical variables, LVEDV and LVEF (Table 5.2.).

5.4.10 QRS score and Kaplan-Meier analysis

Survival curves were compared between patients stratified according to low and high QRS score. Using Kaplan-Meier analysis, death occurred in 9 of 24 patients in the high score group (QRS score ≥6), 5 of 26 patients in the low score group (QRS <6) (P=0.03) (Figure 5.6).

5.5 Discussion

This small, retrospective observational study of CAD patients selected for ICD therapy has shown that Selvester QRS scoring can detect the presence of LV scar with high sensitivity and accuracy, but poor specificity. QRS score correlates moderately well with the extent of scar and scar surface area with the strongest correlation seen in subjects with transmural scar

only, and no association with subendocardial scar. Furthermore, over a mean follow-up period of 42 months, increasing QRS score was associated with an increased risk of mortality (but not an increased occurrence of ventricular arrhythmia). To the best of my knowledge, this study is unique in reporting QRS scores from a cohort in whom both CMR scar burden and clinical outcomes are known.

The utility of the QRS Selvester score to predict presence of myocardial scar has previously been reported by several groups, using magnetic resonance imaging as reference.[178][180][181][182] These studies were performed using the standard Selvester score, requiring the presence of an ECG free of conduction defects, and report a very wide range of correlation between QRS score and CMR scar, varying from poor to good (r=0.33-0.78).

This study used the modified QRS score that has more recently been refined to take account of ECG conduction confounders.[183] In the largest analysis of the updated score, 162 patients with poor LVEF of mixed aetiology were included.[184] Correlation with CMR scar was stronger than that seen in the current study (r=0.74 for the whole group), with even stronger correlation for some ECG subgroups (e.g. LBBB, r=0.80). There are several possible explanations why these previous results seem to suggest stronger QRS scoring performance.

First, patients included in the study by Strauss *et al*. received ICD for primary prevention, and as such had LVEF≤35%. Second, the study manually segmented LGE-CMR and included border zone in the calculation of total scar. By contrast, this study quantified LGE-CMR using a SI ≥50% of the maximum SI, with no reference to peri-infarct zone. A standard method for quantification of peri-infarct zone has not been universally agreed, and at clinical CMR resolutions, peri-infarct zone can be hard to distinguish from partial volume averaging, effects that cannot be accounted for when measuring total scar volume manually.[315][316][317] Irrespective of the methodology used, the role for assessment of border zone does not appear to enhance prediction of arrhythmia risk, compared to quantification of scar size alone.[318] Clearly there is scope to develop improved approaches of CMR scar assessment, including the use of higher field strength to better visualise micro-infarcts, and quantification of diffuse myocardial fibrosis.[319]

Third, the Selvester score was developed in the pre-reperfusion era, using computer simulation and ventriculography data, and subsequently validated with reference to post mortem hearts with single infarcts.[173][174][175][320] In these studies, where higher scoring, larger infarcts tended to extend through the myocardium, transmurality could only be described at three cut surfaces (basal, mid and apical) of the heart. Thus, there are obvious limitations when applying these historically derived data to a contemporary population studied with LGE-CMR. Although some limited data do exist describing transmurality of scar and QRS

scoring in the acute, single location infarction setting[179], the study is, to my knowledge, the first to report how QRS performance may vary with chronic scar thickness in variable locations. In patients with multi-location infarcts of varying thickness, the same linear relationship between scar area, transmurality and QRS score may not hold true. It is therefore possible that the score best reflects single location, transmural scar rather than total scar.

It is well understood that while patients receiving ICD therapy may avoid arrhythmic death, many with low LVEF will still go on to die from pump failure and it was these differences in mode of death that were explored. Variation in end point definitions may account for the lack of clarity in using QRS scoring to predict clinical arrhythmia. A high QRS score has been shown to significantly predict monomorphic VT inducibility in CAD patients receiving ICD therapy (P=0.006), although the authors accept the limitation of this surrogate measure in predicting clinical prognosis.[184] Arrhythmia was also investigated during a median 45.5 month follow up of 797 ICD recipients enrolled in SCD-HeFT (where arrhythmia events were defined as appropriate shock therapy delivered for detected rates ≥188bpm).[185] Although CMR scar data in this group was not known, each 3 point increase in QRS score was significantly related to shock therapy (HR=1.14, P=0.01), and a secondary endpoint of time to incident VT/VF or all-cause mortality (HR=1.13, P=0.01). Mortality alone was not explored. I chose the end points in the ICD population to distinguish the risk of SCD from non SCD. The study is therefore unique in that it includes data on the QRS score, CMR scar, VT/VF and death. Appropriate therapy does not necessarily reflect life threatening VA and it is possible that some VT episodes might have spontaneously reverted without the need for ICD pacing or shock.[59] My research group has however previously reported that CMR scar burden is predictive of appropriate ICD therapy in this patient cohort.[299] Therefore a scoring system that accurately describes scar would also be expected to predict appropriate ICD therapy in this group. In the current study, despite the relatively weak predictive accuracy for extent of scar, QRS score was associated with mortality, but not ventricular arrhythmia.

The arrhythmogenic potential of transmural and subendocardial scar differ, and this may explain why, in this cohort, the score was predictive of death and not associated with ventricular arrhythmia. The study has cast doubt on the accuracy of the Selvester QRS score to accurately describe the type of mixed scar seen in chronic ischaemic cardiomyopathy. A larger, multicentre study is needed to robustly evaluate the limits of the score in clinical practice and determine whether ICD therapy can be effectively targeted based on QRS score. It is arguable that a high score predicts a non-arrhythmic mode of death that will not be prevented by device therapies for ventricular arrhythmia, and could still therefore find application in better targeting of ICD therapy.

5.5.1 Limitations

The present study had several limitations. First, it is an observational study and has all the limitations inherent in such a study design.[321] The performance of QRS score to quantify scar, the lack of arrhythmia prediction, and apparent association between QRS score and mortality may be confounded by an unidentified factor.

Second, ECGs acquired at the time of ICD implantation were part of clinical practice and were not systematically obtained by the same operator. Although all ECG acquisition took place in the context of a tertiary referral cardiac centre with experienced electrocardiographers, it remains possible that slight variation in location of electrodes could affect the resulting QRS score. In addition, since time passed between CMR and ECG acquisition, there may be instances where scar burden may have changed.

Lastly, I included only patients with CAD undergoing CMR before ICD implantation. Although the baseline characteristics between those who did and did not undergo CMR before ICD were similar, very few of the patients had no CMR scar. It may not be possible to generalise these findings to patients receiving ICDs for other indications. Further work is needed to validate the use of QRS scoring to detect myocardial scar in a general unselected population.

5.6 Conclusions

In a small retrospective study of consecutive CAD patients undergoing CMR before ICD implantation, QRS scoring had significant, moderate correlation to CMR quantified transmural scar, and showed association with medium term mortality risk, but not with risk of ventricular arrhythmia. It may be that the score is best suited as a predictor of death that is non-preventable by ICD therapy – i.e. a risk stratifier of those with least potential to benefit from ICD benefit. Further prospectively acquired data in larger cohorts are needed to clarify the potential value of sophisticated ECG scoring and scar burden assessment in targeting ICD therapy.

Variable	QRS score <6 (n=31)	QRS score ≥6 (n=33)	p
Age (y)	68	65	0.26
Male sex	21 (68%)	30 (91%)	0.30
Diabetes	8 (26%)	9 (27%)	1.00
Hypertension	14 (45%)	16 (49%)	0.80
Atrial fibrillation	6 (19%)	11 (33%)	0.26
Previous revascularisation	13 (42%)	15 (46%)	0.49
Amiodarone	8 (26%)	7 (21%)	0.77
Sotalol	1 (3%)	0 (0%)	0.49
B blocker	24 (80%)	27 (26%)	0.34
Ca channel blocker	4 (13%)	6 (19%)	0.39
Digitalis	0	0	
Diuretic	21 (70%)	17 (55%)	0.17
ACE-I/ARB	25 (83%)	28 (90%)	0.42
Primary ICD indication	20 (65%)	14 (42%)	0.64
ICD VT treatment zone lower setting, beats/min	150±15	152±14	0.49
LVEF (%)	36 ±20	30 ±11	0.16
QRS duration, ms	120 ±30	125 ±30	0.49
CMR scar (% LV)	11 ±9	17 ±10	0.19
LV mass	170 ±59	181 ±44	0.47
LVESV, mL	187 ±108	198 ±80	0.63
LVEDV, mL	259 ±115	277 ±82	0.47
QRS estimated scar (% LV)	9.7 ±5	29.8 ±10	<0.001
ECG			
No confounder	15 (48%)	8 (24%)	
LBBB	13 (42%)	13 (39%)	
RBBB	1 (3%)	2 (6%)	0.06
LAFB	0 (%)	5 (15%)	
LAFB+RBBB	2 (7%)	5 (15%)	
LVH	0 (0%)	0 (0%)	

ACE-I, angiotensin-converting enzyme inhibitor; ARB, angiotensin II receptor blocker; ICD, implantable cardioverter defibrillator; VT, ventricular tachycardia; LVEF, left ventricular ejection fraction; CMR, cardiac resonance imaging; LV, left ventricular; LVESV, left ventricular end systolic volume; LVEDV, left ventricular end diastolic volume; ECG, electrocardiogram; LBBB, left bundle branch block; RBBB, right bundle branch block; LAFB, left anterior fascicular block; LVH left ventricular hypertrophy

Table 5.1. Baseline Characteristics.

	All-cause mortality				Any appropriate ICD therapy	
	Univariate		Multivariate		Univariate	
	Hazard ratio (95% CI)	P value	Adjusted Hazard ratio	P value	Hazard ratio (95% CI)	P value
ECG variables						
QRS Score (per 1 point increase)	1.16 (1.03-1.30)	0.01	1.13 (1.01-1.28)	0.04	0.99 (0.91-1.09)	0.89
QRS duration (per 1ms increase)	1.00 (0.99-1.02)	0.71			0.99 (0.98-1.01)	0.48
Normal conduction	1.12 (0.12-10.0)	0.92			1.42 (0.41-5.01)	0.58
LBBB	2.62 (.323-21.2)	0.37			0.65 (0.17-2.47)	0.65
RBBB	0.00 (0.00)	0.99			1.95 (0.32-11.98)	0.47
LAFB	1.04(0.07-16.7)	0.98			1.05 (0.18-6.34)	0.95
CMR variables						
Per cent scar (per 1% increase)	1.01 (0.96-1.07)	0.59			1.04 (1.00-1.08)	0.03
LVEF (per 1% decrease)	0.96 (0.92-1.01)	0.10	0.97 (0.90-1.05)	0.49	1.00 (0.98-1.02)	0.87
LVEDV (per 1% increase)	1.01 (1.00-1.01)	0.04	1.01 (1.00-1.01)	0.12	1.00 (1.00-1.00)	0.70
Clinical variables						
Age (per year increase)	1.01 (0.96-1.06)	0.79			0.98 (0.95-1.02)	0.32
Creatinine (mmol/L increase)	0.89 (0.98-1.01)	0.89	0.99 (0.97-1.01)	0.32	0.99 (0.98-1.00)	0.15
AF	5.74 (0.75-44.0)	0.09	4.90 (0.62-38.8)	0.13	0.56 (0.23-1.39)	0.21
Amiodarone	0.51 (0.17-1.51)	0.22	2.04 (0.58-7.13)	0.26	0.30 (0.09-1.00)	0.05

Table 5.2.Predictors of all-cause mortality and appropriate implantable cardioverter defibrillator therapy

Figure 5.1 Patient with inferior transmural scar. Total points awarded 12. ECG derived scar volume = 36%. CMR derived scar volume = 33%. Example scoring in II and aVF (lead III not included in criteria).

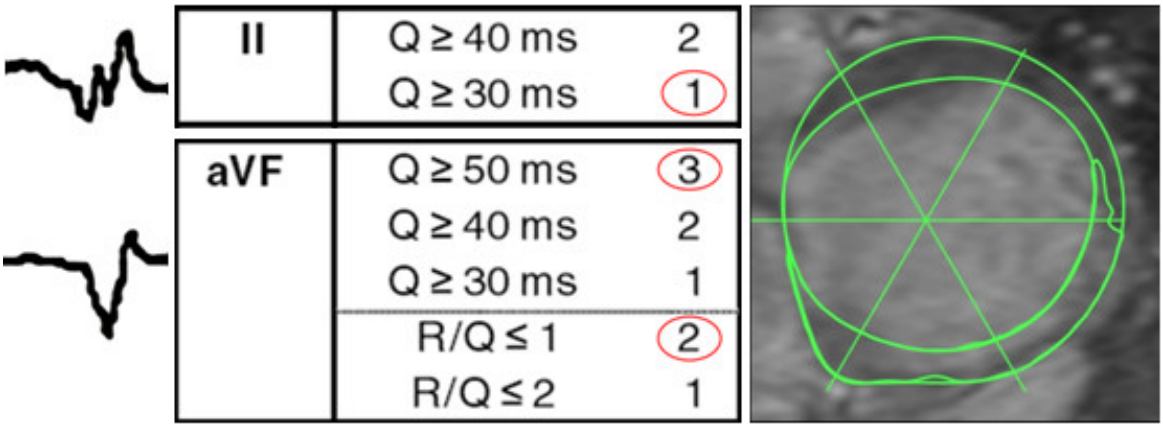

Figure 5.2 Patient with anteroseptal subendocardial scar. Points awarded 2. ECG derived scar volume = 6% CMR derived scar volume = 19%. No score in anteroseptal leads.

V1 Ant.	any Q	1
V2 Ant.	any Q R ≤ 10 ms R ≤ 0.1mV	1
V3	Q ≥ 30 ms R ≤ 10 ms Q ≥ 20 ms R ≤ 20 ms	2 1

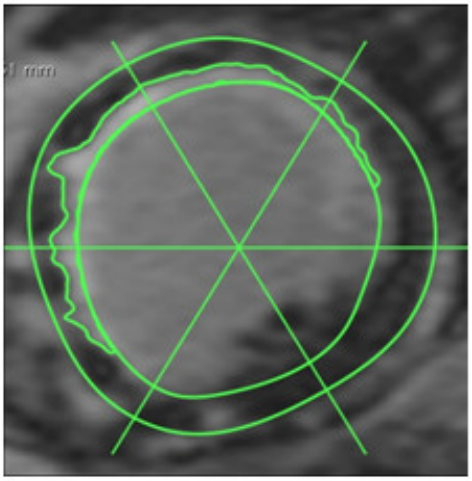

Figure 5.3. Receiver operating characteristic curve of the QRS score to diagnose the presence of CMR scar. Area under the curve (AUC) indicates poor overall test performance.

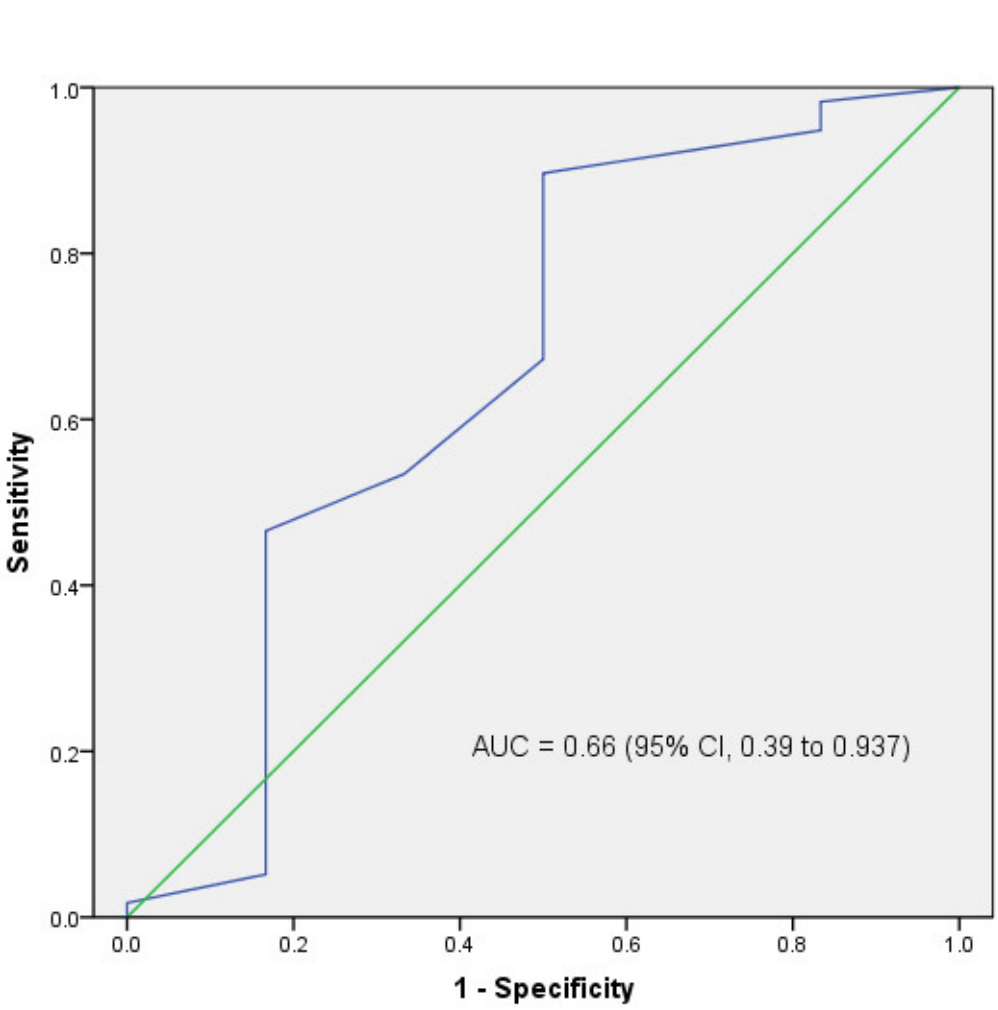

Figure 5.4. Scatterplot of QRS estimated scar and CMR derived scar (%LV). Regression line shown. r=0.42, P=0.001, indicating significant correlation between QRS score and CMR scar.

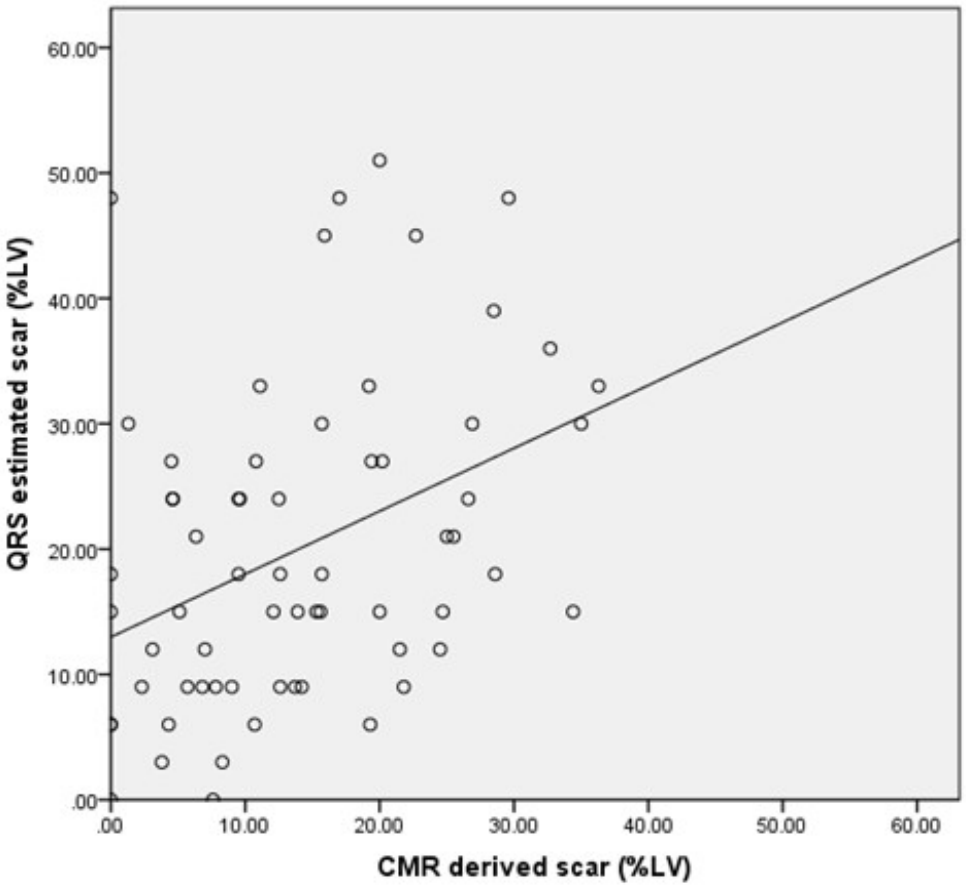

Figure 5.5. Bland-Altman plot of agreement between QRS estimated scar and CMR derived scar. Mean difference in scar size as assessed by these methods was 6%.

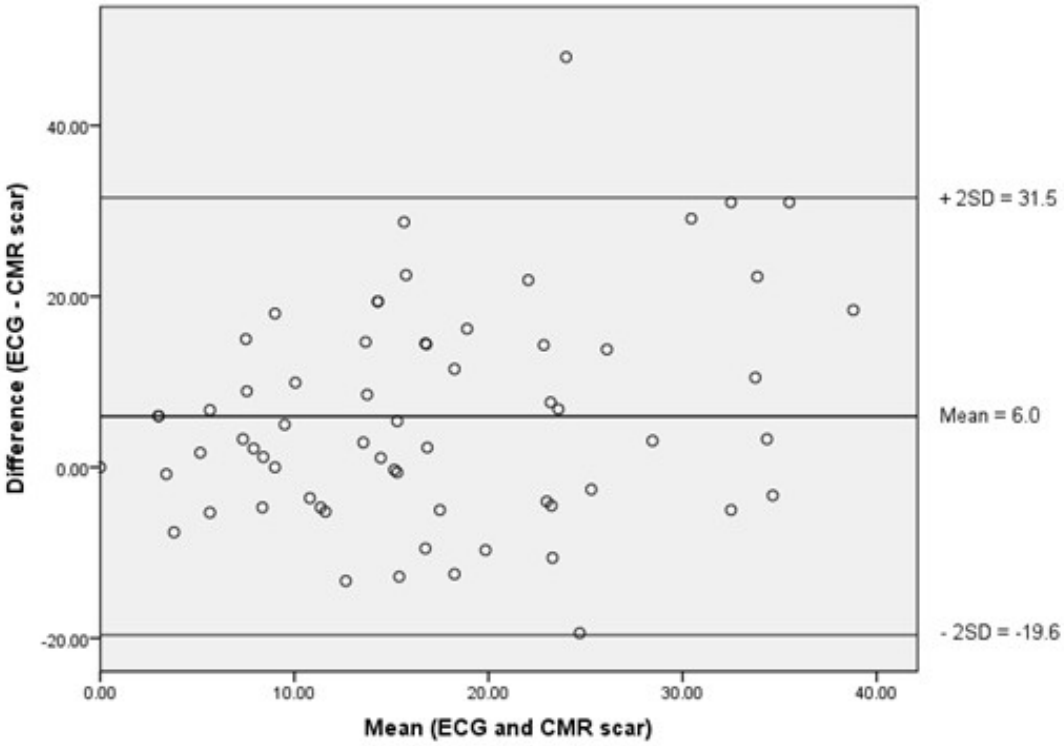

Figure 5.6. Kaplan-Meier survival curves over 60 months for patients with low and high QRS score, determined according to median score of 6. Events represent all cause mortality.

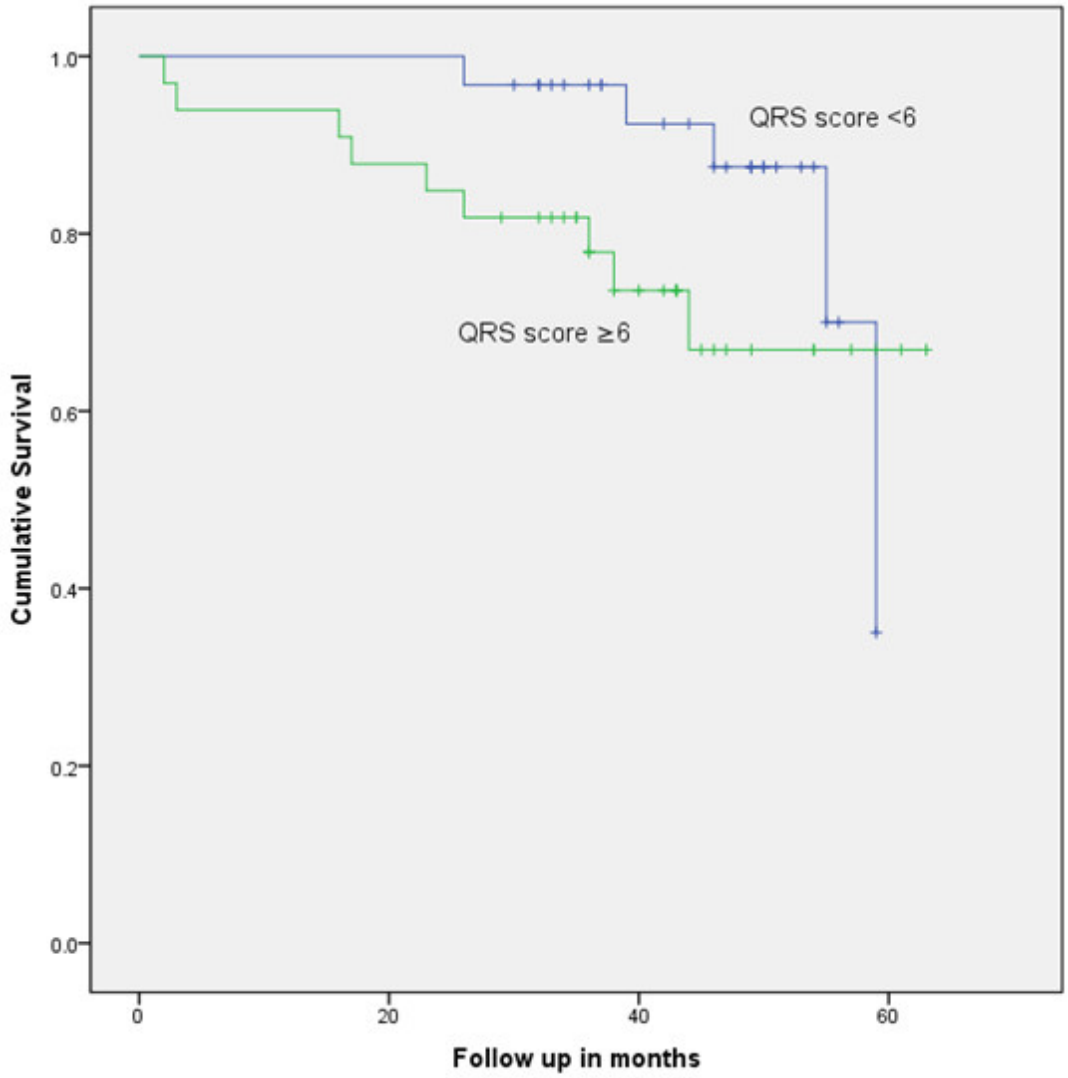

6 Automated QRS score analysis as a screening tool for myocardial scar

6.1 Introduction

Left ventricular scar, characterised by LGE-CMR, is significantly associated with the occurrence of spontaneous ventricular arrhythmias.[299] CMR is not suitable as a bedside test, nor widely available. Using the ECG as a surrogate for scar burden is therefore appealing. The Selvester QRS score is an ECG score, developed using computer modelling and post mortem data, to quantify MI scar. The original method was not suitable for analysis where BBB or ventricular hypertrophy was present, but has recently been updated to take account of these confounders.[183] Despite the renewed interest, the technique has not gained widespread popularity, in part due to technical limitations including the length of time required to manually score each patient, and variation due to inter- and intra- observer error. In addition, the data for its use in predicting clinical outcomes and determining myocardial scar are limited. A retrospective analysis of a selected cohort has reported strong correlation with scar burden.[184] It is unknown whether this scoring system would be of use in quantifying scar in an unselected population studied prospectively.

This study sought to determine if (a) automated analysis improves feasibility and accuracy of the Selvester QRS score and (b) whether this tool could be used as a screening tool for scar in an unselected population.

6.2 Methods

6.2.1 Study population

This was a single centre, prospective, cross sectional study performed at University Hospital Southampton NHS Foundation Trust, a regional tertiary referral centre serving a population of more than 3 million people. All adult patients, who as part of their routine clinical care attended for LGE-CMR of the LV, were eligible for inclusion. No specific referral indications were specified, but morphological studies of adult congenital heart disease were excluded. Recruitment took place over a 2-month period. The study complied with the Declaration of Helsinki and was approved by the local research ethics committee. Written informed consent was obtained from all patients.

6.2.2 *ECG*

6.2.2.1 Acquisition

A standard 12 lead ECG was acquired immediately preceding, or following the CMR. In the case of stress CMR, the ECG was acquired at resting heart rate. Electrodes were placed in standardised positions and acquisition always performed by the same investigators. To enable manual evaluation at magnification and offline computer analysis, the ECG was stored digitally (Spacelabs Healthcare Inc., CardioDirect 12 USB; frequency 2000Hz, 18bit resolution, AC filter 50Hz, 25 mm/s, 10 mm/mV).

6.2.2.2 Manual analysis

ECG scoring was in accordance to the published 50-criteria/31-point modified Selvester QRS method.[312] In summary, ECGs are first categorised according to conduction pattern: LBBB or RBBB), LAFB, LVH, right ventricular hypertrophy, RBBB+LAFB, or a normal pattern. Points are then awarded in leads I, II, aVL, aVF, and V1 through V6 according to presence of QRS notching, duration and amplitude criteria. The criterion thresholds are adjusted to account for younger men with increased voltage and older women with lower voltages. Each point represents 3% of myocardial scar. The Selvester score also generates a local QRS score, based upon the 12-segment model of the LV adopted by the International Society of Computerized Electrocardiography.[322] (Figure 6.1)

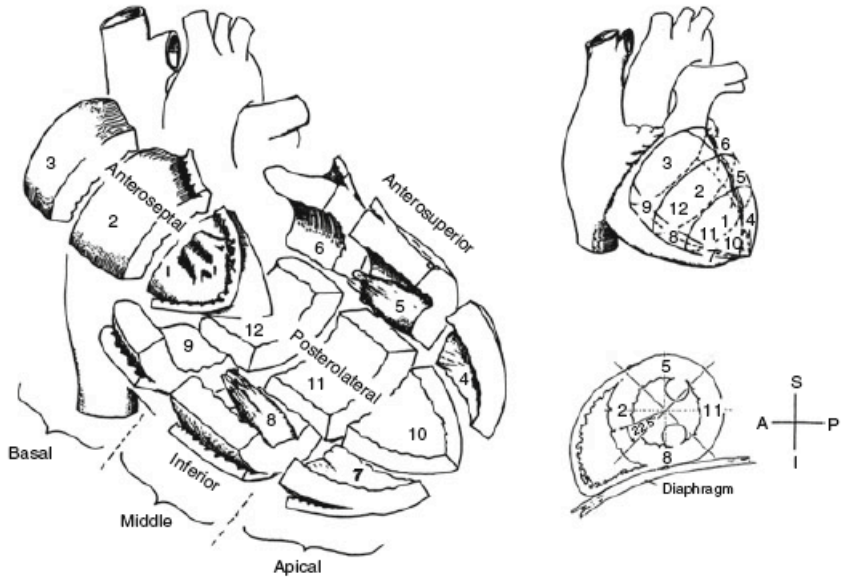

Figure 6.1 12-segment LV subdivision recommended by the Committee on Nomenclature of Myocardial Wall Segments of the International Society of Computerized Electrocardiography.[322]

ECG scoring was performed blinded to the CMR scar analysis. 30 ECGs were re-evaluated by a second scorer to determine inter-rater variability.

6.2.2.3 Automated analysis

The digital ECG signal was imported into MATLAB (R2013b, MathWorks, MA, USA) for analysis. Custom software, developed in collaboration with biomedical engineers, can undertake automated analysis without manual intervention. A full description of the development and testing is beyond the scope of this thesis but has been reported in the biomedical literature. [323] An overview of the automated workflow is shown in Figure 6.2. The process is near instantaneous and has no variability for the same record. The major challenge in developing the algorithm was detection of the full range of conduction defects that affect both "confounder" classification and scar criteria. DSP traditionally employs spectral analysis through the Fourier transformation of a signal into its constituent sinusoids. This technique obscures the time signal, and whilst an R wave can be readily identified by a high frequency component of maximum amplitude, complexity increases when coding for more subtle "slowing", "slurring" or "notching". To this end, wavelet transformation was used to decompose the QRS signal into frequency components whilst still maintaining temporal resolution.[324]

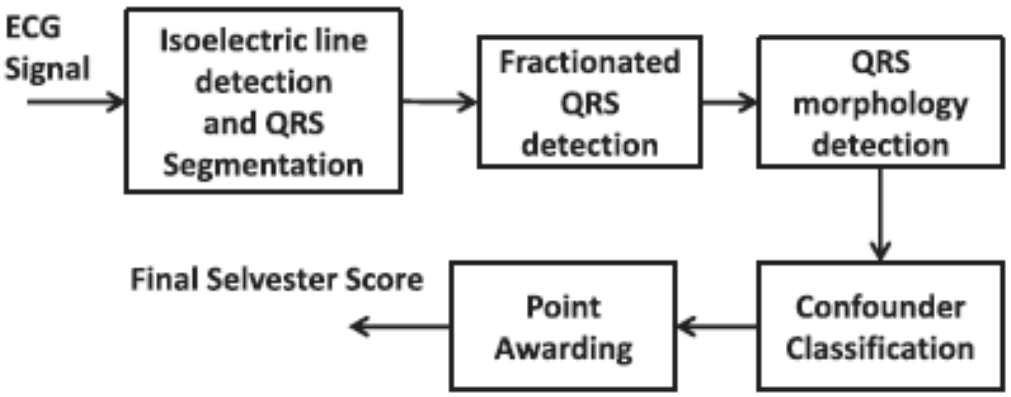

Figure 6.2 Flow diagram of the automated algorithm.

6.2.3 CMR scar assessment

All scans were performed according to the methods described in section 2.5 Cardiac Magnetic ResonanceObservers were blinded to the ECG score.

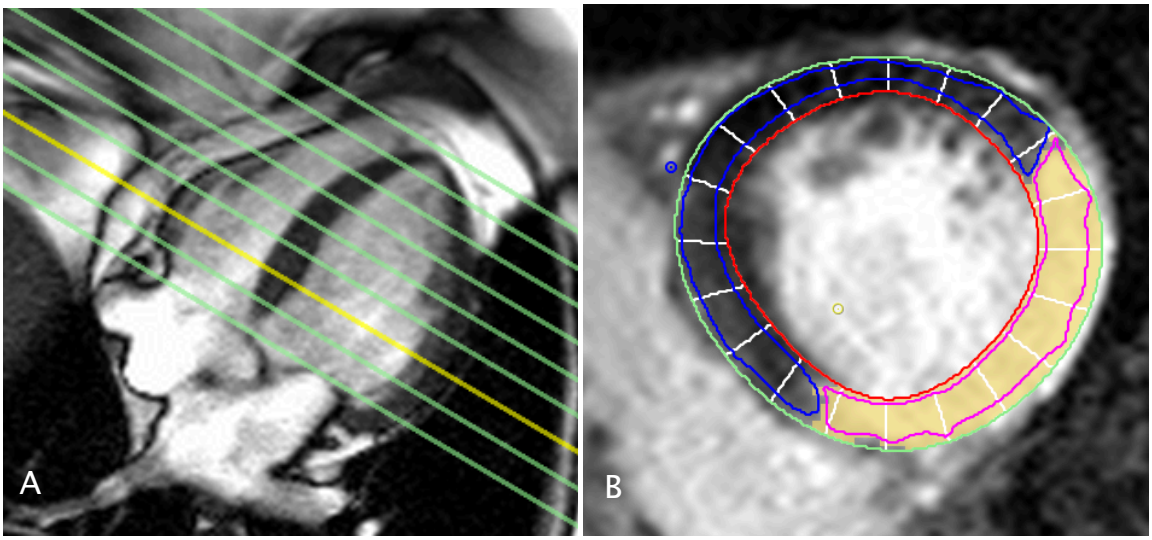

Figure 6.3 Semiautomated scar analysis. Panel A demonstrates long axis reference with LGE-CMR images acquired in the short axis plane from mitral valve to apex (green lines). The yellow line references the "active" short axis image seen in panel B. The myocardial borders are automatically contoured (red and green) with the scar highlighted with yellow shading defined by SI ≥50% of maximum. The area used in scar calculation is bounded by the pink line.

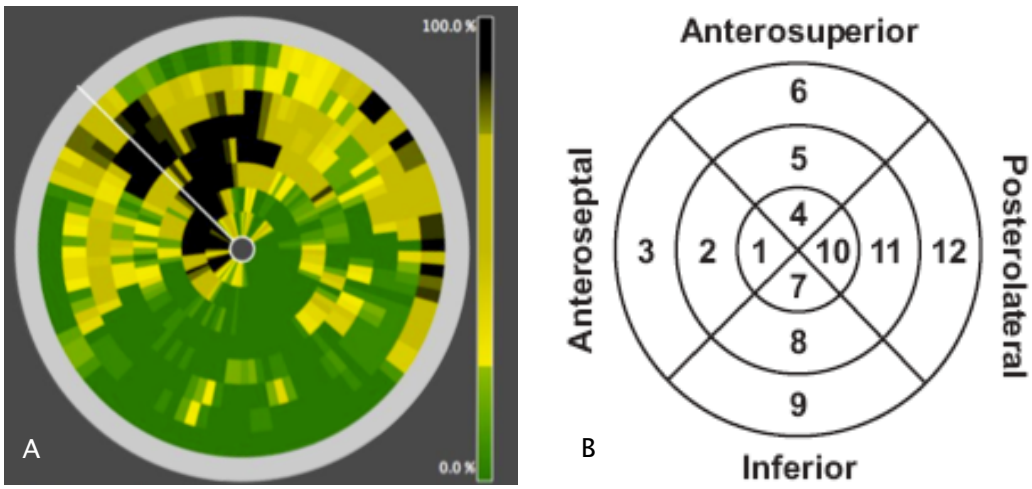

Figure 6.4. A: Polarmap of LV scar. The LV is divided into 100 radial chords. Each of the 8 rings represents a short axis slice. The white radial line is set at the RV insertion point. Panel B demonstrates the polarmap of the 12-segment model.

Each slice was segmented into 100 chords starting from the anterior right ventricular insertion point, and for each chord, the amount and transmural extent of LGE was calculated. To aid assessment this can be represented as a polar map (Figure 6.4A), although for the purposes of this experiment the raw data was exported and analysed offline. In order to compare ECG based QRS scoring, the CMR scar data from each chord was combined to approximate the 12 ECG model segment model: 25 chords per 4 segments of basal, mid and apical slices (Figure 6.4B).

6.2.4 Statistics

Categorical variables are expressed as numbers (percentages). Normally distributed continuous variables are expressed as mean±SD and compared using Student's t-test. Variables not normally distributed are expressed as median (lower quartile to upper quartile) and compared using Wilcoxon–Mann–Whitney test. Inter-observer agreement for ECG measurements was calculated using the ICC for absolute agreement. The relationship between the QRS score and the LV scar variables was determined by Pearson's *r* (chosen because of the large sample size). Bland-Altman plots used to analyse the agreement between the methods. Nonparametric ROC curves were used to assess the ability of the QRS score to diagnose the presence of CMR-LGE scar. In order to detect a correlation between QRS score and CMR scar of at least 0.5, a sample size of 150 was determined to give a power of 80%. [325] Statistical analyses were performed on SPSS Version 20 (IBM SPSS, Chicago, IL, USA). In all analyses a p value of <0.05 was considered significant.

6.3 Results

6.3.1 Study characteristics

From those attending for LGE-CMR, 156 consecutive adults were included in the analysis (Table 6.1). The average age was 64±12 years and 101 (65%) participants were male. CMR gave diagnostic information in all cases. Mean LVEF was 58±16%. 52% had CAD, 13% DCM and 18% had a structurally and functionally normal heart. All ECGs were suitable for analysis. Mean QRS duration was 114±20ms. The majority of patients (71%) had no ECG confounder, whilst around 10% had BBB.

6.3.2 Left ventricular scar

LGE-CMR defined scar was detected in 109 (70%) patients, with the majority (90%) displaying areas of transmural scar. Almost all had some areas of subendocardial scar (96%), although just 6% had scar with subendocardial distribution only. Median total scar burden was 9.6%(4.3-17.3). Patients with CAD had more scar [8.50% (0.25-17.25)] than those without [3.70% [0.00-8.40] (p<0.05).

6.3.3 QRS scoring

138 patients scored at least 1 point. Median QRS score was 5(3-7) equal to estimated LV scar of 15(9-21)%. The ICC was 0.937 indicating good agreement between raters. Average time for calculating score was 5 minutes.

6.3.4 QRS scores and LV scar

QRS scores correctly identified the presence of scar in 99 of 109 (91%) patients. Only 8 of 47 patients were correctly identified as having no LV scar. A detection cut off of 1 point gave a sensitivity of 90% but only specificity of 17%. PPV was 72% and NPV 56%. Using median QRS score of 5 as a cut off resulted sensitivity of 47%, specificity of 30%, PPV of 61% and NPV of 81%. Area under the ROC curve (AUC) for QRS score as a predictor of scar presence was 0.63 (95% CI 0.54-0.71) (Figure 6.5). No optimal cut-point was seen. Evaluating QRS scoring to detect just transmural scar (AUC 0.64, 95% CI 0.56-0.73) or subendocardial scar (AUC 0.64, 95% CI 0.56-0.73), or just in those with CAD (AUC 0.68, 95% CI 0.54-0.71) did not appreciably affect performance.

As a continuous variable, QRS score was only moderately correlated with LV scar ($r=0.392$, $p<0.01$) (Figure 6.6). Bland-Altman analysis suggested a mean difference of ~5% between LV scar measured by CMR and estimated by QRS score, and that the absolute difference was greater as LV scar increased. However, for most individuals the differences fell within the 95% limits of agreement (Figure 6.7).

No difference in correlation was seen amongst those with LVEF <35 or ≥35%. When limiting the analysis just to those with CAD, correlation remained significant and was stronger ($r=0.487$, $p<0.01$). However, in those with non CAD aetiology, correlation was no longer significant ($p=0.142$), and was not improved in any other specific subgroup. When considering those with no ECG confounders, correlation was essentially unchanged ($r=0.397$, $p<0.01$). However, correlation in other confounder groups was non-significant, although each individual group was small.

Correlation between QRS score and CMR LV % scar remained significant when anatomical regions were matched to the same or nearest segment (Table 6.2). This correlation was less strong in the inferior and posterolateral segments.

6.3.5 Automated QRS scoring

Automated QRS scoring was successful on all ECGs. The result was near instantaneous. The ICC between manual and automated scoring was 0.727 indicating moderate agreement between these methods. In the ability to predict presence of CMR measured LV scar, the automated QRS score performed similarly to manual scoring (AUC 0.63 95% CI 0.54-0.74). However, the correlation between automated QRS score and LV % scar was stronger than when calculated manually ($r=0.490$). No significant differences to manual scoring were seen when examining subgroups.

6.4 Discussion

This single centre, prospective cross sectional study of unselected adult patients has shown that Selvester QRS scoring can detect the presence of LV scar with high sensitivity but weak specificity. As a "rule-out" test for scar, QRS scoring may not be best suited; its specificity is weak, and the NPV using the standard cut off value is poor. However, using the median QRS score of 5 may allow for better negative prediction of scar.

QRS scoring correlates moderately well with scar burden, with the strongest correlation seen in those with CAD. In this regard, the results reflect the findings from the retrospective analysis in Chapter 5. The novelty of this investigation was that this was a "real world" cohort of patients referred for LV scar evaluation. However, performance amongst those with non-ischaemic aetiologies seems weak. The score did perform equally in those with and without poor LVEF. However, where ECG "confounders" were present, the score performance was weak, although as acknowledged the numbers in each group were small.

It is encouraging that the correlation between ECG and CMR anatomically matched regions is consistent. In addition, the lack of correlation between non-matched regions adds proof that the score performance is more than just a chance reflection of a confounding factor related to scar.

Whereas in the previous analysis, QRS score was not well associated with subendocardial scar, the same findings were not seen here. This is likely to be in part due to the more sophisticated method used to segment and characterise contrast enhanced regions. Most patients therefore had evidence of both transmural and subendocardial scar, and were characterised as such, reflecting the reality that full thickness of scar will vary between neighbouring regions. Nonetheless, it is possible that this cohort had a different distribution of scar to that seen in the selected, retrospective analysis.

Automated Selvester scoring was successfully performed in the population and when compared to manual scoring resulted in an estimated scar burden closer to the CMR measured score. The reasons for this are unclear. The computer algorithm was coded to process the score as published, and was not designed to improve upon LV scar estimate. However, the analysis was performed on the raw ECG trace and is not subject to the limits of precision that effect manual measurement of a graphically displayed ECG recording. There was good agreement between manual scorers, suggesting that the same limitations exist for all manual scorers. When the algorithm was validated at

the time of development, variation between the manual and automatic scar was noted in six records, only three of which differed by more than one point.[323] When these differences were examined, many were due to precision of timing (40ms is a critical value for classifying points) or calculation of QRS axis (the algorithm calculates the sum limb lead vector using the AUC). However, the automated score is limited by signal noise and inaccuracies of annotation. Therefore it might be by chance that the automated score provides a better of estimate of LV scar.

Previous publications have described computerised evaluation of QRS scoring, although developed in a period before the score was updated to take account of ECG confounders. Early attempts at automation revealed limitations related to manual development of the score, normal measurements having been derived from middle-aged white men.[177,326] Some of the suggested age and gender adjustments have been incorporated into later iterations of the score. When Haisty *et al*. examined the sensitivity and specificity of individual criteria, applied to subjects with a clinical history of infarction (confirmed on ventriculogram), they found that arbitrary thresholds, such as R/S amplitude ratios, were non specific and reflected the compromises made in developing the score for manual application.[177]

Horáček *et al*. developed a Selvester QRS scoring algorithm on a retrospective collection of 705 signal averaged body surface ECGs, from which they derived a standard 12 lead recording.[327] The actual coding is not detailed in their publication, but an iterative process was used to improve the "logic" of the decisions the software needed to perform. By agreement, discrepancies were ignored when they fell within predetermined limits for waveform duration (≤2ms) or amplitude (≤0.01mV). The computer program was then validated in 60 additional ECGs. Disagreement of 2 or more points was seen in 7 of these cases, reinforcing that differences between manual and automated scoring do necessarily exist. However, since that study did not compare the scoring to clinical evidence of scar, it does not add to the observation that automatic scoring performed better than manual scoring in predicting LV scar.

6.4.1 Limitations

This study has some limitations. First, although the analysis used unselected and consecutive patients referred for CMR evaluation, this may not reflect the true population in whom a screening test for LV scar would be desirable. Second, in order that anatomical comparisons were made between CMR scar and ECG scar, some assumptions were made when evaluating CMR late enhancement. The standard model of the left ventricle is 17-segments[301], whereas the Selvester score has been validated against a 12-segment model as described above. It is possible that some scar was

attributed incorrectly to a neighbouring segment, although this is unlikely to have been a significant confounder. Third, the analysis did not take into account the aetiology of the scar. It is known that accuracy of scar analysis can vary according to disease process, although the FWHM method chosen in this study is the most reproducible.[328] Lastly, this study did not investigate clinical outcomes. Whilst it is known that CMR measured LV scar is associated with mortality and arrhythmia, it is not clear whether the burden of scar, measured by CMR or estimated by QRS score, is associated with these end points in this study population.

6.5 Conclusions

In a single centre, prospective cross sectional study, QRS scoring had significant, moderate correlation to CMR measured LV scar. Its performance seems best in those with CAD, and use in non-CAD populations is questionable. Despite updated criteria for use with ECG confounders, QRS scoring was not significant in these groups. Automated scoring improved the strength of correlation between QRS scoring and CMR scar, which may in part be explained by an improvement in classification accuracy. However, the score was developed for manual application. Automated ECG scar analysis need not be limited by manual precision and may be better exploited by custom signal processing algorithms. Such potential is explored in Chapter 7.

Characteristic	
Participants (n)	156
Age (years)	64±12
Male	101 (65%)
LVEF (%)	58±16
Clinical diagnosis	
Normal	28(18%)
CAD	85(55%)
DCM	24(15%)
Hypertrophic Cardiomyopathy	7(5%)
LVH	3(2%)
Myocarditis	4(3%)
Amyloid	1(1%)
Takotsubu	1(1%)
Valve disease	2(1%)
ECG characteristics	
QRS duration (ms)	144±20
No confounder	111(71%)
LBBB	14(9%)
RBBB	5(3%)
LAFB	13(71%)
LAFB+RBBB	1(1%)
LVH	12(7.7)

Table 6.1 Study variables.

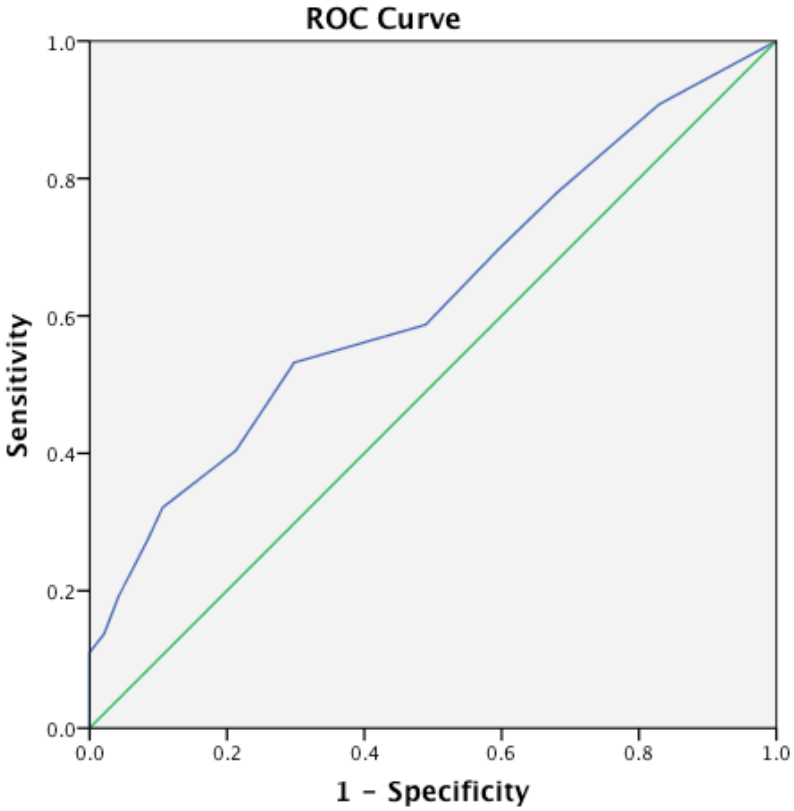

Figure 6.5 Receiver operator characteristic curve of QRS score to predict the presence of left ventricular scar.

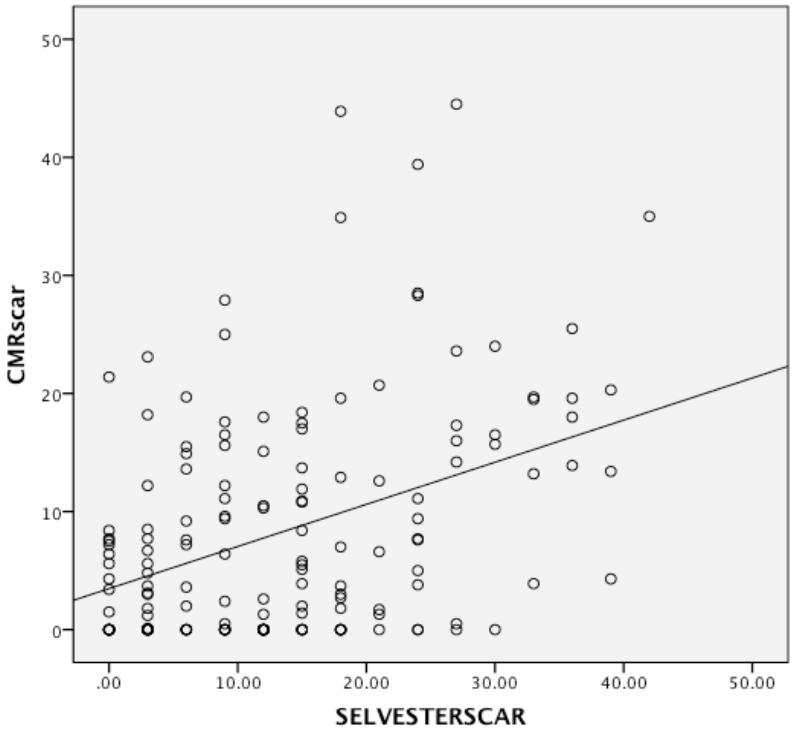

Figure 6.6 Scatterplot fQRS estimated scar and CMR LV scar (%LV). Regression line shown r=0.392, p=<0.01

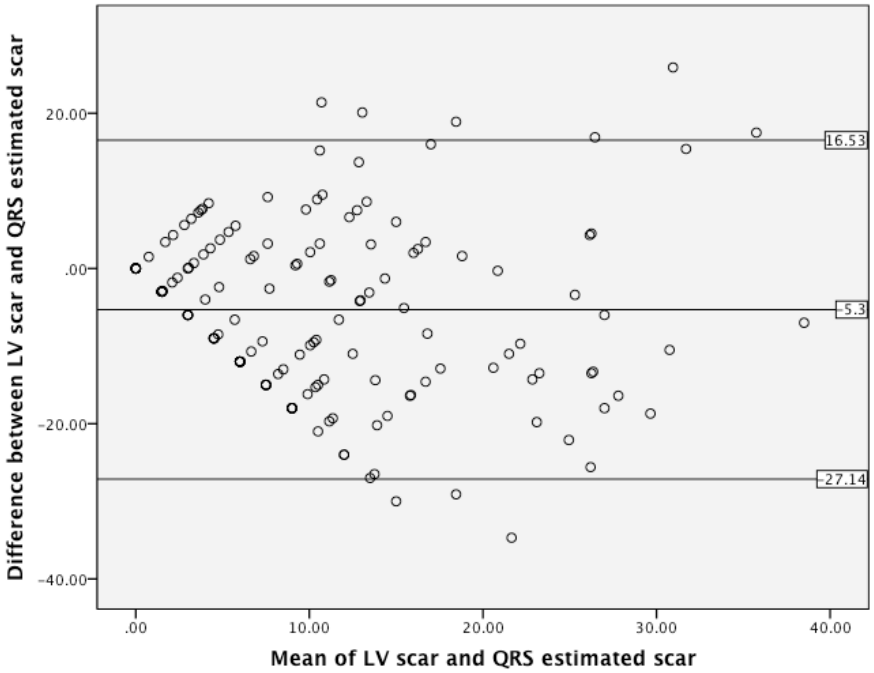

Figure 6.7 Bland-Altman plot of agreement between QRS estimated scar and LV scar

		QRS score %			
	Location	Anteroseptal	Anterosuperior	Inferior	Posterolateral
LV Scar %	Anteroseptal	0.45**	0.368**	NS	0.167*
	Anterosuperior	0.312**	0.33**	NS	NS
	Inferior	NS	NS	0.295**	NS
	Posterolateral	NS	NS	0.479**	0.220**

*p<0.05, **p<0.01, NS=non significant

Table 6.2 Correlation between QRS score and LV scar by anatomical location

7 Novel non invasive detection of arrhythmia substrate

7.1 Introduction

Myocardial scar burden, quantified by CMR, predicts ventricular arrhythmogenesis.[299] CMR use is resource and cost limited whereas conventional 12 lead ECG is readily available. The accepted ECG marker of myocardial scar, the Q wave, is not a specific finding.[153] In light of this, attempts have been made to develop new ECG markers of scar, but these have had only limited clinical uptake. Chapters 1 and 5 describe fQRS and Selvester QRS scoring. Whilst these scores have been shown by others to be more specific than Q waves for the detection of scar,[329] manual assessment of the ECG is labour intensive, and subject to the limits of human precision, and variation due to inter- and intra-observer error. Chapter 6 explored how automated ECG scoring can improve prediction of scar burden, although the level of correlation was only moderate. This may be because the Selvester score, and other similar scores, were developed for manual assessment, and are necessarily limited in complexity. The 12 lead ECG displays voltage information, varying over time. This time domain data has become the standard method by which aspects of the heart rhythm are manually assessed. Temporal information allows the observer to visually assess heart rate and rhythm that may reveal information about conduction system disease. The frequency domain of the ECG describes how much of the signal lies within each given frequency band over a range of frequencies. Whilst this data cannot be intuitively assessed, digital signal processing allows the ECG to be broken down into components suitable for computer assessment.

An SVM is an example of artificial intelligence supervised learning. Given training examples belonging to one of two categories, an SVM training algorithm builds a classifier that assigns new examples into these two categories, or classes.

This study was designed to test the hypothesis that an SVM could be developed, capable of analysing multiple time and frequency domain ECG components, able to screen ECGs for the presence of myocardial scar.

7.2 Methods

7.2.1 Study population

This was a single centre, prospective, cross sectional study performed at University Hospital Southampton NHS Foundation Trust, a regional tertiary referral centre serving a population of more than 3 million people. All adult patients, who as part of their

routine clinical care attended for LGE-CMR of the LV, were eligible for inclusion. No specific referral indications were specified, but morphological studies of adult congenital heart disease were excluded. Recruitment took place over a 2-month period. The study complied with the Declaration of Helsinki and was approved by the local research ethics committee. Written informed consent was obtained from all patients.

7.2.2 ECG **Acquisition**

A standard 12 lead ECG was acquired immediately preceding, or following the CMR. In the case of stress CMR, the ECG was acquired at resting heart rate. Electrodes were placed in standardised positions and acquisition always performed by the same investigators. To enable manual evaluation at magnification and offline computer analysis, the ECG was stored digitally (Spacelabs Healthcare Inc., CardioDirect 12 USB; frequency 2000Hz, 18bit resolution, AC filter 50Hz, 25 mm/s, 10 mm/mV).

7.2.3 CMR scar assessment

All scans were performed according to the methods described in section 2.5 Cardiac Magnetic Resonancewith cmr42 software used for scar analysis.

7.2.4 Support vector machine

From the patient population described in Chapter 6, 45 patients had no scar. In order to create a balanced database, the no scar ECGs were matched with 45 ECGs randomly selected from those with scar. 70% (64) were randomly selected as a balanced training set of 31 records with scar and 33 records with no scar. The SVM was trained using results from time and frequency domain analysis (see below). The SVM was validated with the remaining 28 unseen records. Test ECGs were categorised as “scar” or “no scar” and compared against the CMR result.

The SVM was developed in collaboration with biomedical engineers. A full technical description of feature selection, mathematical equations and SVM development is reported in the biomedical literature.[330] Whilst that paper takes a broad approach to feature selection and mathematical validation, this Chapter describes the experiment from a clinical viewpoint. The SVM was trained with the most novel features of signal analysis, validated in a clinically robust manner.

7.2.4.1 ECG template

The ECGs from those with no scar were signal averaged to create a median “template” beat for each lead, representing a typical non-scarred ECG. This approach was taken to create a template against which a test beat could be compared. It was important that this template ECG was typical of patients who had no LV scar, but was not necessarily

"normal". Had a "normal" ECG been artificially generated then *any* deviation from it may have been learnt as scar. The described method ensured that the presence of common ECG abnormalities, such as QRS prolongation, or signal artefact, would be ignored by the algorithm when categorising features representative of scar. This process was chosen to maximise specificity of the algorithm.

7.2.4.2 Comparative analysis

Statistical comparison between the test beat and template beat was achieved in both the time and frequency domains. *Cross-covariance* is a function of the relative time between the two signals, whilst *cross-correlation* reflects time delay between the two signals. W*avelet transformation* enables the *coherence* (a measure of how perfectly the waves are correlated in frequency) and phase *synchrony* (a measure of how "ahead" (lead) or "behind" (lag) the test signal is in relation to the template beat). A graphical representation of this analysis is shown in Figure 7.1, Figure 7.2 and Figure 7.3.

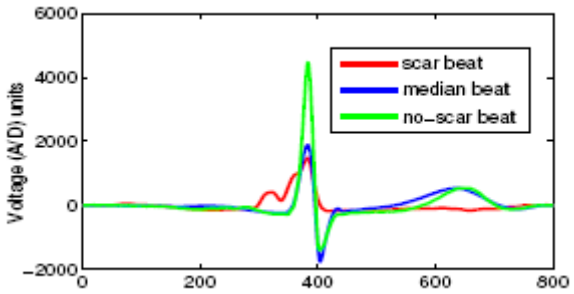

Figure 7.1 Time series representation of template (median) beat, scar and no-scar test beats.

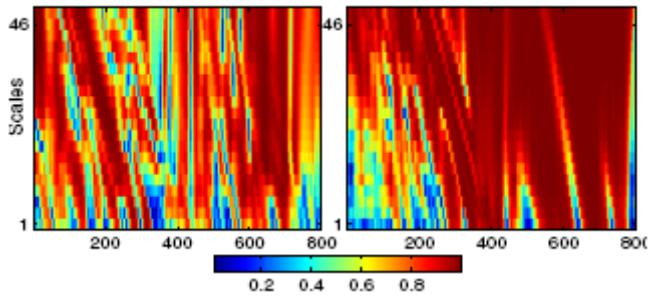

Figure 7.2 Wavelet coherence. Red represents greatest correlation, blue least correlation. X-axis is time series sample, y-axis is frequency range.

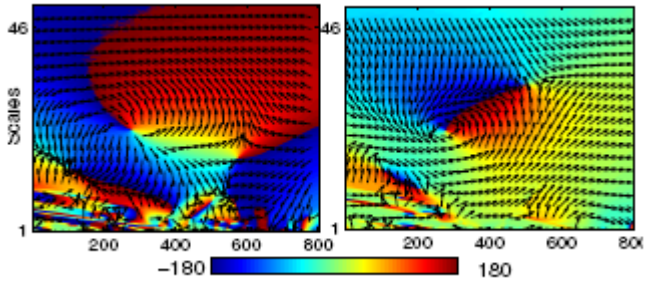

Figure 7.3 Phase synchrony. Red represents phase lead and blue phase lag. X-axis is time series sample, y-axis is frequency range.

7.2.4.3 Descriptive statistics

In addition to template comparison, the test signal itself underwent statistical analysis of the time domain signal (Table 7.1). These features were chosen as a method of capturing the "statistical signature" of the ECG signal in its fullest form.

7.2.5 General statistics

Categorical variables are expressed as numbers (percentages). Normally distributed continuous variables are expressed as mean±SD and compared using Student's t-test. Variables not normally distributed are expressed as median (lower quartile to upper quartile) and compared using Wilcoxon-Mann-Whitney test. Accuracy of the SVM was assessed using 2x2 contingency tables, calculating sensitivity, specificity and overall accuracy.

7.3 Results

Clinical characteristics were similar in those with scar and no scar. Importantly, there was no significant difference in QRS duration between groups (Table 6.1). Of 15 test ECGs with scar, only 1 was incorrectly characterised as no scar. There were 2 false positive tests from a total of 13 ECGs without scar (Table 7.3). Overall, accuracy was 89%. Sensitivity was 93% and specificity 85%. PPV was 86% and NPV was 92%.

7.4 Discussion

This study has shown that an SVM, trained using comparative and descriptive statistical features, is capable of classifying unseen ECGs as scar or no scar. In this analysis, the performance of such as a tool is excellent, with good sensitivity and specificity, and predictive ability that would make it suitable as a screening tool for LV scar.

Machine learning approaches such as SVMs are used in everyday life to manage large volumes of complex data. In contrast to traditional statistical approaches, ML can enable iterative development of algorithms, continually improving the performance of the classifier. Whilst this experiment was developed and validated with separate data sets, such an approach could easily be refined as new ECG examples were learnt.

Ventricular activation is determined by conduction through the His-Purkinje system and propagation through the left and right bundles. Left ventricular scar results in localised conduction delay, which should therefore manifest as changes to the ECG signal. In the simplest form, such delay might result in QRS prolongation. However, QRS duration has not been shown to be a predictor of LV scar, and in this experiment baseline QRS duration was not significantly different in those with and without scar. It is probable that localised delay in conduction results in more subtle changes to the ECG, seen as complex high frequency signals. Despite several proposed methods for manually scoring the ECG for the presence of scar, none has been shown to have a high level of accuracy, and in this work they were found to lack specificity. These scores, such as fQRS and Selvester scoring, are designed for manual assessment of time domain features. Even with precise measurement, such tools cannot systematically record frequency domain components of potential interest. In contrast, both time and frequency domain features were used in classifier development.

Whilst the SVM was developed as a screening tool for the presence of any LV scar, the clinical relevance of this is uncertain. The presence and extent of myocardial scar is associated with clinical outcomes, although the exact burden of scar that predicts adverse outcome is not clear. Whether this SVM could be trained to detect a defined threshold of scar is untested. In addition, it is not known whether the same features would be of use in quantifying myocardial scar. Lastly, whilst the use of fQRS and Selvester scoring in predicting SCD and overall mortality is considered, the association of SVM detected scar and clinical outcomes is as yet unknown.

This SVM was trained with several statistical features from the time and frequency domain. The “black-box” nature of such an algorithm means that it is not known which of these features was most discriminating. Whilst the benefit of such an approach is that the SVM need not be limited in complexity, with an increasing number of variables there is a risk of overfitting the algorithm to the training data. Despite validating the performance on a separate dataset, the test ECGs came from the same population and it is unknown how it would perform in different circumstances.

7.5 Conclusion

Digital ECG analysis, using descriptive and comparative statistical analysis of time and frequency domain features, can be used to train an SVM algorithm capable of classifying myocardial scar. These observations require confirmation in larger prospective studies. Such an approach has a high level of accuracy that might make it an appropriate tool for population screening and risk stratification.

Table 7.1 Statistical feature selection

Statistical feature	Explanation
Median	Average value of the signal. Value separating upper from lower time domain values.
Standard deviation	Signal variation from the average. Measure of signal to noise ratio.
Interquartile range	Describes distribution and normality of signal.
Hjorth complexity	Computational value for shape of signal based upon energy ratio of high frequency components and whole spectrum. Complexity increases with fragmentation.
Hjorth mobility	Computational value of mean frequency.
Hurst exponent	Measure of autocorrelation. Probability that a signal value will be followed by one of similar magnitude. Complex signals will have low autocorrelation.
Kurtosis	Measure of distribution and "peakedness" of the signal. Sharp, complex signals have greater kurtosis.

Table 7.2 Baseline characteristics.

Characteristic	Training			Test		
	Scar	no scar	p	scar	no scar	p
n	31	33		15	13	
Age (years)	66+-10	60+-10	0.58	66+-11	64+-11	0.69
Male gender	20	23	0.79	9	6	0.36
LVEF (%)	55+-17	62+-16	0.13	50+-16	63+-14	0.05
QRS duration (ms)	117+-22	110+-17	0.16	122+-21	109+-22	0.13

Table 7.3 Diagnostic accuracy of the SVM in categorising scar ECGs

		CMR		
		scar	no scar	total
SVM	scar	14	2	16
	no scar	1	11	12
	total	15	13	28

8 High resolution proteomics to detect candidate arrhythmia biomarkers

8.1 Introduction

Despite improvements in healthcare, HF remains a major worldwide cause of mortality. In addition to optimal medical therapy, appropriately selected individuals derive mortality benefit from insertion of an ICD as a means to prevent sudden arrhythmic cardiac death (SCD). The criteria used to identify these individuals has changed little over the last decade, despite the observation that many implanted with an ICD live for years without requiring life saving defibrillation therapy.[314] In addition, many patients suffering with HF will die from progressive pump failure and not benefit from ICD therapy.[331] On this background, ICD therapy uptake is under utilised even amongst those who meet current insertion criteria.

Several strategies have been used to identify those most likely to benefit from ICD implantation. ECG, imaging and electrophysiology markers have each been used with limited success. Combination scores of non-invasive and biochemical markers have been reported, but are yet to be adopted into widespread clinical practice. [332333334] Traditional techniques to identify biomarkers are based upon knowledge of biological pathways and underlying pathophysiology, requiring targeted selection of candidate markers. An alternative approach, *proteomics*, seeks to identify peptide characteristics in clearly defined disease phenotypes. The protein profile, or *proteome*, reflects the complement of proteins expressed in a certain cell/tissue under specified conditions.[239] Mass spectrometry (MS) based approaches can identify the differences in protein expression between these phenotypes. Samples for analysis, often obtained at the point of clinical diagnosis, form the basis of such studies. Whilst these techniques have been employed in HF, the biomarkers identified can only be described as diagnostic. Only through prospective tissue sampling, robust clinical follow up and analysis of differential expression with clear phenotype definition can prognostic biomarkers be proposed.

Proteomics is used widely in cancer sciences where solid tissue from disease sufferers is readily available. Although human cardiac tissue from biopsy, transplant or post mortem is available for proteomic analysis, such techniques fail to identify target proteins that can be readily translated into a clinical tool. For this reason, easily acquired serum and plasma samples appear more attractive targets. The human proteome, however, contains approximately 500,000 proteins, expression of which can vary by 8 orders of magnitude[239]. Low abundant proteins can easily be missed

unless techniques to reduce the complexity of the analyte are employed. Traditionally, methods such as immunodepletion have been used to remove high abundant proteins, although this in itself can lead to co-removal of other proteins of interest. More recently, a novel high resolution proteomic method has been described and validated.[261] Such a technique is able to identify protein candidates across the whole serum proteome. This offers the possibility of accurate identification of expressed biomarkers specific to disease sub-types and reflective of clinical outcomes.

8.1.1 Study Aim

Patients with HF die from SCD or pump failure. It is hypothesised is that in patients with HF, serum biomarker expression is indicative of a phenotype that encompasses future SCD risk. The study aim was to determine if a novel high resolution proteomic technique could be utilised in a prospectively monitored HF population to identify differentially expressed biomarkers reflective of SCD risk by an association with VA occurrence and cardiac mode of death.

8.2 Methods

8.2.1 Patients

All patients included in the study were enrolled in a biomarker analysis research programme recruited from those attending University Hospital Southampton, a tertiary cardiology centre. Participants had either a permanent pacemaker or ICD and were attending for routine device follow up. Exclusion criteria were pregnancy, congenital heart disease, hospital admission or therapy changes within 6 weeks.

At enrolment, baseline demographic and clinical data were recorded, a 12 lead resting ECG performed, and NYHA functional class assessed. All patients had a transthoracic echocardiogram prior to study entry. Blood was drawn from a forearm vein and collected in serum separator tubes. The collection and handling of all samples was in accordance to the recommendations of the Standard Operating Procedure Integration Working Group (SOPIWG)[248]. Briefly, serum samples were allowed to clot for 30 minutes and then centrifuged at 3000 rpm for 10 minutes. Samples were then divided into aliquots and frozen within 1 hour of sampling. Samples were finally stored at -80˚C prior to analysis and underwent no more than two freeze-thaw cycles. The study complied with the Declaration of Helsinki and was approved by the local research ethics committee. Written informed consent was obtained from all patients.

8.2.2 Follow up and end points

All patients were followed up at regular intervals according to standard clinical practice in the UK. For pacemaker patients this was every 6 months or annually. ICD patients had remote or in office follow up every 3 or 6 months. The occurrence of any device detected VA was recorded.

Following a minimum of 24 months follow up, patient samples were pooled into four groups, based upon pre enrolment VA expression and arrhythmia occurrence over the follow-up period:

i) Cardiovascular death
Patients dying of cardiac cause despite pacemaker/ICD

ii) Prior arrhythmia expression without VA during follow up
Patients previously experiencing VT>182bpm/VF but not experiencing arrhythmia during study follow up

iii) VA occurring during follow up
Individuals experiencing VT>182bpm/VF during study follow up

iv) Survival without VA expression
Individuals who had never experienced VA (at any rate) before enrolment or during follow up.

Correct arrhythmia detection/discrimination was confirmed by two electrophysiologists blinded to the proteomic analysis. Cardiovascular death was confirmed by death certificate, review of medical notes, cardiac device interrogation and consultation with the primary physician. Proteomic analysis requires clear phenotype definition, and individuals not reaching one of these endpoints were not included in the analysis.

8.2.3 Proteomic analysis

Proteomic analysis was performed in accordance with the previously reported method of depletion-free, high-performance size exclusion chromatographic separation of proteins, followed by two-dimensional chromatographic separation of their tryptic peptides and their tandem mass spectrometry.[261] The workflow is outlined as follows:

i. High-performance size exclusion chromatography
ii. Dialysis purification
iii. Protein digestion with trypsin
iv. Stable isotope labelling with isobaric stable isotope reagents (iTRAQ), assigned 113,114,115,116 according to the pooling described above.
v. Peptide fractionation using reverse phase chromatography

vi. Liquid chromatography-nano electrospray ionisation-mass spectrometry analysis using the ultra high-resolution nano ESI LTQ-Velos Pro Orbitrap Elite mass spectrometer (Thermo Scientific, Warrington, Cheshire, UK)

8.2.4 Statistics

Categorical variables are expressed as numbers (percentages) and compared using Pearson Chi-Square or Fisher's exact test. Normally distributed continuous variables are expressed as mean±SD and compared using Student's t-test. Variables not normally distributed are expressed as median (lower quartile to upper quartile) and compared using the Mann-Whitney *U*-test. Multiple group comparisons were performed using ANOVA.

Tandem mass spectra were submitted to the Sequest search engine implemented in the Proteome Discoverer 1.4 (Thermo Scientific, MA, USA). All spectra were searched against the UniProtKB SwissProt human proteome database. Identification was based upon a false discovery rate, $q<0.05$. Quantification ratios were median-normalized and transformed to log2 ratios.

8.3 Results

8.3.1 Patient characteristics

A total of 115 patients were enrolled and followed up for 28±4 months (Table 8.1). There were 7 cardiovascular deaths (6%), 48 (41%) had never experienced VA and 25 (22%) had VA prior to enrolment but no VA during follow up. 35 (30%) experienced VT>182bpm/VF. Individuals were deemed not to have reached a study end point if experiencing slower VA, death from a non cardiac cause, or where adjudication of an event following device interrogation was not possible.

There were no significant differences in age or gender, NYHA classification, or presence of diabetes between groups. Compared to others, survivors without VA phenotype expression were more likely to have NYHA I symptoms, normal LVEF, and a NICM ($p\approx0.01$). However, there was no significant difference in age ($p=0.30$), gender ($p=0.99$), LVEF ($p=0.12$), aetiology ($p=0.65$) or presence of diabetes ($p=0.63$) between those suffering cardiovascular death or prospective VA. No patients died during follow up who had NYHA class I symptoms and therefore NYHA class was significantly different in those who died versus those experiencing VA ($p=0.02$).

8.3.2 Protein discovery

Analysis of the sera identified 579 unique proteins and phosphoproteins, with a molecular weight ranging from 5kDa to 772kDa and varying in concentration by 12 orders of magnitude. Full Proteome Discoverer output is included in Appendix A.

8.3.2.1 Biomarkers of heart failure death: group (i) compared to (iv) and (iii) compared to (iv)

The sickest HF sufferers will die, either from pump failure, or SCD. In this study, patients from group (i) died despite the presence of an ICD, and therefore represent death from pump failure. Patients in group (iii) experienced VT>182bpm or VF, and therefore this group is a surrogate for sudden arrhythmic death. Considered together, patients in these two groups represent the sickest HF sufferers. Together, 577 proteins were differentially expressed in these cases compared to those surviving without VA expression. Of these, 34 proteins had more than 2-fold up or down regulation in the death group compared to survivors (Table 8.2). 17 proteins had more than 2-fold up or down regulation in the VA group compared to that of survivors (Table 8.3). Of these proteins, 9 were differentially expressed in both groups (i) and (iii) compared to survivors (iv). 7 proteins with 2 fold differential expression were seen in the VA group, but not death group, compared to survivors.

8.3.2.2 Biomarkers of mode of death: group (i) compared to (iii)

576 proteins were differentially expressed in those experiencing cardiovascular death (pump failure death) versus those experiencing VA (a crude surrogate for sudden arrhythmic death). 9 had expression in the death group more than twice that in the VA group, and 9 less than half that of the VA group (Table 8.4). 8 of these 18 proteins were unique to this comparison and were not differentially expressed against survivors.

8.3.2.3 Biomarkers of ongoing arrhythmia risk: group (iii) compared to (ii)

538 proteins were differentially expressed in those who experienced VA compared to those who did not (but had previously done so). Of these, 10 had expression in the VA group at least twice that seen in those who did not, and 14 had expression less than half (Table 8.5). Of these 24 proteins, 13 were unique to this comparison (i.e. did not have such high differential expression with respect to death) and were therefore markers of ongoing VA risk.

8.4 Discussion

This study of patients with implantable cardiac devices has shown that high-resolution analysis can identify serum proteins from across the whole proteome spectrum, even when abundance varies by 12 orders of magnitude. The study is unique in identifying protein expression present at study entry that was associated with subsequent HF events. As such, this work identified biomarkers indicative of future VA phenotype expression.

When compared to patients with preserved LVEF who did not experience VA during follow up, those who suffered pump failure death or experienced VA had a differential pattern of protein expression. Furthermore, expression of proteins varied between those who died of non-preventable death (pump failure) and those who experienced life saving ICD therapies (surrogate for SCD). Many of the patients in this study had received an ICD after surviving ventricular arrhythmia, and protein expression differed between those who did and did not experience further VA during follow up.

Proteomics provides an ideal platform to determine changes in proteins that might reflect disease states and show promise as biomarkers of diagnosis or prognosis. The choice of biological sample is a key factor in biomarker discovery. Solid tissue may express high levels of disease specific markers, and although biopsy material may be readily available in cancer sciences, access to human *ante mortem* cardiac tissue is limited, and so tissue from animal models is often used. Translating these findings into clinical practice is challenging, and necessitates validating candidate markers in human blood, a step that introduces selection bias. The current approach utilizes human serum that enables direct translation into clinical practice. Blood collection is low risk, minimally invasive and cheap. However, in addition to the great diversity of the human proteome, there is a wide concentration range of plasma protein, exceeding 10 orders of magnitude, beyond the dynamic range of any current analytical instrument. The 20 most abundant proteins represent ~99% of total plasma protein.[244335336] Immunoaffinity depletion is frequently implemented, using immobilized polyclonal antibodies to remove a portion of high abundance proteins, reducing complexity and dynamic range. This approach, however, removes proteins such as albumin that are carrier molecules for other proteins, and in doing so leads to a loss of diagnostic potential.[335] Direct mass spectrometry of the sample enables rapid assessment of the protein profile. A typical approach is use of MALDI to excite the sample into gas phase, before detection ion a Time of Flight (TOF) mass analyser. Although MALDI-TOF can provide rapid comparison of samples, low abundant proteins are left undetected. To overcome this, SELDI utilizes prefractionation and binding of a target protein subset before detection, and the principle of using this tool to identify

biomarkers of HF prognosis has been proven.[269] Despite the method having rapid throughput, resolving power and accuracy is poor, and information about differential protein expression is limited to just mass to charge (*m/z*), rather than protein identification.

Advances in MS/MS, capable of both fragmenting ions and detecting ion fragments, have lead to techniques capable of proteome detection with greater depth, dynamic range and enhanced accuracy. A protein sample undergoes proteolytic cleavage and separation by high performance liquid chromatography (HPLC) methods, before MS/MS and identification of the peptides. Highly complex samples, such as serum or plasma, require a combination of various fractionation and separation methods. This study utilized an approach incorporating strong cation-exchange chromatography HPLC before reverse phase HPLC, known as Multidimensional Protein Identification Technology (MudPIT)[254] further refined to use zwitterion-ion hydrophilic interaction chromatography (ZIC-HILIC) fractionation followed by their online analysis with reversed-phase nano-ultraperformance chromatography (RP-nUPLC).[261] Quantification of proteins and comparison of sample expression was possible with stable isotope labelling though the use of iTRAQ.[337] Utilizing these techniques has enabled identification and quantification of proteins from across the whole serum proteome. More basic proteomic methodology requires extensive validation using traditional biochemistry techniques such as western blotting, ELISA and immunofluorescence, and many novel biomarkers get overlooked due to a lack of suitable or quality detection reagents.[338]

The proteins identified in this study provide validation of markers previously associated with cardiovascular disease, but also represent several novel findings. When taken together, patients in group (i) and (iii) represent HF suffers with the worst prognosis. Biomarkers that can identify these patients would help to target ICD therapy more appropriately, including those without biomarker expression who have a low risk of future events and therefore in whom ICD therapy would be unnecessary.

Four proteins were up-regulated in both groups compared to survivors. **Lysophosphatidylcholine acyltransferase 2** (LPCAT2) is a calcium dependent enzyme involved in platelet activating factor (PAF) biosynthesis under inflammatory conditions. PAF is produced by human heart and is thought to be implicated in HF since it participates in cardiomyocyte apoptosis and causes a negative inotropic effect [339340]. In a small pilot study of healthy volunteers and newly diagnosed HF patients, concentrations of LPCAT2 were shown to increase during follow up.[341] **Interferon Epsilon** (IFε) is a type 1 interferon encoded for at the gene locus 9p21.3. Although the

function is unknown, a meta-analysis of case control studies demonstrates evidence that variants at this locus increase the risk of CAD and MI in individuals of European ancestry.[342] **Alpha-2-HS-glycoprotein**, or *Fetuin-A* acts as an inhibitor of vessel calcification and has been shown to be an independent predictor of insulin resistance. Whilst low levels of fetuin-A may be associated with increased cardiovascular mortality in those with end stage renal disease[343], more recent analysis suggests a more complex association, where higher levels of fetuin-A in those with diabetes, insulin resistance, obesity and metabolic syndrome, were at greater cardiovascular risk.[344345] The association with HF has not been described**. Chromogranin A** is a neuroendocrine protein, secreted widely but shown to be present in the human heart co-localised with natriuretic peptides. Levels are increased in HF and are a predictive factor for mortality.[346347]

Five proteins were downregulated compared to survivors. **Transcription elongation factor SPT6** is a widely expressed nuclear protein which binds histone H3 and plays a key role in the regulation of transcription elongation and mRNA processing. No reports of association with cardiac disease in humans are reported but mutations in this class of protein can cause problems of cardiac differentiation in Zebrafish.[348] **Collagen alpha-1(XI) chain** is a secreted protein involved intracellular assembly of procollagen molecules and the extracellular assembly of collagen fibrils. It is involved in morphogenesis of ventricular muscle.[349] There are no reports of association with cardiac disease. **Zinc finger CCCH domain-containing protein 18, Probable ATP-dependent RNA helicase DDX60-like,** and **Lipase maturation factor 2** are proteins involved in gene encoding and metabolism, but not specific to cardiac tissue. The association with cardiac disease has not been reported.

Several of the proteins expressed in those experiencing VA compared to survivors were not so highly expressed in those who died. In addition, protein expression differed between those who died and those who experienced ventricular arrhythmia. The association of a biomarker with VA rather than pump failure is a unique finding that would identify those patients in whom ICD therapy would prevent SCD, and those with such adverse prognosis that they would die from pump failure despite ICD therapy.

Some structural cardiac muscle proteins, such as **Myosin-7** and **Tropomyosin alpha-3 chain** were highly expressed in those who died compared to those surviving without VA and those who survived with ventricular arrhythmia. It is plausible that end stage HF sufferers have higher circulating levels of these proteins. Indeed, a study using a mouse model of HF identified myosin-7 and found it also present in the plasma of

humans with failing human hearts.[350] Of the several proteins downregulated in those dying compared to those experiencing ventricular arrhythmia, **Vitamin K-dependent protein Z**, has been linked to cardiac disease previously. Low levels of cofactor for the inhibition of activated coagulation factor X are linked to adverse 1 year outcomes in ACS, and are associated with an increased risk of thrombosis in diseases related to vascular thrombosis.[351][352]

Lastly, ongoing arrhythmia risk might be identified, even in those who have previously expressed ventricular arrhythmia. Amongst several differentially expressed proteins, **beta-2-microglobulin** was identified. This protein has been shown to identify worse medium term cardiovascular outcomes amongst those presenting with acute HF.[353]

The latest North American guideline for the management of HF highlights the use of biomarkers for the diagnosis, and to some extent, guidance of management, in HF.[354] BNP has long been used in this context and novel biomarkers must show additional discriminatory power. Although this study was not designed to demonstrate this, it is noted that BNP and atrial natriuretic peptide (ANP) were identified and had high levels of differential expression in those who died compared to survivors without ventricular arrhythmia. In those who had pre study VA, BNP had higher expression amongst those in those who went on to experience further ventricular arrhythmia. However, it should also be noted that other proteins had stronger differential expression than BNP or ANP in all groups. The emerging biomarker galectin-3 is also highlighted in guidelines, and although it was detected in this experiment, its differential expression between HF groups is weaker than the proteins discussed here. This reinforces the message that an unbiased proteomic approach may hold the key to discovering biomarkers with greater potential than those already in clinical practice.

8.4.1 Limitations

The study population was small and the number of samples in each group was limited. Cause of death is challenging to define; non preventable deaths may not have been due to pump failure, and VT >182bpm or VF detected by an implantable cardiac device may not be a surrogate for SCD. These features are, however, indicative of a VA phenotype that is distinct from a phenotype with no VA expression.

Many of the participants were established on HF therapies and may have been several years remote from device implant. Prognostic biomarkers may be best suited to risk stratification at the time of diagnosis and it is not clear whether the molecular portrait identified in this study can be applied to a newly diagnosed population. It is recognised that VA risk will change over time. Characterization of those enrolled in the

study is limited to ventricular arrhythmia/SCD phenotype expression during the follow up period. Nonetheless, it is arguable that knowledge of risk, even over this short time horizon, is of value in determining ICD therapy. A personalized chemical signature giving a temporal arrhythmia risk indicator would enable titration of personalized therapies appropriate to the forthcoming level of risk. It follows that over the very long term, expression of VA phenotype could become ubiquitous. Long-term predictors of VA risk may, in fact, be less discriminating.

The proteomic methodology chosen necessitated sample pooling. It is acknowledged that differential expression of a particular protein may have been driven by a single outlier within the group. However, pooling of samples has been shown to reduce biological variation and the need for replicates.[355356] Nonetheless, the biomarkers identified need validating as SCD/VA risk predicitors in a larger, independent cohort.

8.5 Conclusion

This novel high-resolution proteomic technique can be used in a HF device population to detect candidate prognostic biomarkers. Expression of these markers differs according to survival, VA occurrence and mode of death. This approach needs to be tested in a prospective study of candidate biomarkers, powered to characterise individuals in whom ICD therapy offers benefit.

Table 8.1 Patient characteristics

Group		Cardiovascular Death (n=7)	Prior Arrhythmia (n=25)	VA in follow up (n=35)	Survival (n=48)	*p*
Male		6 (86)	17 (68)	25 (71)	26 (54)	0.32
Aetiology	CAD	4 (57)	18 (72)	27 (77)	12 (25)	<0.01
LVEF	Normal	1 (14)	0 (0)	4 (11)	43 (90)	<0.01
	Mild	0 (0)	0 (0)	0 (0)	0 (0)	
	Modera					
	te	0 (0)	6 (24)	3 (9)	0 (0)	
	Severe	4 (57)	13 (52)	19 (54)	4 (8)	
NYHA	i	0 (0)	6 (24)	15 (43)	32 (67)	0.17
	ii	1 (14)	11 (44)	5 (14)	4 (8)	
	iii	3 (43)	2 (8)	5 (14)	0 (0)	
	iv	0 (0)	0 (0)	1 (3)	0 (0)	
DM		2 (29)	5 (20)	5 (14)	6 (13)	0.89

CAD, coronary artery disease; LVEF, left ventricular function; NYHA, New York Heart Association heart failure classification; DM, diabetes mellitus.

Table 8.2 Protein expression in cardiovascular death compared to survivors without arrhythmia

Protein	Accession Number	MW [kDa]	Fold difference
Pyruvate kinase isozymes M1/M2	P14618	57.9	16.67
Lysophosphatidylcholine acyltransferase 2*	Q7L5N7	60.2	6.71
Myosin-7	P12883	223.0	6.16
Apolipoprotein C-III	P02656	10.8	5.36
Natriuretic peptides A	P01160	16.7	4.57
Creatine kinase M-type	P06732	43.1	4.57
Retinol-binding protein 4	P02753	23.0	4.42
Interferon epsilon*	Q86WN2	24.4	4.40
Heat shock cognate 71	P11142	70.9	4.37
Tropomyosin alpha-3 chain	P06753	32.8	3.61
Thymosin beta-4, Y-chromosomal	O14604	5.0	2.90
Selenoprotein P	P49908	43.2	2.82
PtdIns-3-kinase C2 subunit gamma	O75747	165.6	2.79
Natriuretic peptides B	P16860	14.7	2.53
Trypsin-2	P07478	26.5	2.46
Polyubiquitin-C	P0CG48	77.0	2.45
Alpha-2-HS-glycoprotein*	P02765	39.3	2.38
Chromogranin-A*	P10645	50.7	2.20
FYVE and coiled-coil domain-containing protein 1	Q9BQS8	166.9	2.18
Small G protein signalling modulator 2	O43147	113.2	2.17
Microtubule-associated protein tau	P10636	78.9	2.08
Interferon-induced very large GTPase 1	Q7Z2Y8	278.9	-2.07
Protein piccolo OS=Homo sapiens	Q9Y6V0	552.9	-2.14
Protein deltex-4 OS=Homo sapiens	Q9Y2E6	67.2	-2.27
Transcription elongation factor SPT6*	Q7KZ85	198.9	-2.29
Dynein heavy chain 17, axonemal	Q9UFH2	511.5	-2.80
Collagen alpha-1(XI) chain*	P12107	181.0	-2.85
Zinc finger CCCH domain-containing protein 18*	Q86VM9	106.3	-3.36
Protein ELYS OS=Homo sapiens	Q8WYP5	252.3	-3.41
Ankyrin repeat domain-containing protein 26	Q9UPS8	196.2	-3.50
Probable methyltransferase BCDIN3D	Q7Z5W3	33.2	-4.22
Probable ATP-dependent RNA helicase DDX60-like *	Q5H9U9	197.5	-4.37
Nuclear receptor coactivator 2	Q15596	159.1	-5.81
Lipase maturation factor 2 *	Q9BU23	79.6	-11.63

MW, molecular weight. Fold difference values indicate higher or lower protein levels in cardiovascular death group compared with those surviving without ventricular arrhythmia. *indicates protein also seen in VA group compared to survivors.

Table 8.3 Protein expression in ventricular arrhythmia compared to survivors without arrhythmia

Protein	Accession Number	MW [kDa]	Fold difference
Lysophosphatidylcholine acyltransferase 2*	Q7L5N7	60.2	18.28
Vesicle-fusing ATPase	**P46459**	**82.5**	**5.77**
Interferon epsilon*	Q86WN2	24.4	4.73
Alpha-2-HS-glycoprotein*	P02765	39.3	3.82
Chromogranin-A*	P10645	50.7	3.28
Gamma-tubulin complex component 6	**Q96RT7**	**200.4**	**2.95**
Collagen alpha-1(XVIII) chain	**P39060**	**178.1**	**2.05**
Transcription elongation factor SPT6*	Q7KZ85	198.9	-2.08
Nidogen-1	**P14543**	**136.3**	**-2.18**
Desmoplakin	**P15924**	**331.6**	**-2.73**
Collagen alpha-1(XI) chain*	P12107	181.0	-3.05
Sodium/potassium-transporting ATPase β2	**P14415**	**33.3**	**-3.11**
Probable ATP-dependent RNA helicase DDX60-like*	Q5H9U9	197.5	-4.33
Zinc finger CCCH domain-containing protein 18*	Q86VM9	106.3	-6.33
Lipase maturation factor 2*	Q9BU23	79.6	-8.62
Signal peptidase complex subunit 3	**P61009**	**20.3**	**-11.24**

MW, molecular weight. Fold difference values indicate higher or lower protein levels in ventricular arrhythmia group compared with those surviving without ventricular arrhythmia. *indicates protein also seen in cardiovascular death group compared to survivors. Bold indicates proteins with greater differential expression than seen in cardiovascular death group compared to survivors.

Table 8.4 Protein expression in those experiencing cardiovascular death versus those experiencing VA

Protein	Accession Number	MW [kDa]	Fold difference
Vesicle-fusing ATPase	**P46459**	**82.5**	**6.102**
Myosin-7	P12883	223.0	4.297
Probable ATP-dependent RNA helicase DDX60-like	Q5H9U9	197.5	4.227
WD repeat- and FYVE domain-containing protein 4	**Q6ZS81**	**353.4**	**2.893**
Heat shock cognate 71 kDa protein	P11142	70.9	2.563
Transmembrane channel-like protein 7	**Q7Z402**	**83.4**	**2.272**
Tropomyosin alpha-3 chain	P06753	32.8	2.166
Polyubiquitin-C	P0CG48	77.0	2.131
Interferon-induced very large GTPase 1	Q7Z2Y8	278.9	2.036
Ig lambda chain V-II region NEI	**P01705**	**11.6**	**-2.094**
Vitamin K-dependent protein Z	**P22891**	**44.7**	**-2.102**
Probable methyltransferase BCDIN3D	Q7Z5W3	33.2	-2.159
Double-stranded RNA-specific editase 1	**P78563**	**80.7**	**-2.364**
Alpha-2,8-sialyltransferase 8B	Q92186	42.4	-3.150
Nuclear receptor coactivator 2	Q15596	159.1	-4.336
Protein S100-A7	**P31151**	**11.5**	**-6.002**
Lipase maturation factor 2	Q9BU23	79.6	-18.277
Ras-related protein Rab-5C	**P51148**	**23.5**	**-21.107**

MW, molecular weight. Fold difference values indicate higher or lower protein levels in cardiovascular death group compared with those experiencing ventricular arrhythmia. Bold indicates proteins with greater differential expression than seen in cardiovascular death group compared to survivors.

Table 8.5 Protein expression in those experiencing ventricular arrhythmia compared to those who did not (but had previously done so).

Protein	Accession Number	MW [kDa]	Fold difference
Pyruvate kinase isozymes M1/M2	P14618	57.9	9.316
Zinc finger CCCH domain-containing protein 18	Q86VM9	106.3	8.995
WD repeat- and FYVE domain-containing protein 4	Q6ZS81	353.4	3.294
Chromogranin-A	P10645	50.7	2.973
Protein YIPF3	Q9GZM5	38.2	2.581
Natriuretic peptides B	P16860	14.7	2.557
Microtubule-associated protein tau	P10636	78.9	2.490
Nucleolin	**P19338**	**76.6**	**2.283**
Beta-2-microglobulin	**P61769**	**13.7**	**2.280**
EMILIN-1	**Q9Y6C2**	**106.6**	**2.083**
Platelet glycoprotein Ib alpha chain	**P07359**	**68.9**	**-2.055**
Ig lambda chain V-II region NEI	**P01705**	**11.6**	**-2.070**
Surfeit locus protein 6	O75683	41.4	-2.093
Zinc finger protein 425	Q6IV72	87.7	-2.338
Carbohydrate sulfotransferase 15	**Q7LFX5**	**64.9**	**-2.422**
Keratin, type II cytoskeletal 5	**P13647**	**62.3**	**-2.585**
Double-stranded RNA-specific editase 1	**P78563**	**80.7**	**-2.717**
Keratin, type I cytoskeletal 14	**P02533**	**51.5**	**-3.374**
Alpha-2,8-sialyltransferase 8B	**Q92186**	**42.4**	**-3.955**
Keratin, type II cytoskeletal 1	**P04264**	**66.0**	**-4.567**
Keratin, type I cytoskeletal 9	**P35527**	**62.0**	**-4.733**
Protein S100-A7	P31151	11.5	-8.840
Lipase maturation factor 2	Q9BU23	79.6	-17.793
Ras-related protein Rab-5C	**P51148**	**23.5**	**-19.942**

MW, molecular weight. Fold difference values indicate higher or lower protein levels in ventricular arrhythmia group compared with those who did not (but had previously done so). Bold indicates proteins with greater differential expression than seen in arrhythmia group compared to those dying.

9 Validation of candidate arrhythmia biomarkers

9.1 Introduction

The candidate serum biomarkers presented Chapter 8 represent the broadest range of differentially expressed proteins. The highly sensitive proteomic approach defines biomarker profiles, with the potential to identify a panel of markers that describe distinct clinical risk groups. Whilst these results are encouraging, the findings were not validated through traditional techniques, or in an external clinical cohort. There are several barriers to achieving this. First, the overall number of participants was relatively small, and amongst those, the number of clinically relevant endpoints was low. Therefore, most samples were included in the initial proteomic experiment described, leaving few samples suitable for external validation. Second, the discovery experiment utilised a highly sensitive method. Traditional techniques for protein detection are limited due to cross-reactivity of antibodies, restricted availability of reagents, and the nanogram/millilitre concentration of candidates.[245] Targeted methods such as MRM-MS might find utility in biomarker validation[357], although these techniques are not yet widely used or accepted into clinical practice. On the other hand, technology such as ELISA is clinically recognised, widely used in daily practice and is commonly used in biomarker validation.

With these issues in mind, this study aimed to undertake a limited clinical and technical validation of suitable protein targets generated from the previous experiment.

9.2 Methods

9.2.1 Enzyme-linked immunosorbent assay

ELISA uses the basic immunology concept of an antigen binding to its specific antibody.[358] The "sandwich" technique is used to identify a specific protein antigen. Sample is added to a well, coated with a known quantity of bound *capture* antibody. This antibody is specific for the protein in question and will bind to any protein antigen present in the test sample. A biotin-conjugated anti-protein antibody is added, binding also to the test protein, hence "sandwiching" the protein. A non-specific Avidin conjugated Horseradish Peroxidase (HRP) is added. Following incubation, 3,3',5,5'-Tetramethylbenzidine (TMB) substrate will react where biotin-avidin-HRP is present, giving rise to a colour change, the optical density (OD) of which can be measured spectrophotometrically at a wavelength of 450nm±10nm (Figure 9.1).

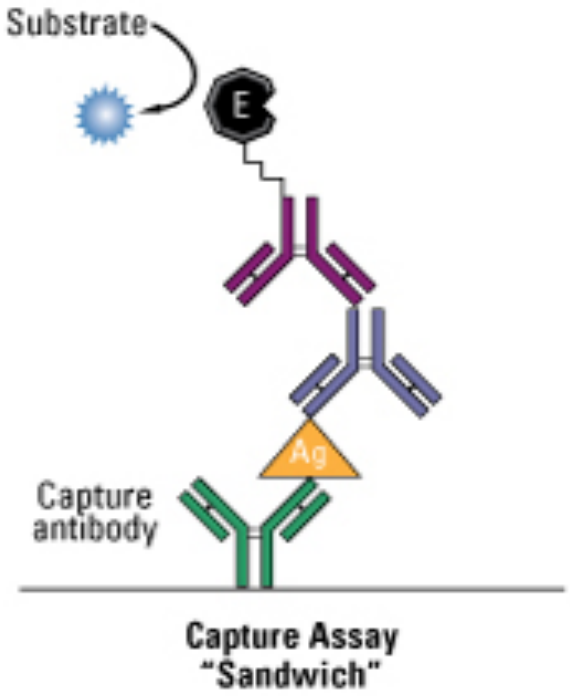

Figure 9.1 Antibody-Protein-antibody sandwich. Ag=protein antigen attached to blue protein. Purple is biotin-conjugated anti-protein. Substrate reacts with anti-protein complex giving rise to colour change.

9.2.1.1 ELISA kit

ELISA kits consisted of pre-coated 96-well strip plate, protein standard, biotin-conjugated antibody, HRP-avidin and TMB substrate (Cusabio Biotech Co. Ltd, Wuhan, China and USCN Life Science Inc. Wuhan, China). Kits were chosen based upon stated quality control. Each kit followed identical workflow.

9.2.1.2 Workflow

i. 100µl prepared standard was added to wells 1-8. 100µL of sample was added to the remaining wells in identical positions.
ii. Plates were incubated for 2 hours at 37˚C before liquid removal.
iii. 100µL of biotin antibody was added to each well before incubating for 1 hour at 37˚C.
iv. Liquid was removed and the wells washed with 200µL wash buffer. This process was repeated for a total of three washes to fully remove unbound protein.
v. 100µL HRP-avidin was added to each well and incubated for 1 hour at 37˚C.
vi. Liquid was removed and the wells washed with 200µL wash buffer. This process was repeated for a total of five washes to fully remove unbound protein.

vii. 90µL TMB substrate was added to each well before incubation at 37˚C for 15-30minutes in darkness.
viii. 50µL stop solution (1mol/L sulphuric acid) was added to each well.
ix. Optical density of each well was read using a microplate reader set to 450nm.

9.2.2 Patients

All patients were enrolled in a biomarker analysis research programme, recruited from those attending University Hospital Southampton for cardiac device follow up. Inclusion and exclusion criteria, enrolment protocol and sample collection were as described in Chapter 8.
With approval of the Faculty of Medicine Ethics Committee, additional "healthy controls" were recruited from University of Southampton students, self-reporting as healthy. Serum was collected and processed in an identical fashion to clinical samples, in accordance with the SOPIWG.[248] However, no clinical follow up was undertaken in this group, and serum was used within 1 month of -80˚C storage.

Within the limitations of the ELISA kit, only 88 samples could be tested (96 well plate, including 8 reference standards). In order to restrict the population along reasoned grounds, the test cohort was restricted to those with CAD, amounting to 86 samples. Disease controls were identified as those individuals in the original cohort who had expressed no arrhythmia prior to enrolment, or during follow up. The two remaining wells were therefore utilised for these disease controls, pooled into one sample, and the healthy controls, pooled into one sample.

9.2.3 Protein candidates

Protein candidates were selected from results generated from the biomarker discovery experiment detailed in Chapter 8. Proteins were chosen from the full list of candidates, based upon differential expression between clinical groupings, but limited to those proteins with a validated, commercially available ELISA kit, capable of detection within the range of the kit. (Table 9.1)

9.2.4 Statistics

Absorbance readings were normalised according to the zero reference and log plotted against the known standards. Regression analysis was used to calculate unknown protein concentration.

Categorical variables were expressed as percentages (numbers). Normally distributed continuous variables are expressed as mean±SD and compared using the independent-samples t-test. Variables not normally distributed are expressed as median (lower quartile to upper quartile) and compared using the Mann–Whitney

U test. Student's one sample T test used to compare protein expression against the control standard. Cox proportional hazards models were used to investigate candidate markers as predictors of death or ventricular arrhythmia.

9.3 Results

From the patients enrolled in the biomarker research programme, 86 patients were identified with CAD who also expressed a clear VA phenotype or died. Half of these participants had been included in the proteomic biomarker discovery experiment (Chapter 8) expressing either VA or cardiovascular death. There were 43 further patients who had been enrolled but had not been included in the discovery phase, and these samples went on to form a validation set. These two groups were similar in age, gender, renal function and LVEF, but differed in the time from sampling to first clinical event (VA or death) (Table 9.2) The disease control group was similar in age, but had preserved LV. Healthy controls were younger.

Full ELISA results are shown in Appendix B. Of 13 ELISA kits, only 9 gave meaningful results. Myosin8, beta actin, BNP and Galectin were not detected consistently in the majority of samples, despite protein standards being read as expected. This suggests the protein concentration was outside the range of detection, although a technical failure cannot be excluded. No further analysis of these proteins was performed.

Protein concentration in the pooled healthy control group was incongruous. Up or down regulation was inconsistent when considering results in the disease control group and HF samples. It is likely this was a reflection of the sample preparation and reduced length of time in storage, although any individual with occult cardiac disease may have skewed the result. These results were therefore not used in any further analysis.

9.3.1 Discovery group

Of the 9 proteins suitable for analysis, 7 demonstrated differential expression when compared to disease controls (Table 9.3). Calpain-2, LPCAT2, tropomyosin, and Voltage-dependent anion-selective channel protein 1 (VDAC1) were differentially expressed in both death and VA groups. With respect to disease control, up and down-regulation matched that seen in the proteomic results (Chapter 8). LPACT2 and tropomyosin had differential expression between death and VA that matched the proteomic experiment.

9.3.2 Validation group

Four proteins demonstrated differential expression when compared to control (Table 9.3). LPACT2, tropmyosin and VDAC1 were differentially expressed in both death and VA groups. Compared to death, the VA group had greater LPACT2 expression and lesser VDAC1 expression, mirroring the proteomic results.

9.3.3 Biomarkers of survival

LPACT2, tropomyosin and VDAC1 showed differential expression in those experiencing death or VA, when compared to controls, and this was seen in both discovery and validation groups. These proteins, along with age, LV function and creatinine at enrolment, were considered as predictors of death or VA is univariable models. None of these were significant predictors of time to these events (Table 9.4).

9.4 Discussion

The main finding of this study is that ELISA can be used to validate candidate biomarker proteins identified through high resolution novel proteomic techniques. LPACT2, tropomyosin and VDAC1 were shown to have different expression in those experiencing VA or death, and those surviving without VA.

LPCAT2 is a calcium dependent enzyme involved PAF biosynthesis under inflammatory conditions. PAF is produced by human heart and is thought to be implicated in HF since it participates in cardiomyocyte apoptosis and causes a negative inotropic effect [339340]. In a small pilot study of healthy volunteers and newly diagnosed HF patients, concentrations of LPCAT2 were shown to increase during follow up.[341]

The tropomyosins are widely distributed actin-binding proteins involved in the contractile system of both striated and smooth muscle. Mutations in the encoding gene are associated with type 3 familial hypertrophic cardiomyopathy, LV non-compaction and dilated cardiomyopathy.[359] The isoform alpha-3 is highly expressed in skeletal muscle and it is also plausible that higher circulating levels of tropomyosin result from the cardiac cachexia seen in advanced HF states.[360]

VDAC1 is a mitochondrial membrane protein, responsible for apoptosis.[361] Increased expression of VDAC1results in mitochondrial permeability to metabolites and exchange of nucleotides. Sequencing has shown up-regulation of the VDAC1 gene in hypertrophic human hearts[362], and Mitra *et al.* found increased expression of the protein in a mouse model of ventricular hypotrophy.[363] Cheng *et al.* examined the effect of nitric oxide on rat cardiac VDAC1, proposing a cardioprotective role of VDAC1, furthering findings that inhibition of VDAC1 phosphorylation was associated

with less ischaemia/reperfusion injury in rabbit hearts.[364] In vivo down-regulation of this protein has not been described previously in an adult ischaemic population. The protein has, however, been associated with many disease processes, reflecting its ubiquitous nature, and it is unlikely to specific for cardiac disease.[365]

These proteins were selected from many differentially expressed proteins, predominantly based upon suitability for ELISA detection, and availability of commercial detection kits. ELISA as a tool for quantification of biomarkers has been used for many years and is common in clinical practice.[358] This study demonstrates that it can be used to validate protein biomarkers, discovered by more sophisticated techniques, but that its use for low concentration proteins is limited. In addition, the patient population, sample preparation and storage may affect results. Technical failings are also possible. Therefore, these results serve to add confidence to the proteomic technique, but cannot fully validate the findings. Validation is likely to require techniques that can match the sensitivity of mass spectrometry, such as MRM-MS. However, such technology is costly and requires specific expertise, and is therefore not available routinely.

9.4.1 Limitations

Whilst these biomarkers might be suitable for identifying different prognostic groups, the potential of every differentially expressed protein has not been investigated. It is likely that there is utility in other candidate proteins, and even if the sensitivity of ELISA is suitable, the time and cost resource would make this prohibitive.

9.5 Conclusion

This study provides clinical and technical validation of protein biomarkers and provides proof of principle that proteomic techniques can identify candidate proteins for use as biomarkers of arrhythmia risk.

ELISA is limited in its sensitivity to detect all proteins, and is subject to technical failure. Further investigation is needed with validation techniques that can match the high sensitivity of proteomics before testing in a prospective setting.

Table 9.1 Protein candidates.

Protein	Accession Number	Death	VA
Actin	P60709	2.72	2.46
Natriuretic peptides A	P01160	2.65	1.92
Natriuretic peptides B	P16860	2.13	1.64
Galectin-3	P17931	1.94	1.38
Apolipoprotein(a)	P08519	1.86	1.62
Lysophosphatidylcholine acyltransferase 2	Q7L5N7	1.46	2.07
Myosin-8	P13535	1.37	0.85
Proteoglycan 4	Q92954	1.34	2.34
Alpha-2-HS-glycoprotein	P02765	1.28	1.76
Tropomyosin alpha-3 chain	P06753	0.44	0.11
Tyrosine-protein kinase BLK	P51451	-1.67	-0.81
Voltage-dependent anion-selective channel protein 1	P21796	-3.17	-3.66
Calpain-2	P17655	-3.69	-3.95

VA,ventricular arrhythmia. Numbers represent fold change compared to survivors, generated from experiment in Chapter 8.

Table 9.2 Baseline characteristics

	Discovery	Validation	*p*	Disease control	Healthy control
n	43	43		11	24
Age	71±8	69±9	0.28	72±7	33±8
Male gender	38	37		6	14
LVEF (%)	29±9	26±8	0.11		
Creatinine	126±42	122±41	0.66	n/a	n/a
Days to event	861+-549	1173+-400	<0.01		

LVEF, left ventricular ejection fraction.

Table 9.3 ELISA validation of candidate proteins.

Protein	Control	Discovery				Validation			
	No VA (n=11)	Death (n=10)	*p*	VA (n=29)	*P*	Death (n=11)	*p*	VA (n=13)	*p*
Natriuretic peptides A	2.01	1.83±0.57	0.34	**1.14±0.85**	**<0.01**	1.88±0.69	0.52	**1.07±0.77**	**<0.01**
Calpain-2	1.26	**1.20±0.08**	**0.06**	**1.24±0.05**	**0.02**	1.26±0.02	0.91	1.25±0.03	0.79
LPCAT 2	0.63	**0.91±0.19**	**<0.01**	**0.98±0.23**	**<0.01**	**0.93±0.17**	**<0.01**	**0.98±0.15**	**<0.01**
Tyrosine-protein kinase BLK	-0.22	**-0.33±0.16**	**0.05**	-0.16±0.2	0.13	-0.19±0.18	0.64	-0.26±0.14	0.36
Tropomyosin alpha-3 chain	-0.41	**-0.06±0.13**	**<0.01**	**-0.10±0.20**	**<0.01**	**-0.53±0.17**	**<0.01**	**-0.11±0.17**	**<0.01**
VDAC1	1.43	**0.85±0.61**	**0.02**	**1.00±0.65**	**<0.01**	**0.98±0.52**	**0.02**	**0.79±0.84**	**0.02**
Proteoglycan 4	0.75	**0.84±0.16**	0.11	0.70±0.32	0.41	0.96±0.41	0.12	0.82±0.47	0.61
Alpha-2-HS-glycoprotein	2.60	**2.77±0.18**	**0.02**	2.52±0.30	0.15	2.79±0.47	0.21	2.78±0.41	0.14
Apolipoprotein(a)	0.52	0.58±0.15	0.26	**0.59±0.12**	**0.01**	0.54±0.14	0.75	0.55±0.10	0.28

VA, ventricular arrhythmia; LPCAT 2, Lysophosphatidylcholine acyltransferase 2; VDAC 1, Voltage-dependent anion-selective channel protein 1. Red indicates down-regulation and blue up-regulation with respect to control. Values represent log concentration. p value represents difference between disease and control group expression.

Table 9.4 Predictors of death or ventricular arrhythmia. HR=hazard ratio

	Death		Ventricular arrhythmia	
	p	HR (95% CI)	p	HR (95% CI)
Age	0.94	1.002 (0.954-1.052)	0.92	1.003 (0.953-1.055)
LVEF (%)	0.72	1.012 (0.947-1.082)	0.63	0.979 (0.900-1.066)
Creatinine	0.80	0.999 (0.988-1.009)	0.21	0.992 (0.979-1.005)
LPACT2	0.25	0.290 (0.035-2.413)	0.24	4.281 (0.389-47.084)
Tropomyosin	0.50	2.198 (0.222-21.557)	0.47	0.431 (0.44-4.253)
VDAC1	0.86	0.941 (0.488-1.8140)	0.99	0.996 (0.487-2.039)

LVEF, left ventricular ejection fraction; LPCAT 2, Lysophosphatidylcholine acyltransferase 2; VDAC 1, Voltage-dependent anion-selective channel protein 1

10 Conclusions

The work presented in this thesis was undertaken to explore how risk stratification of SCD might be refined. Several non-invasive techniques were chosen, and their application to a HF population explored. In addition, I examined the utility of custom developed electrocardiographic and biochemical markers in this role.

10.1 Summary of original findings

10.1.1 The ECG as a marker of risk

Myocardial scar is known to be associated with cardiac mortality and SCD. Detecting myocardial scar through techniques such as CMR requires expertise and is resource limited. I examined ECG markers, which through an association with myocardial scar, might be of use in risk stratification.

The utility of fQRS to predict cardiovascular mortality or VA was studied in Chapter 1. Other groups have explored this marker, publishing data from CAD or NICM populations, but the results are discrepant. I undertook a meta-analysis including data from >5000 patients to better understand the utility of fQRS as a risk stratifier. fQRS was associated with an increased risk of mortality but a greater risk of VA events. Subgroup analysis demonstrated greater mortality and SCD risk in those with LVEF >35% and SCD risk in those with QRS duration <120ms.

ECG markers of ventricular repolarisation have an association with SCD. The relationship between these markers, such as QT interval and TpTe, were explored in Chapter 4. In this retrospective study of patients with CAD, a strong association was seen between the extent of subendocardial LV scar and prolonged QTc, QTD and TpTe. However, no association was seen between these markers and total scar burden, or that extending beyond the sub-endocardium. In addition, in this population, the ECG markers were not associated with VA occurrence. These findings question the assumption that ECG changes might simply reflect myocardial scar. Characteristics of the scar, such as transmural extent, are likely to affect ECG changes, Their significance needs to be considered in this context.

The Selvester QRS score is an ECG test, proposed as a marker of LV scar and SCD. However, it was not known whether the score was predictive of clinical outcomes due to association with myocardial scar, and how the scar characteristics might affect this. The experiment in Chapter 5 explored this, finding that in a retrospective analysis, QRS scoring performed best in quantifying transmural scar, but was not associated with subendocardial scar. The score was predictive of all cause mortality but not VA.

One of the limiting factors of the technique was the considerable time taken to calculate the manual score. If it were to be used as a screening tool for the general population, an automated scoring system would need to speed up the process, whilst maintaining accuracy. Chapter 6 explored this through prospective investigation and supported the use of custom computerized algorithm to achieve this. However, the specificity of the score in detecting LV scar was weak, and therefore its use a "rule out" test for scar is questionable.

The aforementioned ECG techniques were developed for use in manual calculation. In an effort to fully exploit computing techniques in scar detection, Chapter 7 investigated the use of artificial intelligence and developed a novel SVM, trained to differentiate between the ECGs of individuals with and without LV scar. This demonstrated excellent accuracy and negative prediction, making it attractive as a rule out test for myocardial scar.

10.1.2 High resolution proteomics

The utility of biomarkers, such as BNP, in the diagnosis of HF is established. However, blood biomarkers, either singly or in combination, are not predictive or specific for arrhythmic HF outcomes, against which ICD therapy might protect. I investigated the use of a novel high resolution proteomic technique to identify biomarkers that might be useful in this regard. Chapter 8 describes this work, describing the differential expression of proteins at baseline that was predictive of subsequent death or VA.

Whilst more than 500 proteins were differentially expressed between outcome groups, Chapter 9 details the validation of a small number of these using the more established technique, ELISA. The markers Lysophosphatidylcholine acyltransferase 2, tropomyosin and VDAC1 showed differential expression in those experiencing death or VA, when compared to those surviving.

10.2 Limitations

This thesis explored a number of possibilities to refine risk stratification in SCD, and ultimately improve targeting of ICD implantation. However it is difficult to draw firm conclusions from the work, most of which was conducted at a single centre, and some of which involved retrospective analysis, There was significant heterogeneity in the populations studied, with some studies involving only CAD populations, whilst others included those with NICM, or indeed no specific cardiac diagnosis. Therefore, whether these results can be applied to a wider population is not clear.

The proposed ECG and biochemical markers may have a role in SCD risk stratification, but in general the studies have not explored the incremental benefit over and above more established selection tools. In addition, no attempt was made to determine which marker has greatest potential, or indeed whether a multimarker strategy would be show more promise.

Each of these limitations, as well as those discussed in the respective chapters, need addressing in a prospective multicentre, randomized control trial.

10.3 Final conclusion

Identification of patients at risk of SCD remains a challenge. Current risk stratification tools, used in clinical practice to identify ICD recipients, lack specificity for mode of death. Novel non invasive markers, such as serum proteins and computer analysis of the ECG may be valuable tools to improve risk prediction. The incremental benefit of these tools to determine prognosis, and select those in need of ICD therapy, needs addressing in prospective studies.

Appendix A

Full protein quantification output from Proteome Discoverer (Chapter 8). Identification was based upon a false discovery rate, q<0.05. Quantification ratios were median-normalized and transformed to log2 ratios. Up/down regulation indicated by greyscale (white/black), ordered here by 113/116.

Accession	Description	113/116	114/116	113/114	113/115	114/115	115/116
P14618	Pyruvate kinase isozymes M1/M2 OS=Homo sapiens GN=PKM2 PE=1 SV=4 - [KPYM_HUMAN]	4.059	-3.752	-3.837	-0.555	-3.220	0.685
Q7L5N7	Lysophosphatidylcholine acyltransferase 2 OS=Homo sapiens GN=LPCAT2 PE=1 SV=1 - [PCAT2_HUMAN]	2.745	0.314	-0.209	0.327	-0.005	4.192
P12883	Myosin-7 OS=Homo sapiens GN=MYH7 PE=1 SV=5 - [MYH7_HUMAN]	2.622	1.892	2.806	2.103	-0.222	-0.248
P02656	Apolipoprotein C-III OS=Homo sapiens GN=APOC3 PE=1 SV=1 - [APOC3_HUMAN]	2.421	-0.651	0.502	0.192	-0.803	0.001
P01160	Natriuretic peptides A OS=Homo sapiens GN=NPPA PE=1 SV=1 - [ANF_HUMAN]	2.193	-0.556	0.947	0.299	-0.866	0.248
P06732	Creatine kinase M-type OS=Homo sapiens GN=CKM PE=1 SV=2 - [KCRM_HUMAN]	2.191	1.603	3.394	0.876	0.716	-0.646
P02753	Retinol-binding protein 4 OS=Homo sapiens GN=RBP4 PE=1 SV=3 - [RET4_HUMAN]	2.144	-0.302	0.394	0.137	-0.445	0.716
Q86WN2	Interferon epsilon OS=Homo sapiens GN=IFNE PE=2 SV=1 - [IFNE_HUMAN]	2.136	-1.207	-0.202	-0.491	-0.739	2.240
P11142	Heat shock cognate 71 kDa protein OS=Homo sapiens GN=HSPA8 PE=1 SV=1 - [HSP7C_HUMAN]	2.126	0.785	1.246	1.358	-0.583	0.486
P06753	Tropomyosin alpha-3 chain OS=Homo sapiens GN=TPM3 PE=1 SV=1 - [TPM3_HUMAN]	1.850	1.153	2.527	1.115	0.265	-0.320
O14604	Thymosin beta-4, Y-chromosomal OS=Homo sapiens GN=TMSB4Y PE=2 SV=3 - [TYB4Y_HUMAN]	1.536	0.840	1.326	0.909	-0.080	-0.023
P49908	Selenoprotein P OS=Homo sapiens GN=SEPP1 PE=1 SV=3 - [SEPP1_HUMAN]	1.496	-0.274	-0.132	0.129	-0.441	0.291
O75747	Phosphatidylinositol 4-phosphate 3-kinase C2 domain-containing subunit gamma OS=Homo sapiens GN=PIK3C2G PE=1 SV=3 - [P3C2G_HUMAN]	1.478	0.078	1.711	-0.386	0.440	-0.115
P16860	Natriuretic peptides B OS=Homo sapiens GN=NPPB PE=1 SV=1 - [ANFB_HUMAN]	1.338	-0.620	1.297	0.723	-1.354	0.920
P07478	Trypsin-2 OS=Homo sapiens GN=PRSS2 PE=1 SV=1 - [TRY2_HUMAN]	1.296	-0.566	0.255	-0.059	-0.517	0.784
P0CG48	Polyubiquitin-C OS=Homo sapiens GN=UBC PE=1 SV=2 - [UBC_HUMAN]	1.293	0.561	0.859	1.091	-0.542	-0.017
P02765	Alpha-2-HS-glycoprotein OS=Homo sapiens GN=AHSG PE=1 SV=1 - [FETUA_HUMAN]	1.252	-0.346	-0.102	-0.236	-0.086	1.935
P10645	Chromogranin-A OS=Homo sapiens GN=CHGA PE=1 SV=7 - [CMGA_HUMAN]	1.139	-0.913	0.408	0.648	-1.572	1.713
Q9BQS8	FYVE and coiled-coil domain-containing protein 1 OS=Homo sapiens GN=FYCO1 PE=1 SV=3 - [FYCO1_HUMAN]	1.126	-0.462	0.533	-0.207	-0.247	0.402
O43147	Small G protein signaling modulator 2 OS=Homo sapiens GN=SGSM2 PE=1 SV=4 - [SGSM2_HUMAN]	1.114	-0.516	0.086	-0.341	-0.168	0.398
P10636	Microtubule-associated protein tau OS=Homo sapiens GN=MAPT PE=1 SV=5 - [TAU_HUMAN]	1.053	-0.718	1.347	0.576	-1.316	0.546
Q13201	Multimerin-1 OS=Homo sapiens GN=MMRN1 PE=1 SV=3 - [MMRN1_HUMAN]	0.985	-0.217	0.134	0.114	-0.342	0.062
Q9Y6C2	EMILIN-1 OS=Homo sapiens GN=EMILIN1 PE=1 SV=2 - [EMIL1_HUMAN]	0.966	-0.720	0.630	0.328	-1.059	0.558
Q86YW5	Trem-like transcript 1 protein OS=Homo sapiens GN=TREML1 PE=1 SV=2 - [TRML1_HUMAN]	0.957	-0.626	-0.239	-0.070	-0.567	0.099
P0C0S5	Histone H2A.Z OS=Homo sapiens GN=H2AFZ PE=1 SV=2 - [H2AZ_HUMAN]	0.952	-0.228	-0.405	0.544	-0.746	0.554
P69905	Hemoglobin subunit alpha OS=Homo sapiens GN=HBA1 PE=1 SV=2 - [HBA_HUMAN]	0.917	0.292	-0.033	-0.090	0.347	0.426
P78352	Disks large homolog 4 OS=Homo sapiens GN=DLG4 PE=1 SV=3 - [DLG4_HUMAN]	0.913	-0.170	-0.018	0.110	-0.273	0.396
P68431	Histone H3.1 OS=Homo sapiens GN=HIST1H3A PE=1 SV=2 - [H31_HUMAN]	0.883	-0.002	-0.191	0.564	-0.604	0.160

P02655	Apolipoprotein C-II OS=Homo sapiens GN=APOC2 PE=1 SV=1 - [APOC2_HUMAN]	0.880	-0.562	-0.032	-0.722	0.150	0.426
P02743	Serum amyloid P-component OS=Homo sapiens GN=APCS PE=1 SV=2 - [SAMP_HUMAN]	0.876	-0.512	-0.158	-0.231	-0.304	0.214
O60814	Histone H2B type 1-K OS=Homo sapiens GN=HIST1H2BK PE=1 SV=3 - [H2B1K_HUMAN]	0.859	-0.078	-0.153	0.673	-0.864	0.270
P27797	Calreticulin OS=Homo sapiens GN=CALR PE=1 SV=1 - [CALR_HUMAN]	0.803	0.445	0.582	0.068	0.366	-0.074
Q9H299	SH3 domain-binding glutamic acid-rich-like protein 3 OS=Homo sapiens GN=SH3BGRL3 PE=1 SV=1 - [SH3L3_HUMAN]	0.791	-0.820	-0.068	-0.179	-0.652	-0.129
P05154	Plasma serine protease inhibitor OS=Homo sapiens GN=SERPINA5 PE=1 SV=3 - [IPSP_HUMAN]	0.790	-0.305	0.360	-0.014	-0.337	-0.525
P62805	Histone H4 OS=Homo sapiens GN=HIST1H4A PE=1 SV=2 - [H4_HUMAN]	0.770	0.084	-0.078	0.502	-0.251	0.054
Q9UMX5	Neudesin OS=Homo sapiens GN=NENF PE=1 SV=1 - [NENF_HUMAN]	0.749	-0.495	0.195	0.018	-0.523	0.724
Q96JB2	Conserved oligomeric Golgi complex subunit 3 OS=Homo sapiens GN=COG3 PE=1 SV=3 - [COG3_HUMAN]	0.740	-0.343	-0.249	-0.086	-0.269	0.153
Q96RT7	Gamma-tubulin complex component 6 OS=Homo sapiens GN=TUBGCP6 PE=1 SV=3 - [GCP6_HUMAN]	0.735	0.374	0.565	0.431	-0.080	1.563
P02735	Serum amyloid A protein OS=Homo sapiens GN=SAA1 PE=1 SV=2 - [SAA_HUMAN]	0.730	0.016	0.369	0.711	-0.497	0.627
P15924	Desmoplakin OS=Homo sapiens GN=DSP PE=1 SV=3 - [DESP_HUMAN]	0.725	0.693	0.988	0.591	0.090	-1.450
P68871	Hemoglobin subunit beta OS=Homo sapiens GN=HBB PE=1 SV=2 - [HBB_HUMAN]	0.724	0.018	0.015	0.042	-0.012	0.218
Q9Y5S1	Transient receptor potential cation channel subfamily V member 2 OS=Homo sapiens GN=TRPV2 PE=1 SV=1 - [TRPV2_HUMAN]	0.717	0.161	0.758	0.150	-0.001	0.990
P17936	Insulin-like growth factor-binding protein 3 OS=Homo sapiens GN=IGFBP3 PE=1 SV=2 - [IBP3_HUMAN]	0.669	-0.406	-0.076	-0.176	-0.235	0.174
P02766	Transthyretin OS=Homo sapiens GN=TTR PE=1 SV=1 - [TTHY_HUMAN]	0.669	-0.052	0.160	-0.067	-0.029	0.388
P68104	Elongation factor 1-alpha 1 OS=Homo sapiens GN=EEF1A1 PE=1 SV=1 - [EF1A1_HUMAN]	0.640	0.176	0.073	0.300	-0.292	0.003
P46459	Vesicle-fusing ATPase OS=Homo sapiens GN=NSF PE=1 SV=3 - [NSF_HUMAN]	0.639	3.021	2.663	2.609	0.389	2.529
Q6UWF7	Protein FAM55D OS=Homo sapiens GN=FAM55D PE=2 SV=1 - [FA55D_HUMAN]	0.639	-0.258	0.188	-0.362	0.081	0.107
Q07954	Prolow-density lipoprotein receptor-related protein 1 OS=Homo sapiens GN=LRP1 PE=1 SV=2 - [LRP1_HUMAN]	0.629	0.004	-0.030	-0.113	0.113	0.702
Q14587	Zinc finger protein 268 OS=Homo sapiens GN=ZNF268 PE=1 SV=2 - [ZN268_HUMAN]	0.626	0.145	0.143	0.213	-0.079	-0.118
Q68CZ2	Tensin-3 OS=Homo sapiens GN=TNS3 PE=1 SV=2 - [TENS3_HUMAN]	0.625	0.472	-0.208	0.498	-0.037	-0.069
Q92520	Protein FAM3C OS=Homo sapiens GN=FAM3C PE=1 SV=1 - [FAM3C_HUMAN]	0.625	0.170	0.143	0.213	-0.054	-0.069
Q8NFD2	Ankyrin repeat and protein kinase domain-containing protein 1 OS=Homo sapiens GN=ANKK1 PE=1 SV=1 - [ANKK1_HUMAN]	0.625	0.170	0.143	0.213	-0.054	-0.069
Q96PF1	Protein-glutamine gamma-glutamyltransferase Z OS=Homo sapiens GN=TGM7 PE=2 SV=1 - [TGM7_HUMAN]	0.625	0.170	0.143	0.213	-0.054	-0.069
P32004	Neural cell adhesion molecule L1 OS=Homo sapiens GN=L1CAM PE=1 SV=2 - [L1CAM_HUMAN]	0.625	0.170	0.143	0.213	-0.054	-0.069
Q9ULU8	Calcium-dependent secretion activator 1 OS=Homo sapiens GN=CADPS PE=1 SV=3 - [CAPS1_HUMAN]	0.625	0.170	0.143	0.213	-0.054	-0.069
Q9Y4D1	Disheveled-associated activator of morphogenesis 1 OS=Homo sapiens GN=DAAM1 PE=1 SV=2 - [DAAM1_HUMAN]	0.625	0.170	0.143	0.213	-0.054	-0.069
P23468	Receptor-type tyrosine-protein phosphatase delta OS=Homo sapiens GN=PTPRD PE=1 SV=2 - [PTPRD_HUMAN]	0.625	0.170	0.143	0.213	-0.054	-0.069
Q8IVF2	Protein AHNAK2 OS=Homo sapiens GN=AHNAK2 PE=1 SV=2 - [AHNK2_HUMAN]	0.625	0.170	0.143	0.213	-0.054	-0.069
P06733	Alpha-enolase OS=Homo sapiens GN=ENO1 PE=1 SV=2 - [ENOA_HUMAN]	0.601	0.093	0.199	0.243	-0.166	-0.206

P02042	Hemoglobin subunit delta OS=Homo sapiens GN=HBD PE=1 SV=2 - [HBD_HUMAN]	0.598	0.052	0.089	0.011	0.023	0.539
P08294	Extracellular superoxide dismutase [Cu-Zn] OS=Homo sapiens GN=SOD3 PE=1 SV=2 - [SODE_HUMAN]	0.585	0.101	0.421	0.199	-0.109	-0.289
P01880	Ig delta chain C region OS=Homo sapiens GN=IGHD PE=1 SV=2 - [IGHD_HUMAN]	0.574	-0.377	-0.192	0.145	-0.533	0.734
P08519	Apolipoprotein(a) OS=Homo sapiens GN=LPA PE=1 SV=1 - [APOA_HUMAN]	0.551	-0.618	-0.365	0.225	-0.776	0.767
P18428	Lipopolysaccharide-binding protein OS=Homo sapiens GN=LBP PE=1 SV=3 - [LBP_HUMAN]	0.536	0.095	0.296	0.222	-0.092	0.578
P15151	Poliovirus receptor OS=Homo sapiens GN=PVR PE=1 SV=2 - [PVR_HUMAN]	0.536	-0.319	0.475	0.199	-0.528	0.038
P48449	Lanosterol synthase OS=Homo sapiens GN=LSS PE=1 SV=1 - [ERG7_HUMAN]	0.532	-0.601	-0.192	0.196	-0.808	-0.223
Q6P9F7	Leucine-rich repeat-containing protein 8B OS=Homo sapiens GN=LRRC8B PE=2 SV=2 - [LRC8B_HUMAN]	0.513	0.285	-0.404	0.188	0.093	0.352
Q6UXM1	Leucine-rich repeats and immunoglobulin-like domains protein 3 OS=Homo sapiens GN=LRIG3 PE=2 SV=1 - [LRIG3_HUMAN]	0.511	0.050	0.407	0.192	-0.166	-0.369
P13647	Keratin, type II cytoskeletal 5 OS=Homo sapiens GN=KRT5 PE=1 SV=3 - [K2C5_HUMAN]	0.484	0.352	-0.081	-0.249	1.370	0.962
O75911	Short-chain dehydrogenase/reductase 3 OS=Homo sapiens GN=DHRS3 PE=1 SV=2 - [DHRS3_HUMAN]	0.473	-0.511	0.356	0.112	-0.634	0.574
Q96HR3	Mediator of RNA polymerase II transcription subunit 30 OS=Homo sapiens GN=MED30 PE=1 SV=1 - [MED30_HUMAN]	0.462	0.206	0.027	0.212	-0.017	-0.114
P04406	Glyceraldehyde-3-phosphate dehydrogenase OS=Homo sapiens GN=GAPDH PE=1 SV=3 - [G3P_HUMAN]	0.462	0.063	-0.001	0.238	-0.329	-0.222
P01773	Ig heavy chain V-III region BUR OS=Homo sapiens PE=1 SV=1 - [HV312_HUMAN]	0.459	-0.289	-0.408	-0.173	-0.140	-0.287
P02741	C-reactive protein OS=Homo sapiens GN=CRP PE=1 SV=1 - [CRP_HUMAN]	0.456	0.159	0.708	0.781	-0.626	0.482
Q92613	Protein Jade-3 OS=Homo sapiens GN=PHF16 PE=1 SV=1 - [JADE3_HUMAN]	0.454	0.007	-0.042	0.060	-0.064	-0.089
Q6ZRS2	Helicase SRCAP OS=Homo sapiens GN=SRCAP PE=1 SV=3 - [SRCAP_HUMAN]	0.453	-0.135	-0.890	-0.495	0.337	0.217
P01033	Metalloproteinase inhibitor 1 OS=Homo sapiens GN=TIMP1 PE=1 SV=1 - [TIMP1_HUMAN]	0.443	0.645	0.052	0.352	0.281	0.240
P12109	Collagen alpha-1(VI) chain OS=Homo sapiens GN=COL6A1 PE=1 SV=3 - [CO6A1_HUMAN]	0.443	-0.052	-0.072	-0.356	0.280	0.254
P35527	Keratin, type I cytoskeletal 9 OS=Homo sapiens GN=KRT9 PE=1 SV=3 - [K1C9_HUMAN]	0.441	0.870	0.200	-0.444	2.243	0.288
Q99969	Retinoic acid receptor responder protein 2 OS=Homo sapiens GN=RARRES2 PE=1 SV=1 - [RARR2_HUMAN]	0.437	0.274	0.120	0.421	-0.158	0.538
P31151	Protein S100-A7 OS=Homo sapiens GN=S100A7 PE=1 SV=4 - [S10A7_HUMAN]	0.433	0.563	2.075	-2.585	3.144	0.148
P80108	Phosphatidylinositol-glycan-specific phospholipase D OS=Homo sapiens GN=GPLD1 PE=1 SV=3 - [PHLD_HUMAN]	0.415	-0.064	-0.023	-0.174	0.130	0.144
P12259	Coagulation factor V OS=Homo sapiens GN=F5 PE=1 SV=4 - [FA5_HUMAN]	0.406	-0.143	-0.053	-0.080	-0.021	0.076
Q9BVA0	Katanin p80 WD40-containing subunit B1 OS=Homo sapiens GN=KATNB1 PE=1 SV=1 - [KTNB1_HUMAN]	0.406	0.309	0.308	0.012	0.273	0.555
Q08380	Galectin-3-binding protein OS=Homo sapiens GN=LGALS3BP PE=1 SV=1 - [LG3BP_HUMAN]	0.405	0.059	0.046	0.211	0.133	0.015
Q96PX1	RING finger protein 157 OS=Homo sapiens GN=RNF157 PE=1 SV=3 - [RN157_HUMAN]	0.391	-0.387	0.121	0.119	-0.530	-0.082
A6NK25	Putative protein FAM86A-like 3 OS=Homo sapiens PE=5 SV=2 - [F86A3_HUMAN]	0.376	-0.318	-0.228	0.050	-0.391	0.843
P02747	Complement C1q subcomponent subunit C OS=Homo sapiens GN=C1QC PE=1 SV=3 - [C1QC_HUMAN]	0.374	0.275	0.277	-0.314	0.587	0.529
Q9UBN4	Short transient receptor potential channel 4 OS=Homo sapiens GN=TRPC4 PE=1 SV=1 - [TRPC4_HUMAN]	0.373	0.129	1.282	0.216	-0.111	-0.050
P32119	Peroxiredoxin-2 OS=Homo sapiens GN=PRDX2 PE=1 SV=5 - [PRDX2_HUMAN]	0.372	-0.096	-0.134	-0.037	-0.122	0.157
Q9BWP8	Collectin-11 OS=Homo sapiens GN=COLEC11 PE=1 SV=1 - [COL11_HUMAN]	0.366	0.306	0.347	0.223	0.060	0.088
P42695	Condensin-2 complex subunit D3 OS=Homo sapiens GN=NCAPD3 PE=1 SV=2 - [CNDD3_HUMAN]	0.360	-0.345	-0.782	-0.259	-0.079	-0.305
P02671	Fibrinogen alpha chain OS=Homo sapiens GN=FGA PE=1 SV=2 - [FIBA_HUMAN]	0.355	-0.375	0.165	0.065	-0.513	0.017

P60709	Actin, cytoplasmic 1 OS=Homo sapiens GN=ACTB PE=1 SV=1 - [ACTB_HUMAN]	0.352	0.247	0.159	0.151	0.160	-0.027
P01344	Insulin-like growth factor II OS=Homo sapiens GN=IGF2 PE=1 SV=1 - [IGF2_HUMAN]	0.349	1.218	-0.321	0.725	0.483	0.828
Q96TA2	ATP-dependent zinc metalloprotease YME1L1 OS=Homo sapiens GN=YME1L1 PE=1 SV=2 - [YMEL1_HUMAN]	0.331	0.267	-0.043	0.764	-0.502	0.252
P04264	Keratin, type II cytoskeletal 1 OS=Homo sapiens GN=KRT1 PE=1 SV=6 - [K2C1_HUMAN]	0.329	0.763	0.026	-0.339	2.191	0.493
Q96JB1	Dynein heavy chain 8, axonemal OS=Homo sapiens GN=DNAH8 PE=1 SV=2 - [DYH8_HUMAN]	0.326	0.187	0.616	0.075	0.142	0.307
Q8IYK2	Coiled-coil domain-containing protein 105 OS=Homo sapiens GN=CCDC105 PE=2 SV=3 - [CC105_HUMAN]	0.325	1.267	1.178	0.594	0.650	0.940
P12830	Cadherin-1 OS=Homo sapiens GN=CDH1 PE=1 SV=3 - [CADH1_HUMAN]	0.322	0.252	0.159	-0.004	0.233	0.203
P08246	Neutrophil elastase OS=Homo sapiens GN=ELANE PE=1 SV=1 - [ELNE_HUMAN]	0.321	-0.281	0.218	-0.092	-0.200	0.188
Q14D04	Ventricular zone-expressed PH domain-containing protein homolog 1 OS=Homo sapiens GN=VEPH1 PE=1 SV=1 - [MELT_HUMAN]	0.318	-0.402	-0.145	-0.808	0.382	0.867
Q8IWZ3	Ankyrin repeat and KH domain-containing protein 1 OS=Homo sapiens GN=ANKHD1 PE=1 SV=1 - [ANKH1_HUMAN]	0.313	-0.133	-0.956	-0.495	0.339	0.253
Q9H2Q1	Transmembrane protein 133 OS=Homo sapiens GN=TMEM133 PE=2 SV=1 - [TM133_HUMAN]	0.313	-0.150	-0.212	-0.491	0.318	0.253
P50222	Homeobox protein MOX-2 OS=Homo sapiens GN=MEOX2 PE=1 SV=2 - [MEOX2_HUMAN]	0.313	-0.150	-0.212	-0.491	0.318	0.253
Q9H3Y0	Peptidase inhibitor R3HDML OS=Homo sapiens GN=R3HDML PE=1 SV=1 - [CRSPL_HUMAN]	0.313	-0.150	-0.212	-0.491	0.318	0.253
Q5EBM4	Putative zinc finger protein 542 OS=Homo sapiens GN=ZNF542 PE=5 SV=2 - [ZN542_HUMAN]	0.313	-0.150	-0.212	-0.491	0.318	0.253
Q8NBV4	Probable lipid phosphate phosphatase PPAPDC3 OS=Homo sapiens GN=PPAPDC3 PE=2 SV=1 - [PPAC3_HUMAN]	0.313	-0.150	-0.212	-0.491	0.318	0.253
Q12947	Forkhead box protein F2 OS=Homo sapiens GN=FOXF2 PE=1 SV=2 - [FOXF2_HUMAN]	0.313	-0.150	-0.212	-0.491	0.318	0.253
P78318	Immunoglobulin-binding protein 1 OS=Homo sapiens GN=IGBP1 PE=1 SV=1 - [IGBP1_HUMAN]	0.313	-0.150	-0.212	-0.491	0.318	0.253
Q6NX45	Zinc finger protein 774 OS=Homo sapiens GN=ZNF774 PE=2 SV=2 - [ZN774_HUMAN]	0.313	-0.150	-0.212	-0.491	0.318	0.253
Q9BTY2	Plasma alpha-L-fucosidase OS=Homo sapiens GN=FUCA2 PE=1 SV=2 - [FUCO2_HUMAN]	0.313	-0.150	-0.212	-0.491	0.318	0.253
P62495	Eukaryotic peptide chain release factor subunit 1 OS=Homo sapiens GN=ETF1 PE=1 SV=3 - [ERF1_HUMAN]	0.313	-0.150	-0.212	-0.491	0.318	0.253
P0C860	Putative male-specific lethal-3 protein-like 2 OS=Homo sapiens GN=MSL3P1 PE=5 SV=1 - [MS3L2_HUMAN]	0.313	-0.150	-0.212	-0.491	0.318	0.253
Q3LXA3	Bifunctional ATP-dependent dihydroxyacetone kinase/FAD-AMP lyase (cyclizing) OS=Homo sapiens GN=DAK PE=1 SV=2 - [DHAK_HUMAN]	0.313	-0.150	-0.212	-0.491	0.318	0.253
Q9NR82	Potassium voltage-gated channel subfamily KQT member 5 OS=Homo sapiens GN=KCNQ5 PE=1 SV=3 - [KCNQ5_HUMAN]	0.313	-0.150	-0.212	-0.491	0.318	0.253
Q96RD9	Fc receptor-like protein 5 OS=Homo sapiens GN=FCRL5 PE=1 SV=3 - [FCRL5_HUMAN]	0.313	-0.150	-0.212	-0.491	0.318	0.253
P55285	Cadherin-6 OS=Homo sapiens GN=CDH6 PE=1 SV=1 - [CADH6_HUMAN]	0.313	-0.150	-0.212	-0.491	0.318	0.253
Q9H0D6	5'-3' exoribonuclease 2 OS=Homo sapiens GN=XRN2 PE=1 SV=1 - [XRN2_HUMAN]	0.313	-0.150	-0.212	-0.491	0.318	0.253
Q92833	Protein Jumonji OS=Homo sapiens GN=JARID2 PE=1 SV=2 - [JARD2_HUMAN]	0.313	-0.150	-0.212	-0.491	0.318	0.253
Q9HCJ0	Trinucleotide repeat-containing gene 6C protein OS=Homo sapiens GN=TNRC6C PE=1 SV=3 - [TNR6C_HUMAN]	0.313	-0.150	-0.212	-0.491	0.318	0.253
P09884	DNA polymerase alpha catalytic subunit OS=Homo sapiens GN=POLA1 PE=1 SV=2 - [DPOLA_HUMAN]	0.313	-0.150	-0.212	-0.491	0.318	0.253
Q7Z407	CUB and sushi domain-containing protein 3 OS=Homo sapiens GN=CSMD3 PE=2 SV=3 - [CSMD3_HUMAN]	0.313	-0.150	-0.212	-0.491	0.318	0.253
Q7Z6Z7	E3 ubiquitin-protein ligase HUWE1 OS=Homo sapiens GN=HUWE1 PE=1 SV=3 - [HUWE1_HUMAN]	0.313	-0.150	-0.212	-0.491	0.318	0.253

P02533	Keratin, type I cytoskeletal 14 OS=Homo sapiens GN=KRT14 PE=1 SV=4 - [K1C14_HUMAN]	0.306	0.334	-0.197	-1.000	1.755	0.633
P00738	Haptoglobin OS=Homo sapiens GN=HP PE=1 SV=1 - [HPT_HUMAN]	0.302	-0.274	0.110	-0.217	-0.012	0.183
P17931	Galectin-3 OS=Homo sapiens GN=LGALS3 PE=1 SV=5 - [LEG3_HUMAN]	0.299	-0.560	0.155	0.156	-0.727	0.440
O14756	17-beta-hydroxysteroid dehydrogenase type 6 OS=Homo sapiens GN=HSD17B6 PE=1 SV=1 - [H17B6_HUMAN]	0.291	0.075	-0.053	0.227	-0.144	-0.050
Q8WZ75	Roundabout homolog 4 OS=Homo sapiens GN=ROBO4 PE=1 SV=1 - [ROBO4_HUMAN]	0.289	-0.095	0.163	0.102	-0.189	0.756
P04278	Sex hormone-binding globulin OS=Homo sapiens GN=SHBG PE=1 SV=2 - [SHBG_HUMAN]	0.286	0.211	-0.225	-0.225	0.443	0.442
Q12805	EGF-containing fibulin-like extracellular matrix protein 1 OS=Homo sapiens GN=EFEMP1 PE=1 SV=2 - [FBLN3_HUMAN]	0.283	-0.027	0.312	0.538	-0.322	0.027
P08571	Monocyte differentiation antigen CD14 OS=Homo sapiens GN=CD14 PE=1 SV=2 - [CD14_HUMAN]	0.280	0.304	0.104	0.067	0.267	0.333
Q8N0Z9	V-set and immunoglobulin domain-containing protein 10 OS=Homo sapiens GN=VSIG10 PE=2 SV=1 - [VSI10_HUMAN]	0.277	0.087	0.507	0.377	-0.314	-0.889
P02654	Apolipoprotein C-I OS=Homo sapiens GN=APOC1 PE=1 SV=1 - [APOC1_HUMAN]	0.277	0.212	0.436	0.579	-0.204	0.089
P55290	Cadherin-13 OS=Homo sapiens GN=CDH13 PE=1 SV=1 - [CAD13_HUMAN]	0.273	-0.136	0.291	0.128	-0.284	0.151
O43866	CD5 antigen-like OS=Homo sapiens GN=CD5L PE=1 SV=1 - [CD5L_HUMAN]	0.272	-0.084	0.087	-0.054	-0.017	0.195
Q93074	Mediator of RNA polymerase II transcription subunit 12 OS=Homo sapiens GN=MED12 PE=1 SV=4 - [MED12_HUMAN]	0.271	-0.215	-0.486	0.363	-0.601	0.040
P02746	Complement C1q subcomponent subunit B OS=Homo sapiens GN=C1QB PE=1 SV=3 - [C1QB_HUMAN]	0.271	0.021	0.247	-0.022	0.015	0.245
P15814	Immunoglobulin lambda-like polypeptide 1 OS=Homo sapiens GN=IGLL1 PE=1 SV=1 - [IGLL1_HUMAN]	0.266	-0.086	0.162	-0.102	0.012	0.819
P19827	Inter-alpha-trypsin inhibitor heavy chain H1 OS=Homo sapiens GN=ITIH1 PE=1 SV=3 - [ITIH1_HUMAN]	0.266	-0.113	0.238	-0.139	0.080	0.220
Q9BQI7	PH and SEC7 domain-containing protein 2 OS=Homo sapiens GN=PSD2 PE=2 SV=3 - [PSD2_HUMAN]	0.265	-0.822	-0.510	-0.006	-0.839	0.849
P02786	Transferrin receptor protein 1 OS=Homo sapiens GN=TFRC PE=1 SV=2 - [TFR1_HUMAN]	0.263	0.087	0.288	-0.093	0.166	0.180
P05090	Apolipoprotein D OS=Homo sapiens GN=APOD PE=1 SV=1 - [APOD_HUMAN]	0.258	0.007	0.011	0.159	-0.187	-0.130
Q9NQ34	Transmembrane protein 9B OS=Homo sapiens GN=TMEM9B PE=1 SV=1 - [TMM9B_HUMAN]	0.257	0.036	0.100	0.373	-0.341	0.119
Q15847	Adipose most abundant gene transcript 2 protein OS=Homo sapiens GN=APM2 PE=1 SV=1 - [APM2_HUMAN]	0.253	0.102	0.075	0.454	-0.374	-0.930
P07359	Platelet glycoprotein Ib alpha chain OS=Homo sapiens GN=GP1BA PE=1 SV=1 - [GP1BA_HUMAN]	0.251	0.287	-0.191	-0.794	1.039	0.363
P02751	Fibronectin OS=Homo sapiens GN=FN1 PE=1 SV=4 - [FINC_HUMAN]	0.247	0.029	0.164	0.148	-0.114	0.278
P26232	Catenin alpha-2 OS=Homo sapiens GN=CTNNA2 PE=1 SV=5 - [CTNA2_HUMAN]	0.240	-0.071	-0.280	0.076	-0.170	-0.226
P41212	Transcription factor ETV6 OS=Homo sapiens GN=ETV6 PE=1 SV=1 - [ETV6_HUMAN]	0.239	0.198	0.042	-0.151	0.327	-0.197
P02760	Protein AMBP OS=Homo sapiens GN=AMBP PE=1 SV=1 - [AMBP_HUMAN]	0.238	-0.015	0.175	-0.167	0.157	0.225
Q92496	Complement factor H-related protein 4 OS=Homo sapiens GN=CFHR4 PE=1 SV=2 - [FHR4_HUMAN]	0.235	-0.578	-0.606	-0.288	-0.283	0.419
Q9HB20	Pleckstrin homology domain-containing family A member 3 OS=Homo sapiens GN=PLEKHA3 PE=1 SV=2 - [PKHA3_HUMAN]	0.224	-0.229	0.165	0.105	-0.357	0.652
Q6ZS81	WD repeat- and FYVE domain-containing protein 4 OS=Homo sapiens GN=WDFY4 PE=1 SV=3 - [WDFY4_HUMAN]	0.219	-0.164	2.163	1.533	-1.720	0.330
P01617	Ig kappa chain V-II region TEW OS=Homo sapiens PE=1 SV=1 - [KV204_HUMAN]	0.217	0.224	0.281	0.191	0.075	0.267
P01702	Ig lambda chain V-I region NIG-64 OS=Homo sapiens PE=1 SV=1 - [LV104_HUMAN]	0.213	-0.124	0.232	0.065	0.007	-0.095

O00533	Neural cell adhesion molecule L1-like protein OS=Homo sapiens GN=CHL1 PE=1 SV=4 - [CHL1_HUMAN]	0.207	-0.239	0.004	0.166	-0.429	-0.010
Q99996	A-kinase anchor protein 9 OS=Homo sapiens GN=AKAP9 PE=1 SV=3 - [AKAP9_HUMAN]	0.207	0.280	0.657	0.505	-0.249	0.300
Q14112	Nidogen-2 OS=Homo sapiens GN=NID2 PE=1 SV=3 - [NID2_HUMAN]	0.205	0.051	0.317	-0.182	0.209	0.219
P46379	Large proline-rich protein BAG6 OS=Homo sapiens GN=BAG6 PE=1 SV=2 - [BAG6_HUMAN]	0.200	0.159	-0.206	-0.238	0.374	-0.035
P02745	Complement C1q subcomponent subunit A OS=Homo sapiens GN=C1QA PE=1 SV=2 - [C1QA_HUMAN]	0.198	-0.067	0.152	0.234	-0.211	-0.131
P07996	Thrombospondin-1 OS=Homo sapiens GN=THBS1 PE=1 SV=2 - [TSP1_HUMAN]	0.196	-0.093	0.148	-0.075	-0.052	0.352
P07686	Beta-hexosaminidase subunit beta OS=Homo sapiens GN=HEXB PE=1 SV=3 - [HEXB_HUMAN]	0.194	0.484	0.281	0.672	-0.212	-0.130
P10586	Receptor-type tyrosine-protein phosphatase F OS=Homo sapiens GN=PTPRF PE=1 SV=2 - [PTPRF_HUMAN]	0.192	-0.130	-0.077	-0.393	0.240	0.297
O95445	Apolipoprotein M OS=Homo sapiens GN=APOM PE=1 SV=2 - [APOM_HUMAN]	0.191	-0.033	-0.273	-0.142	0.181	-0.106
O14791	Apolipoprotein L1 OS=Homo sapiens GN=APOL1 PE=1 SV=5 - [APOL1_HUMAN]	0.191	-0.412	-0.426	0.026	-0.372	-0.111
O75443	Alpha-tectorin OS=Homo sapiens GN=TECTA PE=1 SV=3 - [TECTA_HUMAN]	0.190	-0.360	-0.103	-0.205	-0.148	0.387
P01815	Ig heavy chain V-II region COR OS=Homo sapiens PE=1 SV=1 - [HV202_HUMAN]	0.189	0.001	0.231	0.190	-0.213	-0.072
Q6ZMR5	Transmembrane protease serine 11A OS=Homo sapiens GN=TMPRSS11A PE=1 SV=1 - [TM11A_HUMAN]	0.184	-0.359	-0.047	-0.077	-0.305	0.239
P19823	Inter-alpha-trypsin inhibitor heavy chain H2 OS=Homo sapiens GN=ITIH2 PE=1 SV=2 - [ITIH2_HUMAN]	0.184	0.000	-0.016	-0.156	0.159	0.058
P01768	Ig heavy chain V-III region CAM OS=Homo sapiens PE=1 SV=1 - [HV307_HUMAN]	0.183	0.099	0.279	-0.090	0.165	0.504
P02675	Fibrinogen beta chain OS=Homo sapiens GN=FGB PE=1 SV=2 - [FIBB_HUMAN]	0.172	0.066	0.507	0.423	-0.381	0.048
P01854	Ig epsilon chain C region OS=Homo sapiens GN=IGHE PE=1 SV=1 - [IGHE_HUMAN]	0.170	-0.631	0.080	0.190	-0.844	0.016
Q9GZM5	Protein YIPF3 OS=Homo sapiens GN=YIPF3 PE=1 SV=1 - [YIPF3_HUMAN]	0.169	-0.703	1.093	0.655	-1.368	0.230
Q14520	Hyaluronan-binding protein 2 OS=Homo sapiens GN=HABP2 PE=1 SV=1 - [HABP2_HUMAN]	0.168	-0.001	-0.049	-0.187	0.123	0.198
P35555	Fibrillin-1 OS=Homo sapiens GN=FBN1 PE=1 SV=3 - [FBN1_HUMAN]	0.168	0.052	0.527	0.231	-0.203	0.176
P14780	Matrix metalloproteinase-9 OS=Homo sapiens GN=MMP9 PE=1 SV=3 - [MMP9_HUMAN]	0.165	-0.057	0.000	-0.293	0.216	0.127
O75534	Cold shock domain-containing protein E1 OS=Homo sapiens GN=CSDE1 PE=1 SV=2 - [CSDE1_HUMAN]	0.164	-0.270	-0.904	-0.609	0.316	-0.079
Q9Y6Z7	Collectin-10 OS=Homo sapiens GN=COLEC10 PE=2 SV=2 - [COL10_HUMAN]	0.160	0.349	0.096	0.200	0.126	-0.286
Q9UK55	Protein Z-dependent protease inhibitor OS=Homo sapiens GN=SERPINA10 PE=1 SV=1 - [ZPI_HUMAN]	0.154	-0.244	-0.338	0.004	-0.330	-0.155
Q9H9S4	Calcium-binding protein 39-like OS=Homo sapiens GN=CAB39L PE=1 SV=3 - [CB39L_HUMAN]	0.153	-0.098	-0.376	-0.761	0.650	0.592
Q02985	Complement factor H-related protein 3 OS=Homo sapiens GN=CFHR3 PE=1 SV=2 - [FHR3_HUMAN]	0.153	-0.229	0.360	0.132	-0.384	0.008
Q5JU67	Uncharacterized protein C9orf117 OS=Homo sapiens GN=C9orf117 PE=2 SV=1 - [CI117_HUMAN]	0.152	-0.316	0.020	-0.255	-0.084	-0.096
Q8TCS8	Polyribonucleotide nucleotidyltransferase 1, mitochondrial OS=Homo sapiens GN=PNPT1 PE=1 SV=2 - [PNPT1_HUMAN]	0.152	0.028	0.005	-0.101	0.162	-0.172
P05452	Tetranectin OS=Homo sapiens GN=CLEC3B PE=1 SV=3 - [TETN_HUMAN]	0.151	-0.406	0.182	0.198	-0.559	-0.390
Q14118	Dystroglycan OS=Homo sapiens GN=DAG1 PE=1 SV=2 - [DAG1_HUMAN]	0.151	-0.516	0.195	-0.053	-0.473	0.118
Q01668	Voltage-dependent L-type calcium channel subunit alpha-1D OS=Homo sapiens GN=CACNA1D PE=1 SV=2 - [CAC1D_HUMAN]	0.151	-0.407	-0.196	-0.162	-0.256	-0.192
P00450	Ceruloplasmin OS=Homo sapiens GN=CP PE=1 SV=1 - [CERU_HUMAN]	0.151	0.153	0.018	0.174	-0.003	0.180
P08697	Alpha-2-antiplasmin OS=Homo sapiens GN=SERPINF2 PE=1 SV=3 - [A2AP_HUMAN]	0.150	0.339	-0.076	0.174	0.153	0.073
P06703	Protein S100-A6 OS=Homo sapiens GN=S100A6 PE=1 SV=1 - [S10A6_HUMAN]	0.149	-0.376	-0.168	0.086	-0.474	-0.470

P02775	Platelet basic protein OS=Homo sapiens GN=PPBP PE=1 SV=3 - [CXCL7_HUMAN]	0.148	0.716	0.274	0.279	0.344	0.263
Q12913	Receptor-type tyrosine-protein phosphatase eta OS=Homo sapiens GN=PTPRJ PE=1 SV=3 - [PTPRJ_HUMAN]	0.147	0.091	-0.033	-0.056	0.142	0.147
P00915	Carbonic anhydrase 1 OS=Homo sapiens GN=CA1 PE=1 SV=2 - [CAH1_HUMAN]	0.146	0.318	-0.058	0.125	0.223	0.310
Q04756	Hepatocyte growth factor activator OS=Homo sapiens GN=HGFAC PE=1 SV=1 - [HGFA_HUMAN]	0.145	-0.071	-0.152	-0.075	0.022	0.161
Q9NZJ4	Sacsin OS=Homo sapiens GN=SACS PE=1 SV=2 - [SACS_HUMAN]	0.144	-0.539	-0.370	-0.323	-0.209	-0.120
P01700	Ig lambda chain V-I region HA OS=Homo sapiens PE=1 SV=1 - [LV102_HUMAN]	0.140	-0.114	0.045	-0.079	-0.021	0.325
P22792	Carboxypeptidase N subunit 2 OS=Homo sapiens GN=CPN2 PE=1 SV=3 - [CPN2_HUMAN]	0.140	0.292	-0.016	-0.186	0.526	0.175
P14543	Nidogen-1 OS=Homo sapiens GN=NID1 PE=1 SV=3 - [NID1_HUMAN]	0.139	0.110	0.547	0.267	-0.180	-1.124
Q9UNN8	Endothelial protein C receptor OS=Homo sapiens GN=PROCR PE=1 SV=1 - [EPCR_HUMAN]	0.139	0.296	0.039	0.332	0.069	-0.003
P51148	Ras-related protein Rab-5C OS=Homo sapiens GN=RAB5C PE=1 SV=2 - [RAB5C_HUMAN]	0.128	-0.059	-0.057	-4.400	4.318	-0.118
Q9UJ83	2-hydroxyacyl-CoA lyase 1 OS=Homo sapiens GN=HACL1 PE=1 SV=2 - [HACL1_HUMAN]	0.124	0.232	0.235	0.206	0.033	0.100
P01031	Complement C5 OS=Homo sapiens GN=C5 PE=1 SV=4 - [CO5_HUMAN]	0.122	0.008	0.018	0.038	-0.059	-0.013
P13473	Lysosome-associated membrane glycoprotein 2 OS=Homo sapiens GN=LAMP2 PE=1 SV=2 - [LAMP2_HUMAN]	0.122	0.000	0.196	0.058	-0.082	0.190
P04433	Ig kappa chain V-III region VG (Fragment) OS=Homo sapiens PE=1 SV=1 - [KV309_HUMAN]	0.121	0.078	0.114	0.081	-0.010	-0.029
P00734	Prothrombin OS=Homo sapiens GN=F2 PE=1 SV=2 - [THRB_HUMAN]	0.119	-0.184	-0.191	-0.605	0.562	0.901
P19320	Vascular cell adhesion protein 1 OS=Homo sapiens GN=VCAM1 PE=1 SV=1 - [VCAM1_HUMAN]	0.118	0.069	0.231	0.234	-0.188	0.139
Q14126	Desmoglein-2 OS=Homo sapiens GN=DSG2 PE=1 SV=2 - [DSG2_HUMAN]	0.114	0.046	0.056	0.213	-0.189	-0.152
P01714	Ig lambda chain V-III region SH OS=Homo sapiens PE=1 SV=1 - [LV301_HUMAN]	0.112	0.056	0.097	0.234	-0.170	0.186
P55056	Apolipoprotein C-IV OS=Homo sapiens GN=APOC4 PE=1 SV=1 - [APOC4_HUMAN]	0.111	-0.237	-0.134	-0.308	-0.027	0.143
P01008	Antithrombin-III OS=Homo sapiens GN=SERPINC1 PE=1 SV=1 - [ANT3_HUMAN]	0.111	0.198	0.062	0.169	0.017	-0.153
P04003	C4b-binding protein alpha chain OS=Homo sapiens GN=C4BPA PE=1 SV=2 - [C4BPA_HUMAN]	0.110	-0.253	-0.320	-0.411	0.225	-0.047
P12111	Collagen alpha-3(VI) chain OS=Homo sapiens GN=COL6A3 PE=1 SV=5 - [CO6A3_HUMAN]	0.110	0.181	0.160	0.251	-0.039	0.176
Q9BZE4	Nucleolar GTP-binding protein 1 OS=Homo sapiens GN=GTPBP4 PE=1 SV=3 - [NOG1_HUMAN]	0.107	0.051	-0.229	-0.382	0.409	0.161
P02763	Alpha-1-acid glycoprotein 1 OS=Homo sapiens GN=ORM1 PE=1 SV=1 - [A1AG1_HUMAN]	0.107	-0.519	-0.006	0.051	0.407	-0.234
P01600	Ig kappa chain V-I region Hau OS=Homo sapiens PE=1 SV=1 - [KV108_HUMAN]	0.105	-0.099	0.493	0.145	-0.268	0.047
A6NKZ8	Putative tubulin beta chain-like protein ENSP00000290377 OS=Homo sapiens PE=5 SV=2 - [YI016_HUMAN]	0.101	1.084	0.091	0.975	0.105	-0.081
P25311	Zinc-alpha-2-glycoprotein OS=Homo sapiens GN=AZGP1 PE=1 SV=2 - [ZA2G_HUMAN]	0.100	-0.231	-0.212	-0.129	-0.112	0.073
Q9BSA9	Transmembrane protein 175 OS=Homo sapiens GN=TMEM175 PE=1 SV=1 - [TM175_HUMAN]	0.099	0.117	1.141	0.482	-0.377	0.219
Q9UGM5	Fetuin-B OS=Homo sapiens GN=FETUB PE=1 SV=2 - [FETUB_HUMAN]	0.098	-0.428	-0.172	0.113	-0.558	0.092
Q13615	Myotubularin-related protein 3 OS=Homo sapiens GN=MTMR3 PE=1 SV=3 - [MTMR3_HUMAN]	0.097	-0.397	-0.218	-0.588	0.168	-0.255
P13645	Keratin, type I cytoskeletal 10 OS=Homo sapiens GN=KRT10 PE=1 SV=6 - [K1C10_HUMAN]	0.095	1.447	0.889	0.969	0.506	0.758
Q06033	Inter-alpha-trypsin inhibitor heavy chain H3 OS=Homo sapiens GN=ITIH3 PE=1 SV=2 - [ITIH3_HUMAN]	0.094	0.246	-0.019	0.306	-0.092	-0.102
P01877	Ig alpha-2 chain C region OS=Homo sapiens GN=IGHA2 PE=1 SV=3 - [IGHA2_HUMAN]	0.093	-0.233	0.219	0.110	-0.243	0.078
P06310	Ig kappa chain V-II region RPMI 6410 OS=Homo sapiens PE=4 SV=1 - [KV206_HUMAN]	0.092	0.366	0.691	1.000	-0.657	-0.605
P09172	Dopamine beta-hydroxylase OS=Homo sapiens GN=DBH PE=1 SV=3 - [DOPO_HUMAN]	0.090	0.025	-0.117	-0.036	0.214	-0.154

P14415	Sodium/potassium-transporting ATPase subunit beta-2 OS=Homo sapiens GN=ATP1B2 PE=1 SV=3 - [AT1B2_HUMAN]	0.088	-0.086	0.749	0.427	-0.536	-1.636
P01876	Ig alpha-1 chain C region OS=Homo sapiens GN=IGHA1 PE=1 SV=2 - [IGHA1_HUMAN]	0.086	0.096	0.213	-0.023	0.111	0.068
P06681	Complement C2 OS=Homo sapiens GN=C2 PE=1 SV=2 - [CO2_HUMAN]	0.086	0.193	0.021	0.233	-0.175	0.012
P00390	Glutathione reductase, mitochondrial OS=Homo sapiens GN=GSR PE=1 SV=2 - [GSHR_HUMAN]	0.086	0.279	0.318	0.451	-0.196	-0.042
P06317	Ig lambda chain V-VI region SUT OS=Homo sapiens PE=1 SV=1 - [LV603_HUMAN]	0.085	0.025	0.155	-0.060	0.075	-0.129
P01707	Ig lambda chain V-II region TRO OS=Homo sapiens PE=1 SV=1 - [LV204_HUMAN]	0.084	0.172	0.173	0.127	0.241	-0.066
Q9NX78	UPF0679 protein C14orf101 OS=Homo sapiens GN=C14orf101 PE=1 SV=3 - [CN101_HUMAN]	0.084	-0.197	0.076	0.302	-0.510	-0.428
P49221	Protein-glutamine gamma-glutamyltransferase 4 OS=Homo sapiens GN=TGM4 PE=1 SV=2 - [TGM4_HUMAN]	0.081	0.091	0.383	0.051	0.023	-0.015
P02652	Apolipoprotein A-II OS=Homo sapiens GN=APOA2 PE=1 SV=1 - [APOA2_HUMAN]	0.078	-0.315	-0.427	0.006	-0.276	-0.047
Q9GZT6	Coiled-coil domain-containing protein 90B, mitochondrial OS=Homo sapiens GN=CCDC90B PE=1 SV=2 - [CC90B_HUMAN]	0.073	0.257	0.414	0.295	-0.062	-0.035
P04275	von Willebrand factor OS=Homo sapiens GN=VWF PE=1 SV=4 - [VWF_HUMAN]	0.073	0.193	0.245	0.373	-0.192	0.010
P00742	Coagulation factor X OS=Homo sapiens GN=F10 PE=1 SV=2 - [FA10_HUMAN]	0.072	-0.299	-0.377	-0.439	0.084	0.155
P05546	Heparin cofactor 2 OS=Homo sapiens GN=SERPIND1 PE=1 SV=3 - [HEP2_HUMAN]	0.072	-0.273	0.043	-0.336	0.035	0.102
P01024	Complement C3 OS=Homo sapiens GN=C3 PE=1 SV=2 - [CO3_HUMAN]	0.069	-0.028	0.078	0.026	-0.025	-0.072
Q14515	SPARC-like protein 1 OS=Homo sapiens GN=SPARCL1 PE=1 SV=2 - [SPRL1_HUMAN]	0.065	0.163	0.238	0.059	0.081	-0.016
Q99784	Noelin OS=Homo sapiens GN=OLFM1 PE=1 SV=4 - [NOE1_HUMAN]	0.064	-0.047	0.121	-0.058	-0.012	-0.071
P35908	Keratin, type II cytoskeletal 2 epidermal OS=Homo sapiens GN=KRT2 PE=1 SV=2 - [K22E_HUMAN]	0.064	1.503	0.886	0.901	0.648	0.414
Q7Z6G3	N-terminal EF-hand calcium-binding protein 2 OS=Homo sapiens GN=NECAB2 PE=1 SV=1 - [NECA2_HUMAN]	0.060	-0.181	-0.447	0.317	-0.490	0.800
Q13936	Voltage-dependent L-type calcium channel subunit alpha-1C OS=Homo sapiens GN=CACNA1C PE=1 SV=4 - [CAC1C_HUMAN]	0.056	0.237	0.821	0.447	-0.234	0.125
P20929	Nebulin OS=Homo sapiens GN=NEB PE=1 SV=4 - [NEBU_HUMAN]	0.055	-0.135	0.067	0.092	-0.247	-0.071
P06702	Protein S100-A9 OS=Homo sapiens GN=S100A9 PE=1 SV=1 - [S10A9_HUMAN]	0.052	-0.202	-0.091	-0.221	0.052	0.120
P00488	Coagulation factor XIII A chain OS=Homo sapiens GN=F13A1 PE=1 SV=4 - [F13A_HUMAN]	0.048	0.264	0.495	0.530	-0.271	0.123
Q8NG04	Solute carrier family 26 member 10 OS=Homo sapiens GN=SLC26A10 PE=2 SV=1 - [S2610_HUMAN]	0.045	-0.091	-0.022	0.112	-0.226	-0.274
Q9NR48	Histone-lysine N-methyltransferase ASH1L OS=Homo sapiens GN=ASH1L PE=1 SV=2 - [ASH1L_HUMAN]	0.043	0.153	-0.480	-0.772	0.902	0.266
P42694	Probable helicase with zinc finger domain OS=Homo sapiens GN=HELZ PE=1 SV=2 - [HELZ_HUMAN]	0.042	0.490	0.361	0.448	0.049	0.169
P02750	Leucine-rich alpha-2-glycoprotein OS=Homo sapiens GN=LRG1 PE=1 SV=2 - [A2GL_HUMAN]	0.040	0.041	0.233	0.121	-0.067	0.304
Q12860	Contactin-1 OS=Homo sapiens GN=CNTN1 PE=1 SV=1 - [CNTN1_HUMAN]	0.039	0.178	-0.148	0.033	0.122	0.040
O00391	Sulfhydryl oxidase 1 OS=Homo sapiens GN=QSOX1 PE=1 SV=3 - [QSOX1_HUMAN]	0.037	0.442	0.240	0.288	0.138	0.003
Q6EMK4	Vasorin OS=Homo sapiens GN=VASN PE=1 SV=1 - [VASN_HUMAN]	0.035	0.240	0.182	-0.307	0.509	0.302
Q9NQC8	Intraflagellar transport protein 46 homolog OS=Homo sapiens GN=IFT46 PE=2 SV=1 - [IFT46_HUMAN]	0.034	0.657	-0.272	-0.029	0.664	-0.507
P37802	Transgelin-2 OS=Homo sapiens GN=TAGLN2 PE=1 SV=3 - [TAGL2_HUMAN]	0.030	0.181	-0.007	-0.143	0.301	0.198

O43526	Potassium voltage-gated channel subfamily KQT member 2 OS=Homo sapiens GN=KCNQ2 PE=1 SV=2 - [KCNQ2_HUMAN]	0.029	0.150	0.314	0.106	0.020	0.090
Q96IY4	Carboxypeptidase B2 OS=Homo sapiens GN=CPB2 PE=1 SV=2 - [CBPB2_HUMAN]	0.028	-0.033	-0.076	0.300	-0.248	-0.006
P02749	Beta-2-glycoprotein 1 OS=Homo sapiens GN=APOH PE=1 SV=3 - [APOH_HUMAN]	0.027	0.078	-0.001	0.094	0.008	0.263
P01775	Ig heavy chain V-III region LAY OS=Homo sapiens PE=1 SV=1 - [HV314_HUMAN]	0.021	-0.177	0.148	0.278	-0.478	-0.147
Q14624	Inter-alpha-trypsin inhibitor heavy chain H4 OS=Homo sapiens GN=ITIH4 PE=1 SV=4 - [ITIH4_HUMAN]	0.020	-0.220	-0.192	-0.271	0.106	0.185
Q15878	Voltage-dependent R-type calcium channel subunit alpha-1E OS=Homo sapiens GN=CACNA1E PE=1 SV=3 - [CAC1E_HUMAN]	0.019	0.136	-0.298	-0.228	0.341	-0.157
P03951	Coagulation factor XI OS=Homo sapiens GN=F11 PE=1 SV=1 - [FA11_HUMAN]	0.015	0.068	-0.109	0.008	0.072	-0.034
Q8N7Z5	Ankyrin repeat domain-containing protein 31 OS=Homo sapiens GN=ANKRD31 PE=5 SV=2 - [ANR31_HUMAN]	0.014	0.079	-0.053	0.140	-0.054	0.026
Q9UF56	F-box/LRR-repeat protein 17 OS=Homo sapiens GN=FBXL17 PE=2 SV=3 - [FXL17_HUMAN]	0.013	0.321	-0.284	0.198	0.099	-0.293
P33151	Cadherin-5 OS=Homo sapiens GN=CDH5 PE=1 SV=5 - [CADH5_HUMAN]	0.013	0.132	0.184	0.340	-0.204	-0.162
P01615	Ig kappa chain V-II region FR OS=Homo sapiens PE=1 SV=1 - [KV202_HUMAN]	0.012	0.068	-0.345	0.000	0.045	-0.179
Q6IV72	Zinc finger protein 425 OS=Homo sapiens GN=ZNF425 PE=2 SV=1 - [ZN425_HUMAN]	0.010	0.308	0.064	-0.941	1.226	0.580
Q86VB7	Scavenger receptor cysteine-rich type 1 protein M130 OS=Homo sapiens GN=CD163 PE=1 SV=2 - [C163A_HUMAN]	0.010	0.319	0.517	0.262	0.004	0.067
E7ETH6	Zinc finger protein 587B OS=Homo sapiens GN=ZNF587B PE=2 SV=1 - [Z587B_HUMAN]	0.006	0.966	-0.643	0.244	0.710	0.019
O75369	Filamin-B OS=Homo sapiens GN=FLNB PE=1 SV=2 - [FLNB_HUMAN]	0.005	0.036	0.109	0.328	-0.285	0.063
P01717	Ig lambda chain V-IV region Hil OS=Homo sapiens PE=1 SV=1 - [LV403_HUMAN]	0.005	-0.156	0.039	-0.194	-0.116	0.196
Q8N3K9	Cardiomyopathy-associated protein 5 OS=Homo sapiens GN=CMYA5 PE=1 SV=3 - [CMYA5_HUMAN]	0.004	0.150	0.238	0.454	-0.297	0.249
Q76LX8	A disintegrin and metalloproteinase with thrombospondin motifs 13 OS=Homo sapiens GN=ADAMTS13 PE=1 SV=1 - [ATS13_HUMAN]	0.004	0.042	0.049	0.073	0.008	-0.030
P01019	Angiotensinogen OS=Homo sapiens GN=AGT PE=1 SV=1 - [ANGT_HUMAN]	0.004	-0.148	-0.274	-0.122	0.023	-0.227
P33908	Mannosyl-oligosaccharide 1,2-alpha-mannosidase IA OS=Homo sapiens GN=MAN1A1 PE=1 SV=3 - [MA1A1_HUMAN]	0.003	0.037	-0.132	0.143	-0.025	0.048
Q9ULI3	Protein HEG homolog 1 OS=Homo sapiens GN=HEG1 PE=1 SV=3 - [HEG1_HUMAN]	0.003	-0.210	-0.099	-0.032	-0.202	0.043
Q92954	Proteoglycan 4 OS=Homo sapiens GN=PRG4 PE=1 SV=2 - [PRG4_HUMAN]	0.002	-0.305	0.082	0.112	-0.441	-0.015
Q12965	Unconventional myosin-Ie OS=Homo sapiens GN=MYO1E PE=1 SV=2 - [MYO1E_HUMAN]	0.002	0.067	0.187	0.723	-0.679	-0.439
P01623	Ig kappa chain V-III region WOL OS=Homo sapiens PE=1 SV=1 - [KV305_HUMAN]	0.002	0.249	-0.151	0.096	0.180	0.118
P01824	Ig heavy chain V-II region WAH OS=Homo sapiens PE=1 SV=1 - [HV206_HUMAN]	0.002	0.137	-0.189	-0.276	0.440	0.097
Q15113	Procollagen C-endopeptidase enhancer 1 OS=Homo sapiens GN=PCOLCE PE=1 SV=2 - [PCOC1_HUMAN]	0.001	0.268	0.107	0.328	-0.053	-0.072
Q13535	Serine/threonine-protein kinase ATR OS=Homo sapiens GN=ATR PE=1 SV=3 - [ATR_HUMAN]	0.001	0.289	-0.241	0.123	0.173	-0.072
Q92186	Alpha-2,8-sialyltransferase 8B OS=Homo sapiens GN=ST8SIA2 PE=2 SV=1 - [SIA8B_HUMAN]	0.000	0.321	0.107	-1.655	1.984	-0.073
Q9Y6K1	DNA (cytosine-5)-methyltransferase 3A OS=Homo sapiens GN=DNMT3A PE=1 SV=4 - [DNM3A_HUMAN]	0.000	0.054	-0.040	-0.125	0.155	-0.155
P41236	Protein phosphatase inhibitor 2 OS=Homo sapiens GN=PPP1R2 PE=1 SV=2 - [IPP2_HUMAN]	0.000	0.321	0.107	0.328	0.000	-0.073
Q9UKM9	RNA-binding protein Raly OS=Homo sapiens GN=RALY PE=1 SV=1 - [RALY_HUMAN]	0.000	0.321	0.107	0.328	0.000	-0.073

P10124	Serglycin OS=Homo sapiens GN=SRGN PE=1 SV=3 - [SRGN_HUMAN]	0.000	0.321	0.107	0.328	0.000	-0.073
P40933	Interleukin-15 OS=Homo sapiens GN=IL15 PE=1 SV=1 - [IL15_HUMAN]	0.000	0.321	0.107	0.328	0.000	-0.073
A0PK00	Transmembrane protein 120B OS=Homo sapiens GN=TMEM120B PE=2 SV=1 - [T120B_HUMAN]	0.000	0.321	0.107	0.328	0.000	-0.073
Q16352	Alpha-internexin OS=Homo sapiens GN=INA PE=1 SV=2 - [AINX_HUMAN]	0.000	0.321	0.107	0.328	0.000	-0.073
Q96GD0	Pyridoxal phosphate phosphatase OS=Homo sapiens GN=PDXP PE=1 SV=2 - [PLPP_HUMAN]	0.000	0.321	0.107	0.328	0.000	-0.073
Q96SY0	UPF0464 protein C15orf44 OS=Homo sapiens GN=C15orf44 PE=1 SV=2 - [CO044_HUMAN]	0.000	0.321	0.107	0.328	0.000	-0.073
Q96R54	Olfactory receptor 14A2 OS=Homo sapiens GN=OR14A2 PE=2 SV=2 - [O14A2_HUMAN]	0.000	0.321	0.107	0.328	0.000	-0.073
Q9Y448	Small kinetochore-associated protein OS=Homo sapiens GN=SKAP PE=1 SV=2 - [SKAP_HUMAN]	0.000	0.321	0.107	0.328	0.000	-0.073
P15559	NAD(P)H dehydrogenase [quinone] 1 OS=Homo sapiens GN=NQO1 PE=1 SV=1 - [NQO1_HUMAN]	0.000	0.321	0.107	0.328	0.000	-0.073
Q8NFR7	Coiled-coil domain-containing protein 148 OS=Homo sapiens GN=CCDC148 PE=2 SV=2 - [CC148_HUMAN]	0.000	0.321	0.107	0.328	0.000	-0.073
Q03924	Zinc finger protein 117 OS=Homo sapiens GN=ZNF117 PE=2 SV=5 - [ZN117_HUMAN]	0.000	0.321	0.107	0.328	0.000	-0.073
O95834	Echinoderm microtubule-associated protein-like 2 OS=Homo sapiens GN=EML2 PE=2 SV=1 - [EMAL2_HUMAN]	0.000	0.321	0.107	0.328	0.000	-0.073
A8MVW0	Protein FAM171A2 OS=Homo sapiens GN=FAM171A2 PE=1 SV=1 - [F1712_HUMAN]	0.000	0.321	0.107	0.328	0.000	-0.073
O00410	Importin-5 OS=Homo sapiens GN=IPO5 PE=1 SV=4 - [IPO5_HUMAN]	0.000	0.321	0.107	0.328	0.000	-0.073
Q5T6X5	G-protein coupled receptor family C group 6 member A OS=Homo sapiens GN=GPRC6A PE=1 SV=1 - [GPC6A_HUMAN]	0.000	0.321	0.107	0.328	0.000	-0.073
Q6Y288	Beta-1,3-glucosyltransferase OS=Homo sapiens GN=B3GALTL PE=1 SV=2 - [B3GLT_HUMAN]	0.000	0.321	0.107	0.328	0.000	-0.073
Q96JN2	Coiled-coil domain-containing protein 136 OS=Homo sapiens GN=CCDC136 PE=2 SV=3 - [CC136_HUMAN]	0.000	0.321	0.107	0.328	0.000	-0.073
Q6AI08	HEAT repeat-containing protein 6 OS=Homo sapiens GN=HEATR6 PE=1 SV=1 - [HEAT6_HUMAN]	0.000	0.321	0.107	0.328	0.000	-0.073
O15389	Sialic acid-binding Ig-like lectin 5 OS=Homo sapiens GN=SIGLEC5 PE=1 SV=1 - [SIGL5_HUMAN]	0.000	0.321	0.107	0.328	0.000	-0.073
P48382	DNA-binding protein RFX5 OS=Homo sapiens GN=RFX5 PE=1 SV=1 - [RFX5_HUMAN]	0.000	0.321	0.107	0.328	0.000	-0.073
Q86VH4	Leucine-rich repeat transmembrane neuronal protein 4 OS=Homo sapiens GN=LRRTM4 PE=2 SV=2 - [LRRT4_HUMAN]	0.000	0.321	0.107	0.328	0.000	-0.073
Q5T6F2	Ubiquitin-associated protein 2 OS=Homo sapiens GN=UBAP2 PE=1 SV=1 - [UBAP2_HUMAN]	0.000	0.321	0.107	0.328	0.000	-0.073
O95470	Sphingosine-1-phosphate lyase 1 OS=Homo sapiens GN=SGPL1 PE=1 SV=3 - [SGPL1_HUMAN]	0.000	0.321	0.107	0.328	0.000	-0.073
Q96P70	Importin-9 OS=Homo sapiens GN=IPO9 PE=1 SV=3 - [IPO9_HUMAN]	0.000	0.321	0.107	0.328	0.000	-0.073
O96020	G1/S-specific cyclin-E2 OS=Homo sapiens GN=CCNE2 PE=1 SV=1 - [CCNE2_HUMAN]	0.000	0.321	0.107	0.328	0.000	-0.073
Q9P2N5	RNA-binding protein 27 OS=Homo sapiens GN=RBM27 PE=1 SV=2 - [RBM27_HUMAN]	0.000	0.321	0.107	0.328	0.000	-0.073
Q15468	SCL-interrupting locus protein OS=Homo sapiens GN=STIL PE=1 SV=2 - [STIL_HUMAN]	0.000	0.321	0.107	0.328	0.000	-0.073
P35556	Fibrillin-2 OS=Homo sapiens GN=FBN2 PE=1 SV=3 - [FBN2_HUMAN]	0.000	0.321	0.107	0.328	0.000	-0.073
Q9P2P1	Protein NYNRIN OS=Homo sapiens GN=NYNRIN PE=1 SV=3 - [NYNRI_HUMAN]	0.000	0.321	0.107	0.328	0.000	-0.073
O43306	Adenylate cyclase type 6 OS=Homo sapiens GN=ADCY6 PE=1 SV=2 - [ADCY6_HUMAN]	0.000	0.321	0.107	0.328	0.000	-0.073
Q8N0W3	L-fucose kinase OS=Homo sapiens GN=FUK PE=2 SV=2 - [FUK_HUMAN]	0.000	0.321	0.107	0.328	0.000	-0.073
Q9HBL0	Tensin-1 OS=Homo sapiens GN=TNS1 PE=1 SV=2 - [TENS1_HUMAN]	0.000	0.321	0.107	0.328	0.000	-0.073
Q96JG9	Zinc finger protein 469 OS=Homo sapiens GN=ZNF469 PE=1 SV=3 - [ZN469_HUMAN]	0.000	0.321	0.107	0.328	0.000	-0.073
O14686	Histone-lysine N-methyltransferase MLL2 OS=Homo sapiens GN=MLL2 PE=1 SV=2 - [MLL2_HUMAN]	0.000	0.321	0.107	0.328	0.000	-0.073

Q14517	Protocadherin Fat 1 OS=Homo sapiens GN=FAT1 PE=1 SV=2 - [FAT1_HUMAN]	0.000	0.321	0.107	0.328	0.000	-0.073
Q8IZF7	Probable G-protein coupled receptor 111 OS=Homo sapiens GN=GPR111 PE=2 SV=1 - [GP111_HUMAN]	-0.001	0.465	0.255	-0.003	0.476	0.187
P06311	Ig kappa chain V-III region IARC/BL41 OS=Homo sapiens PE=1 SV=1 - [KV311_HUMAN]	-0.002	0.055	-0.053	-0.188	0.386	0.306
P00740	Coagulation factor IX OS=Homo sapiens GN=F9 PE=1 SV=2 - [FA9_HUMAN]	-0.004	0.051	-0.402	-0.048	0.140	0.005
P23470	Receptor-type tyrosine-protein phosphatase gamma OS=Homo sapiens GN=PTPRG PE=1 SV=4 - [PTPRG_HUMAN]	-0.004	0.205	-0.015	-0.018	0.200	0.073
Q6UXB8	Peptidase inhibitor 16 OS=Homo sapiens GN=PI16 PE=1 SV=1 - [PI16_HUMAN]	-0.004	0.201	0.284	0.173	-0.044	0.051
P22352	Glutathione peroxidase 3 OS=Homo sapiens GN=GPX3 PE=1 SV=2 - [GPX3_HUMAN]	-0.006	0.714	-0.296	0.054	0.649	-0.065
P23142	Fibulin-1 OS=Homo sapiens GN=FBLN1 PE=1 SV=4 - [FBLN1_HUMAN]	-0.006	0.016	0.277	0.016	-0.002	0.005
P04209	Ig lambda chain V-II region NIG-84 OS=Homo sapiens PE=1 SV=1 - [LV211_HUMAN]	-0.006	0.183	0.435	0.283	-0.123	-0.198
P61009	Signal peptidase complex subunit 3 OS=Homo sapiens GN=SPCS3 PE=1 SV=1 - [SPCS3_HUMAN]	-0.012	0.864	-3.727	0.255	0.617	-3.494
Q68CZ6	HAUS augmin-like complex subunit 3 OS=Homo sapiens GN=HAUS3 PE=1 SV=1 - [HAUS3_HUMAN]	-0.012	-0.164	-0.100	-0.149	-0.007	0.346
P01624	Ig kappa chain V-III region POM OS=Homo sapiens PE=1 SV=1 - [KV306_HUMAN]	-0.012	-0.067	0.473	0.183	-0.386	0.050
Q9NRJ4	Tubby-related protein 4 OS=Homo sapiens GN=TULP4 PE=2 SV=2 - [TULP4_HUMAN]	-0.013	0.095	0.101	0.059	0.013	0.006
Q9H3R1	Bifunctional heparan sulfate N-deacetylase/N-sulfotransferase 4 OS=Homo sapiens GN=NDST4 PE=2 SV=1 - [NDST4_HUMAN]	-0.014	0.550	0.144	0.631	-0.105	-0.042
P01701	Ig lambda chain V-I region NEW OS=Homo sapiens PE=1 SV=1 - [LV103_HUMAN]	-0.014	-0.044	-0.046	-0.292	0.228	0.027
P00751	Complement factor B OS=Homo sapiens GN=CFB PE=1 SV=2 - [CFAB_HUMAN]	-0.014	-0.176	0.108	-0.107	-0.087	0.254
P19338	Nucleolin OS=Homo sapiens GN=NCL PE=1 SV=3 - [NUCL_HUMAN]	-0.016	-0.875	-0.724	0.305	-1.191	-0.255
Q96JC1	Vam6/Vps39-like protein OS=Homo sapiens GN=VPS39 PE=1 SV=2 - [VPS39_HUMAN]	-0.018	0.448	0.579	0.923	-0.498	-0.205
Q92887	Canalicular multispecific organic anion transporter 1 OS=Homo sapiens GN=ABCC2 PE=1 SV=3 - [MRP2_HUMAN]	-0.019	0.242	0.386	-0.040	0.259	0.106
P0C0L5	Complement C4-B OS=Homo sapiens GN=C4B PE=1 SV=1 - [CO4B_HUMAN]	-0.021	0.088	0.114	-0.047	0.169	0.077
P43251	Biotinidase OS=Homo sapiens GN=BTD PE=1 SV=2 - [BTD_HUMAN]	-0.023	-0.284	-0.413	-0.095	-0.211	-0.188
P23610	Factor VIII intron 22 protein OS=Homo sapiens GN=F8A1 PE=1 SV=2 - [F8I2_HUMAN]	-0.024	0.064	0.322	0.112	-0.071	-0.285
P36955	Pigment epithelium-derived factor OS=Homo sapiens GN=SERPINF1 PE=1 SV=4 - [PEDF_HUMAN]	-0.025	-0.056	0.111	-0.006	-0.026	0.027
P00748	Coagulation factor XII OS=Homo sapiens GN=F12 PE=1 SV=3 - [FA12_HUMAN]	-0.025	0.078	-0.035	-0.147	0.250	0.141
P35858	Insulin-like growth factor-binding protein complex acid labile subunit OS=Homo sapiens GN=IGFALS PE=1 SV=1 - [ALS_HUMAN]	-0.027	-0.265	-0.251	-0.458	0.139	0.155
Q9Y3P9	Rab GTPase-activating protein 1 OS=Homo sapiens GN=RABGAP1 PE=1 SV=3 - [RBGP1_HUMAN]	-0.027	-0.015	0.043	0.145	-0.153	0.085
Q13129	Zinc finger protein Rlf OS=Homo sapiens GN=RLF PE=1 SV=2 - [RLF_HUMAN]	-0.027	-0.667	-0.468	-0.114	-0.563	-0.023
Q9NUJ1	Abhydrolase domain-containing protein 10, mitochondrial OS=Homo sapiens GN=ABHD10 PE=1 SV=1 - [ABHDA_HUMAN]	-0.034	-0.467	-0.366	-0.046	-0.414	-0.325
P01625	Ig kappa chain V-IV region Len OS=Homo sapiens PE=1 SV=2 - [KV402_HUMAN]	-0.035	-0.010	-0.007	-0.068	0.016	0.079
P35542	Serum amyloid A-4 protein OS=Homo sapiens GN=SAA4 PE=1 SV=2 - [SAA4_HUMAN]	-0.037	-0.408	-0.595	0.062	-0.431	-0.356
P01777	Ig heavy chain V-III region TEI OS=Homo sapiens PE=1 SV=1 - [HV316_HUMAN]	-0.038	0.084	0.012	-0.023	0.180	0.269
P80748	Ig lambda chain V-III region LOI OS=Homo sapiens PE=1 SV=1 - [LV302_HUMAN]	-0.039	0.004	0.071	0.020	0.015	0.062

P00739	Haptoglobin-related protein OS=Homo sapiens GN=HPR PE=1 SV=2 - [HPTR_HUMAN]	-0.040	-0.252	-0.174	-0.349	0.195	-0.186
P01860	Ig gamma-3 chain C region OS=Homo sapiens GN=IGHG3 PE=1 SV=2 - [IGHG3_HUMAN]	-0.041	0.424	0.480	-0.012	0.205	0.125
P54289	Voltage-dependent calcium channel subunit alpha-2/delta-1 OS=Homo sapiens GN=CACNA2D1 PE=1 SV=3 - [CA2D1_HUMAN]	-0.041	0.065	0.016	0.070	-0.028	0.171
P11226	Mannose-binding protein C OS=Homo sapiens GN=MBL2 PE=1 SV=2 - [MBL2_HUMAN]	-0.045	-0.079	-0.361	-0.638	0.536	0.251
P01781	Ig heavy chain V-III region GAL OS=Homo sapiens PE=1 SV=1 - [HV320_HUMAN]	-0.046	0.002	-0.180	-0.190	0.124	0.092
P01715	Ig lambda chain V-IV region Bau OS=Homo sapiens PE=1 SV=1 - [LV401_HUMAN]	-0.051	-0.103	0.186	0.016	-0.130	-0.156
P01023	Alpha-2-macroglobulin OS=Homo sapiens GN=A2M PE=1 SV=3 - [A2MG_HUMAN]	-0.052	0.594	0.355	0.130	0.422	0.152
P04430	Ig kappa chain V-I region BAN OS=Homo sapiens PE=1 SV=1 - [KV122_HUMAN]	-0.053	0.038	0.067	0.180	-0.153	0.303
P27918	Properdin OS=Homo sapiens GN=CFP PE=1 SV=2 - [PROP_HUMAN]	-0.054	0.004	-0.382	-0.161	0.173	-0.098
P02649	Apolipoprotein E OS=Homo sapiens GN=APOE PE=1 SV=1 - [APOE_HUMAN]	-0.055	-0.067	-0.252	-0.083	0.027	-0.294
P13796	Plastin-2 OS=Homo sapiens GN=LCP1 PE=1 SV=6 - [PLSL_HUMAN]	-0.055	0.345	0.545	0.632	-0.300	0.347
P08185	Corticosteroid-binding globulin OS=Homo sapiens GN=SERPINA6 PE=1 SV=1 - [CBG_HUMAN]	-0.057	0.098	-0.217	-0.368	0.473	0.176
P01764	Ig heavy chain V-III region VH26 OS=Homo sapiens PE=1 SV=1 - [HV303_HUMAN]	-0.057	-0.025	-0.114	-0.441	0.420	-0.052
P16070	CD44 antigen OS=Homo sapiens GN=CD44 PE=1 SV=3 - [CD44_HUMAN]	-0.060	0.100	0.411	0.426	-0.339	-0.035
Q15582	Transforming growth factor-beta-induced protein ig-h3 OS=Homo sapiens GN=TGFBI PE=1 SV=1 - [BGH3_HUMAN]	-0.061	0.029	0.073	-0.087	0.000	-0.097
P27169	Serum paraoxonase/arylesterase 1 OS=Homo sapiens GN=PON1 PE=1 SV=3 - [PON1_HUMAN]	-0.063	-0.119	-0.323	-0.279	0.251	-0.091
P01011	Alpha-1-antichymotrypsin OS=Homo sapiens GN=SERPINA3 PE=1 SV=2 - [AACT_HUMAN]	-0.064	0.062	-0.089	0.017	0.038	0.125
Q6TDU7	Cancer susceptibility candidate protein 1 OS=Homo sapiens GN=CASC1 PE=2 SV=2 - [CASC1_HUMAN]	-0.068	0.757	-0.220	0.454	0.311	0.380
Q9UHK0	Nuclear fragile X mental retardation-interacting protein 1 OS=Homo sapiens GN=NUFIP1 PE=1 SV=2 - [NUFP1_HUMAN]	-0.073	-0.362	-0.287	0.614	-0.968	0.208
P01009	Alpha-1-antitrypsin OS=Homo sapiens GN=SERPINA1 PE=1 SV=3 - [A1AT_HUMAN]	-0.074	0.011	0.007	0.066	-0.043	0.013
P06727	Apolipoprotein A-IV OS=Homo sapiens GN=APOA4 PE=1 SV=3 - [APOA4_HUMAN]	-0.075	-0.153	0.145	0.193	-0.316	0.187
P61769	Beta-2-microglobulin OS=Homo sapiens GN=B2M PE=1 SV=1 - [B2MG_HUMAN]	-0.079	-0.509	-0.001	0.576	-1.189	-0.196
Q6WRI0	Immunoglobulin superfamily member 10 OS=Homo sapiens GN=IGSF10 PE=1 SV=1 - [IGS10_HUMAN]	-0.082	-0.008	0.107	-0.717	0.686	0.091
Q8TEV9	Smith-Magenis syndrome chromosomal region candidate gene 8 protein OS=Homo sapiens GN=SMCR8 PE=1 SV=2 - [SMCR8_HUMAN]	-0.083	0.789	1.111	0.624	0.142	-0.005
P07360	Complement component C8 gamma chain OS=Homo sapiens GN=C8G PE=1 SV=3 - [CO8G_HUMAN]	-0.084	-0.073	-0.045	-0.092	0.023	-0.006
Q9NQ79	Cartilage acidic protein 1 OS=Homo sapiens GN=CRTAC1 PE=1 SV=2 - [CRAC1_HUMAN]	-0.085	0.115	-0.175	-0.051	0.219	0.054
P22105	Tenascin-X OS=Homo sapiens GN=TNXB PE=1 SV=3 - [TENX_HUMAN]	-0.086	0.019	-0.078	-0.199	-0.172	-0.158
Q12967	Ral guanine nucleotide dissociation stimulator OS=Homo sapiens GN=RALGDS PE=1 SV=2 - [GNDS_HUMAN]	-0.086	0.320	0.218	0.157	0.170	-0.432
O75636	Ficolin-3 OS=Homo sapiens GN=FCN3 PE=1 SV=2 - [FCN3_HUMAN]	-0.086	-0.150	-0.235	-0.289	0.270	0.067
P01719	Ig lambda chain V-V region DEL OS=Homo sapiens PE=1 SV=1 - [LV501_HUMAN]	-0.086	0.169	-0.056	-0.167	0.334	0.022
Q9HCS7	Pre-mRNA-splicing factor SYF1 OS=Homo sapiens GN=XAB2 PE=1 SV=2 - [SYF1_HUMAN]	-0.087	-0.046	0.216	0.141	-0.210	0.082
P05155	Plasma protease C1 inhibitor OS=Homo sapiens GN=SERPING1 PE=1 SV=2 - [IC1_HUMAN]	-0.087	0.016	-0.032	-0.150	0.197	0.003

P29622	Kallistatin OS=Homo sapiens GN=SERPINA4 PE=1 SV=3 - [KAIN_HUMAN]	-0.089	-0.148	0.038	-0.264	0.114	-0.061
P04438	Ig heavy chain V-II region SESS OS=Homo sapiens PE=2 SV=1 - [HV208_HUMAN]	-0.089	-0.093	-0.404	-0.500	0.406	-0.118
P04004	Vitronectin OS=Homo sapiens GN=VTN PE=1 SV=1 - [VTNC_HUMAN]	-0.090	0.222	-0.143	0.012	0.132	-0.007
Q6P996	Pyridoxal-dependent decarboxylase domain-containing protein 1 OS=Homo sapiens GN=PDXDC1 PE=1 SV=2 - [PDXD1_HUMAN]	-0.090	0.054	0.265	0.186	-0.155	-0.438
Q96PD5	N-acetylmuramoyl-L-alanine amidase OS=Homo sapiens GN=PGLYRP2 PE=1 SV=1 - [PGRP2_HUMAN]	-0.090	0.095	-0.015	-0.015	0.197	0.334
P04206	Ig kappa chain V-III region GOL OS=Homo sapiens PE=1 SV=1 - [KV307_HUMAN]	-0.093	0.141	-0.012	0.061	0.057	0.198
P04217	Alpha-1B-glycoprotein OS=Homo sapiens GN=A1BG PE=1 SV=4 - [A1BG_HUMAN]	-0.094	-0.096	0.236	-0.192	0.435	0.758
P01833	Polymeric immunoglobulin receptor OS=Homo sapiens GN=PIGR PE=1 SV=4 - [PIGR_HUMAN]	-0.095	-0.067	0.361	-0.105	-0.132	0.226
Q7Z7G8	Vacuolar protein sorting-associated protein 13B OS=Homo sapiens GN=VPS13B PE=1 SV=2 - [VP13B_HUMAN]	-0.095	0.085	-0.092	0.093	-0.031	0.314
P07225	Vitamin K-dependent protein S OS=Homo sapiens GN=PROS1 PE=1 SV=1 - [PROS_HUMAN]	-0.097	-0.390	-0.314	-0.387	0.030	-0.061
P01591	Immunoglobulin J chain OS=Homo sapiens GN=IGJ PE=1 SV=4 - [IGJ_HUMAN]	-0.097	0.079	0.070	0.050	0.035	-0.014
Q6ZMI0	Protein phosphatase 1 regulatory subunit 21 OS=Homo sapiens GN=PPP1R21 PE=1 SV=1 - [PPR21_HUMAN]	-0.097	0.500	0.129	0.243	0.233	0.323
P01772	Ig heavy chain V-III region KOL OS=Homo sapiens PE=1 SV=1 - [HV311_HUMAN]	-0.098	0.237	0.276	0.352	-0.506	0.023
P86790	Vacuolar fusion protein CCZ1 homolog B OS=Homo sapiens GN=CCZ1B PE=1 SV=1 - [CCZ1B_HUMAN]	-0.099	-0.069	-0.221	0.008	-0.069	-0.004
P01705	Ig lambda chain V-II region NEI OS=Homo sapiens PE=1 SV=1 - [LV202_HUMAN]	-0.100	0.007	-0.284	-1.066	1.050	0.461
Q9Y2D4	Exocyst complex component 6B OS=Homo sapiens GN=EXOC6B PE=1 SV=3 - [EXC6B_HUMAN]	-0.100	0.138	0.189	0.636	-0.522	-0.058
P07477	Trypsin-1 OS=Homo sapiens GN=PRSS1 PE=1 SV=1 - [TRY1_HUMAN]	-0.100	0.135	-0.350	-0.023	0.297	-0.141
P04211	Ig lambda chain V region 4A OS=Homo sapiens PE=4 SV=1 - [LV001_HUMAN]	-0.102	-0.113	-0.013	-0.125	0.007	0.038
P20742	Pregnancy zone protein OS=Homo sapiens GN=PZP PE=1 SV=4 - [PZP_HUMAN]	-0.102	-0.327	-0.737	-0.535	0.131	-0.127
P02774	Vitamin D-binding protein OS=Homo sapiens GN=GC PE=1 SV=1 - [VTDB_HUMAN]	-0.105	-0.091	-0.044	0.091	-0.114	-0.011
P15169	Carboxypeptidase N catalytic chain OS=Homo sapiens GN=CPN1 PE=1 SV=1 - [CBPN_HUMAN]	-0.106	-0.037	0.089	-0.194	0.152	-0.053
P02768	Serum albumin OS=Homo sapiens GN=ALB PE=1 SV=2 - [ALBU_HUMAN]	-0.111	0.105	-0.056	0.125	0.008	-0.001
Q16610	Extracellular matrix protein 1 OS=Homo sapiens GN=ECM1 PE=1 SV=2 - [ECM1_HUMAN]	-0.111	0.071	0.173	0.072	-0.002	-0.006
P01699	Ig lambda chain V-I region VOR OS=Homo sapiens PE=1 SV=1 - [LV101_HUMAN]	-0.112	0.106	0.036	-0.054	0.137	-0.258
Q9H8L6	Multimerin-2 OS=Homo sapiens GN=MMRN2 PE=1 SV=2 - [MMRN2_HUMAN]	-0.115	-0.336	0.068	-0.060	-0.287	0.049
P20851	C4b-binding protein beta chain OS=Homo sapiens GN=C4BPB PE=1 SV=1 - [C4BPB_HUMAN]	-0.115	-0.361	-0.012	-0.279	0.023	-0.038
P02748	Complement component C9 OS=Homo sapiens GN=C9 PE=1 SV=2 - [CO9_HUMAN]	-0.119	-0.036	0.039	-0.172	0.161	0.100
Q9BXR6	Complement factor H-related protein 5 OS=Homo sapiens GN=CFHR5 PE=1 SV=1 - [FHR5_HUMAN]	-0.122	-0.279	-0.236	-0.043	-0.238	0.179
Q9UGJ0	5'-AMP-activated protein kinase subunit gamma-2 OS=Homo sapiens GN=PRKAG2 PE=1 SV=1 - [AAKG2_HUMAN]	-0.126	0.109	0.092	0.243	-0.126	-0.196
Q9UK61	Protein FAM208A OS=Homo sapiens GN=FAM208A PE=1 SV=3 - [F208A_HUMAN]	-0.126	-0.192	-0.168	0.035	-0.219	-0.143
P01857	Ig gamma-1 chain C region OS=Homo sapiens GN=IGHG1 PE=1 SV=1 - [IGHG1_HUMAN]	-0.127	-0.017	0.139	0.119	-0.130	-0.181
P01703	Ig lambda chain V-I region NEWM OS=Homo sapiens PE=1 SV=1 - [LV105_HUMAN]	-0.128	-0.125	0.050	-0.160	0.058	-0.048
P15090	Fatty acid-binding protein, adipocyte OS=Homo sapiens GN=FABP4 PE=1 SV=3 - [FABP4_HUMAN]	-0.128	-0.259	0.071	-0.044	-0.226	0.025
O75882	Attractin OS=Homo sapiens GN=ATRN PE=1 SV=2 - [ATRN_HUMAN]	-0.129	0.015	-0.138	-0.096	0.113	-0.059

P04207	Ig kappa chain V-III region CLL OS=Homo sapiens PE=1 SV=2 - [KV308_HUMAN]	-0.129	0.141	0.072	-0.172	0.489	0.145
P04196	Histidine-rich glycoprotein OS=Homo sapiens GN=HRG PE=1 SV=1 - [HRG_HUMAN]	-0.131	-0.077	0.019	-0.086	-0.012	-0.135
Q6UXY1	Brain-specific angiogenesis inhibitor 1-associated protein 2-like protein 2 OS=Homo sapiens GN=BAIAP2L2 PE=1 SV=1 - [BI2L2_HUMAN]	-0.132	0.034	0.648	0.301	-0.271	-0.067
P07358	Complement component C8 beta chain OS=Homo sapiens GN=C8B PE=1 SV=3 - [CO8B_HUMAN]	-0.134	-0.046	-0.097	-0.295	0.370	0.086
P01602	Ig kappa chain V-I region HK102 (Fragment) OS=Homo sapiens GN=IGKV1-5 PE=4 SV=1 - [KV110_HUMAN]	-0.134	0.103	0.809	0.140	-0.060	-0.406
P01042	Kininogen-1 OS=Homo sapiens GN=KNG1 PE=1 SV=2 - [KNG1_HUMAN]	-0.138	-0.018	-0.135	-0.170	0.186	-0.031
Q7LFX5	Carbohydrate sulfotransferase 15 OS=Homo sapiens GN=CHST15 PE=1 SV=1 - [CHSTF_HUMAN]	-0.139	0.635	0.421	-0.665	1.276	-0.175
Q9NYA1	Sphingosine kinase 1 OS=Homo sapiens GN=SPHK1 PE=1 SV=1 - [SPHK1_HUMAN]	-0.143	0.096	0.368	-0.016	0.102	0.252
P07357	Complement component C8 alpha chain OS=Homo sapiens GN=C8A PE=1 SV=2 - [CO8A_HUMAN]	-0.143	-0.164	-0.136	-0.208	0.043	0.053
P19652	Alpha-1-acid glycoprotein 2 OS=Homo sapiens GN=ORM2 PE=1 SV=2 - [A1AG2_HUMAN]	-0.144	0.348	-0.320	0.028	0.208	-0.040
P01767	Ig heavy chain V-III region BUT OS=Homo sapiens PE=1 SV=1 - [HV306_HUMAN]	-0.144	0.134	0.028	-0.049	0.135	0.058
P36980	Complement factor H-related protein 2 OS=Homo sapiens GN=CFHR2 PE=1 SV=1 - [FHR2_HUMAN]	-0.150	0.295	-0.091	0.160	0.124	0.172
P03952	Plasma kallikrein OS=Homo sapiens GN=KLKB1 PE=1 SV=1 - [KLKB1_HUMAN]	-0.160	0.178	-0.319	-0.005	0.213	0.098
Q8N3C7	CAP-Gly domain-containing linker protein 4 OS=Homo sapiens GN=CLIP4 PE=1 SV=1 - [CLIP4_HUMAN]	-0.161	0.006	0.005	-0.233	0.215	-0.143
Q9NUL3	Double-stranded RNA-binding protein Staufen homolog 2 OS=Homo sapiens GN=STAU2 PE=1 SV=1 - [STAU2_HUMAN]	-0.162	-0.431	-0.583	-0.042	-0.413	-0.513
Q99728	BRCA1-associated RING domain protein 1 OS=Homo sapiens GN=BARD1 PE=1 SV=2 - [BARD1_HUMAN]	-0.162	0.056	-0.095	-0.052	0.085	-0.003
P11597	Cholesteryl ester transfer protein OS=Homo sapiens GN=CETP PE=1 SV=2 - [CETP_HUMAN]	-0.164	0.011	-0.345	-0.505	0.492	-0.073
P01598	Ig kappa chain V-I region EU OS=Homo sapiens PE=1 SV=1 - [KV106_HUMAN]	-0.165	0.033	0.058	0.109	-0.128	0.115
P09871	Complement C1s subcomponent OS=Homo sapiens GN=C1S PE=1 SV=1 - [C1S_HUMAN]	-0.165	0.119	0.119	0.011	0.076	-0.091
P01613	Ig kappa chain V-I region Ni OS=Homo sapiens PE=1 SV=1 - [KV121_HUMAN]	-0.165	0.135	-0.056	0.220	-0.334	-0.103
Q9Y2W6	Tudor and KH domain-containing protein OS=Homo sapiens GN=TDRKH PE=1 SV=2 - [TDRKH_HUMAN]	-0.171	0.172	-0.013	0.104	0.075	-0.379
Q9Y5X1	Sorting nexin-9 OS=Homo sapiens GN=SNX9 PE=1 SV=1 - [SNX9_HUMAN]	-0.174	0.164	0.179	0.265	-0.094	-0.176
Q9BZD7	Transmembrane gamma-carboxyglutamic acid protein 3 OS=Homo sapiens GN=PRRG3 PE=2 SV=2 - [TMG3_HUMAN]	-0.175	-0.439	-0.340	-0.097	-0.335	-0.098
Q9HB65	RNA polymerase II elongation factor ELL3 OS=Homo sapiens GN=ELL3 PE=2 SV=2 - [ELL3_HUMAN]	-0.177	-0.036	-0.033	0.015	-0.085	-0.049
P14625	Endoplasmin OS=Homo sapiens GN=HSP90B1 PE=1 SV=1 - [ENPL_HUMAN]	-0.179	0.277	0.293	-0.053	0.306	0.048
P00736	Complement C1r subcomponent OS=Homo sapiens GN=C1R PE=1 SV=2 - [C1R_HUMAN]	-0.179	0.189	-0.077	-0.071	0.249	-0.147
P06396	Gelsolin OS=Homo sapiens GN=GSN PE=1 SV=1 - [GELS_HUMAN]	-0.182	-0.167	-0.019	-0.321	0.182	0.070
P08603	Complement factor H OS=Homo sapiens GN=CFH PE=1 SV=4 - [CFAH_HUMAN]	-0.184	-0.080	-0.064	-0.226	0.116	0.115
Q15848	Adiponectin OS=Homo sapiens GN=ADIPOQ PE=1 SV=1 - [ADIPO_HUMAN]	-0.188	-0.142	-0.302	-0.137	-0.029	0.025
P06331	Ig heavy chain V-II region ARH-77 OS=Homo sapiens PE=4 SV=1 - [HV209_HUMAN]	-0.189	0.074	-0.013	-0.137	0.186	0.073
P01762	Ig heavy chain V-III region TRO OS=Homo sapiens PE=1 SV=1 - [HV301_HUMAN]	-0.189	0.120	-0.015	0.103	0.024	-0.231
P48740	Mannan-binding lectin serine protease 1 OS=Homo sapiens GN=MASP1 PE=1 SV=3 - [MASP1_HUMAN]	-0.190	-0.012	-0.092	-0.091	0.154	0.028
O14815	Calpain-9 OS=Homo sapiens GN=CAPN9 PE=1 SV=1 - [CAN9_HUMAN]	-0.191	-0.530	-0.005	-0.427	-0.126	0.161
Q9UBN7	Histone deacetylase 6 OS=Homo sapiens GN=HDAC6 PE=1 SV=2 - [HDAC6_HUMAN]	-0.193	-0.599	-0.174	-0.109	-0.514	-0.097

P13671	Complement component C6 OS=Homo sapiens GN=C6 PE=1 SV=3 - [CO6_HUMAN]	-0.194	-0.019	-0.058	-0.040	0.018	-0.045
Q15166	Serum paraoxonase/lactonase 3 OS=Homo sapiens GN=PON3 PE=1 SV=3 - [PON3_HUMAN]	-0.194	0.008	-0.294	-0.091	0.140	-0.159
O75052	Carboxyl-terminal PDZ ligand of neuronal nitric oxide synthase protein OS=Homo sapiens GN=NOS1AP PE=1 SV=3 - [CAPON_HUMAN]	-0.195	-0.097	-0.222	-0.104	0.014	0.042
P01871	Ig mu chain C region OS=Homo sapiens GN=IGHM PE=1 SV=3 - [IGHM_HUMAN]	-0.196	0.018	-0.100	-0.247	0.212	-0.026
P55058	Phospholipid transfer protein OS=Homo sapiens GN=PLTP PE=1 SV=1 - [PLTP_HUMAN]	-0.200	0.295	-0.229	0.100	0.369	-0.337
P10909	Clusterin OS=Homo sapiens GN=CLU PE=1 SV=1 - [CLUS_HUMAN]	-0.202	0.043	-0.280	-0.071	0.091	0.435
Q86SQ0	Pleckstrin homology-like domain family B member 2 OS=Homo sapiens GN=PHLDB2 PE=1 SV=2 - [PHLB2_HUMAN]	-0.203	-0.164	-0.315	-0.136	-0.020	0.087
O75683	Surfeit locus protein 6 OS=Homo sapiens GN=SURF6 PE=1 SV=3 - [SURF6_HUMAN]	-0.205	0.406	-1.027	-0.664	1.066	-0.311
Q7Z4S6	Kinesin-like protein KIF21A OS=Homo sapiens GN=KIF21A PE=1 SV=2 - [KI21A_HUMAN]	-0.205	0.445	0.066	0.348	0.092	-0.311
Q8NBW4	Putative sodium-coupled neutral amino acid transporter 9 OS=Homo sapiens GN=SLC38A9 PE=1 SV=2 - [S38A9_HUMAN]	-0.205	0.381	0.000	0.284	0.092	-0.311
A8MUX0	Putative keratin-associated protein 10-like ENSP00000375147 OS=Homo sapiens PE=3 SV=1 - [KR10D_HUMAN]	-0.205	0.381	0.000	0.284	0.092	-0.311
Q8NAM6	Zinc finger and SCAN domain-containing protein 4 OS=Homo sapiens GN=ZSCAN4 PE=2 SV=1 - [ZSCA4_HUMAN]	-0.205	0.381	0.000	0.284	0.092	-0.311
Q86UF2	Putative protein cTAGE-6 OS=Homo sapiens GN=CTAGE6P PE=5 SV=2 - [CTGE6_HUMAN]	-0.205	0.381	0.000	0.284	0.092	-0.311
P10643	Complement component C7 OS=Homo sapiens GN=C7 PE=1 SV=2 - [CO7_HUMAN]	-0.209	0.448	0.378	0.113	0.321	-0.152
O95613	Pericentrin OS=Homo sapiens GN=PCNT PE=1 SV=4 - [PCNT_HUMAN]	-0.209	0.198	0.298	0.938	-0.733	0.031
A6NJ16	Putative V-set and immunoglobulin domain-containing-like protein IGHV4OR15-8 OS=Homo sapiens GN=IGHV4OR15-8 PE=5 SV=2 - [IV4F8_HUMAN]	-0.213	-0.008	-0.154	0.082	-0.074	-0.016
P01604	Ig kappa chain V-I region Kue OS=Homo sapiens PE=1 SV=1 - [KV112_HUMAN]	-0.215	-0.047	-0.103	0.115	-0.185	0.394
P12955	Xaa-Pro dipeptidase OS=Homo sapiens GN=PEPD PE=1 SV=3 - [PEPD_HUMAN]	-0.219	0.384	0.040	0.150	0.134	-0.284
P43652	Afamin OS=Homo sapiens GN=AFM PE=1 SV=1 - [AFAM_HUMAN]	-0.220	0.131	-0.098	0.012	0.119	-0.143
P81605	Dermcidin OS=Homo sapiens GN=DCD PE=1 SV=2 - [DCD_HUMAN]	-0.226	-0.695	0.416	0.122	-0.841	0.109
P01619	Ig kappa chain V-III region B6 OS=Homo sapiens PE=1 SV=1 - [KV301_HUMAN]	-0.228	0.007	-0.221	-0.448	0.503	0.151
Q8IWU9	Tryptophan 5-hydroxylase 2 OS=Homo sapiens GN=TPH2 PE=1 SV=1 - [TPH2_HUMAN]	-0.228	0.282	-0.653	-0.418	0.677	-0.198
Q6UY14	ADAMTS-like protein 4 OS=Homo sapiens GN=ADAMTSL4 PE=1 SV=2 - [ATL4_HUMAN]	-0.229	0.168	0.308	0.048	0.097	0.021
Q7Z478	ATP-dependent RNA helicase DHX29 OS=Homo sapiens GN=DHX29 PE=1 SV=2 - [DHX29_HUMAN]	-0.234	0.031	-0.234	-0.405	0.412	0.306
Q5T5P2	Sickle tail protein homolog OS=Homo sapiens GN=SKT PE=1 SV=2 - [SKT_HUMAN]	-0.239	-0.431	-0.395	-0.708	0.254	-0.161
Q9NQT8	Kinesin-like protein KIF13B OS=Homo sapiens GN=KIF13B PE=1 SV=1 - [KI13B_HUMAN]	-0.241	0.358	0.245	0.662	-0.326	-0.309
B9A064	Immunoglobulin lambda-like polypeptide 5 OS=Homo sapiens GN=IGLL5 PE=2 SV=2 - [IGLL5_HUMAN]	-0.242	-0.039	0.010	0.005	-0.175	-0.149
P23083	Ig heavy chain V-I region V35 OS=Homo sapiens PE=1 SV=1 - [HV103_HUMAN]	-0.243	-0.061	0.516	0.240	-0.346	0.097
P01765	Ig heavy chain V-III region TIL OS=Homo sapiens PE=1 SV=1 - [HV304_HUMAN]	-0.243	-0.050	-0.089	0.272	-0.346	-0.206
Q6P1J9	Parafibromin OS=Homo sapiens GN=CDC73 PE=1 SV=1 - [CDC73_HUMAN]	-0.246	0.490	0.068	0.360	0.107	-0.096
Q9NZP8	Complement C1r subcomponent-like protein OS=Homo sapiens GN=C1RL PE=1 SV=2 - [C1RL_HUMAN]	-0.247	-0.133	-0.218	-0.102	0.039	0.156

P04070	Vitamin K-dependent protein C OS=Homo sapiens GN=PROC PE=1 SV=1 - [PROC_HUMAN]	-0.248	-0.419	-0.818	-0.635	0.202	-0.089
P40197	Platelet glycoprotein V OS=Homo sapiens GN=GP5 PE=1 SV=1 - [GPV_HUMAN]	-0.249	-0.041	-0.083	-0.310	0.245	0.026
P02647	Apolipoprotein A-I OS=Homo sapiens GN=APOA1 PE=1 SV=1 - [APOA1_HUMAN]	-0.250	-0.231	-0.325	0.033	-0.229	-0.065
P05156	Complement factor I OS=Homo sapiens GN=CFI PE=1 SV=2 - [CFAI_HUMAN]	-0.250	0.233	-0.255	0.051	0.181	0.015
P51884	Lumican OS=Homo sapiens GN=LUM PE=1 SV=2 - [LUM_HUMAN]	-0.250	0.238	0.397	0.288	-0.098	-0.216
Q13939	Calicin OS=Homo sapiens GN=CCIN PE=2 SV=3 - [CALI_HUMAN]	-0.250	0.325	-0.060	-0.031	0.332	-0.327
P01742	Ig heavy chain V-I region EU OS=Homo sapiens PE=1 SV=1 - [HV101_HUMAN]	-0.252	-0.015	-0.046	-0.083	0.058	-0.152
Q96KN2	Beta-Ala-His dipeptidase OS=Homo sapiens GN=CNDP1 PE=1 SV=4 - [CNDP1_HUMAN]	-0.260	-0.145	-0.330	-0.028	-0.121	-0.414
Q86TB9	Protein PAT1 homolog 1 OS=Homo sapiens GN=PATL1 PE=1 SV=2 - [PATL1_HUMAN]	-0.263	0.168	0.566	0.288	-0.131	0.022
P01711	Ig lambda chain V-II region VIL OS=Homo sapiens PE=1 SV=1 - [LV208_HUMAN]	-0.266	-0.787	-0.231	-0.658	-0.153	0.178
Q8NHU6	Tudor domain-containing protein 7 OS=Homo sapiens GN=TDRD7 PE=1 SV=2 - [TDRD7_HUMAN]	-0.268	0.343	0.215	0.408	-0.057	-0.147
P01779	Ig heavy chain V-III region TUR OS=Homo sapiens PE=1 SV=1 - [HV318_HUMAN]	-0.271	0.049	0.000	-0.117	0.166	-0.098
P83593	Ig kappa chain V-IV region STH (Fragment) OS=Homo sapiens PE=1 SV=1 - [KV405_HUMAN]	-0.277	0.397	0.014	-0.219	0.593	-0.147
A0M8Q6	Ig lambda-7 chain C region OS=Homo sapiens GN=IGLC7 PE=1 SV=2 - [LAC7_HUMAN]	-0.279	-0.430	0.015	-0.023	-0.430	0.199
P01609	Ig kappa chain V-I region Scw OS=Homo sapiens PE=1 SV=1 - [KV117_HUMAN]	-0.286	0.068	-0.088	-0.013	0.093	0.089
Q03591	Complement factor H-related protein 1 OS=Homo sapiens GN=CFHR1 PE=1 SV=2 - [FHR1_HUMAN]	-0.286	-0.383	-0.087	-0.154	-0.241	0.369
P04114	Apolipoprotein B-100 OS=Homo sapiens GN=APOB PE=1 SV=2 - [APOB_HUMAN]	-0.287	0.250	0.212	0.256	0.115	-0.080
P00747	Plasminogen OS=Homo sapiens GN=PLG PE=1 SV=2 - [PLMN_HUMAN]	-0.288	0.082	-0.061	0.003	-0.034	-0.136
Q8NEV8	Exophilin-5 OS=Homo sapiens GN=EXPH5 PE=1 SV=3 - [EXPH5_HUMAN]	-0.292	-0.087	0.159	-0.096	0.016	0.078
P26927	Hepatocyte growth factor-like protein OS=Homo sapiens GN=MST1 PE=1 SV=2 - [HGFL_HUMAN]	-0.292	0.311	-0.363	-0.025	0.340	0.172
Q16666	Gamma-interferon-inducible protein 16 OS=Homo sapiens GN=IFI16 PE=1 SV=3 - [IF16_HUMAN]	-0.296	0.494	0.300	0.756	-0.255	-0.722
P52848	Bifunctional heparan sulfate N-deacetylase/N-sulfotransferase 1 OS=Homo sapiens GN=NDST1 PE=1 SV=1 - [NDST1_HUMAN]	-0.296	0.176	0.711	0.557	-0.374	-0.025
P01612	Ig kappa chain V-I region Mev OS=Homo sapiens PE=1 SV=1 - [KV120_HUMAN]	-0.300	-0.049	0.146	0.006	-0.009	-0.108
O43805	Sjoegren syndrome nuclear autoantigen 1 OS=Homo sapiens GN=SSNA1 PE=1 SV=2 - [SSNA1_HUMAN]	-0.301	0.198	-0.354	0.054	0.133	-0.113
P01760	Ig heavy chain V-I region WOL OS=Homo sapiens PE=1 SV=1 - [HV105_HUMAN]	-0.303	0.024	0.251	0.418	-0.417	0.300
O00187	Mannan-binding lectin serine protease 2 OS=Homo sapiens GN=MASP2 PE=1 SV=4 - [MASP2_HUMAN]	-0.304	-0.373	0.374	-0.208	-0.175	-0.297
P01611	Ig kappa chain V-I region Wes OS=Homo sapiens PE=1 SV=1 - [KV119_HUMAN]	-0.307	-0.060	0.060	0.115	-0.161	-0.079
Q8NFU5	Inositol polyphosphate multikinase OS=Homo sapiens GN=IPMK PE=1 SV=1 - [IPMK_HUMAN]	-0.307	-0.014	-0.245	-0.109	0.083	-0.218
P01834	Ig kappa chain C region OS=Homo sapiens GN=IGKC PE=1 SV=1 - [IGKC_HUMAN]	-0.311	0.422	0.115	0.164	0.213	-0.030
P05543	Thyroxine-binding globulin OS=Homo sapiens GN=SERPINA7 PE=1 SV=2 - [THBG_HUMAN]	-0.314	-0.206	-0.075	-0.166	0.062	-0.221
P02787	Serotransferrin OS=Homo sapiens GN=TF PE=1 SV=3 - [TRFE_HUMAN]	-0.321	-0.107	-0.123	0.103	-0.192	0.074
O94822	E3 ubiquitin-protein ligase listerin OS=Homo sapiens GN=LTN1 PE=1 SV=6 - [LTN1_HUMAN]	-0.327	0.026	-0.204	-0.100	0.133	0.028
P02790	Hemopexin OS=Homo sapiens GN=HPX PE=1 SV=2 - [HEMO_HUMAN]	-0.332	0.031	-0.092	-0.033	0.080	-0.119
P01861	Ig gamma-4 chain C region OS=Homo sapiens GN=IGHG4 PE=1 SV=1 - [IGHG4_HUMAN]	-0.339	0.024	0.141	-0.022	0.042	-0.070
Q86Y38	Xylosyltransferase 1 OS=Homo sapiens GN=XYLT1 PE=1 SV=1 - [XYLT1_HUMAN]	-0.341	0.546	0.331	0.673	-0.151	-0.028

Q96L93	Kinesin-like protein KIF16B OS=Homo sapiens GN=KIF16B PE=1 SV=2 - [KI16B_HUMAN]	-0.344	0.009	0.049	0.230	-0.213	-0.254
Q9GZV4	Eukaryotic translation initiation factor 5A-2 OS=Homo sapiens GN=EIF5A2 PE=1 SV=3 - [IF5A2_HUMAN]	-0.345	0.325	0.107	0.328	0.004	-0.413
Q5TG30	Rho GTPase-activating protein 40 OS=Homo sapiens GN=ARHGAP40 PE=2 SV=3 - [RHG40_HUMAN]	-0.349	0.448	-0.263	-0.071	0.496	-0.377
Q86UP3	Zinc finger homeobox protein 4 OS=Homo sapiens GN=ZFHX4 PE=1 SV=1 - [ZFHX4_HUMAN]	-0.352	-0.011	-0.109	-0.118	0.188	-0.168
P05160	Coagulation factor XIII B chain OS=Homo sapiens GN=F13B PE=1 SV=3 - [F13B_HUMAN]	-0.352	0.026	-0.108	0.079	-0.075	-0.102
Q6ZN08	Putative zinc finger protein 66 OS=Homo sapiens GN=ZNF66P PE=5 SV=2 - [ZNF66_HUMAN]	-0.355	-0.087	-0.321	-0.176	0.162	-0.199
P0CG05	Ig lambda-2 chain C regions OS=Homo sapiens GN=IGLC2 PE=1 SV=1 - [LAC2_HUMAN]	-0.368	0.003	0.187	0.184	-0.187	-0.027
Q5T2W1	Na(+)/H(+) exchange regulatory cofactor NHE-RF3 OS=Homo sapiens GN=PDZK1 PE=1 SV=2 - [NHRF3_HUMAN]	-0.385	0.268	0.019	0.501	-0.225	-0.146
P01780	Ig heavy chain V-III region JON OS=Homo sapiens PE=1 SV=1 - [HV319_HUMAN]	-0.388	-0.046	0.291	0.365	-0.544	-0.309
P04434	Ig kappa chain V-III region VH (Fragment) OS=Homo sapiens PE=4 SV=1 - [KV310_HUMAN]	-0.400	0.050	0.585	0.580	-0.554	-0.329
Q5R387	Putative inactive group IIC secretory phospholipase A2 OS=Homo sapiens GN=PLA2G2C PE=2 SV=3 - [PA2GC_HUMAN]	-0.402	-0.365	-0.590	-0.477	0.120	-0.067
P00746	Complement factor D OS=Homo sapiens GN=CFD PE=1 SV=5 - [CFAD_HUMAN]	-0.407	-0.088	0.150	0.370	-0.377	-0.078
P18065	Insulin-like growth factor-binding protein 2 OS=Homo sapiens GN=IGFBP2 PE=1 SV=2 - [IBP2_HUMAN]	-0.410	0.320	-0.053	-0.058	0.328	0.446
Q9NPR9	Protein GPR108 OS=Homo sapiens GN=GPR108 PE=2 SV=3 - [GP108_HUMAN]	-0.415	-0.208	0.106	-0.044	-0.187	-0.309
P48643	T-complex protein 1 subunit epsilon OS=Homo sapiens GN=CCT5 PE=1 SV=1 - [TCPE_HUMAN]	-0.424	-0.220	0.097	0.249	-0.492	0.034
P06276	Cholinesterase OS=Homo sapiens GN=BCHE PE=1 SV=1 - [CHLE_HUMAN]	-0.424	-0.453	-0.044	-0.279	-0.192	-0.510
P22891	Vitamin K-dependent protein Z OS=Homo sapiens GN=PROZ PE=1 SV=2 - [PROZ_HUMAN]	-0.427	-0.764	-1.255	-1.072	0.306	-0.354
Q9NQW6	Actin-binding protein anillin OS=Homo sapiens GN=ANLN PE=1 SV=2 - [ANLN_HUMAN]	-0.428	-0.145	-0.064	-0.221	0.053	-0.167
Q15485	Ficolin-2 OS=Homo sapiens GN=FCN2 PE=1 SV=2 - [FCN2_HUMAN]	-0.431	-0.161	-0.651	0.248	-0.258	-0.086
P01859	Ig gamma-2 chain C region OS=Homo sapiens GN=IGHG2 PE=1 SV=2 - [IGHG2_HUMAN]	-0.434	0.022	-0.142	-0.208	0.209	-0.232
P78563	Double-stranded RNA-specific editase 1 OS=Homo sapiens GN=ADARB1 PE=1 SV=1 - [RED1_HUMAN]	-0.442	0.224	0.050	-1.241	1.442	-0.104
P07195	L-lactate dehydrogenase B chain OS=Homo sapiens GN=LDHB PE=1 SV=2 - [LDHB_HUMAN]	-0.444	-0.148	-0.300	-0.130	-0.041	0.084
Q15063	Periostin OS=Homo sapiens GN=POSTN PE=1 SV=2 - [POSTN_HUMAN]	-0.447	-0.154	-0.396	-0.646	0.488	-0.266
Q96JH8	Ras-associating and dilute domain-containing protein OS=Homo sapiens GN=RADIL PE=1 SV=5 - [RADIL_HUMAN]	-0.450	0.356	-0.506	-0.311	0.655	-0.241
Q6UX46	Protein FAM150B OS=Homo sapiens GN=FAM150B PE=2 SV=2 - [F150B_HUMAN]	-0.455	-0.133	-0.153	0.203	-0.360	-0.160
Q5VZR2	Protein FAM22G OS=Homo sapiens GN=FAM22G PE=2 SV=2 - [FA22G_HUMAN]	-0.460	0.285	0.509	0.218	0.044	-0.097
P08684	Cytochrome P450 3A4 OS=Homo sapiens GN=CYP3A4 PE=1 SV=4 - [CP3A4_HUMAN]	-0.481	0.364	0.285	0.254	0.117	-0.147
P52798	Ephrin-A4 OS=Homo sapiens GN=EFNA4 PE=1 SV=1 - [EFNA4_HUMAN]	-0.517	0.393	1.721	-0.085	0.455	-0.160
Q9Y606	tRNA pseudouridine synthase A, mitochondrial OS=Homo sapiens GN=PUS1 PE=1 SV=3 - [TRUA_HUMAN]	-0.522	-0.138	-0.460	-0.258	0.109	-0.413
O95171	Sciellin OS=Homo sapiens GN=SCEL PE=1 SV=2 - [SCEL_HUMAN]	-0.559	0.327	0.368	0.167	0.167	-0.902
Q13023	A-kinase anchor protein 6 OS=Homo sapiens GN=AKAP6 PE=1 SV=3 - [AKAP6_HUMAN]	-0.562	-0.187	-0.168	-0.614	0.404	-0.750
Q6VUC0	Transcription factor AP-2-epsilon OS=Homo sapiens GN=TFAP2E PE=2 SV=1 - [AP2E_HUMAN]	-0.595	0.353	-0.229	0.006	0.354	-0.239
Q9Y6R7	IgGFc-binding protein OS=Homo sapiens GN=FCGBP PE=1 SV=3 - [FCGBP_HUMAN]	-0.644	-0.140	-0.055	0.003	-0.148	-0.299
P56192	Methionine--tRNA ligase, cytoplasmic OS=Homo sapiens GN=MARS PE=1 SV=2 - [SYMC_HUMAN]	-0.652	0.897	1.250	0.628	0.246	-0.633

Q9NS87	Kinesin-like protein KIF15 OS=Homo sapiens GN=KIF15 PE=1 SV=1 - [KIF15_HUMAN]	-0.665	0.193	-0.057	0.112	0.057	-0.239
P39060	Collagen alpha-1(XVIII) chain OS=Homo sapiens GN=COL18A1 PE=1 SV=5 - [COIA1_HUMAN]	-0.667	0.559	0.460	0.446	0.103	1.037
Q8IUC6	TIR domain-containing adapter molecule 1 OS=Homo sapiens GN=TICAM1 PE=1 SV=1 - [TCAM1_HUMAN]	-0.683	-0.230	-0.492	-0.332	0.092	-0.472
Q13228	Selenium-binding protein 1 OS=Homo sapiens GN=SELENBP1 PE=1 SV=2 - [SBP1_HUMAN]	-0.717	-0.059	-0.173	-0.055	-0.015	-0.109
P01605	Ig kappa chain V-I region Lay OS=Homo sapiens PE=1 SV=1 - [KV113_HUMAN]	-0.727	0.032	0.376	0.321	-0.379	-0.166
Q9BZF9	Uveal autoantigen with coiled-coil domains and ankyrin repeats OS=Homo sapiens GN=UACA PE=1 SV=2 - [UACA_HUMAN]	-0.730	-0.054	0.551	-0.033	-0.044	-1.077
Q8N8V2	Guanylate-binding protein 7 OS=Homo sapiens GN=GBP7 PE=2 SV=2 - [GBP7_HUMAN]	-0.732	0.547	-0.062	0.178	0.346	-0.774
Q9H4A3	Serine/threonine-protein kinase WNK1 OS=Homo sapiens GN=WNK1 PE=1 SV=2 - [WNK1_HUMAN]	-0.774	0.285	-0.181	0.370	-0.104	-0.506
Q13439	Golgin subfamily A member 4 OS=Homo sapiens GN=GOLGA4 PE=1 SV=1 - [GOGA4_HUMAN]	-0.905	-0.181	-0.485	-0.391	0.198	-0.558
O75015	Low affinity immunoglobulin gamma Fc region receptor III-B OS=Homo sapiens GN=FCGR3B PE=1 SV=2 - [FCG3B_HUMAN]	-0.915	-0.140	-0.189	-0.005	-0.146	-0.117
Q8NFY9	Kelch repeat and BTB domain-containing protein 8 OS=Homo sapiens GN=KBTBD8 PE=2 SV=2 - [KBTB8_HUMAN]	-0.937	0.000	-0.155	0.329	-0.352	0.565
Q7Z402	Transmembrane channel-like protein 7 OS=Homo sapiens GN=TMC7 PE=2 SV=1 - [TMC7_HUMAN]	-0.960	1.569	1.112	1.184	0.362	0.604
Q7Z2Y8	Interferon-induced very large GTPase 1 OS=Homo sapiens GN=GVINP1 PE=2 SV=2 - [GVIN1_HUMAN]	-1.050	0.433	0.431	1.026	-0.585	-0.096
Q9Y6V0	Protein piccolo OS=Homo sapiens GN=PCLO PE=1 SV=4 - [PCLO_HUMAN]	-1.094	-0.397	-0.536	-0.279	-0.141	-0.419
Q9Y2E6	Protein deltex-4 OS=Homo sapiens GN=DTX4 PE=1 SV=2 - [DTX4_HUMAN]	-1.181	-0.035	-0.351	-0.084	0.056	-0.302
Q7KZ85	Transcription elongation factor SPT6 OS=Homo sapiens GN=SUPT6H PE=1 SV=2 - [SPT6H_HUMAN]	-1.193	0.400	-0.964	0.550	-0.173	-1.054
Q9UFH2	Dynein heavy chain 17, axonemal OS=Homo sapiens GN=DNAH17 PE=2 SV=2 - [DYH17_HUMAN]	-1.486	-0.344	-0.663	-0.271	-0.078	-0.485
P12107	Collagen alpha-1(XI) chain OS=Homo sapiens GN=COL11A1 PE=1 SV=4 - [COBA1_HUMAN]	-1.510	0.346	0.107	0.328	0.024	-1.608
Q86VM9	Zinc finger CCCH domain-containing protein 18 OS=Homo sapiens GN=ZC3H18 PE=1 SV=2 - [ZCH18_HUMAN]	-1.744	-2.696	-2.095	0.462	-3.169	-2.664
Q8WYP5	Protein ELYS OS=Homo sapiens GN=AHCTF1 PE=1 SV=3 - [ELYS_HUMAN]	-1.770	0.189	-0.431	-0.215	0.393	-0.388
Q9UPS8	Ankyrin repeat domain-containing protein 26 OS=Homo sapiens GN=ANKRD26 PE=1 SV=3 - [ANR26_HUMAN]	-1.805	-0.006	-0.402	-0.152	0.136	-0.918
Q7Z5W3	Probable methyltransferase BCDIN3D OS=Homo sapiens GN=BCDIN3D PE=2 SV=1 - [BN3D2_HUMAN]	-2.075	-0.456	-0.750	-1.111	0.631	-0.765
Q5H9U9	Probable ATP-dependent RNA helicase DDX60-like OS=Homo sapiens GN=DDX60L PE=2 SV=2 - [DDX6L_HUMAN]	-2.125	2.478	2.563	2.080	0.375	-2.112
Q15596	Nuclear receptor coactivator 2 OS=Homo sapiens GN=NCOA2 PE=1 SV=2 - [NCOA2_HUMAN]	-2.538	-2.110	0.150	-2.116	0.013	0.216
Q9BU23	Lipase maturation factor 2 OS=Homo sapiens GN=LMF2 PE=1 SV=2 - [LMF2_HUMAN]	-3.542	-0.016	-0.218	-4.192	4.153	-3.106

Appendix B

Full results of ELISA experiment detailed in Chapter 9. Values indicate protein concentration derived from absorbance readings and log plot of reference standards.

	Calpain	ANP	Myosin8	LPCAT	BLK	Tropo-myosin	ActinBeta	BNP	Galectin	VDAC1	PRG4	aHSG	Lpa
	ng/mL	pg/mL	pg/mL	ng/mL	ng/mL	pg/mL	ng/mL	pg/mL	ng/mL	pg/mL	ng/mL	ng/mL	pg/mL
Healthy	1.27	3.03	4.05	0.61	-0.20	-0.04	0.00	-0.46	0.00	1.32	1.14	2.47	0.61
Control	1.26	2.01	3.25	0.63	-0.22	-0.41	0.00	0.00	0.00	1.43	0.75	2.60	0.52
Mean	1.24	1.35	0.45	0.97	-0.22	-0.08	0.02	-0.31	0.00	0.95	0.80	2.67	0.63
SD	0.05	0.81	1.21	0.20	0.19	0.19	0.07	0.25	0.05	0.63	0.37	0.38	0.24
Sample16	1.27	1.49	1.58	0.43	-0.06	-0.22	0.00	-0.25	0.00	1.39	0.32	2.40	0.49
17	1.27	1.02	0.00	0.84	-0.17	-0.36	0.00	-0.55	0.00	0.00	0.49	2.55	0.59
18	1.13	2.28	0.00	1.10	-0.29	0.08	0.00	-0.47	0.00	1.19	1.20	2.83	0.82
22	1.21	0.00	0.00	0.80	-0.30	-0.41	0.00	-0.19	0.00	1.16	0.75	2.78	0.72
24	1.27	0.68	0.00	0.84	-0.31	-0.29	0.00	0.02	0.00	1.00	1.86	3.59	1.27
25	1.25	1.05	0.00	0.82	-0.37	-0.44	0.00	-0.48	0.00	1.38	0.47	2.28	0.30
26	1.24	1.69	0.00	0.90	-0.16	0.00	0.00	0.00	0.00	1.08	1.02	2.97	0.77
30	1.27	0.00	0.00	0.81	-0.47	0.01	0.00	0.00	0.00	0.94	0.87	2.16	0.51
31	1.27	2.45	3.56	0.87	-0.04	0.00	0.00	-0.21	0.00	1.29	0.40	2.51	0.48
33	1.26	2.15	0.00	0.98	-0.19	0.00	0.29	-0.64	0.00	0.98	0.41	2.30	0.33
34	1.18	0.77	0.00	0.61	-0.30	0.00	0.00	0.00	0.00	1.14	0.58	2.39	0.52
36	1.27	1.52	0.00	0.71	-0.47	0.00	0.00	-0.61	0.00	1.13	0.65	2.96	0.52
39	1.27	2.22	0.00	0.57	-0.29	0.00	0.00	0.00	0.00	0.00	0.71	2.52	0.56
40	1.24	0.00	0.00	0.85	-0.38	-0.47	0.00	0.00	0.00	0.00	0.27	2.22	0.46
42	1.24	0.89	0.00	1.19	-0.02	-0.34	0.00	-0.57	0.00	1.37	0.55	2.03	0.59
43	1.22	1.52	0.00	1.17	-0.12	0.00	0.00	-0.41	0.00	1.70	0.81	2.57	0.47
46	1.27	1.98	0.00	0.93	0.13	0.00	0.00	-0.42	0.00	1.11	1.61	3.66	1.16
49	1.25	1.93	0.00	0.99	0.10	0.38	0.00	0.00	0.00	0.94	0.39	2.29	0.54
50	1.27	0.84	0.00	0.95	-0.04	0.00	0.00	-0.53	0.00	1.44	1.11	2.27	0.78
52	1.23	1.47	0.00	1.12	-0.10	0.27	0.00	-0.52	0.00	1.46	0.23	2.67	0.42
53	1.27	1.45	0.00	0.95	-0.27	-0.09	0.00	-0.55	0.41	0.98	0.68	2.55	0.47
65	1.27	1.57	0.00	0.80	-0.10	0.10	0.00	-0.59	0.00	0.00	0.62	2.85	0.57

68	1.17	0.00	0.00	0.73	-0.25	0.00	0.00	-0.52	0.00	1.14	0.86	2.71	0.59
70	1.27	0.84	1.52	0.87	0.02	0.00	0.00	0.00	0.00	1.25	0.88	2.31	0.61
71	1.27	0.47	0.00	0.81	-0.06	-0.23	0.00	-0.58	0.00	1.37	0.57	2.52	0.64
72	1.27	0.00	0.00	0.90	0.16	0.00	0.12	-0.54	0.00	0.00	0.68	2.43	0.60
74	1.27	1.51	0.00	1.48	-0.11	-0.43	0.50	-0.13	0.00	2.41	0.57	2.49	0.72
76	1.20	0.00	0.00	1.19	-0.50	0.00	0.00	-0.31	0.00	1.67	0.63	2.96	0.62
78	1.27	3.39	4.99	1.18	-0.07	0.00	0.00	-0.36	0.00	1.15	1.51	3.62	1.32
79	1.27	0.50	0.00	1.10	-0.10	-0.30	0.00	-0.28	0.00	0.00	0.41	2.59	0.50
80	1.06	1.71	0.00	0.99	-0.31	0.00	0.00	-0.50	0.00	1.50	0.45	2.64	0.54
81	1.22	1.01	0.00	1.04	-0.50	0.00	0.00	0.00	0.00	1.15	0.86	2.61	0.62
82	1.20	1.64	1.76	0.90	-0.36	0.00	0.03	0.00	0.00	1.08	-0.01	2.67	0.59
84	1.04	2.07	0.00	0.83	-0.52	0.00	0.00	-0.63	0.00	0.00	0.89	2.86	0.56
85	1.19	0.89	0.00	0.71	-0.22	-0.47	0.00	0.00	0.00	0.00	0.76	2.77	0.49
87	1.26	0.00	0.00	1.00	-0.20	-0.44	0.00	0.00	0.00	0.00	0.42	2.56	0.57
91	1.27	2.50	2.01	0.92	0.15	0.00	0.00	-0.47	0.00	1.28	0.58	2.72	0.54
92	1.27	1.83	0.00	0.94	-0.16	-0.26	0.00	0.00	0.00	0.00	0.65	2.80	0.57
93	1.24	0.79	0.00	1.34	0.04	0.00	0.00	-0.47	0.00	1.38	0.89	2.78	0.77
94	1.22	1.52	0.00	1.19	-0.37	0.00	0.00	-0.52	0.00	1.42	0.36	2.20	0.50
95	1.27	0.52	0.00	0.93	-0.41	0.00	0.00	0.00	0.00	1.06	1.69	3.68	1.39
98	1.27	1.05	0.00	0.94	-0.25	0.00	0.02	-0.61	0.00	1.29	0.26	2.73	0.65
99	1.27	1.40	0.00	1.28	-0.17	-0.24	0.07	-0.28	0.00	2.52	0.71	2.65	0.51
102	1.22	1.56	0.00	1.00	-0.47	0.16	0.00	-0.49	0.00	0.96	0.32	2.59	0.44
103	1.14	0.81	0.00	0.62	-0.54	-0.25	0.00	-0.51	0.00	0.00	0.48	2.22	0.39
107	1.27	0.00	0.00	0.80	-0.27	0.00	0.00	0.00	0.00	1.20	0.46	2.35	0.52
110	1.23	1.62	0.00	0.79	-0.24	0.00	0.00	-0.38	0.00	0.97	0.83	2.69	0.43
112	1.24	1.19	0.00	1.00	-0.36	0.00	0.00	0.00	0.00	1.09	0.54	2.64	0.78
113	1.27	1.78	0.00	0.69	-0.33	0.00	0.00	-0.53	0.00	1.27	0.30	2.94	0.54
114	1.27	0.64	0.00	1.01	-0.19	0.08	0.00	-0.51	0.00	0.00	0.74	2.42	0.65
115	1.27	1.65	0.00	1.33	0.32	-0.13	0.06	-0.54	0.00	1.46	0.96	2.84	0.75
117	1.27	1.01	0.00	1.26	-0.35	0.00	0.00	-0.62	0.00	1.38	0.74	3.05	0.76
120	1.25	0.52	0.00	1.01	-0.18	0.00	0.00	0.00	0.00	0.00	1.72	3.61	1.47
121	1.21	1.79	0.00	1.11	-0.35	0.00	0.00	0.00	-0.22	1.06	0.77	2.98	0.67
125	1.27	1.41	0.00	0.99	-0.13	0.00	0.00	-0.40	0.00	1.49	0.80	2.96	0.64
126	1.23	2.18	0.00	1.07	-0.12	-0.30	0.00	-0.53	0.00	0.00	0.69	2.32	0.50
130	1.19	0.88	0.00	0.88	-0.44	-0.38	0.00	0.00	0.00	0.00	0.70	2.78	0.28
132	1.27	2.11	0.00	0.81	-0.28	0.00	0.00	0.00	0.00	0.97	1.34	3.06	0.47

134	1.18	2.76	3.99	0.79	-0.09	0.00	0.00	0.00	0.00	1.07	1.06	2.60	0.33
135	1.27	0.95	0.00	1.11	-0.45	-0.41	0.21	0.00	0.00	1.72	0.74	3.10	0.67
136	1.27	2.23	0.00	0.50	-0.42	0.00	0.00	-0.58	0.00	1.27	0.90	2.62	0.59
137	1.27	2.91	4.47	0.99	-0.41	0.00	0.00	-0.54	0.00	0.00	0.95	2.72	0.70
138	1.27	0.00	0.00	1.37	0.32	0.00	0.24	-0.54	0.00	1.69	1.29	2.19	0.80
141	1.27	0.57	0.00	1.23	-0.35	0.00	0.00	-0.62	0.00	1.27	1.05	2.53	0.74
143	1.27	1.82	1.51	1.02	-0.18	0.00	0.00	0.00	0.00	0.00	1.30	3.59	1.33
144	1.17	0.61	0.00	1.01	-0.35	0.00	0.00	0.00	0.00	0.00	0.68	2.58	0.53
146	1.27	0.97	0.00	1.21	-0.13	0.00	0.12	-0.40	0.00	1.50	0.61	2.68	0.52
147	1.27	2.30	0.00	1.18	-0.12	0.00	0.00	-0.53	0.00	1.04	0.89	2.53	0.59
148	1.27	1.08	0.00	1.25	-0.44	0.39	0.00	0.00	0.00	0.00	1.03	2.60	0.56
149	1.27	3.11	4.68	0.83	-0.28	-0.32	0.00	0.00	0.00	0.94	0.84	2.78	0.57
150	1.22	1.33	0.00	0.82	-0.09	-0.47	0.00	0.00	0.00	0.00	0.92	2.55	0.61
151	1.27	1.51	0.00	0.85	-0.45	0.00	0.00	0.00	0.00	0.95	0.88	2.70	0.49
152	1.27	1.03	2.23	0.90	-0.42	-0.09	0.00	-0.58	0.00	1.06	0.89	2.34	0.58
153	1.24	1.98	0.00	0.87	-0.41	0.00	0.00	-0.54	0.00	0.00	0.57	2.62	0.71
154	1.27	0.78	0.00	1.21	0.02	-0.34	0.01	0.00	0.00	1.58	0.90	2.73	0.69
156	1.25	1.46	0.00	1.14	-0.31	0.00	0.00	-0.54	0.00	1.49	1.06	2.52	0.65
158	1.27	1.94	0.00	1.17	-0.19	0.00	0.00	-0.50	0.00	1.60	1.90	3.66	1.32
160	1.27	1.28	0.00	1.29	-0.18	0.00	0.00	0.00	0.00	0.00	1.17	2.38	0.83
163	1.24	3.39	4.92	0.96	-0.23	0.00	0.00	-0.52	0.00	1.16	0.60	1.82	0.44
166	1.27	1.02	0.00	1.09	-0.08	0.02	0.00	-0.45	0.00	1.55	0.56	2.67	0.58
168	1.27	2.21	0.00	1.01	-0.45	0.00	0.00	-0.48	0.00	1.43	1.08	2.62	0.66
170	1.27	1.61	0.00	1.01	0.00	0.14	0.03	-0.20	0.00	1.17	1.19	2.59	0.54
179	1.27	1.15	0.00	0.94	-0.22	0.00	0.00	-0.34	0.00	1.36	0.81	2.33	0.39
181	1.27	0.00	0.00	1.03	-0.24	-0.44	0.00	-0.59	0.00	0.00	0.98	2.47	0.48
182	1.13	1.72	0.00	1.08	-0.03	-0.17	0.00	-0.54	0.00	1.44	0.87	2.46	0.50
191	1.15	2.20	1.87	1.05	-0.16	0.00	0.00	-0.45	0.00	1.27	0.76	2.26	0.59

List of References

1. Authors/Task Force Members, Dickstein K, Cohen-Solal A, Filippatos G, McMurray JJV, Ponikowski P, et al. ESC Guidelines for the diagnosis and treatment of acute and chronic heart failure 2008: The Task Force for the Diagnosis and Treatment of Acute and Chronic Heart Failure 2008 of the European Society of Cardiology. Developed in collaboration with the Heart Failure Association of the ESC (HFA) and endorsed by the European Society of Intensive Care Medicine (ESICM). European Heart Journal. 2008 Sep 17;29(19):2388–442.

2. Cowie MR, Wood DA, Coats AJ, Thompson SG, Poole-Wilson PA, Suresh V, et al. Incidence and aetiology of heart failure; a population-based study. Eur Heart J. 1999 Mar;20(6):421–8.

3. Levy D, Kenchaiah S, Larson MG, Benjamin EJ, Kupka MJ, Ho KKL, et al. Long-term trends in the incidence of and survival with heart failure. N Engl J Med. 2002 Oct 31;347(18):1397–402.

4. Lloyd-Jones D, Adams RJ, Brown TM, Carnethon M, Dai S, De Simone G, et al. Heart disease and stroke statistics--2010 update: a report from the American Heart Association. Circulation. 2010 Feb 23;121(7):e46–215.

5. Stewart S, Jenkins A, Buchan S, McGuire A, Capewell S, McMurray JJJV. The current cost of heart failure to the National Health Service in the UK. Eur J Heart Fail. 2002 Jun;4(3):361–71.

6. Hogg K, Swedberg K, McMurray J. Heart failure with preserved left ventricular systolic function; epidemiology, clinical characteristics, and prognosis. J Am Coll Cardiol. 2004 Feb 4;43(3):317–27.

7. MacIver DH, Dayer MJ, Harrison AJI. A general theory of acute and chronic heart failure. International Journal of Cardiology [Internet]. 2012 Apr [cited 2012 Apr 17]; Available from: http://linkinghub.elsevier.com/retrieve/pii/S0167527312003002

8. Stewart S, MacIntyre K, Hole DJ, Capewell S, McMurray JJ. More “malignant” than cancer? Five-year survival following a first admission for heart failure. Eur J Heart Fail. 2001 Jun;3(3):315–22.

9. Bleumink GS, Knetsch AM, Sturkenboom MCJM, Straus SMJM, Hofman A, Deckers JW, et al. Quantifying the heart failure epidemic: prevalence, incidence rate, lifetime risk and prognosis of heart failure The Rotterdam Study. Eur Heart J. 2004 Sep;25(18):1614–9.

10. Goldberg RJ, Ciampa J, Lessard D, Meyer TE, Spencer FA. Long-term survival after heart failure: a contemporary population-based perspective. Arch Intern Med. 2007 Mar 12;167(5):490–6.

11. Bueno H, Ross JS, Wang Y, Chen J, Vidán MT, Normand S-LT, et al. Trends in length of stay and short-term outcomes among Medicare patients hospitalized for heart failure, 1993-2006. JAMA. 2010 Jun 2;303(21):2141–7.

12. Jhund PS, Macintyre K, Simpson CR, Lewsey JD, Stewart S, Redpath A, et al. Long-term trends in first hospitalization for heart failure and subsequent survival between 1986 and 2003: a population study of 5.1 million people. Circulation. 2009 Feb 3;119(4):515–23.

13. Kannel WB, Plehn JF, Cupples LA. Cardiac failure and sudden death in the Framingham Study. American Heart Journal. 1988 Apr;115(4):869–75.

14. Mehta PA, Dubrey SW, McIntyre HF, Walker DM, Hardman SMC, Sutton GC, et al. Mode of Death in Patients with Newly Diagnosed Heart Failure in the General Population. Eur J Heart Fail. 2008 Nov 1;10(11):1108–16.

15. Cubbon RM, Gale CP, Kearney LC, Schechter CB, Brooksby WP, Nolan J, et al. Changing Characteristics and Mode of Death Associated With Chronic Heart Failure Caused by Left Ventricular Systolic DysfunctionClinical Perspective A Study Across Therapeutic Eras. Circ Heart Fail. 2011 Jul 1;4(4):396–403.

16. Effect of metoprolol CR/XL in chronic heart failure: Metoprolol CR/XL Randomised Intervention Trial in Congestive Heart Failure (MERIT-HF). Lancet. 1999 Jun 12;353(9169):2001–7.

17. Pitt B, Zannad F, Remme WJ, Cody R, Castaigne A, Perez A, et al. The effect of spironolactone on morbidity and mortality in patients with severe heart failure. Randomized Aldactone Evaluation Study Investigators. N Engl J Med. 1999 Sep 2;341(10):709–17.

18. Poole-Wilson PA, Uretsky BF, Thygesen K, Cleland JGF, Massie BM, Rydén L. Mode of death in heart failure: findings from the ATLAS trial. Heart. 2003 Jan 1;89(1):42–8.

19. Narang R, Cleland JGF, Erhardt L, Ball SG, Coats AJS, Cowley AJ, et al. Mode of death in chronic heart failure A request and proposition for more accurate classification. European heart journal. 1996;17(9):1390–403.

20. Mozaffarian D, Anker SD, Anand I, Linker DT, Sullivan MD, Cleland JGF, et al. Prediction of Mode of Death in Heart Failure: The Seattle Heart Failure Model. Circulation. 2007 Jul 24;116(4):392–8.

21. Braunwald's heart disease: a textbook of cardiovascular medicine. 9th ed. / edited by Robert O. Bonow ... [et al. I-56 p.

22. Priori SG, Aliot E, Blømstrom-Lundqvist C, Bossaert L, Breithardt G, Brugada P, et al. Task Force on Sudden Cardiac Death, European Society of Cardiology Summary of Recommendations. Europace. 2002;4(1):3–18.

23. Pratt CM, Greenway PS, Schoenfeld MH, Hibben ML, Reiffel JA. Exploration of the precision of classifying sudden cardiac death. Implications for the interpretation of clinical trials. Circulation. 1996 Feb 1;93(3):519–24.

24. Chugh SS, Reinier K, Teodorescu C, Evanado A, Kehr E, Samara MA, et al. Epidemiology of Sudden Cardiac Death: Clinical and Research Implications. Prog Cardiovasc Dis. 2008;51(3):213–28.

25. Kuller L, Lilienfeld A, Fisher R. An epidemiological study of sudden and unexpected deaths in adults. Medicine (Baltimore). 1967 Jul;46(4):341–61.

26. De Vreede-Swagemakers JJ, Gorgels AP, Dubois-Arbouw WI, van Ree JW, Daemen MJ, Houben LG, et al. Out-of-hospital cardiac arrest in the 1990's: a population-based study in the Maastricht area on incidence, characteristics and survival. J Am Coll Cardiol. 1997 Nov 15;30(6):1500–5.

27. Myerburg RJ. Sudden cardiac death: exploring the limits of our knowledge. J Cardiovasc Electrophysiol. 2001 Mar;12(3):369–81.

28. Desai AS, Fang JC, Maisel WH, Baughman KL. Implantable defibrillators for the prevention of mortality in patients with nonischemic cardiomyopathy: A meta-analysis of randomized controlled trials. JAMA. 2004 Dec 15;292(23):2874–9.

29. Myerburg RJ, Interian A Jr, Mitrani RM, Kessler KM, Castellanos A. Frequency of sudden cardiac death and profiles of risk. Am J Cardiol. 1997 Sep 11;80(5B):10F – 19F.

30. Goldberger JJ, Basu A, Boineau R, Buxton AE, Cain ME, Canty JM, et al. Risk Stratification for Sudden Cardiac Death A Plan for the Future. Circulation. 2014 Jan 28;129(4):516–26.

31. Zipes DP, Wellens HJ. Sudden cardiac death. Circulation. 1998 Nov 24;98(21):2334–51.

32. Huikuri HV, Castellanos A, Myerburg RJ. Sudden death due to cardiac arrhythmias. N Engl J Med. 2001 Nov 15;345(20):1473–82.

33. Bayés de Luna A, Coumel P, Leclercq JF. Ambulatory sudden cardiac death: mechanisms of production of fatal arrhythmia on the basis of data from 157 cases. Am Heart J. 1989 Jan;117(1):151–9.

34. Stevenson WG, Stevenson LW, Middlekauff HR, Saxon LA. Sudden death prevention in patients with advanced ventricular dysfunction. Circulation. 1993 Dec;88(6):2953–61.

35. Luu M, Stevenson WG, Stevenson LW, Baron K, Walden J. Diverse mechanisms of unexpected cardiac arrest in advanced heart failure. Circulation. 1989 Dec;80(6):1675–80.

36. Turakhia M, Tseng ZH. Sudden Cardiac Death: Epidemiology, Mechanisms, and Therapy. Current Problems in Cardiology. 2007 Sep;32(9):501–46.

37. Mirowski M, Reid PR, Mower MM, Watkins L, Gott VL, Schauble JF, et al. Termination of Malignant Ventricular Arrhythmias with an Implanted Automatic Defibrillator in Human Beings. New England Journal of Medicine. 1980;303(6):322–4.

38. Cannom DS, Prystowsky EN. The Evolution of the Implantable Cardioverter Defibrillator. Pacing and Clinical Electrophysiology. 2004 Mar 1;27(3):419–31.

39. Glikson M, Friedman PA. The implantable cardioverter defibrillator. The Lancet. 2001 Apr 7;357(9262):1107–17.

40. A comparison of antiarrhythmic-drug therapy with implantable defibrillators in patients resuscitated from near-fatal ventricular arrhythmias. The Antiarrhythmics versus Implantable Defibrillators (AVID) Investigators. N Engl J Med. 1997 Nov 27;337(22):1576–83.

41. Domanski MJ, Sakseena S, Epstein AE, Hallstrom AP, Brodsky MA, Kim S, et al. Relative effectiveness of the implantable cardioverter-defibrillator and antiarrhythmic drugs in patients with varying degrees of left ventricular dysfunction who have survived malignant ventricular arrhythmias. AVID Investigators. Antiarrhythmics Versus Implantable Defibrillators. J Am Coll Cardiol. 1999 Oct;34(4):1090–5.

42. Connolly SJ, Gent M, Roberts RS, Dorian P, Roy D, Sheldon RS, et al. Canadian implantable defibrillator study (CIDS) : a randomized trial of the implantable cardioverter defibrillator against amiodarone. Circulation. 2000 Mar 21;101(11):1297–302.

43. Sheldon R, Connolly S, Krahn A, Roberts R, Gent M, Gardner M. Identification of patients most likely to benefit from implantable cardioverter-defibrillator therapy: the Canadian Implantable Defibrillator Study. Circulation. 2000 Apr 11;101(14):1660–4.

44. Kuck KH, Cappato R, Siebels J, Rüppel R. Randomized comparison of antiarrhythmic drug therapy with implantable defibrillators in patients resuscitated from cardiac arrest : the Cardiac Arrest Study Hamburg (CASH). Circulation. 2000 Aug 15;102(7):748–54.

45. Connolly SJ, Hallstrom AP, Cappato R, Schron EB, Kuck KH, Zipes DP, et al. Meta-analysis of the implantable cardioverter defibrillator secondary prevention trials. AVID, CASH and CIDS studies. Antiarrhythmics vs Implantable Defibrillator study. Cardiac Arrest Study Hamburg . Canadian Implantable Defibrillator Study. Eur Heart J. 2000 Dec;21(24):2071–8.

46. Bigger JT. Prophylactic Use of Implanted Cardiac Defibrillators in Patients at High Risk for Ventricular Arrhythmias after Coronary-Artery Bypass Graft Surgery. New England Journal of Medicine. 1997;337(22):1569–75.

47. Moss AJ, Hall WJ, Cannom DS, Daubert JP, Higgins SL, Klein H, et al. Improved survival with an implanted defibrillator in patients with coronary disease at high risk for ventricular arrhythmia. Multicenter Automatic Defibrillator Implantation Trial Investigators. N Engl J Med. 1996 Dec 26;335(26):1933–40.

48. Buxton AE, Lee KL, Fisher JD, Josephson ME, Prystowsky EN, Hafley G. A randomized study of the prevention of sudden death in patients with coronary artery disease. Multicenter Unsustained Tachycardia Trial Investigators. N Engl J Med. 1999 Dec 16;341(25):1882–90.

49. Moss AJ, Zareba W, Hall WJ, Klein H, Wilber DJ, Cannom DS, et al. Prophylactic implantation of a defibrillator in patients with myocardial infarction and reduced ejection fraction. N Engl J Med. 2002 Mar 21;346(12):877–83.

50. Hohnloser SH, Kuck KH, Dorian P, Roberts RS, Hampton JR, Hatala R, et al. Prophylactic use of an implantable cardioverter-defibrillator after acute myocardial infarction. N Engl J Med. 2004 Dec 9;351(24):2481–8.

51. Strickberger SA, Hummel JD, Bartlett TG, Frumin HI, Schuger CD, Beau SL, et al. Amiodarone versus implantable cardioverter-defibrillator:randomized trial in patients with nonischemic dilated cardiomyopathy and asymptomatic nonsustained ventricular tachycardia--AMIOVIRT. J Am Coll Cardiol. 2003 May 21;41(10):1707–12.

52. Ezekowitz JA, Rowe BH, Dryden DM, Hooton N, Vandermeer B, Spooner C, et al. Systematic review: implantable cardioverter defibrillators for adults with left ventricular systolic dysfunction. Ann Intern Med. 2007 Aug 21;147(4):251–62.

53. Al-Khatib SM, Sanders GD, Mark DB, Lee KL, Bardy GH, Bigger JT, et al. Implantable cardioverter defibrillators and cardiac resynchronization therapy in patients with left ventricular dysfunction: randomized trial evidence through 2004. Am Heart J. 2005 Jun;149(6):1020–34.

54. Nanthakumar K, Epstein AE, Kay GN, Plumb VJ, Lee DS. Prophylactic implantable cardioverter-defibrillator therapy in patients with left ventricular systolic dysfunction: a pooled analysis of 10 primary prevention trials. J Am Coll Cardiol. 2004 Dec 7;44(11):2166–72.

55. Theuns DAMJ, Smith T, Hunink MGM, Bardy GH, Jordaens L. Effectiveness of prophylactic implantation of cardioverter-defibrillators without cardiac resynchronization therapy in patients with ischaemic or non-ischaemic heart disease: a systematic review and meta-analysis. Europace. 2010 Oct;12(11):1564–70.

56. Camm J, Klein H, Nisam S. The cost of implantable defibrillators: perceptions and reality. Eur Heart J. 2007 Feb 1;28(4):392–7.

57. Sanders GD, Hlatky MA, Owens DK. Cost-effectiveness of implantable cardioverter-defibrillators. N Engl J Med. 2005 Oct 6;353(14):1471–80.

58. Smith T, Jordaens L, Theuns DAMJ, Dessel PF van, Wilde AA, Hunink MGM. The cost-effectiveness of primary prophylactic implantable defibrillator therapy in patients with ischaemic or non-ischaemic heart disease: a European analysis. Eur Heart J. 2013 Jan 14;34(3):211–9.

59. Tung R, Zimetbaum P, Josephson ME. A Critical Appraisal of Implantable Cardioverter-Defibrillator Therapy for the Prevention of Sudden Cardiac Death. Journal of the American College of Cardiology. 2008 Sep;52(14):1111–21.

60. Anderson KP. Sudden cardiac death unresponsive to implantable defibrillator therapy: an urgent target for clinicians, industry and government. J Interv Card Electrophysiol. 2005 Nov;14(2):71–8.

61. NICE. Implantable cardioverter defibrillators and cardiac resynchronisation...TA314 Guidance [Internet]. [cited 2014 Jul 22]. Available from: http://publications.nice.org.uk/implantable-cardioverter-defibrillators-and-cardiac-resynchronisation-therapy-for-arrhythmias-and-ta314

62. McMurray JJV, Adamopoulos S, Anker SD, Auricchio A, Böhm M, Dickstein K, et al. ESC Guidelines for the diagnosis and treatment of acute and chronic heart failure 2012: The Task Force for the Diagnosis and Treatment of Acute and Chronic Heart

Failure 2012 of the European Society of Cardiology. Developed in collaboration with the Heart Failure Association (HFA) of the ESC. Eur Heart J. 2012 Jul;33(14):1787–847.

63. Tracy CM, Epstein AE, Darbar D, DiMarco JP, Dunbar SB, Estes NAM, et al. 2012 ACCF/AHA/HRS Focused Update of the 2008 Guidelines for Device-Based Therapy of Cardiac Rhythm AbnormalitiesA Report of the American College of Cardiology Foundation/American Heart Association Task Force on Practice Guidelines. J Am Coll Cardiol. 2012 Oct 2;60(14):1297–313.

64. NICE. Arrhythmia - implantable cardioverter defibrillators (ICDs) (review) [Internet]. NICE. [cited 2014 Apr 19]. Available from: http://www.nice.org.uk/

65. Bigger JT Jr, Fleiss JL, Kleiger R, Miller JP, Rolnitzky LM. The relationships among ventricular arrhythmias, left ventricular dysfunction, and mortality in the 2 years after myocardial infarction. Circulation. 1984 Feb;69(2):250–8.

66. Kusmirek SL, Gold MR. Sudden cardiac death: The role of risk stratification. American Heart Journal. 2007 Apr;153(4):25–33.

67. Solomon SD, Anavekar N, Skali H, McMurray JJV, Swedberg K, Yusuf S, et al. Influence of ejection fraction on cardiovascular outcomes in a broad spectrum of heart failure patients. Circulation. 2005 Dec 13;112(24):3738–44.

68. Kadish A, Dyer A, Daubert JP, Quigg R, Estes NAM, Anderson KP, et al. Prophylactic defibrillator implantation in patients with nonischemic dilated cardiomyopathy. N Engl J Med. 2004 May 20;350(21):2151–8.

69. Bardy GH, Lee KL, Mark DB, Poole JE, Packer DL, Boineau R, et al. Amiodarone or an implantable cardioverter-defibrillator for congestive heart failure. N Engl J Med. 2005 Jan 20;352(3):225–37.

70. Germano JJ, Reynolds M, Essebag V, Josephson ME. Frequency and causes of implantable cardioverter-defibrillator therapies: is device therapy proarrhythmic? Am J Cardiol. 2006 Apr 15;97(8):1255–61.

71. Koller MT, Schaer B, Wolbers M, Sticherling C, Bucher HC, Osswald S. Death without prior appropriate implantable cardioverter-defibrillator therapy: a competing risk study. Circulation. 2008 Apr 15;117(15):1918–26.

72. Otmani A, Trinquart L, Marijon E, Lavergne T, Waintraub X, Lepillier A, et al. Rates and predictors of appropriate implantable cardioverter-defibrillator therapy delivery: results from the EVADEF cohort study. Am Heart J. 2009 Aug;158(2):230–7.e1.

73. Buxton AE, Ellison KE, Lorvidhaya P, Ziv O. Left ventricular ejection fraction for sudden death risk stratification and guiding implantable cardioverter-defibrillators implantation. J Cardiovasc Pharmacol. 2010 May;55(5):450–5.

74. Hartikainen JE, Malik M, Staunton A, Poloniecki J, Camm AJ. Distinction between arrhythmic and nonarrhythmic death after acute myocardial infarction based on heart rate variability, signal-averaged electrocardiogram, ventricular arrhythmias and left ventricular ejection fraction. J Am Coll Cardiol. 1996 Aug;28(2):296–304.

75. Mäkikallio TH, Barthel P, Schneider R, Bauer A, Tapanainen JM, Tulppo MP, et al. Prediction of sudden cardiac death after acute myocardial infarction: role of Holter monitoring in the modern treatment era. Eur Heart J. 2005 Apr;26(8):762–9.

76. Mittal S, Iwai S, Stein KM, Markowitz SM, Slotwiner DJ, Lerman BB. Long-term outcome of patients with unexplained syncope treated with an electrophysiologic-guided approach in the implantable cardioverter-defibrillator era. J Am Coll Cardiol. 1999 Oct;34(4):1082–9.

77. Wilber DJ, Olshansky B, Moran JF, Scanlon PJ. Electrophysiological testing and nonsustained ventricular tachycardia. Use and limitations in patients with coronary artery disease and impaired ventricular function. Circulation. 1990 Aug;82(2):350–8.

78. Poll DS, Marchlinski FE, Buxton AE, Josephson ME. Usefulness of programmed stimulation in idiopathic dilated cardiomyopathy. Am J Cardiol. 1986 Nov 1;58(10):992–7.

79. Meinertz T, Treese N, Kasper W, Geibel A, Hofmann T, Zehender M, et al. Determinants of prognosis in idiopathic dilated cardiomyopathy as determined by programmed electrical stimulation. Am J Cardiol. 1985 Aug 1;56(4):337–41.

80. Maggioni AP, Zuanetti G, Franzosi MG, Rovelli F, Santoro E, Staszewsky L, et al. Prevalence and prognostic significance of ventricular arrhythmias after acute myocardial infarction in the fibrinolytic era. GISSI-2 results. Circulation. 1993 Feb;87(2):312–22.

81. Grimm W, Christ M, Bach J, Müller H-H, Maisch B. Noninvasive arrhythmia risk stratification in idiopathic dilated cardiomyopathy: results of the Marburg Cardiomyopathy Study. Circulation. 2003 Dec 9;108(23):2883–91.

82. Gehi AK, Stein RH, Metz LD, Gomes JA. Microvolt T-Wave Alternans for the Risk Stratification of Ventricular Tachyarrhythmic Events. Journal of the American College of Cardiology. 2005 Jul;46(1):75–82.

83. Gupta A, Hoang DD, Karliner L, Tice JA, Heidenreich P, Wang PJ, et al. Ability of microvolt T-wave alternans to modify risk assessment of ventricular tachyarrhythmic events: a meta-analysis. Am Heart J. 2012 Mar;163(3):354–64.

84. Costantini O, Hohnloser SH, Kirk MM, Lerman BB, Baker JH 2nd, Sethuraman B, et al. The ABCD (Alternans Before Cardioverter Defibrillator) Trial: strategies using T-wave alternans to improve efficiency of sudden cardiac death prevention. J Am Coll Cardiol. 2009 Feb 10;53(6):471–9.

85. Gold MR, Spencer W. T wave alternans for ventricular arrhythmia risk stratification: Current Opinion in Cardiology. 2003 Jan;18(1):1–5.

86. Van Ravenswaaij-Arts CM, Kollée LA, Hopman JC, Stoelinga GB, van Geijn HP. Heart rate variability. Ann Intern Med. 1993 Mar 15;118(6):436–47.

87. Kleiger RE, Miller JP, Bigger JT Jr, Moss AJ. Decreased heart rate variability and its association with increased mortality after acute myocardial infarction. Am J Cardiol. 1987 Feb 1;59(4):256–62.

88. Nolan J, Batin PD, Andrews R, Lindsay SJ, Brooksby P, Mullen M, et al. Prospective study of heart rate variability and mortality in chronic heart failure: results of the United Kingdom heart failure evaluation and assessment of risk trial (UK-heart). Circulation. 1998 Oct 13;98(15):1510–6.

89. Rovere MTL, Bigger JT, Marcus FI, Mortara A, Schwartz PJ. Baroreflex sensitivity and heart-rate variability in prediction of total cardiac mortality after myocardial infarction. The Lancet. 1998 Feb;351(9101):478–84.

90. Erdogan A, Coch M, Bilgin M, Parahuleva M, Tillmanns H, Waldecker B, et al. Prognostic value of heart rate variability after acute myocardial infarction in the era of immediate reperfusion. Herzschrittmacherther Elektrophysiol. 2008 Dec;19(4):161–8.

91. Huikuri HV, Exner DV, Kavanagh KM, Aggarwal SG, Mitchell LB, Messier MD, et al. Attenuated recovery of heart rate turbulence early after myocardial infarction identifies patients at high risk for fatal or near-fatal arrhythmic events. Heart Rhythm. 2010;7(2):229–35.

92. Huikuri HV, Stein PK. Heart Rate Variability in Risk Stratification of Cardiac Patients. Progress in Cardiovascular Diseases. 2013 Sep;56(2):153–9.

93. Breithardt G, Schwarzmaier J, Borggrefe M, Haerten K, Seipel L. Prognostic significance of late ventricular potentials after acute myocardial infarction. Eur Heart J. 1983 Jul;4(7):487–95.

94. Steinberg JS, Berbari EJ. The signal-averaged electrocardiogram: update on clinical applications. J Cardiovasc Electrophysiol. 1996 Oct;7(10):972-88.

95. Gomes JA, Cain ME, Buxton AE, Josephson ME, Lee KL, Hafley GE. Prediction of long-term outcomes by signal-averaged electrocardiography in patients with unsustained ventricular tachycardia, coronary artery disease, and left ventricular dysfunction. Circulation. 2001 Jul 24;104(4):436-41.

96. Denes P, el-Sherif N, Katz R, Capone R, Carlson M, Mitchell LB, et al. Prognostic significance of signal-averaged electrocardiogram after thrombolytic therapy and/or angioplasty during acute myocardial infarction (CAST substudy). Cardiac Arrhythmia Suppression Trial (CAST) SAECG Substudy Investigators. Am J Cardiol. 1994 Aug 1;74(3):216-20.

97. Bauer A, Guzik P, Barthel P, Schneider R, Ulm K, Watanabe MA, et al. Reduced prognostic power of ventricular late potentials in post-infarction patients of the reperfusion era. Eur Heart J. 2005 Apr;26(8):755-61.

98. Grimm W, Hoffmann J, Knop U, Winzenburg J, Menz V, Maisch B. Value of time- and frequency-domain analysis of signal-averaged electrocardiography for arrhythmia risk prediction in idiopathic dilated cardiomyopathy. Pacing Clin Electrophysiol. 1996 Nov;19(11 Pt 2):1923-7.

99. Yi G, Hnatkova K, Mahon NG, Keeling PJ, Reardon M, Camm AJ, et al. Predictive value of wavelet decomposition of the signal-averaged electrocardiogram in idiopathic dilated cardiomyopathy. Eur Heart J. 2000 Jun;21(12):1015-22.

100. Hathaway WR, Peterson ED, Wagner GS, Granger CB, Zabel KM, Pieper KS, et al. Prognostic significance of the initial electrocardiogram in patients with acute myocardial infarction. GUSTO-I Investigators. Global Utilization of Streptokinase and t-PA for Occluded Coronary Arteries. JAMA. 1998 Feb 4;279(5):387-91.

101. Petrina M, Goodman SG, Eagle KA. The 12-lead electrocardiogram as a predictive tool of mortality after acute myocardial infarction: current status in an era of revascularization and reperfusion. Am Heart J. 2006 Jul;152(1):11-8.

102. Zimetbaum PJ, Buxton AE, Batsford W, Fisher JD, Hafley GE, Lee KL, et al. Electrocardiographic predictors of arrhythmic death and total mortality in the multicenter unsustained tachycardia trial. Circulation. 2004 Aug 17;110(7):766-9.

103. Buxton AE, Sweeney MO, Wathen MS, Josephson ME, Otterness MF, Hogan-Miller E, et al. QRS duration does not predict occurrence of ventricular tachyarrhythmias in

patients with implanted cardioverter-defibrillators. J Am Coll Cardiol. 2005 Jul 19;46(2):310–6.

104. Hofmann T, Meinertz T, Kasper W, Geibel A, Zehender M, Hohnloser S, et al. Mode of death in idiopathic dilated cardiomyopathy: a multivariate analysis of prognostic determinants. Am Heart J. 1988 Dec;116(6 Pt 1):1455–63.

105. Schwartz PJ, Wolf S. QT interval prolongation as predictor of sudden death in patients with myocardial infarction. Circulation. 1978 Jun;57(6):1074–7.

106. Schwartz PJ, Ackerman MJ. The long QT syndrome: a transatlantic clinical approach to diagnosis and therapy. Eur Heart J. 2013 Mar 18;eht089.

107. Peters RW, Byington RP, Barker A, Yusuf S. Prognostic value of prolonged ventricular repolarization following myocardial infarction: the BHAT experience. The BHAT Study Group. J Clin Epidemiol. 1990;43(2):167–72.

108. Schouten EG, Dekker JM, Meppelink P, Kok FJ, Vandenbroucke JP, Pool J. QT interval prolongation predicts cardiovascular mortality in an apparently healthy population. Circulation. 1991 Oct;84(4):1516–23.

109. Karjalainen J, Reunanen A, Ristola P, Viitasalo M. QT interval as a cardiac risk factor in a middle aged population. Heart. 1997 Jun;77(6):543–8.

110. Algra A, Tijssen JG, Roelandt JR, Pool J, Lubsen J. QTc prolongation measured by standard 12-lead electrocardiography is an independent risk factor for sudden death due to cardiac arrest. Circulation. 1991 Jun;83(6):1888–94.

111. Brooksby P, Batin PD, Nolan J, Lindsay SJ, Andrews R, Mullen M, et al. The relationship between QT intervals and mortality in ambulant patients with chronic heart failure. The united kingdom heart failure evaluation and assessment of risk trial (UK-HEART). Eur Heart J. 1999 Sep;20(18):1335–41.

112. Noseworthy PA, Peloso GM, Hwang S-J, Larson MG, Levy D, O'Donnell CJ, et al. QT interval and long-term mortality risk in the Framingham Heart Study. Ann Noninvasive Electrocardiol. 2012 Oct;17(4):340–8.

113. Elming H, Holm E, Jun L, Torp-Pedersen C, Køber L, Kircshoff M, et al. The prognostic value of the QT interval and QT interval dispersion in all-cause and cardiac mortality and morbidity in a population of Danish citizens. Eur Heart J. 1998 Sep;19(9):1391–400.

114. Brendorp B, Elming H, Jun L, Køber L, Malik M, Jensen GB, et al. Qt dispersion has no prognostic information for patients with advanced congestive heart failure and reduced left ventricular systolic function. Circulation. 2001 Feb 13;103(6):831–5.

115. Taggart P, Sutton PM, Opthof T, Coronel R, Trimlett R, Pugsley W, et al. Transmural repolarisation in the left ventricle in humans during normoxia and ischaemia. Cardiovasc Res. 2001 Jun;50(3):454–62.

116. Opthof T, Coronel R, Janse MJ. Is there a significant transmural gradient in repolarization time in the intact heart?: Repolarization Gradients in the Intact Heart. Circ Arrhythm Electrophysiol. 2009 Feb;2(1):89–96.

117. Antzelevitch C, Sicouri S, Litovsky SH, Lukas A, Krishnan SC, Di Diego JM, et al. Heterogeneity within the ventricular wall. Electrophysiology and pharmacology of epicardial, endocardial, and M cells. Circ Res. 1991 Dec;69(6):1427–49.

118. Yan GX, Antzelevitch C. Cellular basis for the normal T wave and the electrocardiographic manifestations of the long-QT syndrome. Circulation. 1998 Nov 3;98(18):1928–36.

119. Antzelevitch C, Shimizu W, Yan GX, Sicouri S. Cellular basis for QT dispersion. J Electrocardiol. 1998;30 Suppl:168–75.

120. Xia Y, Liang Y, Kongstad O, Liao Q, Holm M, Olsson B, et al. In vivo validation of the coincidence of the peak and end of the T wave with full repolarization of the epicardium and endocardium in swine. Heart Rhythm. 2005 Feb;2(2):162–9.

121. Van Huysduynen BH, Swenne CA, Draisma HHM, Antoni ML, Van De Vooren H, Van Der Wall EE, et al. Validation of ECG indices of ventricular repolarization heterogeneity: a computer simulation study. J Cardiovasc Electrophysiol. 2005 Oct;16(10):1097–103.

122. Haarmark C, Graff C, Andersen MP, Hardahl T, Struijk JJ, Toft E, et al. Reference values of electrocardiogram repolarization variables in a healthy population. Journal of Electrocardiology. 2010;43(1):31–9.

123. Tatlisu MA, Ozcan KS, Güngör B, Ekmekçi A, Cekirdekçi EI, Aruğarslan E, et al. Can the T-peak to T-end interval be a predictor of mortality in patients with ST-elevation myocardial infarction? Coron Artery Dis. 2014 Mar 10;

124. Panikkath R, Reinier K, Uy-Evanado A, Teodorescu C, Hattenhauer J, Mariani R, et al. Prolonged Tpeak-to-tend interval on the resting ECG is associated with increased risk of sudden cardiac death. Circ Arrhythm Electrophysiol. 2011 Aug;4(4):441–7.

125. Porthan K, Viitasalo M, Toivonen L, Havulinna AS, Jula A, Tikkanen JT, et al. Predictive value of electrocardiographic T-wave morphology parameters and T-wave peak to T-wave end interval for sudden cardiac death in the general population. Circ Arrhythm Electrophysiol. 2013 Aug;6(4):690–6.

126. Hlaing T, DiMino T, Kowey PR, Yan G-X. ECG repolarization waves: their genesis and clinical implications. Ann Noninvasive Electrocardiol. 2005 Apr;10(2):211–23.

127. Haïssaguerre M, Derval N, Sacher F, Jesel L, Deisenhofer I, de Roy L, et al. Sudden cardiac arrest associated with early repolarization. N Engl J Med. 2008 May 8;358(19):2016–23.

128. Tikkanen JT, Anttonen O, Junttila MJ, Aro AL, Kerola T, Rissanen HA, et al. Long-term outcome associated with early repolarization on electrocardiography. N Engl J Med. 2009 Dec 24;361(26):2529–37.

129. Sinner MF, Reinhard W, Müller M, Beckmann B-M, Martens E, Perz S, et al. Association of early repolarization pattern on ECG with risk of cardiac and all-cause mortality: a population-based prospective cohort study (MONICA/KORA). PLoS Med. 2010 Jul;7(7):e1000314.

130. Haruta D, Matsuo K, Tsuneto A, Ichimaru S, Hida A, Sera N, et al. Incidence and prognostic value of early repolarization pattern in the 12-lead electrocardiogram. Circulation. 2011 Jun 28;123(25):2931–7.

131. Junttila MJ, Sager SJ, Tikkanen JT, Anttonen O, Huikuri HV, Myerburg RJ. Clinical significance of variants of J-points and J-waves: early repolarization patterns and risk. Eur Heart J. 2012 Nov 1;33(21):2639–43.

132. Tikkanen JT, Wichmann V, Junttila MJ, Rainio M, Hookana E, Lappi O-P, et al. Association of Early Repolarization and Sudden Cardiac Death During an Acute Coronary Event. Circ Arrhythm Electrophysiol. 2012 Aug 1;5(4):714–8.

133. Machecourt J, Longère P, Fagret D, Vanzetto G, Wolf JE, Polidori C, et al. Prognostic value of thallium-201 single-photon emission computed tomographic myocardial perfusion imaging according to extent of myocardial defect. Study in 1,926 patients with follow-up at 33 months. J Am Coll Cardiol. 1994 Apr;23(5):1096–106.

134. Dorbala S, Hachamovitch R, Curillova Z, Thomas D, Vangala D, Kwong RY, et al. Incremental prognostic value of gated Rb-82 positron emission tomography myocardial perfusion imaging over clinical variables and rest LVEF. JACC Cardiovasc Imaging. 2009 Jul;2(7):846–54.

135. Van der Burg AEB, Bax JJ, Boersma E, Pauwels EKJ, van der Wall EE, Schalij MJ. Impact of viability, ischemia, scar tissue, and revascularization on outcome after aborted sudden death. Circulation. 2003 Oct 21;108(16):1954–9.

136. Tamaki S, Yamada T, Okuyama Y, Morita T, Sanada S, Tsukamoto Y, et al. Cardiac iodine-123 metaiodobenzylguanidine imaging predicts sudden cardiac death independently of left ventricular ejection fraction in patients with chronic heart failure and left ventricular systolic dysfunction: results from a comparative study with signal-averaged electrocardiogram, heart rate variability, and QT dispersion. J Am Coll Cardiol. 2009 Feb 3;53(5):426–35.

137. Verberne HJ, Brewster LM, Somsen GA, van Eck-Smit BLF. Prognostic value of myocardial 123I-metaiodobenzylguanidine (MIBG) parameters in patients with heart failure: a systematic review. Eur Heart J. 2008 May;29(9):1147–59.

138. Jacobson AF, Senior R, Cerqueira MD, Wong ND, Thomas GS, Lopez VA, et al. Myocardial iodine-123 meta-iodobenzylguanidine imaging and cardiac events in heart failure. Results of the prospective ADMIRE-HF (AdreView Myocardial Imaging for Risk Evaluation in Heart Failure) study. J Am Coll Cardiol. 2010 May 18;55(20):2212–21.

139. Boogers MJ, Borleffs CJW, Henneman MM, van Bommel RJ, van Ramshorst J, Boersma E, et al. Cardiac sympathetic denervation assessed with 123-iodine metaiodobenzylguanidine imaging predicts ventricular arrhythmias in implantable cardioverter-defibrillator patients. J Am Coll Cardiol. 2010 Jun 15;55(24):2769–77.

140. McCrohon JA, Moon JCC, Prasad SK, McKenna WJ, Lorenz CH, Coats AJS, et al. Differentiation of heart failure related to dilated cardiomyopathy and coronary artery disease using gadolinium-enhanced cardiovascular magnetic resonance. Circulation. 2003 Jul 8;108(1):54–9.

141. Pereira RS, Prato FS, Wisenberg G, Sykes J, Yvorchuk KJ. The use of Gd-DTPA as a marker of myocardial viability in reperfused acute myocardial infarction. Int J Cardiovasc Imaging. 2001 Oct;17(5):395–404.

142. Wu E, Judd RM, Vargas JD, Klocke FJ, Bonow RO, Kim RJ. Visualisation of presence, location, and transmural extent of healed Q-wave and non-Q-wave myocardial infarction. Lancet. 2001 Jan 6;357(9249):21–8.

143. Schmidt A, Azevedo CF, Cheng A, Gupta SN, Bluemke DA, Foo TK, et al. Infarct Tissue Heterogeneity by Magnetic Resonance Imaging Identifies Enhanced Cardiac Arrhythmia Susceptibility in Patients With Left Ventricular Dysfunction. Circulation. 2007 Apr 17;115(15):2006–14.

144. Roes SD, Borleffs CJW, van der Geest RJ, Westenberg JJM, Marsan NA, Kaandorp TAM, et al. Infarct tissue heterogeneity assessed with contrast-enhanced MRI predicts spontaneous ventricular arrhythmia in patients with ischemic cardiomyopathy and implantable cardioverter-defibrillator. Circ Cardiovasc Imaging. 2009 May;2(3):183–90.

145. Scott PA, Rosengarten JA, Curzen NP, Morgan JM. Late gadolinium enhancement cardiac magnetic resonance imaging for the prediction of ventricular tachyarrhythmic events: a meta-analysis. European Journal of Heart Failure. 2013 Sep;15(9):1019–27.

146. Saeed M, Lund G, Wendland MF, Bremerich J, Weinmann H, Higgins CB. Magnetic resonance characterization of the peri-infarction zone of reperfused myocardial infarction with necrosis-specific and extracellular nonspecific contrast media. Circulation. 2001 Feb 13;103(6):871–6.

147. Yan AT, Shayne AJ, Brown KA, Gupta SN, Chan CW, Luu TM, et al. Characterization of the peri-infarct zone by contrast-enhanced cardiac magnetic resonance imaging is a powerful predictor of post-myocardial infarction mortality. Circulation. 2006 Jul 4;114(1):32–9.

148. Kadish AH, Bello D, Finn JP, Bonow RO, Schaechter A, Subacius H, et al. Rationale and design for the Defibrillators to Reduce Risk by Magnetic Resonance Imaging Evaluation (DETERMINE) trial. J Cardiovasc Electrophysiol. 2009 Sep;20(9):982–7.

149. Cassidy DM, Vassallo JA, Marchlinski FE, Buxton AE, Untereker WJ, Josephson ME. Endocardial mapping in humans in sinus rhythm with normal left ventricles: activation patterns and characteristics of electrograms. Circulation. 1984 Jul;70(1):37–42.

150. Schamroth L. An introduction to electrocardiography. Oxford: Blackwell Scientific; 1993.

151. PRINZMETAL M, SHAW CM Jr, MAXWELL MH, FLAMM EJ, GOLDMAN A, KIMURA N, et al. Studies on the mechanism of ventricular activity. VI. The depolarization complex in pure subendocardial infarction; role of the subendocardial region in the normal electrocardiogram. Am J Med. 1954 Apr;16(4):469–89.

152. PIPBERGER H, SCHWARTZ L, MASSUMI RA, WEINER SM, PRINZMETAL M. Studies on the mechanism of ventricular activity. XXI. The origin of the depolarization complex, with clinical applications. Am Heart J. 1957 Oct;54(4):511–30.

153. Phibbs BP, Marcus FI. Perpetuation of the myth of the Q-wave versus the non-Q-wave myocardial infarction. Journal of the American College of Cardiology. 2002 Feb 6;39(3):556–7.

154. Pipberger HV, Lopez EA. “Silent” subendocardial infarcts: fact or fiction? Am Heart J. 1980 Nov;100(5):597–9.

155. Phibbs B. “Transmural” versus “subendocardial” myocardial infarction: an electrocardiographic myth. J Am Coll Cardiol. 1983 Feb;1(2 Pt 1):561–4.

156. Spodick DH. Q-wave infarction versus S-T infarction: Nonspecificity of electrocardiographic criteria for differentiating transmural and nontransmural lesions. The American Journal of Cardiology. 1983 Mar 1;51(5):913–5.

157. Phibbs B, Marcus F, Marriott HJ, Moss A, Spodick DH. Q-wave versus non-Q wave myocardial infarction: a meaningless distinction. J Am Coll Cardiol. 1999 Feb;33(2):576–82.

158. Selvester RH, Strauss DG, Wagner GS. Myocardial Infarction. In: Macfarlane PW, Oosterom A van, Pahlm O, Kligfield P, Janse M, Camm J, editors. Comprehensive Electrocardiology [Internet]. Springer London; 2010 [cited 2014 Jan 16]. p. 651–746. Available from: http://link.springer.com/referenceworkentry/10.1007/978-1-84882-046-3_16

159. Lima JA, Judd RM, Bazille A, Schulman SP, Atalar E, Zerhouni EA. Regional heterogeneity of human myocardial infarcts demonstrated by contrast-enhanced MRI. Potential mechanisms. Circulation. 1995 Sep 1;92(5):1117–25.

160. Kim RJ, Fieno DS, Parrish TB, Harris K, Chen EL, Simonetti O, et al. Relationship of MRI delayed contrast enhancement to irreversible injury, infarct age, and contractile function. Circulation. 1999 Nov 9;100(19):1992–2002.

161. Moon JCC, De Arenaza DP, Elkington AG, Taneja AK, John AS, Wang D, et al. The pathologic basis of Q-wave and non-Q-wave myocardial infarction: a cardiovascular magnetic resonance study. J Am Coll Cardiol. 2004 Aug 4;44(3):554–60.

162. Flowers NC, Horan LG, Thomas JR, Tolleson WJ. The anatomic basis for high-frequency components in the electrocardiogram. Circulation. 1969 Apr;39(4):531–9.

163. Reddy CVR, Cheriparambill K, Saul B, Makan M, Kassotis J, Kumar A, et al. Fragmented left sided QRS in absence of bundle branch block: sign of left ventricular aneurysm. Ann Noninvasive Electrocardiol. 2006 Apr;11(2):132–8.

164. Das MK, Khan B, Jacob S, Kumar A, Mahenthiran J. Significance of a Fragmented QRS Complex Versus a Q Wave in Patients With Coronary Artery Disease. Circulation. 2006 May 30;113(21):2495–501.

165. Das MK, Saha C, El Masry H, Peng J, Dandamudi G, Mahenthiran J, et al. Fragmented QRS on a 12-lead ECG: a predictor of mortality and cardiac events in patients with coronary artery disease. Heart Rhythm. 2007 Nov;4(11):1385-92.

166. Das MK, Suradi H, Maskoun W, Michael MA, Shen C, Peng J, et al. Fragmented Wide QRS on a 12-Lead ECG A Sign of Myocardial Scar and Poor Prognosis. Circ Arrhythm Electrophysiol. 2008 Oct 1;1(4):258-68.

167. Maskoun W, Suradi H, Mahenthiran J, Bhakta D, Das MK. Fragmented QRS complexes on a 12-lead ECG predict arrhythmic events in patietns with ischemic cardiolmyopathy who receive an ICD for primary prophylaxis. Heart Rhythm. 2007 May;4(5):S211-2.

168. Michael MA, Das MK. Fragmented QRS (fQRS) on 12-lead EKG is a predictor of arrhythmic events and mortality in patients with dilated cardiomyopathy. Heart Rhythm. 2006 May;3(5):S103-4.

169. Forleo GB, Della Rocca DG, Papavasileiou LP, Panattoni G, Sergi D, Duro L, et al. Predictive value of fragmented QRS in primary prevention implantable cardioverter defibrillator recipients with left ventricular dysfunction. J Cardiovasc Med (Hagerstown). 2011 Nov;12(11):779-84.

170. Brenyo A, Pietrasik G, Barsheshet A, Huang DT, Polonsky B, McNITT S, et al. QRS Fragmentation and the Risk of Sudden Cardiac Death in MADIT II. Journal of Cardiovascular Electrophysiology. 2012;23(12):1343-8.

171. Morita H, Kusano KF, Miura D, Nagase S, Nakamura K, Morita ST, et al. Fragmented QRS as a marker of conduction abnormality and a predictor of prognosis of Brugada syndrome. Circulation. 2008 Oct 21;118(17):1697-704.

172. Selvester R, Wagner J, Rubin H. Quantitation of myocardial infarct size and location by electrocardiogram and vectorcardiogram. Quantitative Cardiology. 1972;31.

173. Wagner GS, Freye CJ, Palmeri ST, Roark SF, Stack NC, Ideker RE, et al. Evaluation of a QRS scoring system for estimating myocardial infarct size. I. Specificity and observer agreement. Circulation. 1982 Feb;65(2):342-7.

174. Ideker RE, Wagner GS, Ruth WK, Alonso DR, Bishop SP, Bloor CM, et al. Evaluation of a QRS scoring system for estimating myocardial infarct size. II. Correlation with quantitative anatomic findings for anterior infarcts. Am J Cardiol. 1982 May;49(7):1604-14.

175. Roark SF, Ideker RE, Wagner GS, Alonso DR, Bishop SP, Bloor CM, et al. Evaluation of a QRS scoring system for estimating myocardial infarct size. III. Correlation with quantitative anatomic findings for inferior infarcts. Am J Cardiol. 1983 Feb;51(3):382–9.

176. Palmeri ST, Harrison DG, Cobb FR, Morris KG, Harrell FE, Ideker RE, et al. A QRS scoring system for assessing left ventricular function after myocardial infarction. N Engl J Med. 1982 Jan 7;306(1):4–9.

177. Haisty WK Jr, Pahlm O, Wagner NB, Pope JE, Wagner GS. Performance of the automated complete Selvester QRS scoring system in normal subjects and patients with single and multiple myocardial infarctions. J Am Coll Cardiol. 1992 Feb;19(2):341–6.

178. Engblom H, Wagner GS, Setser RM, Selvester RH, Billgren T, Kasper JM, et al. Quantitative clinical assessment of chronic anterior myocardial infarction with delayed enhancement magnetic resonance imaging and QRS scoring. American Heart Journal. 2003 Aug;146(2):359–66.

179. Engblom H, Hedström E, Heiberg E, Wagner GS, Pahlm O, Arheden H. Size and transmural extent of first-time reperfused myocardial infarction assessed by cardiac magnetic resonance can be estimated by 12-lead electrocardiogram. American Heart Journal. 2005 Nov;150(5):920.e1–920.e9.

180. Bang LE, Ripa RS, Grande P, Kastrup J, Clemmensen PM, Wagner GS. Comparison of infarct size changes with delayed contrast-enhanced magnetic resonance imaging and electrocardiogram QRS scoring during the 6 months after acutely reperfused myocardial infarction. Journal of Electrocardiology. 2008;41(6):609–13.

181. Geerse DA, Wu KC, Gorgels AP, Zimmet J, Wagner GS, Miller JM. Comparison between contrast-enhanced magnetic resonance imaging and Selvester QRS scoring system in estimating changes in infarct size between the acute and chronic phases of myocardial infarction. Ann Noninvasive Electrocardiol. 2009 Oct;14(4):360–5.

182. Weir RAP, Martin TN, Murphy CA, Petrie CJ, Clements S, Steedman T, et al. Comparison of serial measurements of infarct size and left ventricular ejection fraction by contrast-enhanced cardiac magnetic resonance imaging and electrocardiographic QRS scoring in reperfused anterior ST-elevation myocardial infarction. J Electrocardiol. 2010 Jun;43(3):230–6.

183. Strauss D, Selvester R. The QRS complex—a biomarker that “images” the heart: QRS scores to quantify myocardial scar in the presence of normal and abnormal ventricular conduction☆. Journal of Electrocardiology. 2009 Jan;42(1):85–96.

184. Strauss DG, Selvester RH, Lima JAC, Arheden H, Miller JM, Gerstenblith G, et al. ECG quantification of myocardial scar in cardiomyopathy patients with or without conduction defects: correlation with cardiac magnetic resonance and arrhythmogenesis. Circ Arrhythm Electrophysiol. 2008 Dec;1(5):327–36.

185. Strauss DG, Poole JE, Wagner GS, Selvester RH, Miller JM, Anderson J, et al. An ECG index of myocardial scar enhances prediction of defibrillator shocks: An analysis of the Sudden Cardiac Death in Heart Failure Trial. Heart Rhythm. 2011 Jan;8(1):38–45.

186. Kligfield P, Gettes LS, Bailey JJ, Childers R, Deal BJ, Hancock EW, et al. Recommendations for the Standardization and Interpretation of the Electrocardiogram. Journal of the American College of Cardiology. 2007 Mar;49(10):1109–27.

187. Bailey JJ, Berson AS, Garson A, Horan LG, Macfarlane PW, Mortara DW, et al. Recommendations for standardization and specifications in automated electrocardiography: bandwidth and digital signal processing. A report for health professionals by an ad hoc writing group of the Committee on Electrocardiography and Cardiac Electrophysiology of the Council on Clinical Cardiology, American Heart Association. Circulation. 1990 Feb 1;81(2):730–9.

188. Sörnmo L, Laguna P. Electrocardiogram (ECG) Signal Processing. Wiley Encyclopedia of Biomedical Engineering [Internet]. John Wiley & Sons, Inc.; 2006 [cited 2013 Dec 10]. Available from: http://onlinelibrary.wiley.com/doi/10.1002/9780471740360.ebs1482/abstract

189. Venkatachalam et al. - 2011 - Signals and Signal Processing for the Electrophysi.pdf [Internet]. [cited 2013 Dec 11]. Available from: http://circep.ahajournals.org/content/4/6/965.full.pdf

190. Bragg-Remschel DA, Anderson CM, Winkle RA. Frequency response characteristics of ambulatory ECG monitoring systems and their implications for ST segment analysis. Am Heart J. 1982 Jan;103(1):20–31.

191. Berson AS, Pipberger HV. Electrocardiographic distortions caused by inadequate high-frequency response of direct-writing electrocardiographs. Am Heart J. 1967 Aug;74(2):208–18.

192. Venkatachalam KL, Herbrandson JE, Asirvatham SJ. Signals and Signal Processing for the Electrophysiologist: Part I: Electrogram Acquisition. Circulation: Arrhythmia and Electrophysiology. 2011 Dec 20;4(6):965–73.

193. Rangayyan RM. Biomedical signal analysis a case-study approach [Internet]. [Piscataway, NJ]; New York, N.Y.: IEEE Press ; Wiley-Interscience; 2002 [cited 2012 Apr 12]. Available from: http://www.knovel.com/knovel2/Toc.jsp?BookID=2105

194. Shannon CE. Communication in the Presence of Noise. Proceedings of the IRE. 1949;37(1):10–21.

195. Nyquist H. Certain Topics in Telegraph Transmission Theory. American Institute of Electrical Engineers, Transactions of the. 1928;47(2):617–44.

196. Smith SW. Digital signal processing : a practical guide for engineers and scientists. Amsterdam; Boston: Newnes; 2003.

197. Clifford GD, Azuaje F, McSharry P. Advanced methods and tools for ECG data analysis. Boston: Artech House; 2006.

198. Waljee AK, Higgins PDR. Machine Learning in Medicine: A Primer for Physicians. The American Journal of Gastroenterology. 2010 Jun;105(6):1224–6.

199. Clifton DA, Gibbons J, Davies J, Tarassenko L. Machine learning and software engineering in health informatics. Realizing Artificial Intelligence Synergies in Software Engineering (RAISE), 2012 First International Workshop on [Internet]. IEEE; 2012 [cited 2014 May 18]. p. 37–41. Available from: http://ieeexplore.ieee.org/xpls/abs_all.jsp?arnumber=6227968

200. Alderson M. A review of the National Health Service's computing policy in the 1970s. Br J Prev Soc Med. 1976 Mar;30(1):11–6.

201. Kaplan B. The Computer Prescription: Medical Computing, Public Policy, and Views of History. Science Technology Human Values. 1995 Jan 1;20(1):5–38.

202. Sonnenburg S, Braun ML, Cheng Soon Ong, Bengio S, Bottou L, Holmes G, et al. The Need for Open Source Software in Machine Learning. Journal of Machine Learning Research. 2007 10/1/2007;8(10):2443–66.

203. Yoda T. Cooperation between medical doctors and engineers for developing advanced medical devices. Science and Innovation Policy, 2009 Atlanta Conference on [Internet]. IEEE; 2009 [cited 2014 May 17]. p. 1–9. Available from: http://ieeexplore.ieee.org/xpls/abs_all.jsp?arnumber=5367815

204. Home - PubMed - NCBI [Internet]. [cited 2014 May 17]. Available from: http://www.ncbi.nlm.nih.gov/pubmed/

205. Noble WS. What is a support vector machine? Nat Biotech. 2006 Dec;24(12):1565–7.

206. Kotsiantis SB. Supervised machine learning: a review of classification techniques. Informatica (03505596) [Internet]. 2007 [cited 2014 May 10];31(3). Available from: http://search.ebscohost.com/login.aspx?direct=true&profile=ehost&scope=site&authtype=crawler&jrnl=03505596&AN=27465122&h=VMAgAuewyNBrx%2FDfebgHwCDcan9ALMlP2wbdgKSOXURW6tKtOZq8G0vdpdBesF3OThGRDyM4Qbr8AoQ7964XcA%3D%3D&crl=c

207. Osowski S, Hoai LT, Markiewicz T. Support vector machine-based expert system for reliable heartbeat recognition. IEEE Transactions on Biomedical Engineering. 2004 Apr;51(4):582–9.

208. Mohebbi M, Ghassemian H. Detection of atrial fibrillation episodes using SVM. 30th Annual International Conference of the IEEE Engineering in Medicine and Biology Society, 2008 EMBS 2008. 2008. p. 177–80.

209. Goldberger AL, Amaral LAN, Glass L, Hausdorff JM, Ivanov PC, Mark RG, et al. PhysioBank, PhysioToolkit, and PhysioNet Components of a New Research Resource for Complex Physiologic Signals. Circulation. 2000 Jun 13;101(23):e215–20.

210. Namarvar HH, Shahidi AV. Cardiac arrhythmias predictive detection methods with wavelet-SVD analysis and support vector machines. 26th Annual International Conference of the IEEE Engineering in Medicine and Biology Society, 2004 IEMBS '04. 2004. p. 365–8.

211. Parvaneh S, Golpayegani MRH, Firoozabadi M, Haghjoo M. Predicting the spontaneous termination of atrial fibrillation based on poincare section in the electrocardiogram phase space. Proc Inst Mech Eng H. 2012 Jan;226(1):3–20.

212. Shandilya S, Ward K, Kurz M, Najarian K. Non-linear dynamical signal characterization for prediction of defibrillation success through machine learning. BMC Medical Informatics and Decision Making. 2012 Oct 15;12(1):116.

213. Ramirez-Villegas JF, Lam-Espinosa E, Ramirez-Moreno DF, Calvo-Echeverry PC, Agredo-Rodriguez W. Heart Rate Variability Dynamics for the Prognosis of Cardiovascular Risk. PLoS ONE. 2011 Feb 28;6(2):e17060.

214. Yokokawa M, Liu T-Y, Yoshida K, Scott C, Hero A, Good E, et al. Automated analysis of the 12-lead electrocardiogram to identify the exit site of postinfarction ventricular tachycardia. Heart Rhythm. 2012 Mar;9(3):330–4.

215. Ridker PM, Buring JE, Shih J, Matias M, Hennekens CH. Prospective study of C-reactive protein and the risk of future cardiovascular events among apparently healthy women. Circulation. 1998 Aug 25;98(8):731–3.

216. Burke AP, Tracy RP, Kolodgie F, Malcom GT, Zieske A, Kutys R, et al. Elevated C-reactive protein values and atherosclerosis in sudden coronary death: association with different pathologies. Circulation. 2002 Apr 30;105(17):2019–23.

217. Blangy H, Sadoul N, Dousset B, Radauceanu A, Fay R, Aliot E, et al. Serum BNP, hs-C-reactive protein, procollagen to assess the risk of ventricular tachycardia in ICD recipients after myocardial infarction. Europace. 2007 Sep 1;9(9):724–9.

218. Albert CM, Ma J, Rifai N, Stampfer MJ, Ridker PM. Prospective Study of C-Reactive Protein, Homocysteine, and Plasma Lipid Levels as Predictors of Sudden Cardiac Death. Circulation. 2002 Jun 4;105(22):2595–9.

219. Korngold EC, Januzzi JL, Gantzer ML, Moorthy MV, Cook NR, Albert CM. Amino-Terminal Pro-B-Type Natriuretic Peptide and High-Sensitivity C-Reactive Protein as Predictors of Sudden Cardiac Death Among Women. Circulation. 2009 Jun 9;119(22):2868–76.

220. Empana J-P, Jouven X, Canouï-Poitrine F, Luc G, Tafflet M, Haas B, et al. C-Reactive Protein, Interleukin 6, Fibrinogen and Risk of Sudden Death in European Middle-Aged Men: The PRIME Study. Arterioscler Thromb Vasc Biol. 2010 Oct 1;30(10):2047–52.

221. Horwich TB, Patel J, MacLellan WR, Fonarow GC. Cardiac troponin I is associated with impaired hemodynamics, progressive left ventricular dysfunction, and increased mortality rates in advanced heart failure. Circulation. 2003 Aug 19;108(7):833–8.

222. Peacock WF 4th, De Marco T, Fonarow GC, Diercks D, Wynne J, Apple FS, et al. Cardiac troponin and outcome in acute heart failure. N Engl J Med. 2008 May 15;358(20):2117–26.

223. Hussein AA, Gottdiener JS, Bartz TM, Sotoodehnia N, deFilippi C, Dickfeld T, et al. Cardiomyocyte Injury Assessed by a Highly Sensitive Troponin Assay and Sudden Cardiac Death in the Community: The Cardiovascular Health Study. Journal of the American College of Cardiology. 2013 Dec 3;62(22):2112–20.

224. Thygesen K, Mair J, Mueller C, Huber K, Weber M, Plebani M, et al. Recommendations for the use of natriuretic peptides in acute cardiac care A position statement from the Study Group on Biomarkers in Cardiology of the ESC Working Group on Acute Cardiac Care. Eur Heart J. 2011 Feb 2;ehq509.

225. Scott PA, Barry J, Roberts PR, Morgan JM. Brain natriuretic peptide for the prediction of sudden cardiac death and ventricular arrhythmias: a meta-analysis. European journal of heart failure. 2009;11(10):958–66.

226. Patton KK, Sotoodehnia N, DeFilippi C, Siscovick DS, Gottdiener JS, Kronmal RA. N-terminal pro-B-type natriuretic peptide is associated with sudden cardiac death risk: the Cardiovascular Health Study. Heart Rhythm. 2011 Feb;8(2):228–33.

227. Weinberg EO, Shimpo M, De Keulenaer GW, MacGillivray C, Tominaga S, Solomon SD, et al. Expression and regulation of ST2, an interleukin-1 receptor family member, in cardiomyocytes and myocardial infarction. Circulation. 2002 Dec 3;106(23):2961–6.

228. Rehman SU, Mueller T, Januzzi JL Jr. Characteristics of the novel interleukin family biomarker ST2 in patients with acute heart failure. J Am Coll Cardiol. 2008 Oct 28;52(18):1458–65.

229. Sabatine MS, Morrow DA, Higgins LJ, MacGillivray C, Guo W, Bode C, et al. Complementary roles for biomarkers of biomechanical strain ST2 and N-terminal prohormone B-type natriuretic peptide in patients with ST-elevation myocardial infarction. Circulation. 2008 Apr 15;117(15):1936–44.

230. Pascual-Figal DA, Ordoñez-Llanos J, Tornel PL, Vázquez R, Puig T, Valdés M, et al. Soluble ST2 for Predicting Sudden Cardiac Death in Patients With Chronic Heart Failure and Left Ventricular Systolic Dysfunction. Journal of the American College of Cardiology. 2009 Dec 1;54(23):2174–9.

231. Melander O, Newton-Cheh C, Almgren P, Hedblad B, Berglund G, Engström G, et al. Novel and conventional biomarkers for prediction of incident cardiovascular events in the community. JAMA. 2009 Jul 1;302(1):49–57.

232. Zethelius B, Berglund L, Sundström J, Ingelsson E, Basu S, Larsson A, et al. Use of multiple biomarkers to improve the prediction of death from cardiovascular causes. N Engl J Med. 2008 May 15;358(20):2107–16.

233. Kistorp C, Raymond I, Pedersen F, Gustafsson F, Faber J, Hildebrandt P. N-terminal pro-brain natriuretic peptide, C-reactive protein, and urinary albumin levels as predictors of mortality and cardiovascular events in older adults. JAMA. 2005 Apr 6;293(13):1609–16.

234. Shlipak MG, Fried LF, Cushman M, Manolio TA, Peterson D, Stehman-Breen C, et al. Cardiovascular mortality risk in chronic kidney disease: comparison of traditional and novel risk factors. JAMA. 2005 Apr 13;293(14):1737–45.

235. Wang TJ. Multiple Biomarkers for Predicting Cardiovascular Events: Lessons Learned. Journal of the American College of Cardiology. 2010 May 11;55(19):2092–5.

236. Scott PA, Townsend PA, Ng LL, Zeb M, Harris S, Roderick PJ, et al. Defining potential to benefit from implantable cardioverter defibrillator therapy: the role of biomarkers. Europace. 2011 Oct;13(10):1419–27.

237. Azuaje FJ, Dewey FE, Brutsaert DL, Devaux Y, Ashley EA, Wagner DR. Systems-Based Approaches to Cardiovascular Biomarker Discovery. Circ Cardiovasc Genet. 2012 Jun 1;5(3):360–7.

238. McGregor E. Proteomics of the Heart: Unraveling Disease. Circulation Research. 2006 Feb;98(3):309–21.

239. H.W. Dekkers D, Bezstarosti K, Kuster D, J.M. Verhoeven A, K. Das D. Application of Proteomics in Cardiovascular Research. Current Proteomics. 2010;7(2):108–15.

240. Anderson NG, Anderson L. The Human Protein Index. Clin Chem. 1982 Apr;28(4 Pt 2):739–48.

241. Rifai N, Gillette MA, Carr SA. Protein biomarker discovery and validation: the long and uncertain path to clinical utility. Nat Biotechnol. 2006 Aug;24(8):971–83.

242. Guo Y, Fu Z, Van Eyk JE. A Proteomic Primer for the Clinician. Proceedings of the American Thoracic Society. 2007 Jan 1;4(1):9–17.

243. Vitzthum F, Behrens F, Anderson NL, Shaw JH. Proteomics: from basic research to diagnostic application. A review of requirements & needs. J Proteome Res. 2005 Aug;4(4):1086–97.

244. Tambor V, Fucíková A, Lenco J, Kacerovskỳ M, Rehácek V, Stulík J, et al. Application of proteomics in biomarker discovery: a primer for the clinician. Physiol Res. 2010;59:471–97.

245. Dubois E, Fertin M, Burdese J, Amouyel P, Bauters C, Pinet F. Cardiovascular proteomics: Translational studies to develop novel biomarkers in heart failure and left ventricular remodeling. Proteomics Clin Appl [Internet]. 2010 Dec 6 [cited 2011 Jan 24]; Available from: http://www.ncbi.nlm.nih.gov/pubmed/21246740

246. States DJ, Omenn GS, Blackwell TW, Fermin D, Eng J, Speicher DW, et al. Challenges in deriving high-confidence protein identifications from data gathered by a HUPO plasma proteome collaborative study. Nat Biotechnol. 2006 Mar;24(3):333–8.

247. Banks RE. Preanalytical influences in clinical proteomic studies: raising awareness of fundamental issues in sample banking. Clin Chem. 2008 Jan;54(1):6–7.

248. Tuck MK, Chan DW, Chia D, Godwin AK, Grizzle WE, Krueger KE, et al. Standard Operating Procedures for Serum and Plasma Collection: Early Detection Research

Network Consensus Statement *Standard Operating Procedure Integration Working Group*. J Proteome Res. 2009 Jan;8(1):113–7.

249. Barnouin K. Two-dimensional gel electrophoresis for analysis of protein complexes. Methods Mol Biol. 2004;261:479–98.

250. Chugh S, Suen C, Gramolini A. Proteomics and Mass Spectrometry: What Have We Learned About The Heart? Curr Cardiol Rev. 2010 May;6(2):124–33.

251. Lewis C, Jockusch H, Ohlendieck K. Proteomic Profiling of the Dystrophin-Deficient MDX Heart Reveals Drastically Altered Levels of Key Metabolic and Contractile Proteins. J Biomed Biotechnol [Internet]. 2010 [cited 2014 Jul 22];2010. Available from: http://www.ncbi.nlm.nih.gov/pmc/articles/PMC2874991/

252. Hortin GL. The MALDI-TOF mass spectrometric view of the plasma proteome and peptidome. Clin Chem. 2006 Jul;52(7):1223–37.

253. Domon B, Aebersold R. Mass spectrometry and protein analysis. Science. 2006 Apr 14;312(5771):212–7.

254. Wolters DA, Washburn MP, Yates JR 3rd. An automated multidimensional protein identification technology for shotgun proteomics. Anal Chem. 2001 Dec 1;73(23):5683–90.

255. Chugh S, Sharma P, Kislinger T, Gramolini AO. Clinical Proteomics Getting to the Heart of the Matter. Circ Cardiovasc Genet. 2012 Jun 1;5(3):377–377.

256. Craig R, Beavis RC. TANDEM: matching proteins with tandem mass spectra. Bioinformatics. 2004 Jun 12;20(9):1466–7.

257. Thompson A, Schäfer J, Kuhn K, Kienle S, Schwarz J, Schmidt G, et al. Tandem mass tags: a novel quantification strategy for comparative analysis of complex protein mixtures by MS/MS. Anal Chem. 2003 Apr 15;75(8):1895–904.

258. Anderson L. Candidate-based proteomics in the search for biomarkers of cardiovascular disease. The Journal of Physiology. 2004 Dec 20;563(1):23–60.

259. Tam SW, Pirro J, Hinerfeld D. Depletion and fractionation technologies in plasma proteomic analysis. Expert Rev Proteomics. 2004 Dec;1(4):411–20.

260. Liu T, Qian W-J, Mottaz HM, Gritsenko MA, Norbeck AD, Moore RJ, et al. Evaluation of multiprotein immunoaffinity subtraction for plasma proteomics and candidate biomarker discovery using mass spectrometry. Mol Cell Proteomics. 2006 Nov;5(11):2167–74.

261. Garbis SD, Roumeliotis TI, Tyritzis SI, Zorpas KM, Pavlakis K, Constantinides CA. A Novel Multidimensional Protein Identification Technology Approach Combining Protein Size Exclusion Prefractionation, Peptide Zwitterion−Ion Hydrophilic Interaction Chromatography, and Nano-Ultraperformance RP Chromatography/nESI-MS ^{2} for the in-Depth Analysis of the Serum Proteome and Phosphoproteome: Application to Clinical Sera Derived from Humans with Benign Prostate Hyperplasia </title>. Anal Chem. 2011 Feb;83(3):708–18.

262. Wolf-Yadlin A, Hautaniemi S, Lauffenburger DA, White FM. Multiple reaction monitoring for robust quantitative proteomic analysis of cellular signaling networks. Proc Natl Acad Sci USA. 2007 Apr 3;104(14):5860–5.

263. Kislinger T, Gramolini AO, MacLennan DH, Emili A. Multidimensional protein identification technology (MudPIT): technical overview of a profiling method optimized for the comprehensive proteomic investigation of normal and diseased heart tissue. Journal of the American Society for Mass Spectrometry. 2005;16(8):1207–20.

264. Pohlner K, Portig I, Pankuweit S, Lottspeich F, Maisch B. Identification of mitochondrial antigens recognized by antibodies in sera of patients with idiopathic dilated cardiomyopathy by two-dimensional gel electrophoresis and protein sequencing. Am J Cardiol. 1997 Oct 15;80(8):1040–5.

265. Chen C-H, Budas GR, Churchill EN, Disatnik M-H, Hurley TD, Mochly-Rosen D. Activation of aldehyde dehydrogenase-2 reduces ischemic damage to the heart. Science. 2008 Sep 12;321(5895):1493–5.

266. Cuesta F de la, Alvarez-Llamas G, Maroto AS, Donado A, Zubiri I, Posada M, et al. A Proteomic Focus on the Alterations Occurring at the Human Atherosclerotic Coronary Intima. Mol Cell Proteomics. 2011 Apr 1;10(4):M110.003517.

267. Hammer E, Goritzka M, Ameling S, Darm K, Steil L, Klingel K, et al. Characterization of the human myocardial proteome in inflammatory dilated cardiomyopathy by label-free quantitative shotgun proteomics of heart biopsies. J Proteome Res. 2011 May 6;10(5):2161–71.

268. Jones DJL, Willingale R, Quinn PA, Lamb JH, Farmer PB, Davies JE, et al. Improving the diagnostic accuracy of N-terminal B-type natriuretic peptide in human systolic heart failure by plasma profiling using mass spectrometry. J Proteome Res. 2007 Aug;6(8):3329–34.

269. Scott PA, Zeidan B, Ng LL, Zeb M, Rosengarten JA, Garbis S, et al. Proteomic profiling to identify prognostic biomarkers in heart failure. In Vivo. 2012 Nov;26(6):875–82.

270. Hollander Z, Lazárová M, Lam KKY, Ignaszewski A, Oudit GY, Dyck JRB, et al. Proteomic biomarkers of recovered heart function: Proteomic biomarkers of recovered heart function. European Journal of Heart Failure. 2014 May;16(5):551–9.

271. Rosset A, Spadola L, Ratib O. OsiriX: an open-source software for navigating in multidimensional DICOM images. J Digit Imaging. 2004 Sep;17(3):205–16.

272. Passman R, Goldberger JJ. Predicting the Future: Risk Stratification for Sudden Cardiac Death in Patients With Left Ventricular Dysfunction. Circulation. 2012 Jun 18;125(24):3031–7.

273. Das MK, Maskoun W, Shen C, Michael MA, Suradi H, Desai M, et al. Fragmented QRS on twelve-lead electrocardiogram predicts arrhythmic events in patients with ischemic and nonischemic cardiomyopathy. Heart Rhythm. 2010 Jan;7(1):74–80.

274. Hayden JA, van der Windt DA, Cartwright JL, Côté P, Bombardier C. Assessing bias in studies of prognostic factors. Ann Intern Med. 2013 Feb 19;158(4):280–6.

275. The Cochrane Collaboration. Review Manager (RevMan). Copenhagen: The Nordic Cochrane Centre;

276. Zamora J, Abraira V, Muriel A, Khan K, Coomarasamy A. Meta-DiSc: a software for meta-analysis of test accuracy data. BMC Medical Research Methodology. 2006 Jul 12;6(1):31.

277. Deeks JJ, Altman DG. Diagnostic tests 4: likelihood ratios. BMJ. 2004 Jul 17;329(7458):168–9.

278. Higgins JPT, Thompson SG. Quantifying heterogeneity in a meta-analysis. Stat Med. 2002 Jun 15;21(11):1539–58.

279. DerSimonian R, Laird N. Meta-analysis in clinical trials. Control Clin Trials. 1986 Sep;7(3):177–88.

280. Korhonen P, Husa T, Konttila T, Tierala I, Mäkijärvi M, Väänänen H, et al. Fragmented QRS in Prediction of Cardiac Deaths and Heart Failure Hospitalizations after Myocardial Infarction. Annals of Noninvasive Electrocardiology. 2010;15(2):130–7.

281. Torigoe K, Tamura A, Kawano Y, Shinozaki K, Kotoku M, Kadota J. The number of leads with fragmented QRS is independently associated with cardiac death or hospitalization for heart failure in patients with prior myocardial infarction. Journal of Cardiology. 2012 Jan;59(1):36–41.

282. Sheng Q, Hsu C-C, Li J, Hong T, Huo Y. Correlation between fragmented QRS and the short-term prognosis of patients with acute myocardial infarction. J Zhejiang Univ Sci B. 2014 Jan;15(1):67–74.

283. Sha J, Zhang S, Tang M, Chen K, Zhao X, Wang F. Fragmented QRS Is Associated with All-Cause Mortality and Ventricular Arrhythmias in Patient with Idiopathic Dilated Cardiomyopathy. Annals of Noninvasive Electrocardiology. 2011;16(3):270–5.

284. Apiyasawat S, Sahasthas D, Ngarmukos T, Chandanamattha P, Likittanasombat K. Fragmented QRS as a Predictor of Appropriate Implantable Cardioverter-defibrillator Therapy. Indian Pacing Electrophysiol J. 2014 Jan;14(1):4–11.

285. Lorgis L, Jourda F, Hachet O, Zeller M, Gudjoncik A, Dentan G, et al. Prognostic value of fragmented QRS on a 12-lead ECG in patients with acute myocardial infarction. Heart Lung. 2013 Oct;42(5):326–31.

286. Rickard J, Zardkoohi O, Popovic Z, Verhaert D, Sraow D, Baranowski B, et al. QRS fragmentation is not associated with poor response to cardiac resynchronization therapy. Annals of Noninvasive Electrocardiology. 2011;16(2):165–71.

287. Cheema A, Khalid A, Wimmer A, Bartone C, Chow T, Spertus JA, et al. Fragmented QRS and Mortality Risk in Patients With Left Ventricular Dysfunction. Circ Arrhythm Electrophysiol. 2010 Aug 1;3(4):339–44.

288. Pei J, Li N, Gao Y, Wang Z, Li X, Zhang Y, et al. The J wave and fragmented QRS complexes in inferior leads associated with sudden cardiac death in patients with chronic heart failure. Europace. 2012 Aug 1;14(8):1180–7.

289. Ahn M-S, Kim J-B, Joung B, Lee M-H, Kim S-S. Prognostic implications of fragmented QRS and its relationship with delayed contrast-enhanced cardiovascular magnetic resonance imaging in patients with non-ischemic dilated cardiomyopathy. Int J Cardiol. 2013 Aug 20;167(4):1417–22.

290. Ozcan S, Cakmak HA, Ikitimur B, Yurtseven E, Stavileci B, Tufekcioglu EY, et al. The Prognostic Significance of Narrow Fragmented QRS on Admission Electrocardiogram in Patients Hospitalized for Decompensated Systolic Heart Failure. Clinical Cardiology. 2013;36(9):560–4.

291. Yan G-H, Wang M, Yiu K-H, Lau C-P, Zhi G, Lee SWL, et al. Subclinical left ventricular dysfunction revealed by circumferential 2D strain imaging in patients with coronary artery disease and fragmented QRS complex. Heart Rhythm. 2012 Jun;9(6):928–35.

292. Ellenbogen KA. Are Implantable Cardioverter Defibrillator Shocks a Surrogate for Sudden Cardiac Death in Patients With Nonischemic Cardiomyopathy? Circulation. 2006 Feb;113(6):776–82.

293. Wissner E, Stevenson WG, Kuck K-H. Catheter ablation of ventricular tachycardia in ischaemic and non-ischaemic cardiomyopathy: where are we today? A clinical review. Eur Heart J. 2012 Jun 1;33(12):1440–50.

294. Antzelevitch C. Ionic, molecular, and cellular bases of QT-interval prolongation and torsade de pointes. Europace. 2007 Sep;9 Suppl 4:iv4–15.

295. Straus SMJM, Kors JA, De Bruin ML, van der Hooft CS, Hofman A, Heeringa J, et al. Prolonged QTc interval and risk of sudden cardiac death in a population of older adults. J Am Coll Cardiol. 2006 Jan 17;47(2):362–7.

296. Fu GS, Meissner A, Simon R. Repolarization dispersion and sudden cardiac death in patients with impaired left ventricular function. Eur Heart J. 1997 Feb;18(2):281–9.

297. Mahrholdt H, Wagner A, Holly TA, Elliott MD, Bonow RO, Kim RJ, et al. Reproducibility of chronic infarct size measurement by contrast-enhanced magnetic resonance imaging. Circulation. 2002 Oct 29;106(18):2322–7.

298. Kwon DH, Halley CM, Carrigan TP, Zysek V, Popovic ZB, Setser R, et al. Extent of left ventricular scar predicts outcomes in ischemic cardiomyopathy patients with significantly reduced systolic function: a delayed hyperenhancement cardiac magnetic resonance study. JACC Cardiovasc Imaging. 2009 Jan;2(1):34–44.

299. Scott PA, Morgan JM, Carroll N, Murday DC, Roberts PR, Peebles CR, et al. The extent of left ventricular scar quantified by late gadolinium enhancement MRI is associated with spontaneous ventricular arrhythmias in patients with coronary artery disease and implantable cardioverter-defibrillators. Circ Arrhythm Electrophysiol. 2011 Jun 1;4(3):324–30.

300. Haqqani HM, Marchlinski FE. Electrophysiologic substrate underlying postinfarction ventricular tachycardia: characterization and role in catheter ablation. Heart Rhythm. 2009 Aug;6(8 Suppl):S70–6.

301. Cerqueira MD, Weissman NJ, Dilsizian V, Jacobs AK, Kaul S, Laskey WK, et al. Standardized myocardial segmentation and nomenclature for tomographic imaging of the heart. A statement for healthcare professionals from the Cardiac Imaging Committee of the Council on Clinical Cardiology of the American Heart Association. Int J Cardiovasc Imaging. 2002 Feb;18(1):539–42.

302. Kasamaki Y, Ozawa Y, Ohta M, Sezai A, Yamaki T, Kaneko M, et al. Automated versus manual measurement of the QT interval and corrected QT interval. Ann Noninvasive Electrocardiol. 2011 Apr;16(2):156–64.

303. Ahnve S. Correction of the QT interval for heart rate: review of different formulas and the use of Bazett's formula in myocardial infarction. Am Heart J. 1985 Mar;109(3 Pt 1):568–74.

304. Chugh SS, Reinier K, Singh T, Uy-Evanado A, Socoteanu C, Peters D, et al. Determinants of prolonged QT interval and their contribution to sudden death risk in coronary artery disease: the Oregon Sudden Unexpected Death Study. Circulation. 2009 Feb 10;119(5):663–70.

305. Lellouche N, De Diego C, Akopyan G, Boyle NG, Mahajan A, Cesario DA, et al. Changes and predictive value of dispersion of repolarization parameters for appropriate therapy in patients with biventricular implantable cardioverter-defibrillators. Heart Rhythm. 2007 Oct;4(10):1274–83.

306. Chalil S, Yousef ZR, Muyhaldeen SA, Smith REA, Jordan P, Gibbs CR, et al. Pacing-induced increase in QT dispersion predicts sudden cardiac death following cardiac resynchronization therapy. J Am Coll Cardiol. 2006 Jun 20;47(12):2486–92.

307. Zipes DP, Camm AJ, Borggrefe M, Buxton AE, Chaitman B, Fromer M, et al. ACC/AHA/ESC 2006 guidelines for management of patients with ventricular arrhythmias and the prevention of sudden cardiac death: a report of the American College of Cardiology/American Heart Association Task Force and the European Society of Cardiology Committee for Practice Guidelines (Writing Committee to Develop guidelines for management of patients with ventricular arrhythmias and the prevention of sudden cardiac death) developed in collaboration with the European Heart Rhythm Association and the Heart Rhythm Society. Europace. 2006 Sep;8(9):746–837.

308. Damman P, Hirsch A, Windhausen F, Tijssen JGP, de Winter RJ, ICTUS Investigators. 5-year clinical outcomes in the ICTUS (Invasive versus Conservative Treatment in Unstable coronary Syndromes) trial a randomized comparison of an early invasive versus selective invasive management in patients with non-ST-segment elevation acute coronary syndrome. J Am Coll Cardiol. 2010 Mar 2;55(9):858–64.

309. Davies MJ. Anatomic features in victims of sudden coronary death. Coronary artery pathology. Circulation. 1992 Jan;85(1 Suppl):I19–24.

310. Chauhan VS, Tang AS. Dynamic changes of QT interval and QT dispersion in non-Q-wave and Q-wave myocardial infarction. J Electrocardiol. 2001 Apr;34(2):109–17.

311. Patel C, Burke JF, Patel H, Gupta P, Kowey PR, Antzelevitch C, et al. Is there a significant transmural gradient in repolarization time in the intact heart? Cellular basis of the T wave: a century of controversy. Circ Arrhythm Electrophysiol. 2009 Feb;2(1):80–8.

312. Loring Z, Chelliah S, Selvester RH, Wagner G, Strauss DG. A detailed guide for quantification of myocardial scar with the Selvester QRS score in the presence of electrocardiogram confounders. J Electrocardiol. 2011 Oct;44(5):544–54.

313. Wathen MS, DeGroot PJ, Sweeney MO, Stark AJ, Otterness MF, Adkisson WO, et al. Prospective Randomized Multicenter Trial of Empirical Antitachycardia Pacing Versus Shocks for Spontaneous Rapid Ventricular Tachycardia in Patients With Implantable Cardioverter-Defibrillators Pacing Fast Ventricular Tachycardia Reduces Shock Therapies (PainFREE Rx II) Trial Results. Circulation. 2004 Oct 26;110(17):2591–6.

314. Goldenberg I, Vyas AK, Hall WJ, Moss AJ, Wang H, He H, et al. Risk Stratification for Primary Implantation of a Cardioverter-Defibrillator in Patients With Ischemic Left Ventricular Dysfunction. Journal of the American College of Cardiology. 2008 Jan;51(3):288–96.

315. Schelbert EB, Hsu L-Y, Anderson SA, Mohanty BD, Karim SM, Kellman P, et al. Late gadolinium-enhancement cardiac magnetic resonance identifies postinfarction myocardial fibrosis and the border zone at the near cellular level in ex vivo rat heart. Circ Cardiovasc Imaging. 2010 Nov;3(6):743–52.

316. Welinder A, Hakacova N, Martin T, Engblom H. Importance of standardized assessment of late gadolinium enhancement for quantification of infarct size by cardiac magnetic resonance: implications for comparison with electrocardiogram. Journal of Electrocardiology. 2011 Sep;44(5):538–43.

317. Carlsen EA, Bang LE, Ahtarovski KA, Engstrøm T, Køber L, Kelbæk H, et al. Comparison of Selvester QRS score with magnetic resonance imaging measured infarct size in patients with ST elevation myocardial infarction. Journal of Electrocardiology. 2012 Jul;45(4):414–9.

318. De Haan S, Meijers TA, Knaapen P, Beek AM, van Rossum AC, Allaart CP. Scar size and characteristics assessed by CMR predict ventricular arrhythmias in ischaemic cardiomyopathy: comparison of previously validated models. Heart. 2011 Sep 13;97(23):1951–6.

319. Iles L, Pfluger H, Phrommintikul A, Cherayath J, Aksit P, Gupta SN, et al. Evaluation of diffuse myocardial fibrosis in heart failure with cardiac magnetic

resonance contrast-enhanced T1 mapping. J Am Coll Cardiol. 2008 Nov 4;52(19):1574–80.

320. Hindman NB, Schocken DD, Widmann M, Anderson WD, White RD, Leggett S, et al. Evaluation of a QRS scoring system for estimating myocardial infarct size. V. Specificity and method of application of the complete system. Am J Cardiol. 1985 Jun 1;55(13 Pt 1):1485–90.

321. Jepsen P, Johnsen SP, Gillman MW, Sørensen HT. Interpretation of observational studies. Heart. 2004 Aug;90(8):956–60.

322. Wagner GS, Cowan M, Flowers NC, Ginzton LE, Ideker RE, Laks MM, et al. Nomenclature of myocardial wall segments. Committee report. Computerized Interpretation of the ECG VIII. Proceedings of the Engineering Foundation Conference. 1983.

323. Bono V, Mazomenos EB, Chen T, Rosengarten JA, Acharyya A, Maharatna K, et al. Development of an automated updated Selvester QRS scoring system using SWT-based QRS fractionation detection and classification. IEEE J Biomed Health Inform. 2014 Jan;18(1):193–204.

324. Addison PS. Wavelet transforms and the ECG: a review. Physiological Measurement. 2005 Oct 1;26(5):R155–99.

325. R Lenth. Java Applets for Power and Sample Size [Internet]. 2006. Available from: http://www.stat.uiowa.edu/~rlenth/Power.

326. Pope JE, Wagner NB, Dubow D, Edmonds JH, Wagner GS, Haisty WK Jr. Development and validation of an automated method of the Selvester QRS scoring system for myocardial infarct size. Am J Cardiol. 1988 Apr 1;61(10):734–8.

327. Horáček BM, Warren JW, Albano A, Palmeri MA, Rembert JC, Greenfield Jr. JC, et al. Development of an automated Selvester Scoring System for estimating the size of myocardial infarction from the electrocardiogram. Journal of Electrocardiology. 2006 Apr;39(2):162–8.

328. Flett AS, Hasleton J, Cook C, Hausenloy D, Quarta G, Ariti C, et al. Evaluation of Techniques for the Quantification of Myocardial Scar of Differing Etiology Using Cardiac Magnetic Resonance. JACC: Cardiovascular Imaging. 2011 Feb;4(2):150–6.

329. Carey MG, Luisi AJ Jr, Baldwa S, Al-Zaiti S, Veneziano MJ, deKemp RA, et al. The Selvester QRS Score is more accurate than Q waves and fragmented QRS complexes using the Mason-Likar configuration in estimating infarct volume in patients with ischemic cardiomyopathy. J Electrocardiol. 2010 Aug;43(4):318–25.

330. Dima S-M, Panagiotou C, Mazomenos EB, Rosengarten JA, Maharatna K, Gialelis JV, et al. On the Detection of Myocadial Scar Based on ECG/VCG Analysis. IEEE Transactions on Biomedical Engineering. 2013 Dec;60(12):3399–409.

331. Buxton AE, Lee KL, Hafley GE, Pires LA, Fisher JD, Gold MR, et al. Limitations of ejection fraction for prediction of sudden death risk in patients with coronary artery disease: lessons from the MUSTT study. J Am Coll Cardiol. 2007 Sep 18;50(12):1150–7.

332. Levy WC, Lee KL, Hellkamp AS, Poole JE, Mozaffarian D, Linker DT, et al. Maximizing Survival Benefit With Primary Prevention Implantable Cardioverter-Defibrillator Therapy in a Heart Failure Population. Circulation. 2009 Sep 8;120(10):835–42.

333. Barsheshet A, Moss AJ, Huang DT, McNitt S, Zareba W, Goldenberg I. Applicability of a risk score for prediction of the long-term (8-year) benefit of the implantable cardioverter-defibrillator. J Am Coll Cardiol. 2012 Jun 5;59(23):2075–9.

334. Wu KC, Gerstenblith G, Guallar E, Marine JE, Dalal D, Cheng A, et al. Combined Cardiac Magnetic Resonance Imaging and C-Reactive Protein Levels Identify a Cohort at Low Risk for Defibrillator Firings and Death. Circ Cardiovasc Imaging. 2012 Mar 1;5(2):178–86.

335. Anderson NL, Anderson NG. The human plasma proteome: history, character, and diagnostic prospects. Mol Cell Proteomics. 2002 Nov;1(11):845–67.

336. Veenstra TD, Conrads TP, Hood BL, Avellino AM, Ellenbogen RG, Morrison RS. Biomarkers: Mining the Biofluid Proteome. Mol Cell Proteomics. 2005 Apr 1;4(4):409–18.

337. Ross PL, Huang YN, Marchese JN, Williamson B, Parker K, Hattan S, et al. Multiplexed protein quantitation in Saccharomyces cerevisiae using amine-reactive isobaric tagging reagents. Mol Cell Proteomics. 2004 Dec;3(12):1154–69.

338. Sharma P, Cosme J, Gramolini AO. Recent proteomic advances in cardiac cells. J Proteomics. 2013 Apr 9;81:3–14.

339. Zhao D, Chu W-F, Wu L, Li J, Liu Q-M, Lu Y-J, et al. PAF exerts a direct apoptotic effect on the rat H9c2 cardiomyocytes in Ca2+-dependent manner. Int J Cardiol. 2010 Aug 6;143(1):86–93.

340. Montrucchio G, Alloatti G, Camussi G. Role of platelet-activating factor in cardiovascular pathophysiology. Physiol Rev. 2000 Oct;80(4):1669–99.

341. Detopoulou P, Fragopoulou E, Nomikos T, Antonopoulou S, Kotroyiannis I, Vassiliadou C, et al. Baseline and 6-Week Follow-Up Levels of PAF and Activity of Its Metabolic Enzymes in Patients With Heart Failure and Healthy Volunteers--A Pilot Study. Angiology. 2012 Sep 21;64(7):522–8.

342. Schunkert H, Götz A, Braund P, McGinnis R, Tregouet D-A, Mangino M, et al. Repeated Replication and a Prospective Meta-Analysis of the Association Between Chromosome 9p21.3 and Coronary Artery Disease. Circulation. 2008 Apr 1;117(13):1675–84.

343. Ketteler M, Bongartz P, Westenfeld R, Wildberger JE, Mahnken AH, Böhm R, et al. Association of low fetuin-A (AHSG) concentrations in serum with cardiovascular mortality in patients on dialysis: a cross-sectional study. Lancet. 2003 Mar 8;361(9360):827–33.

344. Laughlin GA, Cummins KM, Wassel CL, Daniels LB, Ix JH. The Association of Fetuin-A With Cardiovascular Disease Mortality in Older Community-Dwelling AdultsThe Rancho Bernardo Study. J Am Coll Cardiol. 2012 May 8;59(19):1688–96.

345. Jensen MK, Bartz TM, Mukamal KJ, Djoussé L, Kizer JR, Tracy RP, et al. Fetuin-A, Type 2 Diabetes, and Risk of Cardiovascular Disease in Older Adults The Cardiovascular Health Study. Dia Care. 2013 May 1;36(5):1222–8.

346. Ceconi C. Chromogranin A in heart failure. A novel neurohumoral factor and a predictor for mortality. European Heart Journal. 2002 Jun 15;23(12):967–74.

347. Angelone T, Mazza R, Cerra MC. Chromogranin-A: a multifaceted cardiovascular role in health and disease. Curr Med Chem. 2012;19(24):4042–50.

348. Keegan BR, Feldman JL, Lee DH, Koos DS, Ho RK, Stainier DYR, et al. The elongation factors Pandora/Spt6 and Foggy/Spt5 promote transcription in the zebrafish embryo. Development. 2002 Apr;129(7):1623–32.

349. COL11A1 collagen, type XI, alpha 1 [Homo sapiens (human)] - Gene - NCBI [Internet]. [cited 2013 Nov 20]. Available from: http://www.ncbi.nlm.nih.gov/gene/?term=1301%5Buid%5D

350. Chugh S, Ouzounian M, Lu Z, Mohamed S, Li W, Bousette N, et al. Pilot study identifying myosin heavy chain 7, desmin, insulin-like growth factor 7, and annexin A2 as circulating biomarkers of human heart failure. Proteomics. 2013 Aug;13(15):2324–34.

351. Sofi F, Cesari F, Marcucci R, Fatini C, Gori AM, Giglioli C, et al. Protein Z levels and prognosis in patients with acute coronary syndromes. Clin Chem Lab Med. 2006;44(9):1098–102.

352. Sofi F, Cesari F, Abbate R, Gensini GF, Broze G Jr, Fedi S. A meta-analysis of potential risks of low levels of protein Z for diseases related to vascular thrombosis. Thromb Haemost. 2010 Apr;103(4):749–56.

353. Kawai K, Kawashima S, Miyazaki T, Tajiri E, Mori M, Kitazaki K, et al. Serum beta2-microglobulin concentration as a novel marker to distinguish levels of risk in acute heart failure patients. J Cardiol. 2010 Jan;55(1):99–107.

354. 2009 WRITING GROUP TO REVIEW NEW EVIDENCE AND UPDATE THE 2005 GUIDELINE FOR THE MANAGEMENT OF PATIENTS WITH CHRONIC HEART FAILURE WRITING ON BEHALF OF THE 2005 HEART FAILURE WRITING COMMITTEE, Jessup M, Abraham WT, Casey DE, Feldman AM, Francis GS, et al. 2009 Focused Update: ACCF/AHA Guidelines for the Diagnosis and Management of Heart Failure in Adults: A Report of the American College of Cardiology Foundation/American Heart Association Task Force on Practice Guidelines: Developed in Collaboration With the International Society for Heart and Lung Transplantation. Circulation. 2009 Mar 26;119(14):1977–2016.

355. Karp NA, Lilley KS. Investigating sample pooling strategies for DIGE experiments to address biological variability. PROTEOMICS. 2009;9(2):388–97.

356. Diz AP, Truebano M, Skibinski DOF. The consequences of sample pooling in proteomics: An empirical study. ELECTROPHORESIS. 2009;30(17):2967–75.

357. Zhang P, Kirk JA, Ji W, Remedios CG dos, Kass DA, Eyk JEV, et al. Multiple Reaction Monitoring to Identify Site-Specific Troponin I Phosphorylated Residues in the Failing Human Heart. Circulation [Internet]. 2012 Sep 12 [cited 2012 Oct 1]; Available from: http://circ.ahajournals.org/content/early/2012/09/11/CIRCULATIONAHA.112.096388

358. Crowther JR. The ELISA Guidebook. Springer; 2000. 426 p.

359. Wieczorek DF, Jagatheesan G, Rajan S. The role of tropomyosin in heart disease. Adv Exp Med Biol. 2008;644:132–42.

360. Anker SD, Sharma R. The syndrome of cardiac cachexia. International Journal of Cardiology. 2002 Sep;85(1):51–66.

361. Yuqi L, Lei G, Yang L, Zongbin L, Hua X, Lin W, et al. Voltage-dependent anion channel (VDAC) is involved in apoptosis of cell lines carrying the mitochondrial DNA mutation. BMC Medical Genetics. 2009 Nov 9;10(1):114.

362. Lim DS, Roberts R, Marian AJ. Expression profiling of cardiac genes in human hypertrophic cardiomyopathy: insight into the pathogenesis of phenotypes. J Am Coll Cardiol. 2001 Oct;38(4):1175–80.

363. Mitra A, Basak T, Datta K, Naskar S, Sengupta S, Sarkar S. Role of α-crystallin B as a regulatory switch in modulating cardiomyocyte apoptosis by mitochondria or endoplasmic reticulum during cardiac hypertrophy and myocardial infarction. Cell Death Dis. 2013 Apr 4;4(4):e582.

364. Schwertz H, Carter JM, Abdudureheman M, Russ M, Buerke U, Schlitt A, et al. Myocardial ischemia/reperfusion causes VDAC phosphorylation which is reduced by cardioprotection with a p38 MAP kinase inhibitor. Proteomics. 2007 Dec 1;7(24):4579–88.

365. Shoshan-Barmatz V, Ben-Hail D. VDAC, a multi-functional mitochondrial protein as a pharmacological target. Mitochondrion. 2012 Jan;12(1):24–34.